



UNIVERSITÀ DEGLI STUDI DI TRIESTE

XXIX CYCLE OF THE PH.D. DOCTORAL SCHOOL IN EARTH SCIENCE AND FLUID MECHANICS

Evolution and stability of tidal inlets: a comparison between two natural cases along human-affected coastlines

Settore scientifico-disciplinare:
GEO/04 GEOGRAFIA FISICA E GEOMORFOLOGIA

**DOTTORANDA
CHIARA POPESSO**

Ph.D. program Coordinator
PROF. PIERPAOLO OMARI

Thesis Supervisor
PROF. GIORGIO FONTOLAN

Thesis Co-Supervisors
**PROF. OSCAR FERREIRA
DOC. ANDRE' PACHECO**

ANNO ACCADEMICO 2015/2016

Abstract

Tidal inlets are located within barrier island systems and are distributed worldwide in a variety of geologic and oceanographic settings, primarily on coastal plain shorelines (FitzGerald, 1988). The simultaneous presence of more than one tidal inlet makes the barrier island system susceptible to change. There exists a delicate balance within the competence of each inlet in terms of tidal prism (Pacheco *et al.*, 2010) in such a way that modifications (natural or man-made) in some part of the multi-inlet system could induce hydrodynamic and morphodynamic changes at a larger scale. Various conflicts between natural-unconstrained evolution of the system and human needs are responsible for disrupting equilibrium configurations.

The evolution of two unconstrained tidal inlets (not fixed), Ancão and S. Andrea Inlets, located in different human-affected multi-tidal inlet systems is considered in this thesis. The focus is on how natural features of tidal inlets can be indirectly conditioned by the presence of man and by the natural events in the system. The aim is to understand the conflicts generated by the unconstrained behaviour of the inlets in relation to human needs and uses. Through an analysis of morphological and hydrodynamic data, some guidelines are proposed in relation to the changes in the inlets and in the system.

Ancão Inlet is an artificial inlet, opened (relocated) on the known natural migration path. Once opened, it is allowed to migrate naturally. It is a small eastward-migrating inlet in the mesotidal multi tidal inlets system of Ria Formosa (south of Portugal), which at present consists of six tidal inlets. Following Salles *et al.* (2005), from the hydrodynamic point of view, Ria Formosa inlets are separated into three sub-embayments, each of which could be considered as an autonomous tidal inlet system with minimal interaction with the rest of the system. The lagoon system has been affected by some strong human interventions that modified the former hydrodynamic condition. The most important changes were due to the opening and stabilization of Faro-Olhão Inlet that caused the narrowing of the nearby Armona inlet, associated to the same sub-embayment. Ancão Inlet is the third inlet of this sub-embayment. Migrating toward the east, the inlet gradually diminishes the connection with the other inlets of the sub-embayment,

becoming more and more independent: only during certain tide conditions (e.g. spring tide), is the connection active (Pacheco *et al.*, 2010). The inlet region has been constantly monitored since 1997. Hydro-morphodynamic data were collected during several topobathymetric surveys. Morphological parameters and migration rates were subsequently measured and correlated with wave and water level data to evaluate the importance of different mechanisms in the evolutionary phases of the inlet. The migration trend and the variations of the main morphodynamic data seem to be mainly related to the dominant southwest sea conditions, demonstrating the predominance of the wave climate over tidal currents. The latter are not strong enough to resist the longshore sediment transport and maintain a stable inlet position. The unconstrained nature of the inlet allows it to respond to natural forcings by channel migration. This creates some problems in the water circulation in the backbarrier area, as well as hampering navigation. For these reasons, the position of Ancão Inlet is currently controlled by periodic updrift relocation, to maintain navigability and good oxygen and nutrient exchange. Additional management provisions are proposed and discussed.

The second study case is the small natural S. Andrea Inlet, located in Italy, in the Marano and Grado Lagoon (MGL, North Adriatic Sea), another multi tidal inlet system. This differs from the Ria Formosa system because of the microtidal regime and low wave-dominance, making this lagoon a relatively tide-dominated environment. During the 20th century, land reclamations, waterway dredging and, especially, inlet stabilizations, caused significant changes within the system. These may have been enhanced by natural extreme events (two strong consecutive floodings due to a concomitance of low pressure, spring tide and storm surge). S. Andrea Inlet is one of the two natural openings located in the MGL. On maps, it appears since 1600s but its persistence is uncertain. It is located between the two most efficient inlets in the lagoon i.e. Lignano and Buso Inlets, whose artificial stabilization began in the 1960s in order to improve navigability. These factors led to an increase of efficiency of those inlets at the expense of the S. Andrea Inlet. During the last two decades, morphological monitoring data shows a progressive shallowing of the main ebb channel, as well as a halving of the cross section area and, consequently, tidal prism. In contrast, the ebb tidal delta volume, although compressed in its own area, remained surprisingly unchanged, despite many formulations in literature attest a direct relation between tidal prism and ebb tidal delta volume (see e.g. Walton and Adams,

1976), demonstrating the inertia of the sedimentary body to adapt to changes. The low wave energy that affects this region is insufficient to rework the delta. Although it does not change its position, S. Andrea Inlet could potentially suffer the same conflicts as Ancão Inlet: poor water circulation and thus a bad oxygenation of the backbarrier area, and a difficult navigation of the channel. These conflicts with human needs result from the unconstrained behaviour of the inlet as it adapts to system changes. Considering the limited extent of the S. Andrea basin, the issues caused by the atrophy of the inlet are not yet critical, but if the prism reduction continues, some possible management measures must be adopted. Various options are suggested and discussed.

Riassunto

Le bocche lagunari (tidal inlets) fanno parte di sistemi di isole di barriera e sono distribuite in tutto il mondo in una varietà di ambienti geologici e oceanografici, principalmente sulle zone costiere (FitzGerald, 1988). La presenza simultanea di più di una bocca rende il sistema di isole barriera suscettibile di cambiamento. Esiste infatti un delicato equilibrio nella competenza di ciascuna apertura in termini di prisma di marea (Pacheco *et al.*, 2010) tale per cui eventuali modificazioni (naturali o artificiali) in una parte del sistema multi-inlet potrebbero indurre cambiamenti morfodinamici e idrodinamici in una scala più ampia all'interno dello stesso sistema. Vari conflitti tra evoluzione naturale e libera di bocche non stabilizzate e appartenenti al sistema possono essere responsabili di cambiamenti nelle configurazioni di equilibrio.

In questa tesi è stata presa in considerazione l'evoluzione di due bocche lagunari non stabilizzate con moli o altre strutture rigide, le bocche di Ancão e S. Andrea, situate in due diversi sistemi multi-inlet influenzati dall'uomo. Vorremmo concentrarci sulle modalità secondo la quali le caratteristiche naturali delle bocche mareali possono essere indirettamente condizionate dalla presenza dell'uomo e dagli eventi naturali capitati al sistema. L'obiettivo è quello di riconoscere e comprendere i conflitti generati dal comportamento libero (senza restrizioni dovute a irrigidimento delle bocche) dei tidal inlet studiati in relazione alle esigenze e agli usi dell'uomo. Attraverso un'analisi di dati morfologici ed idrodinamici, vengono proposte alcune linee guida in relazione ai cambiamenti morfologici delle bocche e del sistema di appartenenza.

La bocca di Ancão è un'apertura artificiale, scavata (più precisamente, rilocata) lungo il suo conosciuto passato percorso migratorio. Una volta aperta, gli è permesso di riprendere naturalmente il suo percorso di migrazione. Si tratta di una piccola bocca, migrante verso est, nel sistema multi-inlet della laguna mesotidale di Ria Formosa (situata a sud del Portogallo), attualmente costituito da sei isole di marea. Seguendo Salles *et al.* (2005), dal punto di vista idrodinamico, le bocche della Ria Formosa sono separate in tre sotto - compartimenti, ognuno dei quali può essere considerato come un sistema (singolo o multiplo) autonomo, con interazione minima con i compartimenti adiacenti. La Ria

Formosa è stata interessata da alcuni cospicui interventi antropici che hanno modificato l'ex condizione idrodinamica. I cambiamenti più importanti sono dovuti all'apertura e alla stabilizzazione della bocca di Faro-Olhão, la bocca più efficiente della laguna, le quali hanno causato il restringimento della vicina bocca di Armona, associata allo stesso sotto-compartimento. La bocca di Ancão è la terza apertura di questo sotto-compartimento. Man mano che la migrazione di Ancão procede verso est, la bocca riduce gradualmente la connessione con le altre bocche appartenenti allo stesso sotto-compartimento, diventando sempre più indipendente: solo durante determinate condizioni di marea (ad es. sigiziale) la connessione è attiva (Pacheco *et al.*, 2010). L'area della suddetta bocca è costantemente monitorata dal 1997. I dati idro-morfodinamici sono stati raccolti durante diversi rilevamenti topo-batimetrici. I parametri morfologici e i tassi di migrazione sono stati successivamente misurati e correlati con i dati di altezza d'onda e di marea, tenendo anche in considerazione eventuali storm surge, al fine di valutare l'importanza dei diversi meccanismi nelle fasi evolutive della bocca. Il trend di migrazione e le variazioni dei principali dati morfodinamici sembrano essere legati principalmente alle condizioni dominanti del mare da sud-ovest, dimostrando la predominanza del clima d'onda sulle correnti di marea. Queste ultime non sono abbastanza forti da contrastare il trasporto del sedimento lungo costa e garantire quindi una posizione stabile della bocca. La natura non vincolata della bocca di Ancão, consente di rispondere alle forze naturali attraverso la migrazione del suo canale principale. Ciò crea alcuni problemi nella circolazione dell'acqua nell'area di laguna retrostante oltre a ostacolare la navigazione. Per queste ragioni, la posizione della bocca di Ancão è attualmente controllata e gestita con periodiche rilocalizzazioni updrift della stessa, per mantenere la navigabilità, la buona ossigenazione e lo scambio di nutrienti nell'area lagunare di competenza. Sono proposte e discusse disposizioni aggiuntive di gestione.

Il secondo caso studio è la piccola apertura naturale di S. Andrea, situata in Italia, nella Laguna di Marano e Grado (MGL, Mare Adriatico), un altro sistema multiplo. Questo differisce dal sistema della Ria Formosa a causa del regime microtidale e un meno prepotente clima d'onda, rendendo questa laguna un ambiente relativamente diretto dalla marea. Nel corso del ventesimo secolo, le bonifiche di terreni, il dragaggio dei canali e, soprattutto, le stabilizzazioni di bocche, hanno causato significativi cambiamenti all'interno del sistema. Questi sono poi stati amplificati da estremi eventi naturali (due

pesanti inondazioni, nel 1966 a 1969, causate dalla concomitanza di bassa pressione, marea sigiziale e storm surge). La bocca di S. Andrea è una delle due aperture naturali situate nel MGL. Nelle mappe, appare già dal 1600 ma la sua futura persistenza è incerta. Si trova tra le due bocche più efficienti della laguna, le bocche di Lignano e di Buso, le cui stabilizzazioni artificiali sono iniziate negli anni '60, al fine di migliorare la navigabilità dei loro canali. Questi interventi, artificiali e naturali, hanno portato ad un aumento dell'efficienza di queste bocche a scapito di quella di S. Andrea. Negli ultimi due decenni i dati di monitoraggio morfologico mostrano un progressivo insabbiamento del canale principale, nonché una diminuzione della sua area di sezione trasversale e, di conseguenza, del prisma di marea. Al contrario, il volume di delta di riflusso, sebbene compresso nell'area, rimane sorprendentemente invariato, nonostante molte formulazioni empiriche in letteratura attestino una relazione diretta tra il prisma di marea e il volume del delta di riflusso (vedi ad esempio Walton e Adams, 1976), dimostrando l'inerzia di questo corpo sedimentario ad adattarsi ai cambiamenti. La bassa energia d'onda che colpisce questa area è insufficiente a rielaborare il delta. Anche se non cambia la sua posizione, la bocca di S. Andrea potrebbe mostrare gli stessi conflitti della bocca di Ancão: una scarsa circolazione dell'acqua e quindi una cattiva ossigenazione dell'area di laguna di sua competenza e una difficile navigazione lungo il canale. Questi conflitti generati dai bisogni umani derivano dal comportamento non vincolato della bocca in quanto essa può liberamente adattarsi alle modifiche del sistema. Considerando la limitata portata del bacino di S. Andrea, i problemi causati dall'atrofia dell'entrata non hanno ancora raggiunto un livello di criticità, ma se la riduzione del prisma continuasse, in futuro occorrerebbe adottare alcune misure di gestione. Sono proposte e discusse varie opzioni.

Contents

Abstract	2
Riassunto	5
Notation.....	16
Introduction.....	20
1. Review on stability of multiple inlet systems: coastal management interventions responsible for disrupting natural equilibriums.....	29
1.1 Tidal inlets morphology	33
1.1.1 Tidal deltas.....	35
1.1.2 By-pass processes.....	39
1.2 Stability criteria	40
Final remarks	46
1.3 Examples of coastal management interventions responsible for disrupting natural equilibriums.....	46
1.3.1 Dutch Wadden Sea, The Netherlands	47
1.3.2 Western-central Florida barrier-inlet systems	50
1.3.3 Matagorda Bay, Texas	53
1.3.4 Venice Lagoon, Italy: a case of forced stable multi-inlet system	56
1.3.5 Final remarks	58
2. Ria Formosa and Marano and Grado Lagoon: contrasting coastal environments .	60
2.1 Ria Formosa Lagoon.....	62
2.1.1 Tide, wind and wave climate.....	65
2.1.2 Natural processes and anthropic conflicts	66
2.2 Marano and Grado Lagoon.....	69
2.2.1 Tide, wind and wave climate.....	72
2.2.2 Natural processes and anthropic conflicts	74
2.1 Final remarks.....	75
3. The case of Ria Formosa: relocation and life cycle of an artificial opening inlet allowed migrate naturally	76
3.1 Study area: Ancão Inlet.....	77

3.2	Material and methods	80
3.3	Results.....	87
3.4	Discussions and concluding remarks	100
3.5	Chapter summary	103
4.	The case of Marano Lagunare: past, present and future trends of a natural inlet in a lagoon system highly changed by anthropic actions.....	105
4.1	Study area: S. Andrea Inlet	106
4.2	Material and methods	108
4.3	Results.....	116
4.4	Discussions and concluding remarks	131
4.5	Chapter summary	135
5.	Management practices and perspectives	138
5.1	Inlet stabilization practices	139
5.2	Relocation management practices	143
5.3	Dredging operations practices.....	147
5.4	Ancão inlet perspective	149
5.5	S. Andrea Inlet perspective	150
6.	Concluding remarks.....	153
	References	157
	Appendix.....	181

Figures index

Fig. 1.1 Morphological model of a typical Microtidal, Mesotidal and Macrotidal coastal regime (adapted from Hayes, 1979)	31
Fig. 1.2 Mean wave height vs mean tidal range classification (adapted from Davis and Hayes, 1984).....	32
Fig. 1.3 Tidal inlet morphological scheme (adapted from USACE, 2002).	34
Fig. 1.4 Three configuration of tidal inlets (adapted from Lynch-Blosse and Kumar, 1976).....	35
Fig. 1.5 Common ebb tidal delta morphology (adapted from Hayes, 1980).....	38
Fig. 1.6 Stability diagram of a tidal inlet (adapted from Escoffier, 1940).	40
Fig. 1.7 Mean wave height vs mean tidal range classification of four multi-tidal inlet systems addressed in this study (adapted from Davis and Hayes, 1984).	47
Fig. 1.8 Physiography of the Dutch Wadden Sea (adapted from Steijn, 1991).....	48
Fig. 1.9 Map showing the study area with inlets referred in text underlined (adapted from Davis and Barnard, 2000).....	51
Fig. 1.10 Detail map of Matagorda Bay and East Matagorda Bay (adapted from Kraus and Batten, 2008).....	54
Fig. 1.11 Map of Venice Lagoon. Four sub-embayments (A–D) are separated by broken lines (adapted by Sarretta <i>et al.</i> , 2010)	57
Fig. 2.1 Mean wave height vs mean tidal range classification for Ria Formosa (RF) and Marano and Grado Lagoon (MGL). Adapted from Davis and Hayes (1984).	62
Fig. 2.2 Ria Formosa multi inlet barrier island system (adapted from Popesso <i>et al.</i> , 2016).	63
Fig. 2.3 The Marano and Grado Lagoon (from Bezzi, 2013).....	70

Fig. 2.4 Wind data from the stations of Lignano and Fossalon, along the Marano and Grado Lagoon coastline..... 73

Fig. 3.1 Ancão Inlet migration patterns (adapted from Vila-Concejo *et al.*, 2002). 77

Fig. 3.2 Four stage conceptual model for the natural evolution of Ancão Inlet, after relocation (adapted from Vila-Concejo *et al.*, 2003)..... 78

Fig. 3.3 Example of bathymetric surface maps (May 2011), with the sketch of ten profiles (lines in black) to define the minimum cross sectional area and the points (red crosses) to compute the mean orientation between segments that covered the channel pathway.... 83

Fig. 3.4 Correlations and tendency lines for data coupling from different gauges. 85

Fig. 3.5 Topo-bathymetric maps corresponding to the three new surveys of April 2010 (A), May 2011 (LIDAR survey, B) and May 2015 (C). 89

Fig. 3.6 A) Minimum cross sectional area A_c , inlet width I_w and maximum depth $MaxD$ trends and B) migration tendency, for the last Ancão Inlet cycle. 91

Fig. 3.7 Cumulative migration (gray circles) compared with $Wp\#$ for three directions: $\leq 200^\circ$ (A), $200 < dir < 220^\circ$ (B), and $\geq 220^\circ$ (C). Updrift breaching (Ub) and downdrift breaching ($1Db$ and $2Db$) events are represented by triangles..... 94

Fig. 3.8 Cross-sectional area (A_c , gray circles) compared with the mean $P/\sum Wp\#$ ratio (horizontal lines) for four selected macro-intervals: a) unstable, due to morphological adaptation (which includes the phases described by Vila-Concejo *et al.*, 2003); b) equilibrium 1, while capturing prism and migrating; c) equilibrium 2, without capturing prism but with migration; and d) critical, toward closure/infilling. 95

Fig. 3.9 Migration trends of previous Ancão cycles (Vila-Concejo *et al.*, 2002, 2004) integrated with the last Ancão cycle data (1997–2015). Points represent inlet channel positions observed in aerial photographs or surveys. The dashed line represents the supposed continuity of the migration rate before the 2010 and 2015 jumps..... 96

Fig. 4.1 Detail of “Le Frioul” by Monsieur Blaeu, 1620, Amsterdam (copy from the original, Library I.G.M., Firenze)..... 106

Fig. 4.2 Profiles tracks from Sartori (1995, A) and from Segala (1999, B). Base: restitution from a 1990 orthophoto. 110

Fig. 4.3 Tracks followed during the 2002 survey (Cirilli, 2004)..... 111

Fig. 4.4 Topo-bathymetric tracks of the 2016 survey. Base: restitution from a 1990 orthophoto..... 112

Fig. 4.5 Ten profiles with equal intervals through the inlet cross-section in order to identify the A_c (example for the 2016 survey). 114

Fig. 4.6 Localization of DWRG1 wave-directional buoy offshore the MGL (www.protezionecivile.fvg.it)..... 116

Fig. 4.7 *DEM* for the 1994 survey (using the data collected by Sartori, 1995). Base: restitution from a 1990 orthophoto..... 117

Fig. 4.8 *DEM* for the 1999 survey (using the data collected by Segala, 1999). Base: restitution from a 1990 orthophoto..... 118

Fig. 4.9 *DEM* for the 2016 survey (using the data collected during July 2016). Base: restitution from a 1990 orthophoto..... 119

Fig. 4.10 Northern sector. P3 – P10 – P11: sections on Sartori (1995) tracks; M8 –M9 – M10: sections on Segala (1999) tracks..... 121

Fig. 4.11 Southern sector. P4 – P5 – P6: sections on Sartori (1995) tracks; M5 –M6 – M7: sections on Segala (1999) tracks. 123

Fig. 4.12 Residual map of the differences in volume of the main channel area for the period 1994 – 1999. Base: restitution from a 1990 orthophoto..... 125

Fig. 4.13 Residual map of the differences in volume of the main channel area for the period 1999 – 2016. Base: restitution from a 1990 orthophoto..... 126

Fig. 4.14 Residual map of the differences in volume of the main channel area for the entire period investigated: 1994 – 2016. Base: restitution from a 1990 orthophoto. ... 126

Fig. 4.15 Ebb tidal delta volume computation following the *ADP* procedure: polynomial surfaces of first (on the left) or second on the right) order were subtracting to the *DEM* of 2002 configuration, obtaining two different Residual Map (A and B). 129

Fig. 4.16 Ebb tidal delta volume computation following the *ADP* procedure: polynomial surfaces of first (on the left) or second order on the right) were subtracting to the *DEM* of 2016 configuration, obtaining two different Residual Map (A and B). 130

Fig. 4.17 Storm event directions distribution between 2004 and 2016. 131

Fig. 4.18 Main channel displacement trend during the last 20 years, differentiated in northern NS and southern SS sector. Base: restitution from a 1990 orthophoto..... 132

Fig. 5.1 Ebb-tidal delta development at untrained (A) and trained (B) inlets (adapted from Marino and Mehta, 1988). 140

Fig. 5.2 Ebb tidal delta morphology prior and after jetties extension (adapted from Tomlinson, 1991). 140

Fig. 5.3 Conceptual model of a stabilized ebb-dominated tidal inlet (adapted from Pope, 1991). A: collapse of ebb-tidal delta lobe. B: erosion of ebb-tidal delta platform..... 141

Fig. 5.4 Beach accretion at Punta Sabbioni beach after jettiy construction (adapted from Consorzio Venezia Nuova, 1989)..... 142

Fig. 5.5 Tubbs inlet evolution between 1959 and 1970. The + marks are in the same positions on all drawings (adapted from Masterson *et al.*, 1973)..... 145

Fig. 5.6 Historical changes in the position of Captain Sams Inlet between 1696 and 1979 (adapted from Hayes *et al.*, 1979). 146

Fig. 5.7 Conceptual scheme for Ancão Inlet situation. 149

Fig. 5.8 Conceptual scheme for S. Andrea Inlet situation. 151

Tables index

Table 1.1 Examples of empirical relationships and formulae where: A_c minimum cross sectional area, P spring tidal prism, V ebb tidal delta volume and Q longshore sediment transport, C and n free parameters.....	42
Table 2.1 Wave climate (Costa, 1994). H_s : mean significant height; T_p : mean peak period.	65
Table 2.2 Hydrographic data of the six tidal inlets of Marano and Grado Lagoon (adapted from Fontolan <i>et al.</i> , 2007a).....	71
Table 3.1 Three morphological states based on the three hydrodynamic regimes of Ancão Inlet (adapted from Williams <i>et al.</i> , 2003). H1 – non-storm conditions (A and L subscripts traduce mean Atlantic, W-SW and “ <i>Levante</i> ”, E-SE, wave approach, respectively), H2 – storm conditions for W-SW waves and H3 – storm conditions for E-SE waves.	80
Table 3.2 Topo-bathymetric and <i>LIDAR</i> surveys performed at Ancão Inlet during the investigated period.....	81
Table 3.3 Residual statistics using the cross-validation function for the different interpolators. With: Kr=Kriging Method, TWLI=Triangulation with Linear Interpolation Method, IDTAP=Inverse Distance to a Power Method, RBF=Radial Basis Function Method, MC=Minimum Curvature Method.....	82
Table 3.4 Data of minimum cross sectional area (A_c), tidal prism (P) computed according the empirical relationship by Jarrett (1976), inlet width (I_w), maximum inlet depth, measured on A_c ($MaxD$), thalweg orientation (O), migration (M) and cumulative migration (<i>cum M</i>). The – sign in M denotes a westward migration. The new surveys are highlighted in yellow.	91
Table 3.5 Mean and max values of H_s (significant wave height) and T_p (peak period), and percentages of waves occurrence from three directions ($\leq 200^\circ$, $200 < dir < 220$ and $\geq 220^\circ$), between August 1997 and May 2015.	93
Table 3.6 <i>Pearson Pe</i> and <i>Spearman Sp</i> correlation with the evidences of the couples that are statistically significant (red, $p < 0.1$). ΔA_c , ΔI_w , $\Delta MaxD$, ΔO , ΔM : variations of inlet	

parameters between two consecutive surveys; $\overline{Wp\#}$ ($\overline{Wpn\#}$) and $\Sigma Wp\#$ ($\Sigma Wpn\#$):
 mean and sum $Wp\#$ ($Wpn\#$) of the storms coming from three directions ($\leq 200^\circ$,
 $200^\circ < dir < 220^\circ$, $\geq 220^\circ$), respectively..... 98

Table 4.1 List of surveys used in this thesis for the investigated area. 108

Table 4.2 Evolution of $MaxD$ in depth (*vertical displ.*) and position (*horizontal displ.*),
 along the main-channel sections, during the investigated period. Negative and positive
 values mean, respectively, a westward or eastward movement (for horizontal displ.) or a
 deepening or infilling situation (for vertical displ.). 124

Table 4.3 Differences of volume (m^3) calculated by comparison of *DEMs* in the main
 channel area. 127

Table 4.4 Tidal prism computation for each year using the North Adriatic empirical
 relationship. 127

Table 4.5 Positive anomalies from the *ADP* deployment..... 128

Notation

ΔA_c	difference between cross-sectional area A_c measured in two consecutive surveys (m^2)
ΔI_w	difference between inlet width I_w measured in two consecutive surveys (m)
ΔM	difference between $MaxD$ position in two consecutive surveys (m)
$\Delta MaxD$	difference between maximum depth $MaxD$ measured in two consecutive surveys (m)
ΔO	difference between thalweg orientation O measured in two consecutive surveys ($^\circ$)
η_{dtr}	daily tidal range (m)
η^*_{dtr}	maximum tidal range (m)
$h\eta_{dtr}$	hourly water level (m)
$h\eta^*_{dtr}$	maximum water level reached during the period of time examined (since 1997) (m)
ξ	coefficient of equilibrium (dimensionless)
ADP	Semi-Automatic Detrending Procedure (Fontolan <i>et al.</i> , 2007a,b; Delli Quadri, 2007)
ρ	sea water density (assumed as $1,026 \text{ Kg/m}^3$)
A_c	minimum cross-sectional area of the inlet throat (m^2)
A_b	lagoon basin surface (m^2)
C_g	group velocity (m/s)
D_{max}	discharge at the inlet during spring tide conditions (m^3/s)
E_w	wave energy (J/m^2)

<i>g</i>	gravity acceleration (9.8 m/s ²)
<i>H_s</i>	Significant wave height (m)
<i>I_w</i>	inlet width at minimum cross-sectional area (m)
<i>K</i>	Keulegan coefficient (dimensionless)
<i>M</i>	migration (m)
<i>MaxD</i>	maximum depth at minimum cross-sectional area (m)
<i>Q_{mean}</i>	mean rate of longshore sediment transport at the inlet (m ³ /y)
<i>m.s.l.</i>	mean sea level (m)
<i>O</i>	channel orientation (°)
<i>P</i>	tidal prism (m ³)
<i>Pe</i>	Pearson correlation
<i>Q</i>	longshore sediment transport (m ³ /y)
<i>Sp</i>	Spearman correlation
<i>T_p</i>	wave peak period (s)
<i>U_e</i>	equilibrium velocity (m/s)
<i>U_m</i>	maximum cross-section averaged velocity (m/s)
<i>V</i>	sand volume of the ebb-tidal delta (m ³)
<i>W_p</i>	mean wave power calculated for a storm (W/m)
<i>W_{pn}</i>	mean normalized wave power calculated for a storm (W/m)
<i>W_{p#}</i>	mean wave power calculated for a storm, multiplied by its duration (W/m*s)
<i>W_{pn#}</i>	mean normalized wave power calculated for a storm, multiplied by its duration (W/m*s)

$\overline{Wp\#}$	mean $Wp\#$ of the storms occurred during two consecutive surveys (W/m*s)
$\overline{Wpn\#}$	mean $Wpn\#$ of the storms occurred during two consecutive surveys (W/m*s)
$\Sigma Wp\#$	sum of $Wp\#$ of the storms occurred during two consecutive surveys (W/m*s)
$\Sigma Wpn\#$	sum of $Wpn\#$ of the storms occurred during two consecutive surveys (W/m*s)

Introduction

During recent years, interest in lagoons has increased, especially from the point of view of their conservation. A lagoon is a complex environment because its history is closely related to the events that affect not only the coast, but also the hinterland. Any change in the sedimentation rate, sea level or any natural/anthropic intervention could cause an immediate response since the lagoon is a dynamic environment.

Lagoons occupy 13% of the world's coastlines and they vary in physical-geographic parameters, such as size and shape, the type of climate, freshwater input, type of exchange with the open sea and the human footprint that they have undergone (Barnes, 1980; Nixon, 1982). Lagoons are geologically young features (Martin and Dominguez, 1994) and they are most common on coastal plain coasts with a micro-meso tidal range and a wide continental shelf (Bird, 1994).

Lagoons are separated from the sea/ocean by barriers or barrier islands and the exchange of water occurs through one (single inlet system) or more (multi-inlet system) openings among the barriers, called tidal inlets (Isla, 1995), whose morphology is subject to the action of waves and tides. Only 3% of the world's coasts contain lagoon systems with three or more tidal inlets (Cleary and Pilkey, 1996). The ability to understand and predict the morphological behaviour of barrier island coasts, tidal inlets and basins, is an important issue in coastal zone management, which requires the accurate prediction of equilibrium morphologies. It is important to give decision-makers the ability to determine optimal management schemes, in order to maintain inlet efficiency and thus an overall persistence of the system. Studies on stability and persistence of a tidal inlet system are imperative to provide background knowledge to understand and predict the morphological changes of the system before any engineering solution can be applied (Tung *et al.*, 2009).

Based on the nature of the channel(s) that connect the basin with the ocean, Kjerfve (1986) classified coastal lagoons into three main groups: *choked*, *leaky* and *restricted* systems. *Choked* and *leaky* systems represent the end-members of the classification while the *restricted* lagoon takes an intermediate position between them. A *choked* lagoon presents a unique entrance connecting the basin to the ocean. It is characterized by a quite small ratio between minimum cross sectional area (A_c) and surface area of the basin (A_b); and it is overall dominated by hydrologic/riverine cycles. For this reason it has a limited

short-term marine variability, it is wind forced and experiences a long water residence time. *Choked* lagoons are frequently located on coasts with medium/high wave energy and low tidal range. Consequently, the tidal circulation is restricted close to the opening. Following the Kjerfve (1986) considerations, some examples of this type of lagoon are Coorong Lagoon (Australia), Lagoa dos Patos (Brazil) and Lake St. Lucia (South Africa). On the other side, *leaky* lagoons are effectively multi-inlet system. Rather than *choked* lagoons, *leaky* systems show wide tidal channels and a large A_c/A_b ratio and are marine-dominated, i.e. are located along coasts with variable tidal and wave characteristics. Accordingly, *leaky* lagoons exist along coasts with both high wave energy and tidal range or, vice versa, in the case of both low wave energy and tidal range. Kjerfve arranged in this category the Wadden Sea (Netherlands) and Mississippi Sound (Gulf of Mexico, USA) as examples of environments with both high or both low wave energy and tidal range, respectively. Tidal circulation patterns are usually well defined but are sometimes modified by wind forcing. Kjerfve (1986) continued reporting that a *leaky* lagoon can also present more than one type of barriers: sand islands (as in Mississippi Sound, Gulf of Mexico, USA), or reef of coral/sandstone origin (as in the case of the Great Barrier Reef in Australia and the coasts on north-eastern Brazil, respectively). *Restricted* lagoons have mixed characteristics between *choked* and *leaky* systems. They are usually connected with the ocean by two or more openings. In general, they are situated on low/medium wave energy coasts with a low tidal range. Kjerfve (1986) mentioned, as examples, Laguna de Términos, Mexico, Gulf of Mexico and Lake Pontchartrain, in Louisiana, USA. The lagoons examined in this thesis, Ria Formosa (Portugal) and Marano and Grado Lagoon (Italy), can both be placed in the *restricted* lagoon classification. The first environment has a large tidal range and wave energy while the second one presents lower tidal range and wave energy. Both lagoons show a quite large number of tidal inlets but their dimensions are not as large as in a *leaky* lagoon-type (e.g. tidal inlets in Wadden Sea).

The openings that permit the exchange of water between lagoon environment and ocean/sea, namely the tidal inlets, are essential elements in the barrier-lagoon system. They provide sediment sources for adjacent beaches, and are conduits that allow exchange of nutrients between backbarrier systems and the coastal zone (FitzGerald, 1996). They play also an important role in navigation, often representing the only access to some

harbours or coastal populations. For this reason, many studies have been focused on inlet evolution and behaviour (i.e., Hicks and Hume, 1997; Ranasinghe *et al.*, 1998; Stauble, 1998; Williams *et al.*, 1998; Marden and Cleary, 1999; Johnsen *et al.*, 1999; Morang, 1999; Ranasinghe and Pattiaratchi, 1999; FitzGerald *et al.*, 2001; Williams *et al.*, 2003). These studies derive from a need to improve the knowledge on these environments, and are useful in planning effective coastal management (i.e., Kana and Mason, 1988; Cialone *et al.*, 1999; Forbes and Solomon, 1999; Galgano and Leatherman, 1999), since a great number of inlets have direct and indirect impacts on human economy (navigation, aquaculture, etc.). Hard structures are the traditional engineering responses to tidal inlet coastal hazards. Inlet stabilisation using jetties is intensively used (e.g. Venice Lagoon, Consorzio Venezia Nuova, 1989), to make navigation safer and channel maintenance cheaper. The effects of inlet stabilization, however, may be also modify the shape and seaward extent of the ebb-tidal delta (Pope, 1991), by interrupting the longshore sediment transport. Long jetties extending thousands of metres into the sea may trap and retain millions of cubic metres of sand on the updrift side (i.e., Penland, 1979; Pilkey and Neal, 1980; C.E.R.C., 1984). Furthermore, jetties can cause a great improve of the efficiency of the inlet, often assimilating the tidal prism of nearby tidal inlets related to the same multi-inlet system (e.g. Faro-Olhão Inlet, Esaguy, 1984). Only recently, the coastal managers began to use a particular soft protection engineering technique that, when applied to migrating inlets, involves the artificial opening of a new tidal inlet along the historic migration path of the inlet. A principal example will be given in the next chapters.

Many coastal regions are affected by strong longshore sediment transport. This can cause an accumulation of sand on the updrift side and on the ebb-tidal delta of a tidal inlet, resulting in a modification of the thalweg (Bruun and Gerritsen, 1959), which affects the normal tidal flow and reduces its efficiency. Since the sediment carried by the currents can accumulate on the updrift side of an inlet, in some cases, the opposite side can be eroded, thus causing migration (Johnson, 1919). The rate of migration depends on various factors. First of all, the contribution of sediments; secondly, the wave energy, tidal currents and the size of the main channel (Vila-Concejo *et al.*, 2002; Popesso *et al.*, 2016). Where inlet migration represents a risk for the population or a factor that can affect the navigability or the regular passage of water and nutrients, coastal managers acted using different methods. Inlet stabilization with jetties is common solution but, as before

mentioned, can cause some unexpected problems. Inlet relocation, instead, is a soft protection management tool that permits the defence of the coastal zone without implying a large environmental impact. The concept of this approach is to work with natural processes, rather than confronting nature. It simply reproduces, when done correctly, the natural evolution of a migrating inlet and consists on relocating the opening along its historical path, leaving the old inlet open, waiting for the capture of its prism by the new inlet, or closing it artificially. Kana (2003) reports that another benefit of inlet relocation is the release of sediment from the abandoned inlet, especially for the sediment accumulated in the ebb tidal delta that can move onshore and naturally nourish the downdrift beach. According to Vila-Concejo (2003), once the inlet is relocated, the degree of success depends on: (1) the hydrodynamic efficiency of the new inlet to remain open and (2) that the new inlet is not causing the same problems as the old one. However, this practice is not widely used. Relocation, as soft protection, is not a 'permanent' solution. After some time (typically decades), the inlet will likely reach the same starting position and cause the same problems as before the relocation. For this reason, it is necessary to program a new intervention. Only few examples of inlet relocation are reported in literature. The oldest record of this kind of intervention is the relocation of Tubbs Inlet (North Carolina, USA). During XX century, the inlet migrated westward by 2.0 km (Marden and Cleary, 1999). In order to mitigate the rapid erosion of the downdrift littoral, the inlet was artificially relocated in December 1969 to a position 1.0 km eastward that approximated its position in 1938 (Masterson *et al.*, 1973). After a period of adjustment to the new hydrodynamic conditions, Tubbs Inlet reversed its migration direction and started drifting eastward, although the longshore sediment drift comes from the other direction (Marden and Cleary, 1999). According to Budde & Cleary (2006), this reversal was due to the alteration of the backbarrier channels carried out in those years. No other relocation episode of Tubbs inlet is known since that time onwards. The relocation of Captain Sam's Inlet (South Carolina, USA) is one of the best-known cases. According to many authors (e.g., Mason, 1986; Kana and Mason, 1988; Kana and McKee, 2003), Captain Sam's is a small mesotidal inlet that was relocated in February 1983 because its migration and realignment of the channel was threatening for the coastal population. The relocation was successful but the inlet started soon to migrate again and, by 1995, it reached the position where it was before the relocation (CSE, 1995). Therefore, another

relocation was programmed and undertaken in April 1996 (CSE, 2001). Kana & McKee (2003) give an exhaustive description of the relocation procedures.

At the end of the 1990s, two inlets, Ancão and Fuzeta, were relocated in the Ria Formosa Lagoon (Southern Portugal), in 1997 and 1999, respectively. The aim was to enhance circulation of water and nutrients in the backbarrier zone. Both inlets, after a brief period of adjustment, started again to migrate eastward. In November 2015, a new relocation was carried out for Ancão Inlet. This and subsequent developments are reported in Chapter 3 of this thesis. In March 2002, Mason Inlet (North Carolina, USA) was relocated as it was threatening a coastal population (Broders, 2002; Cleary, 2002; Erickson *et al.*, 2003). Property owners paid for this intervention and agreed also on a 30-year maintenance dredging commitment, which enables them to re-dredge the inlet up to 9 times in the next 30 years if the inlet begins to move outside a defined corridor (Broders, 2002). The new inlet position remained stable for the first year after relocation, but then it started infilling (Erickson *et al.*, 2003). According to Cleary and FitzGerald (2003), this sediment comes from the former ebb-tidal delta and, once dismantled, the downdrift side of the relocated opening started to erode. In literature some other inlet relocations were proposed as, for example, the case of Fire Island Inlet (New York, USA). It still remaining only a project.

Many authors (Brouwer, 2013; Brouwer *et al.*, 2008, 2012, 2013; van de Kreeke *et al.*, 2008; deSwart and Volp, 2012; Roos *et al.*, 2013), affirm that the equilibrium of multiple-inlet systems depends on the degree of connectivity between the inlet basins. Changes in one of the interconnected inlets or associated basins can generate further modifications due to the natural tendency of the system to reach a new equilibrium. Wetland reclamation for urban and agricultural purposes (e.g. Marano and Grado Lagoon, Gatto and Marocco, 1992), storm surge protection (Wadden Sea, Eelkema *et al.*, 2013), drainage of channels (e.g. Matagorda Bay, Kraus and Batten, 2008), inlet stabilization (e.g. Ria Formosa Lagoon, Vila-Concejo *et al.*, 2002) or strong natural events (e.g. western-central Florida barrier-inlet system, Davis and Barnard, 2000) can cause natural adjustments of the interconnected inlets. Depending on the size of the basins, these can lead to an increase or decrease in tidal prism and a corresponding change in inlet current velocity, until possible “atrophy” and closure of one of the openings.

Worldwide, the cases of reduction of tidal prism and size of tidal inlet due to intervention in the related basin are numerous. One of the earliest and impressive examples reported was the case of Faro-Olhão inlet, in Ria Formosa Lagoon (southern Portugal), in the first half of XX century. The inlet was dredged and fixed by two long jetties in an area where another (sediment *choked* and very shallow) inlet existed before (the “Bispo” inlet). The jetties were projected to protect the access channel from the prevailing eastward longshore sediment drift and to assure a proper depth in the access to the navigation channel, leading to mainland (Esaguy, 1986b). This intervention led to important effects on the littoral of Ria Formosa, as well as on the hydrodynamic behavior of the lagoon (Andrade, 1990). According to Salles (2001), the major effect was the drastic reduction of the downdrift sediment contribution, making the nearby (eastern) barrier island more vulnerable to erosion. Furthermore, the width of Armona Inlet (situated E of Faro-Olhão Inlet) started to decrease at very high rates (from almost 4 km to few hundred meters), losing some of its hydrodynamic efficiency (Andrade, 1990; Vila-Concejo *et al.*, 2002). Another example is Pass Cavallo Inlet, in Matagorda Bay (Texas, USA). It was historically stable until the 20th century but the deltaic progradation of Colorado River Delta caused an initial tidal prism decrease, leading to shoaling and increase navigation problems (Harwood, 1973). For this reason, between 1963-1966, the U.S. Army Corps of Engineers (USACE) decided to dredge the Matagorda Ship Channel (MSC), an artificial and jettied channel close to Pass Cavallo Inlet, creating a more efficient tidal channel, which was planned to connect with the deeper and more central portion of the bay. This intervention caused a degeneration of the hydrodynamic efficiency of Pass Cavallo Inlet, with an abrupt decrease of the tidal prism and subsequent decrease of the inlet width (by 2.76 km, Batten *et al.*, 2007).

More or less in the same period, occurred the stabilization of Buso Inlet (1964–1969) in the Marano and Grado Lagoon (MGL, Italy) through jetties and dredging of a more straight connection with the mainland to provide greater draft for navigation (Brambati, 1987; 1996; Ferla *et al.*, 2012). This intervention was responsible for a strong reduction of the nearby S. Andrea and Morgo tidal prisms and the enlargement from 27% to 35% of the tidal prism of the Buso Inlet (Ferla *et al.*, 2012). In addition, other inlet basins were affected by this important change. The tidal prism of Lignano, the westernmost inlet of the MGL, reduced from 44% to 35% of the total lagoon prism. In 1969, a part of Dutch

Wadden Sea (Lauwers Sea) was closed. This fact determined a reduction of the closest tidal inlet basin (Frisian Inlet) by approximately 30%. This led to a decrease in inlet channel velocities and tidal prism and a gradual decrease of the channel cross-sectional area (van de Kreeke, 2004). More recently, in the early 1980s, natural and anthropogenic changes to the Sarasota Bay multi tidal inlet system (Eastern-central Florida) affected the distribution of tidal prism shared by its six openings. According to Dabees and Moore (2011), at that time, the most efficient inlet was Big Sarasota Pass that exchanged about 40% of the total amount of tidal prism while one of the smallest was Midnight Pass. The modification led Midnight Pass to initially migrate northward and later to approach closure in 1983; accordingly, the tidal prism of the other inlets of the system slightly decreased (Davis *et al.*, 1987; Dabees and Moore, 2011).

Aim of this study

There exists a delicate balance within the competence of each inlet in terms of tidal prism (Pacheco *et al.*, 2010) in such a way that natural or man-made modifications could induce hydrodynamic and morphodynamic changes at a larger scale in some part of a multi-inlet system. The migration or atrophy of unconstrained inlets can be both causes and consequences of these changes and need an adequate and careful management plan to permit safe navigation and regular water exchange.

The main aim of this thesis is to study the behaviour and the evolution of two unconstrained inlets, located in dissimilar natural and human affected environments. Ancão Inlet in the Ria Formosa Lagoon (Portugal) and S. Andrea Inlet, in the Marano and Grado Lagoon (Italy). This work aims to understand the conflicts associated with the unconstrained behaviour of the inlets in relation to human needs and uses.

The thesis is structured according to the following outline; the methods, discussions and results of each case study (Ancão or S. Andrea Inlets) are described in separate chapters.

The main part of the first study area (Ancão Inlet) was presented at an international conference and the paper was published in the proceedings of the conference, as the Special Issue of a peer-review journal (Proceedings of the 14th International Coastal Symposium, Sydney, Australia. Journal of Coastal Research, Special Issue, No. 75, pp. 233-237). The paper is attached in the *Appendix* section.

Outline

Studies were undertaken on the relocated Ancão Inlet, the westernmost inlet of the Ria Formosa barrier island system (Southern Portugal) and on S. Andrea Inlet, a natural inlet in the Marano and Grado Lagoon (North Adriatic, Italy). To achieve the above-mentioned objectives, this thesis is structured as follows:

- Chapter 1 is dedicated to a general review of tidal inlet dynamics. A brief review of the main studies on tidal inlet stability criteria is presented as are some examples that illustrate human interventions responsible for disrupting the natural equilibrium of multi tidal inlet systems;
- In Chapter 2 the two different lagoons are briefly introduced. The main differences between these environments and the associated human context are shown;
- The first case study (Ancão Inlet) is presented in Chapter 3. A brief overview of the main characteristics of this relocated inlet is given. The methodology followed and the results of the studies are illustrated in the same chapter;
- The second case study, S. Andrea Inlet, is introduced in Chapter 4. The methodology used both for acquiring the data and for analysing them is also explained and the results are discussed;
- Some management interventions are suggested in Chapter 5, as well as a short description of past management activities on tidal inlets worldwide;
- A final and concepts-summarizing chapter is given in the end (Chapter 6).

1.

***Review on stability of multiple inlet systems:
coastal management interventions responsible
for disrupting natural equilibriums***

A general review of tidal inlet morphodynamics and stability criteria applied over them and over (multi) tidal inlet systems is presented in this chapter. Due to their environmental and economic importance, tidal inlets and the associated barrier/lagoon systems have been the object of many investigations for many years all around the world. The chapter concludes with some examples of disruption of the natural environment-equilibrium of multi tidal-inlet systems around the world .

FitzGerald (1996) defines tidal inlets as openings that interrupt the regular continuation of the shoreline, through which water penetrates the land and provides a connection between the ocean and bays, lagoons or marsh and tidal creek systems. Escoffier (1940) affirmed that the main channel of a tidal inlet is maintained by tidal currents. According to FitzGerald (1996), the second part of this definition distinguishes tidal inlets from open embayments or rock-bound passage-ways where there is little or no mobile sediment. However, according to the same author, one side of the inlet may consist of bedrock. Tidal inlets are complex regions whose morphology perpetually changes, due to the combination of wave and tidal forces acting on the nearshore sediments (Huntley and Nummedal, 1978). Isla (1995) highlighted that tidal inlets are also relevant in the behaviour of coastal lagoons, since they condition sediment, salinity, nutrients, pollutant and organism dispersal between the lagoon and the ocean, i.e. the very existence of the lagoon.

Davies (1964) recognized the importance of the tidal amplitude in shaping the world's coastlines, classifying them as: microtidal when the tidal range is less than 2 m, mesotidal when the range is between 2 and 4 m, macrotidal if it exceeds 4 m. Based on this classification, Hayes *et al.* (1973) and Hayes (1975; 1979) described the configuration of barrier-lagoon coasts associating to the tidal regime and secondarily wave processes (Fig. 1.1):

- *Microtidal coasts* are characterized by long, narrow, and rectilinear barrier islands, interrupted by few wide mouths. The washover structures are pronounced, the flood-tidal delta is usually well developed, while the ebb-tidal delta is small or absent (Hayes 1975; 1979);

- *Mesotidal coasts* have short and large barrier islands, jagged, and frequently interrupted by several not very large mouths; they have a configuration similar to a drumstick (Hayes, 1975; 1979). The ebb-tidal deltas are well developed due to the strong tidal currents and wave effects that shape those morphologies;
- *Macrotidal coasts* do not develop barriers and inlets because of the strong tidal currents; instead, it is possible to see inlets/estuaries in the shape of funnel, containing linear sand bodies parallel to the main tidal flow (Hayes, 1975; 1979).

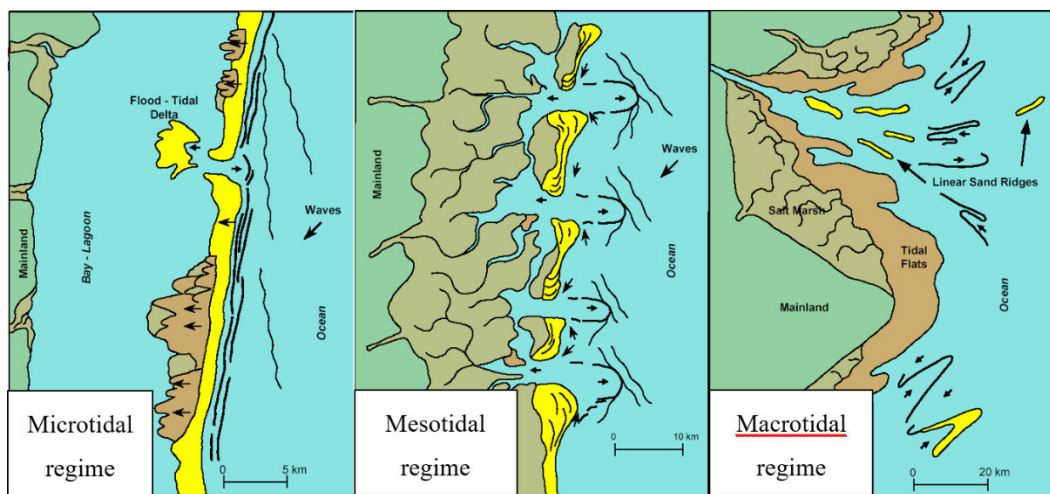


Fig. 1.1 Morphological model of a typical Microtidal, Mesotidal and Macrotidal coastal regime (adapted from Hayes, 1979)

After further studies, Hayes (1979) concluded that there is a close relationship between tide amplitude and waves. According to Davis and Hayes (1984), the above-mentioned classification uses tidal ranges that tend to develop similar morphologies through a spectrum of wave climates. Hence, the classification is generally restricted to coastal areas with moderate wave energy. Hayes (1979) proposed another classification for coastal barrier islands based on the interaction between tidal range and wave energy action, which was subsequently improved by Davis and Hayes (1984, Fig. 1.2).

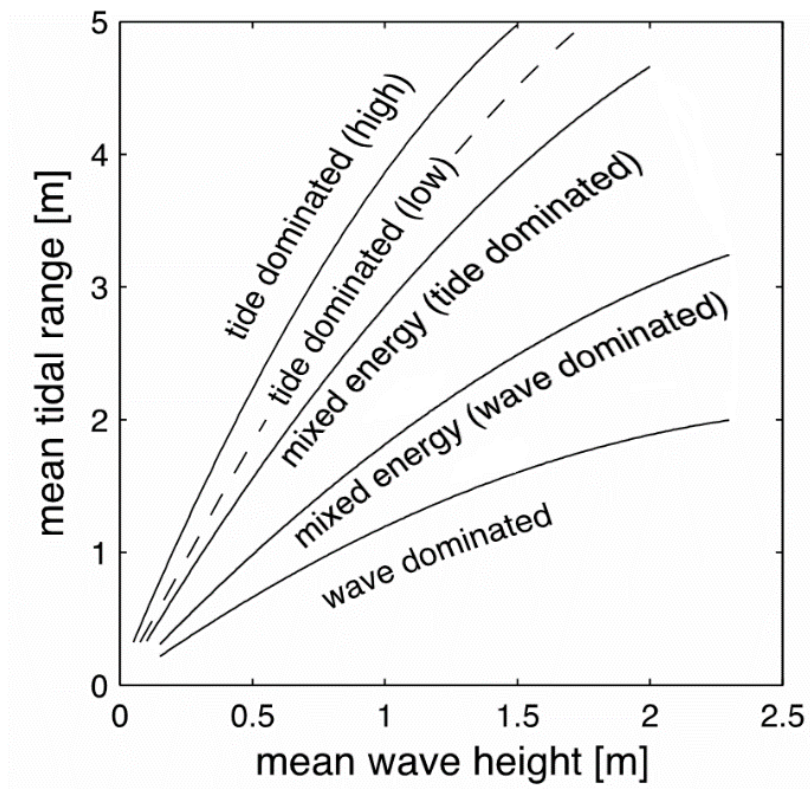


Fig. 1.2 Mean wave height vs mean tidal range classification (adapted from Davis and Hayes, 1984).

Hubbard (1977) and Nummedal *et al.* (1977) applied these concepts directly to tidal inlets. They concluded that within the microtidal and mesotidal ranges, a spectrum of inlet configurations exists, primarily as a response to the dominance of either tidal or wave forces. On the basis of their general morphology and of sedimentary structures distribution in the proximity of the channel, Hubbard *et al.* (1979) described inlets from the Atlantic Coast of USA which are exposed to different wave energy regimes and tidal currents. The description can be generalized to different contexts and involves the following classification:

- *tide-dominated inlets*: the inlet and its evolution is dominated by the action of the tides, where it can be observed high dimension bed-forms, such as bars and subaqueous dunes, combined with the higher velocities of the axial jet. They are also characterized by the presence of a main ebb channel rather broad and deep, stable and symmetric (Davis and Gibeaut, 1990), flanked by channel margin long and linear bars; the ebb-tidal delta is

always present and well defined, since the ebb currents are extremely strong; on the contrary, the flood-tidal delta is small in size or even absent;

- *wave-dominated inlets*: the inlet and its evolution is dominated by the action of waves. On those coastlines, wave action causes significant sediment transport and prevails over the effect of the tide. In this case, the majority of the sediment is pushed through the opening or is bypassed around the inlet. The flood-delta is normally well defined because of the strong wave energy, and it is lobed. The channels are dominated by the flood currents and the inlets are shallow and present an asymmetric section, basically prone to rapid migration or closure if not artificially stabilized (Davis and Gibeaut, 1990);
- *transitional inlets*: this group is more complex due to the variety of factors involved. Their evolution is determined by the balance between the tidal and wave currents. The morphologies are dependent on the current (tidal or wave current) acting at a particular moment (tidal or wave current). The sand bodies vary widely in morphology and geometry; they are concentrated into the throat of the channel, which is dominated by the ebb currents (Davis and Gibeaut, 1990).

The length of islands along a barrier system can be correlated to tidal range and wave energy (Hayes, 1979) because these factors and others, particularly backbarrier area, control the size and number of tidal inlets (FitzGerald, 1988). Following Salles (2001), the typical shape and morphologic evolution of a general multi-tidal inlet system results from (1) the geological origin and evolution of the system, and its response to relative sea-level rise (time scale of thousands of years), (2) the exposure to different wave and current conditions on either side of the system (scale of years), and (3) the effects of storms (scale of weeks).

1.1 Tidal inlets morphology

A tidal inlet contains three main morphological features: i) the mouth (*throat*) typically characterized by the minimum cross section area (A_c), ii) the area with the greatest depth (*gorge*), and, iii) the *channel*, the main scouring pathway (Hayes, 1969, 1979; Oertel, 1988) (Fig. 1.3).

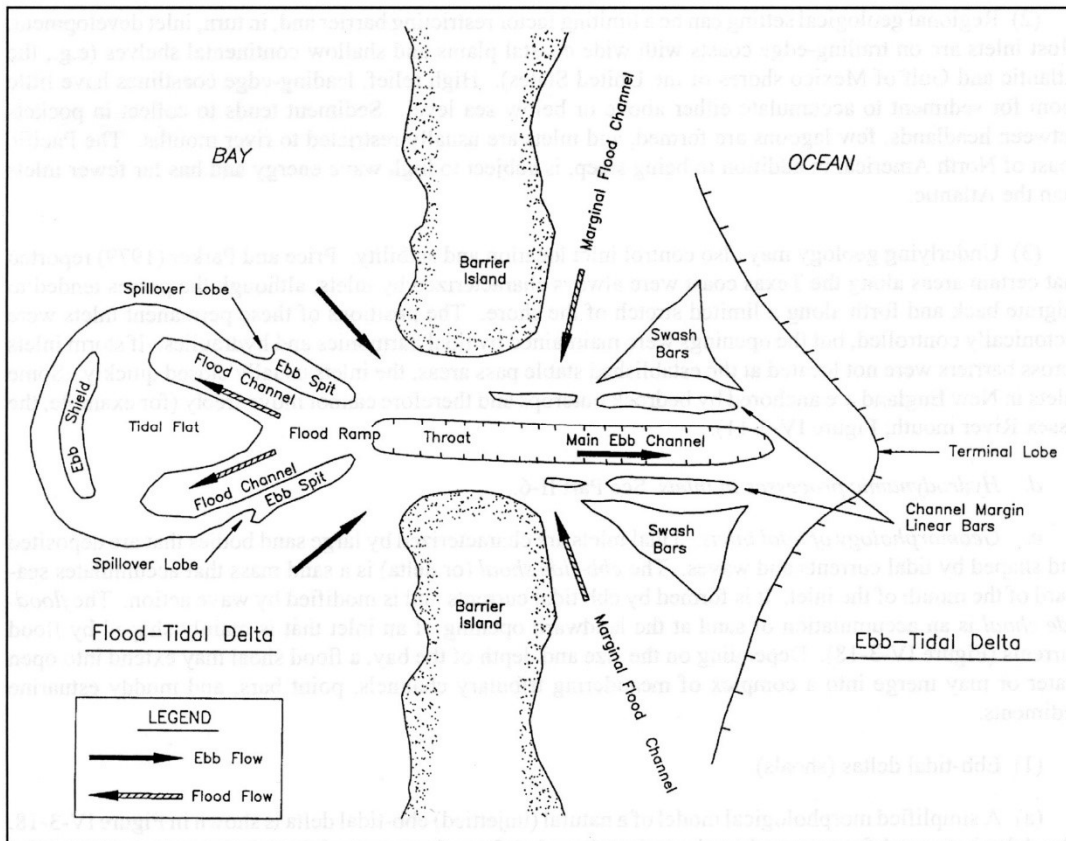


Fig. 1.3 Tidal inlet morphological scheme (adapted from USACE, 2002).

The number and size of tidal inlets is highly dependent on both the lagoon basin surface (Ab) and the tidal range. O'Brien (1931), following Le Conte's (1905) first hypothesis, observed that the inlet-throat width is related to the spring tidal prism (P), the exposure to wave energy and bottom material characteristics.

Tidal inlets can assume different planimetric arrangements in response to the mutual interference between longshore flow and tidal currents (Lynch-Blosse and Kumar, 1976, Fig. 1.4):

- *straight*: it develops when the erosion by wave activity is perfectly compensated by the contribution of sediments from longshore currents. Updrift and downdrift shorelines are located along the same straight line as the downdrift one. With this configuration, it is not easy to infer on the direction of net drift;
- *updrift-offset*: it occurs in the case where there is a surplus of sediment accumulated on the updrift side of the inlet, which is more enriched in sediment

than the downdrift section, resulting in seaward advancement of the shoreline updrift of the inlet and overlapping of barrier tips;

- *downdrift- offset*: it is the opposite situation i.e. the downdrift area is in a more advanced position in the sea because of the interaction between tidal and longshore currents leads to sediment accumulation downdrift of the inlet. These more complex tidal inlets are characterized by an updrift side with a pointed shape and a wider downdrift area. The interaction between longshore and tidal currents creates a limited portion along the shore where the residual direction of longshore flow is opposite to that of the regional longshore current.

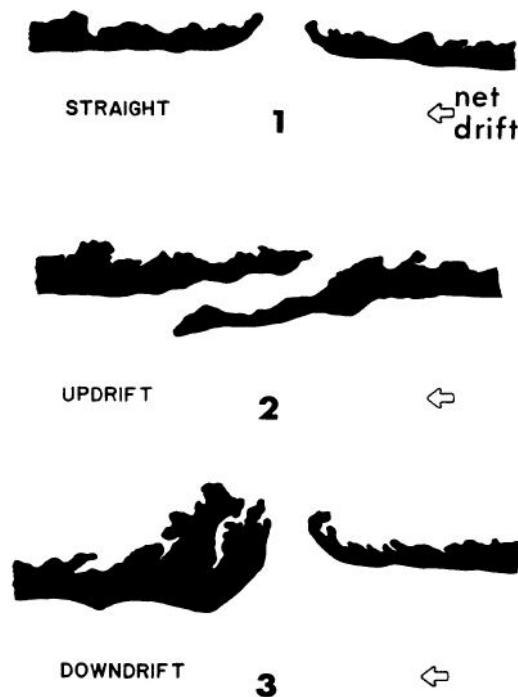


Fig. 1.4 Three configuration of tidal inlets (adapted from Lynch-Blosse and Kumar, 1976).

1.1.1 Tidal deltas

Tidal range and wave height variation have important effects on the processes that act on tidal inlets and their morphology. These two factors control the distribution of sand bodies both landward and seaward. The most impressive morphologies are the tidal deltas. Tidal deltas are depositional forms with a fan-shape that originates from sediment deposition

due to the decrease of the velocity of the wave, tide and current induced transport passing through the tidal inlet.

Tidal deltas can be classified into two types, according to the dominance of the ebb or flood currents, thus giving rise to a different organization of the related morphologies (Hayes, 1969; Hubbard, 1977) (Fig. 1.3):

- *Flood deltas sediment reservoirs*, located landward close to the throat and inside the lagoon basin. These morphologic features are formed by the dissipation of the flood-tide currents and, especially, by the wave action that pushes the sediment inside the lagoon, contributing to the delta growth;
- *Ebb deltas sediment reservoirs*, located seaward at the immediate end of the throat. These morphologic features are developed as a result of ebb-tidal currents decrease due to the spreading of the axial jet seaward. In environments dominated by waves, the ebb-tidal delta development is hampered.

Usually flood deltas are poorly developed or even absent in mesotidal and high mesotidal, tide-dominated inlets because of the combined action of a clear dominance of the outgoing currents (ebb) with a prevalence of the tide effects at the throat due to a high tidal range and low wave height (Hubbard, 1977). Many authors studied the different types and shapes of flood deltas and their bottom forms (e.g. Hayes, 1969; Boothroyd and Hubbard, 1975; Hine, 1975). According to the descriptive model of Hayes and Kana (1976), the flood delta body consists of several structures (Fig. 1.3):

- *flood ramp*: a ramp located inside the lagoon at the end of the main channel with inclination towards the sea. The morphology is characterized by a weak slope and by the presence of subaqueous dunes (sand waves) oriented according to the incoming current flow. The ramp undergoes the highest action of the current because in this section the flow velocity, during flood, reaches the maximum values;
- *flood channels*: channels along which the entering current conveys into the lagoon. Once the ramp is exceeded, channels fork and end on the deposition plain of the flood delta (tidal flat);

- *ebb shield*: an elevation placed in the flood delta terminal border. It acts as a screen against possible changes by outgoing flow;
- *ebb spits*: sand bodies accumulated on the sides of the delta formed by the outgoing flow;
- *spillover lobes*: lobed structures (Ball *et al.*, 1967) created by ebb currents that reshape the sediments placed on the outer edge of the delta.

The main forms of the bottom are marked by the rising tide, while smaller forms, like ripples and megaripples, vary in orientation following the alternation of the two tidal flows (i.e. ebb and flood flows).

Ebb-tidal delta structure and size are functions of tidal prism and exposure to wave energy (Walton and Adams, 1976; Nummedal *et al.*, 1977; Hayes, 1994). The size of the ebb-tidal delta also depends on the "age" parameter: a newly formed inlet can take time to develop an ebb delta while an older inlet should have a larger delta that has reached a balance between hydrodynamics and morphological structure (FitzGerald, 1984). Walton and Adams (1976) were the first to propose an empirical relationship between the size of the ebb delta and the tidal prism relative to a given inlet:

$$V = 6.56 * 10^{-3} * P^{1.23} \quad (\text{Eq. 1.1})$$

where V is the volume of the ebb-tidal delta and P the volume of the spring tidal prism (both expressed in m^3).

Following the same authors, the formula could be expressed with different proportionality factors because, for the same tidal prism, the delta volume tends to be smaller or bigger according to the degree of exposure to wave energy.

The typical structures of an ebb-tidal delta system are reported by Hayes and Kana (1976) and are represented on Fig. 1.3 and Fig. 1.5:

- *main channel*: the ebb water masses move through it. Continuing from the inlet towards the sea, the water flow tends to spread. When the main channel is developed, it extends toward the sea and stops the currents parallel to the shore (Sha, 1989). The boundaries of the main channel to the open sea lie in a sandy plain;

- *swash platform*: a sandy area flanking the edges of the main channel where sediments are deposited and then reworked by the waves;
- *swash bars*: structures formed due to waves (King, 1972) consisting of sediments that are deposited in the terminal part of the swash platform and across this platform by the ebb tidal currents and especially by the action of breaking and broken waves ;
- *terminal lobe*: structures formed due to waves (King, 1972) consisting of sediments that are deposited in the terminal part of the swash platform by the ebb tidal currents;
- *channel margin linear bars*: elongated sand deposits that develop on one or both sides of the main channel. These morphologies are formed by the encounter between currents with different direction i.e. both the flood and ebb tidal currents prevent the transit of the longshore sedimentary load, perpendicular to the channel, thus enhancing sedimentation;
- *marginal flood channels*: located at the boundaries of the inlet, close the barrier islands that surround it. These channels are the water path for flood currents, especially active during the phase delay occurring during the tidal inversion from ebb to flood.

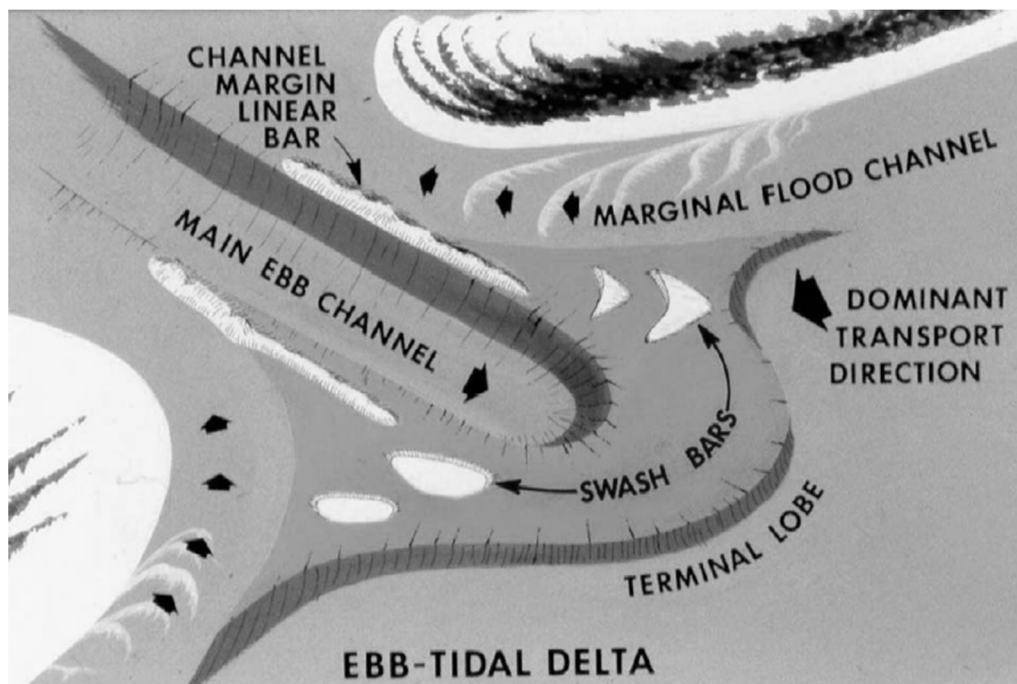


Fig. 1.5 Common ebb tidal delta morphology (adapted from Hayes, 1980).

A change in the ebb tidal-delta shape or size could result in significant variations on the coastline adjacent to the inlet (FitzGerald *et al.*, 1978; FitzGerald, 1988).

1.1.2 By-pass processes

The by-pass of sediment at the inlet is the process by which sediments move from the updrift to the downdrift side, involving both the inlet channel and the ebb delta (FitzGerald *et al.*, 2001).

The perpendicular movement of the water-jet (associated with tidal flow) present at the tidal inlet performs two different functions: first, it interrupts the longshore transport; and second it captures part of the material transported along the shore, which can then be redistributed inside the lagoon or in front of the inlet, generating depositional bodies like the ebb- or the flood-tidal deltas. Only a part of the sediment is captured by the inlet while the remaining volume by-passes the inlet to the downdrift side.

Bruun and Gerritsen (1959) first described the by-pass mechanisms of sediments using the following ratio:

$$r = Q_{mean} / D_{max} \quad (\text{Eq. 1.2})$$

where Q_{mean} indicates the mean rate of longshore sediment transport at the inlet (in m^3/y) and D_{max} is the discharge at the inlet during spring tide conditions (expressed in m^3/s). Those authors defined three processes by which the sand is able to "by-pass" the inlet:

- transport induced by waves along the boundary of the ebb-delta;
- transport by tidal currents along the channels;
- migration and accretion of tidal channels and sand bars.

Inlets with high r ratio ($r=200-300$) by-pass the sands according to the first mode and do not manage to extract sediment from longshore current. This permits a good supply to the downdrift sector. Conversely, inlets with a low ratio ($r=10-20$) are those by-passing the sediment following the last two modes. These inlets manage to intercept much of the sediment carried by longshore currents so the accretion of the downdrift sector is weak since sediment does not by-pass the inlet.

FitzGerald *et al.* (2001), added to the previous works of Bruun and Gerritsen (1959) and Bruun (1966), and improved the studies on inlet by-passing, proposing nine conceptual models summarizing the mechanisms of sediment bypassing along microtidal and mesotidal coasts. They include many processes either natural (e.g. inlet migration, spit or ebb-tidal delta breaching) or human-induced (e.g. due to jetty construction).

1.2 Stability criteria

Empirical equilibrium-state relationships are used to study the stability of both single and multiple inlet systems. These models describe the most relevant physical processes acting on tidal inlets. Regarding single inlet systems, the first analytical approach for inlet stability analysis was developed by Escoffier (1940) that followed a method previously derived by Brown (1928, in O'Brien, 1969). Escoffier (1940) proposed a diagram of the closure curve, which is defined by the inlet channel cross-sectional flow area (A_c) on the abscissa, and by the maximum cross-section averaged velocity on the ordinate (U_m), the latter assumed to be a measure of the sediment transport capacity of inlets currents (Fig. 1.6). The straight line represents the equilibrium velocity curve (U_e).

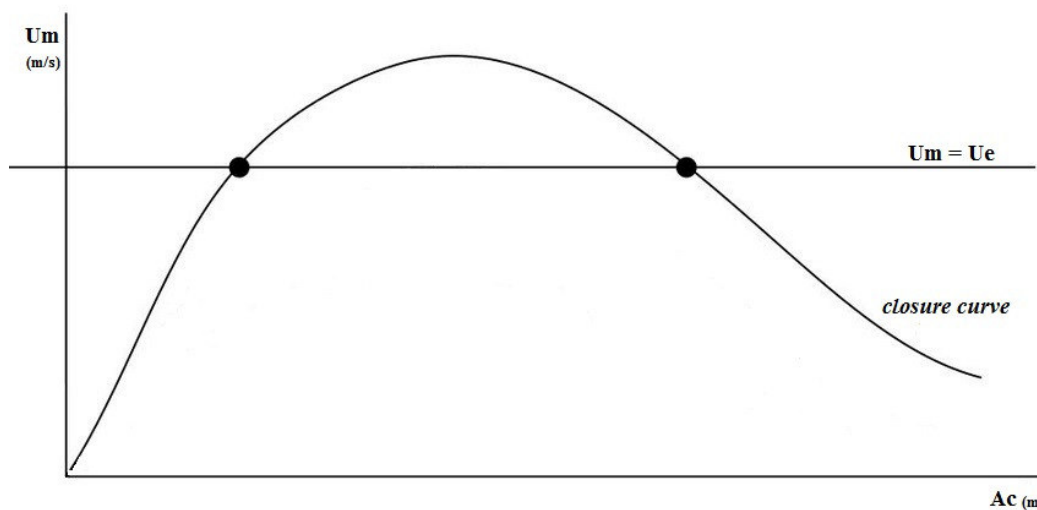


Fig. 1.6 Stability diagram of a tidal inlet (adapted from Escoffier, 1940).

When U_m equals U_e , the sediment transport capacity of the inlet currents is just sufficient to remove the sediment deposited at the inlet. This approach is still widely used in inlet stability evaluation and in engineering design projects. Early studies focused on how to

determine Um in the channel cross section due to the ocean tide and tidal elevation change in the bay. Keulegan (1967) analytically solved the one-dimensional, depth-averaged shallow water equation for flow, considering a simplified model of an inlet. Later he tried to apply his findings to irregular channels; however, his simplifications were only possible when applied to wide channels, where the average depth of a cross-section can be taken as equal to the hydraulic radius of the section. Furthermore, Keulegan (1967) and later O'Brien (1969) reviewed the Brown's (1928 in Keulegan, 1967) work presenting strong arguments against Brown's approach, essentially because of oversimplified hydraulic and geometrical assumptions, and proposing a new analytical solution. The effect of inertia was added by King (1974) to Keulegan's equations. However both Keulegan's and King's assumptions of prismatic channels greatly simplify prototype conditions, because natural inlets have complex morphologies, making accurate determination of several parameters (e.g. cross-section, hydraulic radius, bay surface area) a difficult task (Seabergh, 2002).

Another well-known empirical stability approach uses the spring tidal prism (P) as a fundamental parameter to investigate the stability of an inlet (Table 1.1). According to these formulas, the coupling between P and parameters like cross sectional area (Ac), ebb tidal delta volume (V), and longshore sediment transport (Q) can be used as a stability criteria. However, significant data scatter exists which results in only but rough estimates of the equilibrium conditions. Also, the O'Brien type of formula does not make distinction between flood versus ebb and spring versus neap-tides tidal prisms, which can vary significantly especially on multi-inlet systems where inlets can exhibit significant differences between inflow/ and outflow volumes, due to the existence of large residual flow between hydrodynamic connected inlets (Salles, 2001; Pacheco *et al.*, 2010; Brouwer, 2013); Bruun's P/Q ratio depends on the computation of Q which has a high degree of uncertainty; and Walton and Adams' (1976) relationship does not account for the natural volumetric variability in the ebb-tidal deltas, caused by many secondary external controls such as sediment supply, basin geometry, sedimentation history and regional stratigraphy, which can influence the inlet behaviour (FitzGerald, 1996; FitzGerald *et al.*, 2001). Finally, the use of two constant parameters to fit P/Ac or P/V type equations vary widely over the different regions i.e. the relationships are not universal and are dependent on the local conditions that play an important role in

equilibrium (Bruun, 1978; Mason, 1986; Gao and Collins, 1994a, 1994b; Pacheco *et al.*, 2010).

Table 1.1 Examples of empirical relationships and formulae where: A_c minimum cross sectional area, P spring tidal prism, V ebb tidal delta volume and Q longshore sediment transport, C and n free parameters

Stability criteria		Application
$A_c = C P^n$ O'Brien (1931), based on Le Conte (1905)	Minimum cross-sectional area of an inlet is related to the spring tidal prism, depending on two free parameters.	Equations for different parts of the world, with different tidal and wave characteristics: <u>USA</u> : Johnson (1972), Jarrett (1976); <u>AUSTRALIA</u> : Riedel and Gourlay (1980); <u>NEW ZELAND</u> : Hume and Herdendorf (1993); <u>JAPAN</u> : Shigemura, (1981); <u>WADDEN SEA</u> : Bruun and Gerritsen (1960), Eysink (1990), Gerritsen (1990); <u>NORTH ADRIATIC</u> : Fontolan <i>et al.</i> (2007 a,b)
P/Q Bruun <i>et al.</i> (1974)	$P/Q > 300$: inlets have a high degree of stability. $P/Q < 100$: inlets could be rather unstable.	
$V = C P^n$ Walton and Adams (1976)	Tidal prism governs the volume of sand contained in the ebb-tidal delta.	Validated for inlets in Florida by Marino and Mehta (1987); validated for New Zealand by Hicks and Hume (1996); also available for the northern Adriatic (Fontolan <i>et al.</i> , 2007)

Escoffier (1977) was the first to apply a stability criterion specifically developed for multiple tidal inlet systems. He suggested that the closure curve concept could be applied to these systems by making use of the finite-difference method developed by Dronkers (1964): it is necessary to define two A_c for each inlet (i.e. an initial size and a larger or smaller hypothetical size that would represent the result of accretion/erosion processes), and thus determining Um for each case. If Um is found to decrease when the size of A_c increases, or vice versa, the inlet can be considered stable. Otherwise, it should be unstable. Furthermore, Escoffier (1977) proposed that the total repletion coefficient K (as defined by Keulegan, 1967) of a multi-inlet system should be equal to the sum of K of

each individual inlet. He then used the O'Brien equation (1967) and expressed the coefficient of equilibrium (ζ), assuming that, for multi-inlet equilibrium, the value of ζ should be equal/similar to all inlets related to the same multi-inlet system. The system is unstable if ζ for any inlet is slightly greater than the values for the other inlets, which in turn would cause the development of a higher velocity at that inlet in relation to the others. The inlet would then enlarge until it captures the tidal prism of the surrounding inlets and eventually the entire tidal prism of the system. Escoffier (1977) proposes that stability of multi-inlet systems should be also determined by computing the amplitude and the phase lag of the tide in the bay.

Later, van de Kreeke (1990) derived empirical approaches for multiple inlet systems considering the changes on the total tidal prism caused by the opening of a new inlet. The author concluded that two-inlet bay systems are unstable and cannot coexist for a long time without maintenance works on at least one of the inlets.

According to Salles (2001), multiple inlet systems should not be approached in terms of the stability of each single inlet, but rather on the overall persistence of a barrier island system through time. Using Ria Formosa (Portugal) multiple inlet system as example, Salles (2001) demonstrated that complex intertidal areas show important variations in bay surface slopes, resulting in changes in the friction coefficients throughout the tidal cycle, a fact previously pointed out by Escoffier (1977). The existence of these variations contributes to the development of strong nonlinearities as the tide is distorted when propagating into shallow water systems, i.e., generating tidal asymmetries (Salles, 2001). Tidal asymmetry is common in tidal inlets (Militello and Hughes, 2000). Shallow bays and backbarrier areas are frictionally dominated and therefore produce a variety of nonlinearities associated with friction and time varying channel depth and widths (Aubrey and Speer, 1983; Friedrich *et al.*, 1993). Several studies have documented the nonlinear interaction of the offshore tidal constituents, showing how the offshore tide becomes strongly distorted as it propagates to shallow estuarine systems (Boon and Byrne, 1981; Speer and Aubrey, 1985; Friedrich and Aubrey, 1988; Friedrich and Madsen, 1992). Fry and Aubrey (1990) found that the rate of growth of tidal constituent $M4$ relates directly to the flood versus ebb dominance of the bay. Therefore, the ratio of amplitude of tidal constituents $M4/M2$ is a direct measure of the degree of nonlinear tidal distortion. This

ratio has been used in previous studies to determine the velocity asymmetry of a bay; high $M4/M2$ ratios suggest flood dominance, and low $M4/M2$ ratios indicate ebb dominance (Nummedal and Humphries, 1978; Speer and Aubrey, 1985; Aubrey and Speer, 1983). Several authors mentioned the implication of tidal asymmetries (e.g. velocity and duration) on the sediment transport patterns, suggesting that flood-dominant inlets have a tendency to transport sediment landward (Postma 1961, 1967; Boon and Byrne, 1981; Aubrey, 1986).

Salles (2001) also analysed the $M4/M2$ ratio and tidal velocity distortion but concluded that in multi-inlet systems, as opposed to the behaviour in single inlet systems, the duration of flood/ebb is not a determinant factor for flow dominance. Longer flood (ebb) can be associated with flood (ebb) dominance, due to the existence of strong residual circulation between inlets. In fact, multi-inlet systems servicing a single basin, in contrast to single inlet-systems, confer particular global hydrodynamic characteristics such as the potential existence of residual discharges and currents through the inlets. These aforementioned added processes, together with the magnitude and direction of the maximum velocity, are in fact the processes and characteristics that ultimately determine the flow dominance and the sediment flushing capacity in a given inlet, and can outweigh the effects of tidal distortion (Salles, 2001; Salles *et al.*, 2005). The importance of nonlinear processes on hydrodynamic multi-inlet systems such as tidal distortion, ebb/flood dominance and residual flow patterns was demonstrated and reinforces the need to consider those processes when analysing inlet stability in such systems.

Pacheco *et al.* (2008, 2010, 2011a,b) performed hydrodynamics and sediment transport patterns studies over a spring-neap tidal cycle in the Ria Formosa multiple-inlet system. The findings support the hypothesis proposed by Salles *et al.* (2005) i.e. the capacity to exchange large portions of the tidal prism while maintaining independent behaviour for the majority of the neap-spring tidal cycle, can contribute to the stability of multiple inlets by altering the residual flow and, consequently, the transport capacity of water and sediment. This transport capacity can also be enhanced by the morphology of the channels connecting both inlets, or by the different amplitude or phases of the offshore tides at the inlets (van de Kreeke *et al.*, 2008), although these dynamics require further research.

Using morphological datasets of two inlets of the same Portuguese system, Pacheco *et al.* (2008, 2011a) established equilibrium relationships between barrier island dimensions, inlet cross-section/width, and tidal prism, demonstrating the importance of ebb-tidal deltas in maintaining the equilibrium of a multi inlet system. Those authors concluded that the equilibrium condition depends largely on the ebb-delta sediment reservoir and on the sediment transport capacity of waves during moderate and extreme storm events. These conclusions were synthesized by de Swart and Zimmerman (2009) who argued that a full evaluation of the stability of inlet systems requires a detailed coupling of nonlinear dynamics in the backbarrier area, the inlet, and the ebb-tidal delta, including the effect of waves over the delta and in the adjacent coastal zone; furthermore, the residual flow between inlets which in turn can be affected by the morphology of the inner channels connecting the inlets.

Other recent works (Brouwer, 2013; Brouwer *et al.*, 2008, 2012, 2013; van de Kreeke *et al.*, 2008; deSwart and Volp, 2012; Roos *et al.*, 2013), confirmed that the equilibrium of multiple-inlet systems depends on the degree of connectivity between the basins. Using idealized models, suitable to obtain insight into basic physical mechanisms of equilibrium and stability of multiple inlet systems, those authors demonstrated that spatially varying water levels (i.e. entrance/exit losses, and topographic high) are crucial to explain the stability of multiple inlet system. The same authors used as an example the Wadden Sea (The Netherlands), a multi inlet system where the backbarrier lagoon consists of a series of basins separated by topographic highs, rather than one single basin. van de Kreeke *et al.* (2008) pointed out that van de Kreeke's (1985, 1990) early assumptions might have been too restrictive. The different topographic highs limit (but do not exclude) the interconnection between the sub-embayments. For basins that are connected by a large, wetted cross-section opening over the topographic high, approaching the situation of a single basin, there are no stable equilibria. In contrast, a set of equilibrium cross-sectional areas can coexist for basins that are weakly coupled, approaching a two single-inlet bay configuration. For intermediate wetted cross-sections, the results become more complex, i.e., depending on the length and friction factor of the inlet channels there can be stable configurations.

Brouwer (2013) and Brouwer *et al.* (2013) analysed the competition between a destabilizing mechanism (caused by bottom friction in the inlet, tending to close inlets) and a stabilising one (caused by spatially varying pressure gradients over the inlets, tending to keep inlets open). Both studies brought insights as how a double inlet system either could persist on the long term with two inlets open or could reduce to a single inlet system. Later, Roos *et al.* (2013) reproduced stable and unstable configurations by changing spatial variations in the surface elevation. The authors concluded that possible equilibrium states exist which are in conformity with observations (Wadden Sea, The Netherlands; Ria Formosa, Portugal and Georgia Bight, USA), i.e. spatially varying pressure gradients over the inlets trigger a stabilising mechanism that tend to keep the inlets open, confirming Brouwer (2013) and Brouwer *et al.* (2013) previous assumptions.

Final remarks

Summarizing, there exists a delicate balance between the size and the number of tidal inlets in a (multi) tidal inlet system. Varying the basin or the opening, due to natural factors or anthropic interference, can cause unexpected consequences that often make necessary some (other) human intervention to contrast a possible dangerous situation for the nearby population. In the next paragraph, some examples of interruption of natural equilibrium from multi tidal inlet system are reported.

1.3 Examples of coastal management interventions responsible for disrupting natural equilibriums

Some cases of inefficient management are briefly presented below. The environments addressed, all multi-tidal inlet systems, have been examined from the point of view large scale changes caused by natural forcing and human interventions. Following Hayes (1979) classification, the four multi-tidal inlet systems herein taken as examples show dissimilar tide and wave climate conditions (Fig. 1.7): Dutch Wadden Sea (DWS) system falls into the mixed energy (wave dominated) field, just as do the Western-Central Florida systems, but with different absolute values of tide and wave settings; Matagorda Bay

comes out as an almost exclusively wave dominated environment while Venice Lagoon system is mixed energy but more tide dominated.

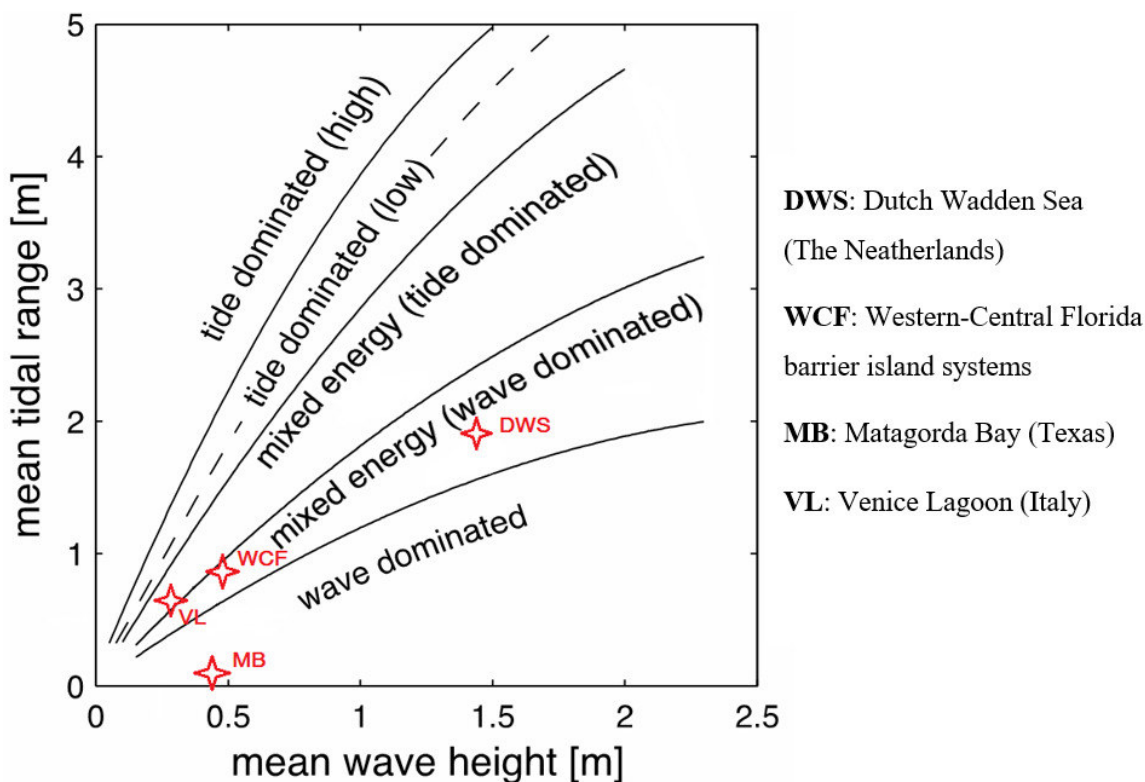


Fig. 1.7 Mean wave height vs mean tidal range classification of four multi-tidal inlet systems addressed in this study (adapted from Davis and Hayes, 1984).

1.3.1 Dutch Wadden Sea, The Netherlands

The Dutch Wadden Sea (Fig. 1.8) consists of a system of five main barrier islands, separated by five tidal inlets. The tide is semidiurnal with increasing mean annual ranges of 2.4 m in the west to 3.0 m in the east while the mean offshore significant wave height is about 1.4 m (Herrling and Winter, 2015). Kjerfve (1986) classified this multi tidal inlet system as a *leaky* lagoon, due to its high tidal range and high wave power in addition to the quite large size of all tidal inlets. According to Hayes' (1979) classification, it corresponds to a mixed energy, wave-dominated environment (Fig. 1.7). The main openings, in the south west of the system, are Texel, Eyerlandse Gat, Vlie, Amelande Gat and Frisian inlets (Fig. 1.8) and their tidal basins are divided by watersheds (Brouwer, 2013).

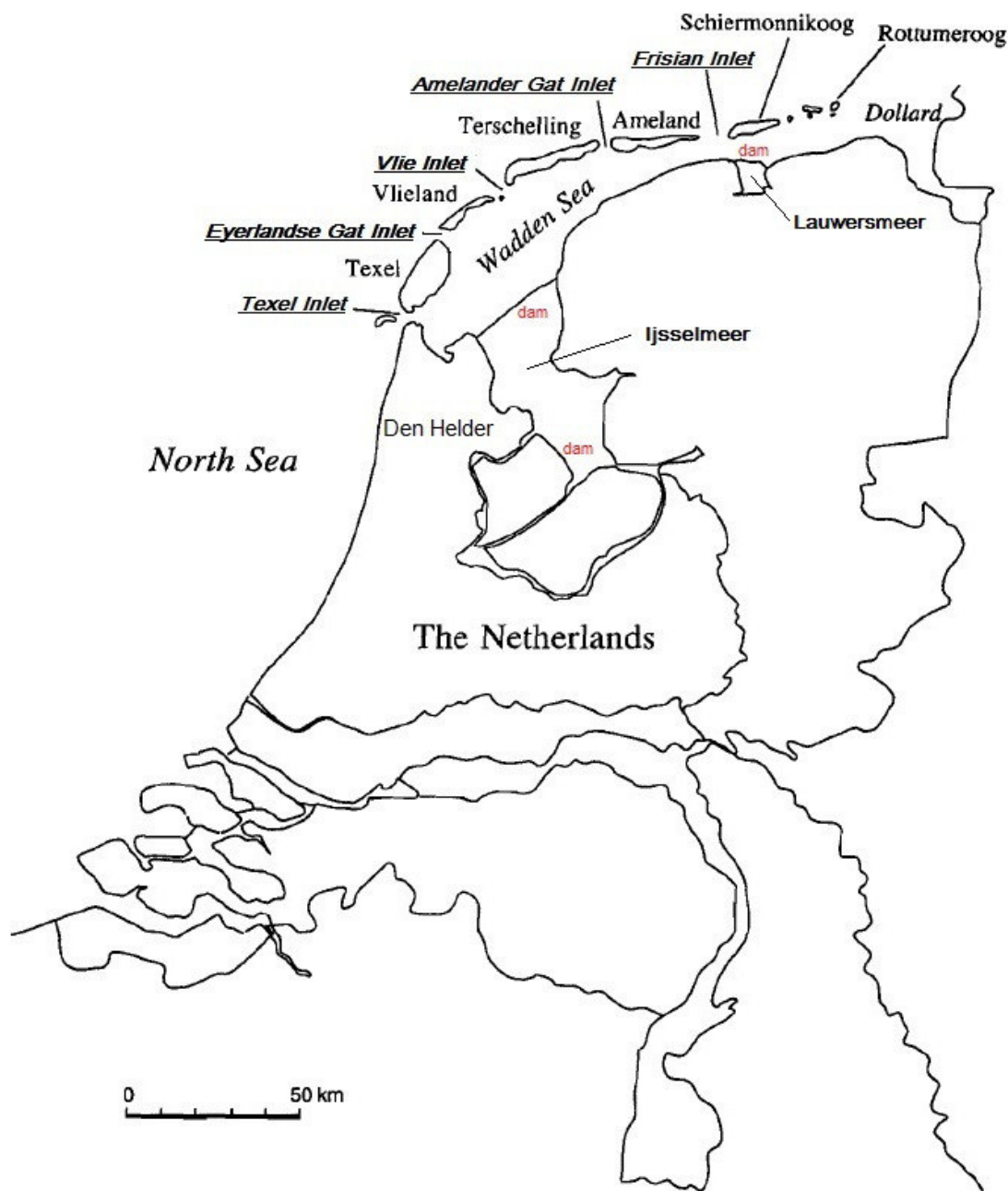


Fig. 1.8 Physiography of the Dutch Wadden Sea (adapted from Steijn, 1991)

Texel Inlet (Fig. 1.8), the southernmost opening, is the largest inlet and separates Den Helder region and the Texel barrier island. An important characteristic of its basin (i.e. Texel basin) is that it does not form a closed system but the basin connects to the neighbouring Vlie basin allowing for water exchange between the two systems (Elias and van der Spek, 2006). This inlet is probably the longest regularly monitored inlet worldwide with bathymetric datasets available since the 16th century (Elias *et al.*, 2006).

The basin drained by the Eyerlandse Gat Inlet, the opening placed between Texel and Vlie inlets, can be considered as an independent inlet system, which hardly influences the water motion in the Texel-Vlie system (Zimmerman, 1976). The major change on the entire system occurred in 1932 when the Zuiderzee (now called IJsselmeer) was separated from the Wadden Sea by a long artificial barrier. The closure of the Zuiderzee induced extensive morphological changes that distorted the equilibrium state for more than 40 years, especially at Texel Inlet where the main channel switched to a southward course and remained stable ever since (Elias and van der Spek, 2006). The length of the main drainage channel, which used to flow through Vlie Inlet was reduced by about 2/3 changing the nature of the tidal wave entering the Dutch Wadden Sea. On the contrary, the Texel inlet system expanded by capturing parts of the Vlie system (Oost, 1995). As a result, the tidal amplitude near Texel Inlet increased some 20% and the main channel became deeper (Sha, 1990; Oost, 1995). These substantial changes in the evolution of Texel Inlet provide a clear example of the responses of an inlet system to the cumulative effects of human interventions. From the point of view of the stability, this system reached a new equilibrium setting after the human intervention (Brouwer, 2013).

Other small example from Dutch Wadden Sea is the case reported by van de Kreeke (2004). The authors described the recent evolution of Frisian Inlet, placed close to the German Wadden Sea boundary and predicted a possible development using mathematical models. In 1969, Lauwersmeer, a part of the Frisian Inlet basin, was closed. Before this event, channel depth, width and cross-sectional area were 10 m, 1,000 m and 10,000 m², respectively. Closure of Lauwersmeer determined a reduction of the inlet basin by approximately 30%, leading to a decrease in inlet channel velocities and tidal prism and a gradual decrease of the channel cross-sectional area (van de Kreeke, 2004). Following the same author, the cross-sectional area was expected to tend towards a new equilibrium. The adaptation time scale was estimated to 30 years. Based on an exponential fit to the observed cross-sectional areas over the period 1970– 1987, the new equilibrium cross-sectional area is expected to reach a value between 12,000 and 16,000 m² (van de Kreeke, 1998).

1.3.2 Western-central Florida barrier-inlet systems

The western-central coast of Florida includes several barrier islands, bays and tidal inlets. Following Davis (1989) there are over 30 barrier islands and inlets along that coast but these numbers can easily change, especially due to intensive hurricanes activity. Inlets can be differently classified, as tide-dominated, wave-dominated and mixed-energy (Davis and Gibeaut, 1990), as meteo-marine parameters falls near the boundary between these two fields (Fig. 1.7). This is due to a combination of low wave energy of about 40 cm, a mean tidal range of one meter or less and a wide range in volume of tidal prisms (Davis and Barnard, 2003). These aspects makes the western-central coasts of Florida (Fig. 1.9) a *leaky* basin, following the Kjerfve (1986) classification.

Davis and Barnard (2000; 2003) and Dabees and Moore (2011) analysed both the anthropogenic and natural modifications in the backbarrier area and how these changes could influence tidal inlet stability. Since the early 1920s, several fill-in causeways connecting the mainland to the barrier islands were constructed. Within two decades, more or less all barrier islands had at least one such thoroughfare connecting barriers with the mainland. Later, to provide additional space to place houses, the “dredge and fill” procedure was adopted, that is to dredge from one area and fill in another one (in this case in the backbarrier area), thereby creating buildable upland in areas that were originally intertidal or subtidal environments (Davis and Barnard, 2000). Finally, a net of channels was dredged to allow commercial boat traffic (Intracoastal Waterway, ICW), with side cast disposal of spoil along the margins of the channels. These works on the backbarrier area and sound caused a dramatic change in hydrodynamics and tidal prism of the interconnected inlets, leading to instability and successive inlet migration or closure (Davis and Barnard, 2000; 2003). Three examples of equilibrium loss in this environment are presented in the following line.

At about the end of 19th century, the present day Dunedin Pass (Fig. 1.9) was a large inlet called Big Pass, with a cross sectional area of 1,200 m² (Lynch-Blosse & Davis 1977). The same authors reported that in 1921 a hurricane and associated storm surge of about 3 m caused a breach along the coastline only 3.5 km north of Dunedin Pass, forming Hurricane Pass (Fig. 1.9). This new inlet rapidly became stable. Only five years later, in 1926, the first nearby causeway was completed. Both these events, one natural and one

human-induced, caused changes to the tidal prism of Dunedin Pass (Big Pass), reducing of its cross sectional area by about 200 m² in 30 years (Davis and Barnard, 2000).

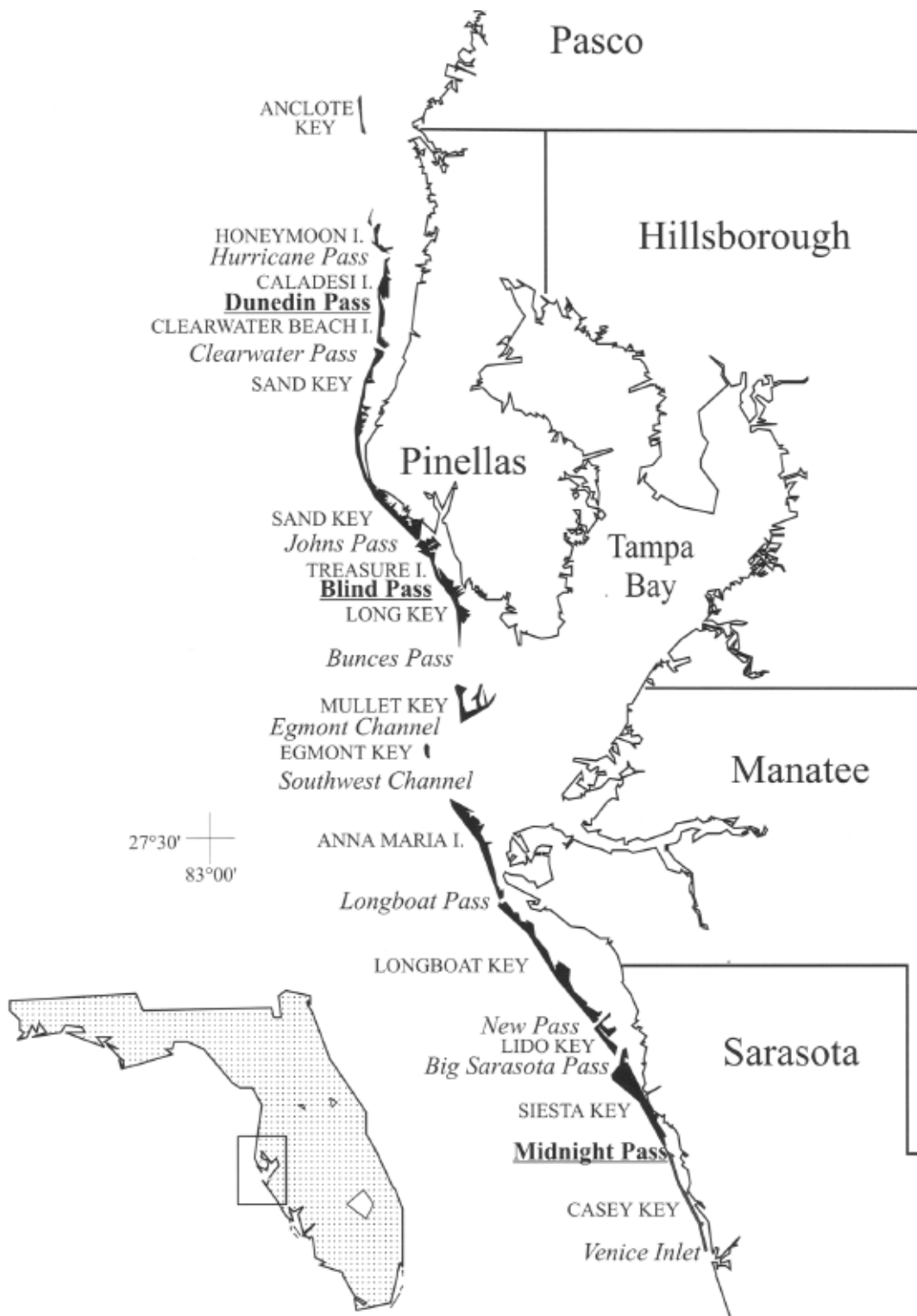


Fig. 1.9 Map showing the study area with inlets referred in text underlined (adapted from Davis and Barnard, 2000).

In 1964, another fill-in causeway was completed, further compartmentalizing the back-barrier lagoon and suddenly accelerating the reduction of tidal prism available to the inlet. In fact, in 100 years, Dunedin Pass (Big Pass) reduced its cross sectional area by about 90%, to only about 200 m² in 1975 (Davis and Barnard, 2000). according to the same authors, ten years later, the inlet channel was only about 50 m wide and 1.5 m deep with a very small tidal flux. For this reason, passage of the Hurricane Helena in the same year caused its complete closure. Davis and Barnard (2000) noted that, although this storm did not made landfall near Dunedin Pass, it generated enough wave energy to remove its ebb-tidal delta. Subsequently, the channel infilled within three years due to the northward longshore sediment transport. The same authors concluded that this is an excellent example of how human activities on the multi inlet system coupled with natural phenomena have caused the demise of a once large tidal inlet.

Other example involves three adjacent inlets in central Pinellas County (Tampa Bay): from north to south, Indian Pass, Johns Pass and Blind Pass (Fig. 1.9). Blind Pass (Fig. 1.9) is an embanked inlet located on the SW-facing portion of the barrier island system in Pinellas County. Twelve kilometres to the north was Indian Pass, a small natural inlet that is now closed. In the middle of the 19th century, the inlets were natural and quite large but after the 1848 hurricane opened Johns Pass (Fig. 1.9) between Indian and Blind Pass, both inlets began to be instable (Davis and Barnard, 2003). The newly formed inlet captured a large amount of the tidal prism and a marked reduction in the size of Indian and Blind Pass was recorded, also forcing the latter inlet to migrate southward (Davis and Barnard, 2000; 2003). By 1926, the time of construction of a nearby fill-in causeway, the mouth of Blind Pass had moved more than 2 km and its inlet throat reduced from about 500 m² to less than 200 m² (Davis and Barnard, 2003). Indian Pass, instead, closed in 1931. When the northern causeway was completed in 1937, the US Army Corps of Engineers decided to stabilize the first inlet, constructing a stone jetty on the south side of the channel (Mehta *et al.*, 1976). The successive decrease in surface area of Boca Ciega Bay, the backbarrier area of Johns and Blind Pass, due to dredge and fill practice (about 28%, following Mehta *et al.*, 1976) caused another strong reduction of the Blind Pass tidal prism. In the meantime, the northern Johns Pass (i.e. the new inlet) increased in size. A north jetty was added to Blind Pass in 1968 to oppose to the littoral drift from the north

(that was threatening to obstruct the inlet), but regular works must be done to guarantee adequate inlet hydrodynamics (Davis and Barnard, 2000; 2003).

Sarasota Bay, to the South, provides another good example of changes in hydrodynamics and tidal prism of interconnected inlets. Sarasota Bay is a multi-inlet system connected with the ocean by a variable number of tidal inlets, strongly depending on the activity of natural events like hurricanes (Davis and Barnard, 2000). Until the early 1980s, six major inlets, Anna Maria, Longboat, New, Big Sarasota, Midnight and Venice Pass that competed for the total tidal prism (Fig. 1.9) (Dabees and Moore, 2011). At that time, the most efficient inlet was Big Sarasota Pass, which exchanged about 40% of the total tidal prism while one of the smallest was Midnight Pass, to the south (Fig. 1.9). As in the north, natural and anthropogenic changes to the system affected the distribution of tidal prism shares between Sarasota Bay inlets, leading Midnight Pass to migrate northward and, at a later time, towards closure in 1983. Its tidal prism was in fact captured by the nearby tidal inlets; the tidal prism of Anna Maria, Longboat, New and Venice Pass increased, while the Big Sarasota Pass prism slightly decreased (Davis *et al.*, 1987; Dabees and Moore, 2011). Again, both natural and anthropogenic factors have contributed to the instability of the inlets.

1.3.3 Matagorda Bay, Texas

Matagorda Bay is a *restricted* lagoon, corresponding to a quite large double-inlet system in the western part of Gulf of Mexico in Texas (Fig. 1.10). It has a microtidal regime, with tidal range between 10 and 60 cm (Kraus and Militello, 1999), but wind-driven flows frequently dominate the weak astronomical tide. The average value of the offshore mean wave height recorded in five different stations, between 1980 and 2014 is less than 1 m (0.94 m, <http://wis.usace.army.mil/>). According to Hayes' (1979) classification, it falls within the wave dominated environment category (Fig. 1.7). It is connected to the Gulf of Mexico by the natural Pass Cavallo inlet and the jettied artificial Matagorda Ship Channel (MSC, Fig. 1.10).

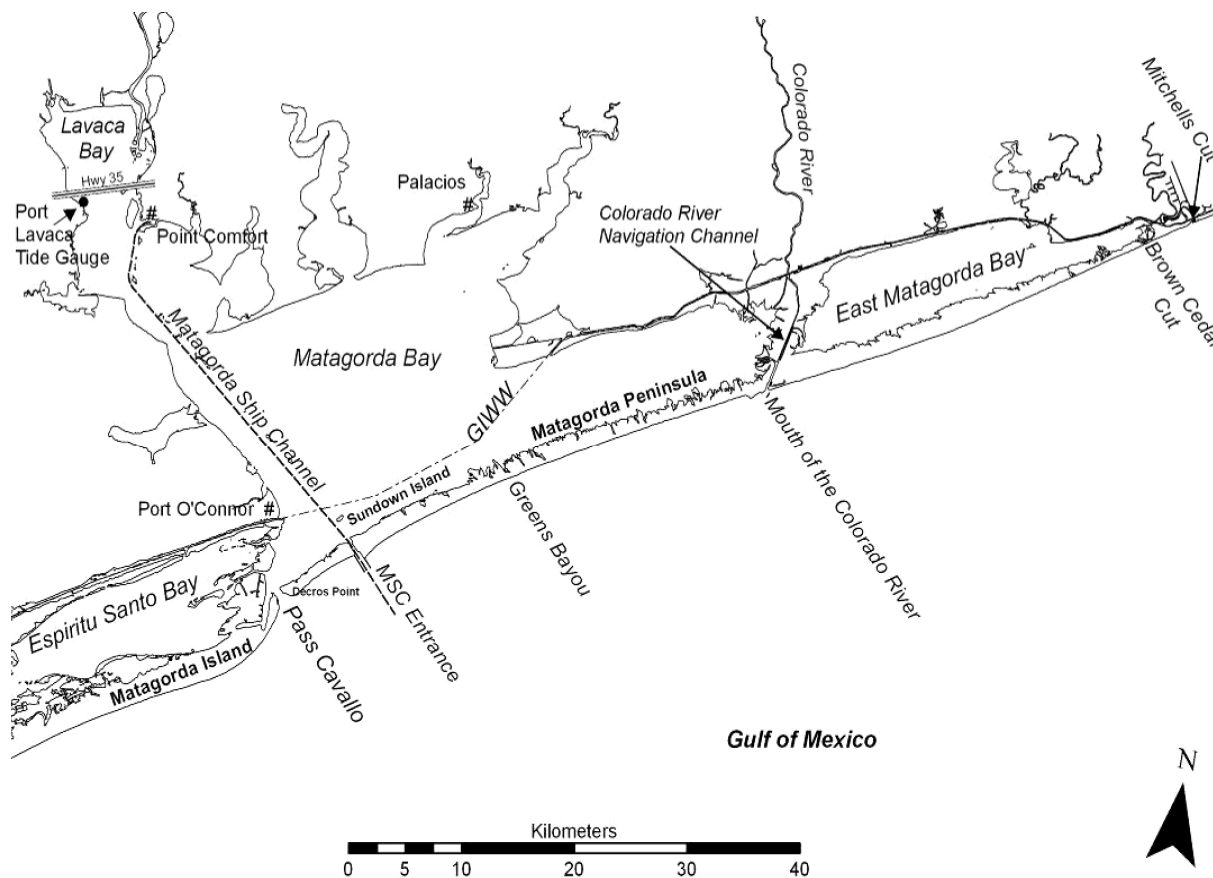


Fig. 1.10 Detail map of Matagorda Bay and East Matagorda Bay (adapted from Kraus and Batten, 2008).

Pass Cavallo inlet (Fig. 1.10) has existed for at least 2,600 years, being approximately at the same location for the last 200 years (Harwood, 1973). Satellite images evidence the presence, in the past, of many ephemeral inlets (e.g. Greens Bayou and Brown Cedar Cut that were opened through Matagorda Peninsula by large storms, but eventually closed in favour of Pass Cavallo, Kraus and Batten, 2008). This bay is the western part of the historic larger Matagorda Bay, splitted in two by the growth of the Colorado River Delta between 1929 and 1935 (Wadsworth, 1966; Bouma and Bryant, 1969). The two parts are connected by the Gulf Intracoastal Waterway (GIWW) that is a part of the Intracoastal Waterway, consisting in a set of navigable channels connecting the rivers that flow into the Gulf of Mexico.

Pass Cavallo Inlet (Fig. 1.10) was historically stable until the 20th century but the deltaic progradation of Colorado River Delta caused an initial tidal prism decrease, leading to

shoaling and increasing navigation problems (Harwood, 1973). For this reason, between 1963-1966, the USACE dredged the MSC, creating a more efficient tidal channel which was planned to connect with the deeper and more central portion of the bay, about 5.5 km updrift of Pass Cavallo (Fig. 1.10). This intervention caused a degeneration of the hydrodynamic efficiency of Pass Cavallo Inlet, with loss of tidal prism and decrease in inlet width (by 2.76 km). In contrast, the adjacent Matagorda Island (downdrift side) and Matagorda Peninsula (updrift) prograded towards the inlet: 3.45 km between 1974 and 2003 and 1.56 km between 1963 and 2003, respectively (Batten *et al.*, 2007). Following Harwood (1973) and Ward (1982), surveys carried out prior and after the opening of the MSC show a halving of Pass Cavallo tidal prism. Ward (1982) also pointed out that, during the 1970s, tidal prisms of Pass Cavallo and MSC inlets were approximately the same. According to the more recent calculation for 2004 situation by Kraus and Batten (2008), based on a calibrated two-dimensional model created by Kraus *et al.* (2006), tidal prism at MSC was approximately three times larger than at Pass Cavallo Inlet. Ward (1982) defined the inlet as “shoal unstable” and Van de Kreeke (1985) stated that Pass Cavallo would ultimately close because of the presence of the MSC entrance. In fact, it was exactly following the above study cases, that van de Kreeke (1990) concluded that multiple inlets that drain the same bay system cannot co-exist for long time periods and that, eventually, only one would remain open. This consideration was afterward denied. van de Kreeke *et al.* (2008) pointed out that van de Kreeke’s (1985, 1990) early assumptions might have been too restrictive. On the other hand, Price (1952) and Kraus (2007) noted that Texas coast is subject to North-Northeasterly winds during wintertime, and this seems to force water into the southwest corners of Texas bays, which promotes the existence and persistence of channels in those corners (the Pass Cavallo Inlet). Furthermore, an ebb discharge is produced in Matagorda Bay by the combination of its southwest shore and the wind setup of water and adds to that of the astronomical tide. Based on this last consideration and on geomorphic analysis, Harwood (1973) concluded that Pass Cavallo Inlet would remain open. Finally, Batten *et al.* (2007), through measurements and modelling, confirmed that Pass Cavallo Inlet has reached a dynamic equilibrium and is not likely to close in the near future, maintaining Matagorda Bay as a multiple tidal-inlet system.

1.3.4 Venice Lagoon, Italy: a case of forced stable multi-inlet system

The Lagoon of Venice (Fig. 1.11) represents an emblematic example of an environment where extreme human intervention has disrupted the natural equilibrium of a multi-inlet system. This lagoon is located in the northeast of Italy on the Adriatic Sea. According to Dal Cin and Simeoni, (1994), mean significant annual wave height is lower than 0.5 m, while the highest offshore wave height, both for *Bora* and *Scirocco* storms (two of the strongest winds in the region), is about 5 m (Cavaleri *et al.*, 1996). Recent studies performed from 1958 to 1999 on wave data give a more precise value for the annual-average significant wave height, 0.27 m (Martucci *et al.*, 2010). Hayes (1979) classification sets this lagoon inside the tide dominated (mixed energy) field (Fig. 1.7). It is the largest wetland district in the Mediterranean Sea, covering an area of about 550 km², and is separated from the sea by a barrier island system, with three tidal inlets, Lido, Malamocco and Chioggia (Fig. 1.11). Each inlet is stabilised with two long jetties. For this reason, the lagoon can be considered as a human-induced stable multi-inlet system. As the nearby MGL, Venice Lagoon can be classified as a *restricted* lagoon (Kjerfve, 1986), even if its natural status is very compromised.

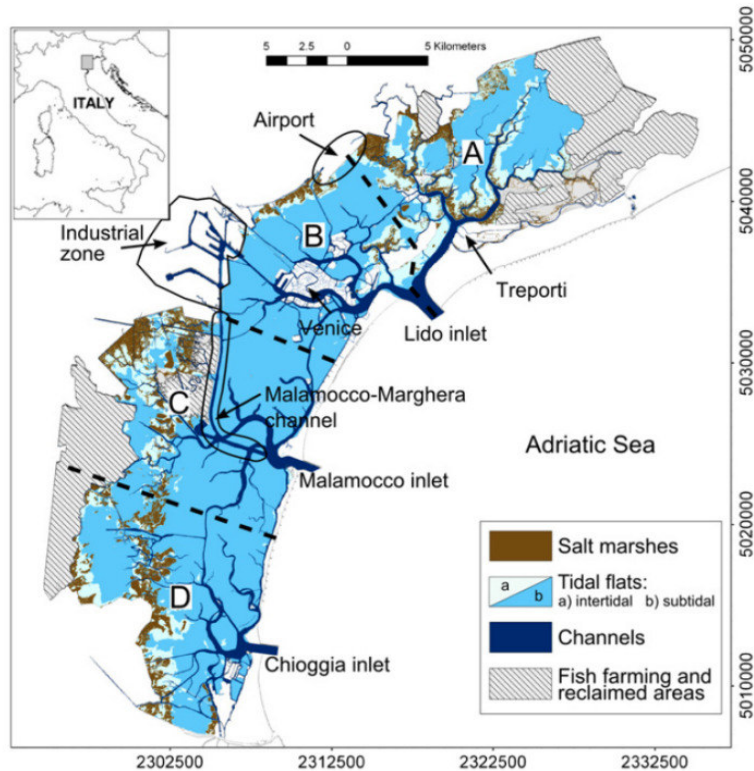


Fig. 1.11 Map of Venice Lagoon. Four sub-embayments (A–D) are separated by broken lines (adapted by Sarretta *et al.*, 2010)

Since the 9th century, Venice Lagoon has been strongly altered by human interventions (Day *et al.*, 1998). The modifications were made with the first aim of protecting the city of Venice (located in an island and nowadays connected to the mainland by an embankment) and also to adapt the system to new human activities e.g. such as the improvement of the navigation for commercial purposes (Ravera, 2000). Following those new developments, the lagoon physiography started to be dominated by river diversion, wetland reclamation, channel excavation, construction of industrial complexes, and enclosure of lagoon areas for fish farms (about one-sixth of the Venice lagoon is at present occupied by fish farms, Dorigo, 1965; Sarretta *et al.*, 2010).

During the period 1840-1872 the jetties at Malamocco Inlet were built to avoid shoaling inside the channel and to improve navigability; for the same reason jetties were also built at the Lido (1882-1910) and Chioggia (1911-1933) Inlets. Until 1882, three different inlets occupied the area of the present Lido Inlet. However, after the construction of the jetties, the three channels were merged together to form the single Lido Inlet (Muraca, 1982). The most devastating effect on the natural hydraulics of the central lagoonal region

was the excavation of more than 40 million cubic meters of sediments to create the navigational channel connecting Malamocco inlet to the industrial zone of Marghera (Ferla *et al.*, 2012).

In the last century, Venice lagoon was subject to continuous subsidence generated both by natural causes (e.g. rising sea level and natural erosion of the seabed) and man-induced activities like groundwater extraction (Cavazzoni and Gottardo, 1983; Sarretta *et al.*, 2010). Sarretta *et al.* (2010) showed that the lagoon was transformed from a highly complex, well-developed microtidal lagoon during the 1930s, to a sediment-starved and subsidence-dominated lagoon in the 1970s. Since then the system has been adapting to the high energy-dominated, flatter-bottomed and more open (bay-like) environment of today, where the simplified morphology and increase of lagoonal depth has favoured water exchange with the sea, weakening the lagoon's estuarine features. Special mention must be made of MOSE, a system that aims to protect the lagoon from highest water levels during surge events. The entire area is subject to subsidence and to strong storm-surge episodes responsible for increasing the water level and causing the famous "acqua alta" phenomena. The construction of MOSE started in 2003 and its conclusion is foreseen to 2018. The aim is to totally control the water exchange between the lagoon and the sea, thus preventing the flooding of the town during the extreme events.

1.3.5 Final remarks

Other cases of disruption of the natural equilibrium due to coastal management interventions will be presented in the next chapter. They concern the Ria Formosa and Marano and Grado lagoons, focuses of this thesis.

This last section has shown some very dissimilar cases where human action and, sometimes, natural events modify the equilibrium of multi-tidal inlet systems that then tries to adapt to the new situation by varying the size, morphology and/or position of any unconstrained inlets. These adaptations can generate some issues for coastal populations as a different configuration of inlet area can affect navigability, exchange of water and nutrients and can also threaten nearby human establishments. A good knowledge of the

functioning of these delicate systems is essential to define appropriate coastal management that can benefit the system itself and the people that live around.

2.

***Ria Formosa and Marano and Grado
Lagoon: contrasting coastal environments***

Many similarities can be found in coastal lagoons worldwide. They usually present different salinity than that of the connected ocean or sea. Salinity is usually lower, because of the introduction of freshwater by tributaries but it may also be higher due to evaporation; this restricts species to those that are resistant to salinity variation. Very few species can survive in this type of environment; however, the number of individuals in each species may be very high. The presence of a tidal regime is the main common factor, but, at the same time, it is also one of the major issues of difference. A small tidal range generates deeply different physiography than that related to medium or high tidal range. Generally, a lagoon can form in a micro or meso-tidal range environment, which permits the formation of a barrier island system and one or more tidal inlets that allows for exchange of water. Macrotidal regimes, over 4 m, inhibits formation of barrier islands due to strong tidal currents (Hayes *et al.*, 1973; Hayes, 1975; 1979). Other important factor that influences the lagoon morphology, especially its external part, is the wave climate. A lagoon in a semi-closed sea is usually exposed to a calmer weather than a lagoon fronting the open ocean. Thus, tidal range and wave climate are two of the major factors that can shape a coastal lagoon.

This chapter intends to give an overview of the dissimilar contexts of the two lagoon environments that are objects of this thesis. Both of these multi-tidal inlet systems can be classified as mixed energy environments, with a pronounced tendency toward tide-dominated (Hayes, 1979, Fig. 2.1), but their conditions of tide and wave climate are very different. The first, Ria Formosa lagoon, has a meso-tidal regime and fronts the open Atlantic Ocean, while Marano and Grado Lagoon, the second environment, is characterized by a micro-tidal regime and is located in the semi-closed basin of the North Adriatic Sea. An overview of the major events both natural and anthropic, is also presented.

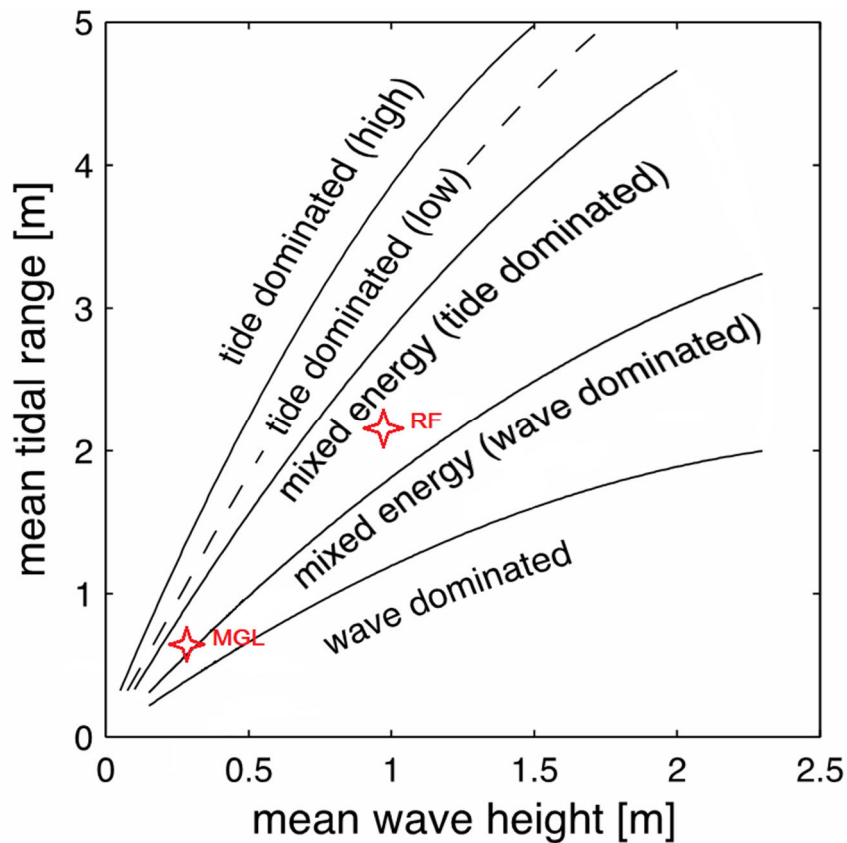


Fig. 2.1 Mean wave height vs mean tidal range classification for Ria Formosa (RF) and Marano and Grado Lagoon (MGL). Adapted from Davis and Hayes (1984).

2.1 Ria Formosa Lagoon

Ria Formosa Lagoon (Fig. 2.2) is integrated in a natural park located in Southern Portugal and, following Kjerfve (1986) classification, is considered at the limit between *leaky* and *restricted* lagoon, since it shows a quite large number of tidal inlets (corresponding to *leaky* lagoon), but of small size. It falls into the mixed energy (tide dominated) environment field, according to the Hayes (1979) classification (Fig. 2.1). It is a multi-inlet barrier island system presently consisting of five elongated islands and two peninsulas separated by six tidal inlets. They are natural, relocated or constrained by jetties, distributed as: two relocated inlets (Ancão and Fuseta), three artificially opened inlets (Faro-Olhão, Tavira and Cacela inlets), and one natural inlet (Armona Inlet. Fig. 2.2). Faro-Olhão and Tavira inlets are also stabilized with a dual system of jetties. Being

an extremely dynamic environment, the number of tidal inlets varied several times over time (Weinholtz, 1964; Esaguy, 1986a). The lagoon extends approximately over 184 km², along about 55 km of coast. The backbarrier area has a complicated pattern of tidal channels and creeks, featuring an average depth of 4 m relative to mean sea level (m.s.l.). The barrier islands, are located up to 6 km offshore of the mainland at the widest point of the lagoon (Andrade, 1990; Ramos and Dias, 2000; Williams *et al.*, 2003).



Fig. 2.2 Ria Formosa multi inlet barrier island system (adapted from Popesso *et al.*, 2016).

The beach and dune systems occupy 13% of the total system among which more than 6% are dunes with high featuring of habitat type (Ferreira *et al.*, 2016a). Beaches are generally narrow and are reflective to intermediate at the western end of the system, with an average beach face slope of 0.11 (Ferreira *et al.*, 1997) and predominately dissipative at the eastern end (Dias *et al.*, 2003) with minimum slopes around 0.04 for Cacela peninsula (Matias *et al.*, 1999). This barrier system is extremely dynamic. It is influenced by longshore drift (e.g. Ciavola *et al.*, 1997), tidal inlet evolution (e.g. Vila-Concejo *et al.*, 2002, 2006; Pacheco *et al.*, 2010), shoreline evolution (e.g. Ferreira *et al.*, 2006), overwash processes (e.g. Matias *et al.*, 2008), dune formation (e.g. Gomes *et al.*, 1994), backbarrier processes (e.g. Carrasco *et al.*, 2011) and artificial nourishment actions (Dias *et al.*, 2003).

Furthermore, it is in active landward migration phase, as other similar systems in the world, likely due to the general sea level rise (e.g. Dias, 1988; Pilkey *et al.*, 1989).

Ria Formosa is one of the few barrier island systems in the world with a cusped shape (Fig. 2.2, Bettencourt, 1994). This feature produces two different areas in terms of exposure to wave action. The west flank is more energetic, being under the direct influence of the dominant wave conditions, while the east flank is only directly exposed to the less energetic wave conditions from SE, locally known as “*Levante*”.

This region is affected by an important longshore sediment transport, from west to east. Recent studies evaluated the rate as $1.1 \times 10^5 \text{ m}^3/\text{year}$ (Teixeira, 2013), which is in accordance with the values of $\sim 0.9 \times 10^5 \text{ m}^3/\text{year}$ determined in the early 1990s by Andrade (1990). According to Pilkey *et al.* (1989) and more recently Ferreira *et al.* (2016a), the sediment supply has its origins in the cliff recession west of the Ria Formosa, with negligible supply from estuarine runoff due to the low rainfall of the region.

Following Salles *et al.* (2005), the system is hydrodynamically divided into three quasi-independent sub-embayments: the western sub-embayment including Ancão, Faro-Olhão and Armona inlets; the adjacent sub-embayment with Fuzeta and Tavira inlets, and the eastern sub-embayment with Cacela Inlet, that is practically an independent system. Each sub-embayment can be considered as an autonomous embayment-tidal inlet system with minimal interaction with the remaining system. The boundary between sub-embayment were defined by Salles *et al.*, (2005) as the areas where the flow volume was less than 1% of the flow through the adjacent inlets.

Regarding the population of the region, the number of residents inhabiting the Ria Formosa drainage basin increased by circa 60% between 1970 and 2001 (Ferreira *et al.*, 2016b). Urban development in Ria Formosa is relatively low and occupies a very small area of the system, concentrated mainly in five small villages, most of them located in the backbarrier area in Faro, Culatra e Armona.

2.1.1 Tide, wind and wave climate

The coast of South Portugal is under a mesotidal regime. Tides in the Ria Formosa lagoon are semi-diurnal with average ranges of 2.8 m for spring tides and 1.3 m for neap tides. Maximum spring ranges can reach 3.5 m. Wave climate in the area is moderate to high (Ciavola *et al.*, 1997). According to Pessanha and Pires, (1981), the storm threshold for this region is defined as the *significant wave height* (H_s) > 3 m but for the purposes of this work, the threshold of storm waves was lowered to 2.5 m. See paragraph 3.2 for furthermore information. Due to its orientation (ca. N132°), Ancão Peninsula is directly exposed to incident waves from the W-SW whilst waves coming from E-SE are strongly refracted (Vila-Concejo *et al.*, 2003). Costa (1994) collected wave data obtained offshore the study area between September 1986 and December 1993. The average seasonal and annual wave conditions are shown in Table 2.1. During winter (October to March) mean H_s and peak periods (T_p) are higher than in summer (April to September) and incident waves coming from the west are dominant. South-easterly wave events (“*Levante*”) are always less relevant. They are usually events during whit waves approaching the coast with large angles, generating strong longshore currents and sediment transport, and inducing erosion along the barrier islands beach due to high steepness (Andrade, 1990).

Table 2.1 Wave climate (Costa, 1994). H_s : mean significant height; T_p : mean peak period.

	Mean		Directions (%)				
	H_s (m)	T_p (s)	W	SW	S	SE	E
Summer	0.8	7.1	56.8	13.4	2.2	23.8	2.7
Winter	1.1	9.2	42.8	21.2	1.9	26.9	6.9
Annual	0.9	8.0	51.5	16.3	2.1	25.0	4.2

Later, Costa *et al.* (2001), extending the period of study to December 2000 and confirmed the annual significant offshore wave height H_s , attesting that most of the values are slightly lower than 1 m (0.92 m, 68%). The same authors found an average T_p of 8.2 s, over the examined period. They observed predominant wave directions from the W-SW

(approximately 71%), while waves coming from the SE only account for 23% of the observations.

Using 14 years of wave data, Almeida *et al.* (2011a,b) confirmed that the largest waves, generated by deep atmospheric low-pressure systems, travel from the SW direction. During SW storms, H_s may reach 4 m, more than once a year in average, and in general these storms occur mainly during winter (December–March); however, there are events that can reach $H_s \sim 7$ m. SE storms occur when a strong “*Levante*” (easterly to southeasterly wind) is blowing at Gibraltar Strait. SE storms are mainly due to mesoscale atmospheric patterns while the SW storms are related to synoptic scales, SE storms occur mainly between October and May and typically with $H_s < 4$ m. The maximum H_s recorded during SE storms is < 6 m (Almeida *et al.*, 2011a,b). Updated percentages, covering the study period considered here, are presented later (see paragraph 3.3).

2.1.2 Natural processes and anthropic conflicts

Both flanks of Ria Formosa coastline have had a variable number of inlets over time. Andrade (1990) and Salles *et al.* (2005) showed that although the system has historically responded to both natural and artificial disturbances, with significant changes in the overall morphology, it has always maintained between four and seven inlets. According to Weinholtz (1964) and Esaguy (1986a), the western flank, that nowadays has only one inlet (Ancão Inlet), at various times in the past has had up to three tidal inlets. The eastern flank also underwent various changes but the present configuration shows five inlets (Fig. 2.2): Faro-Olhão, Armona, Fuseta, Tavira and Cacela Inlets. Faro-Olhão and Tavira inlets were artificially opened and stabilized with groynes in 1929-1955 (Esaguy, 1984) and 1927-1985 (Esaguy, 1987), respectively. Esaguy (1986b) reported that Faro-Olhão Inlet was dredged at a location where another inlet had existed before. The previous unstable and fast-silting inlet (Bispo Inlet), opened in 1861 and was almost completely infilled when the construction of Faro-Olhão Inlet began (Salles, 2001). Tavira Inlet stabilization, instead, was more complicated. It was artificially opened for the first time in 1927 but it soon closed (Esaguy, 1987). The same author reports that in 1936 it was artificially re-

opened and stabilized but it closed again by 1950. Finally, it was re-opened again after a storm in 1961, dredged and stabilized in 1985 (Esaguy, 1987). Both Ancão and Fuseta inlets show a clear pattern of cyclic migration toward the east and they were relocated many times (Vila-Concejo *et al.*, 2002; Popesso *et al.*, 2016). Vila-Concejo *et al.* (2002) proposed a different migration type for both flanks, observing that the inlets on the western flank migrate with a high-energy pattern (Ancão Inlet) while a low energy migration pattern characterizes the inlets located in the eastern flank, such as Fuseta Inlet. In this latter case the channel migration is accompanied by strong constructional processes on the updrift barrier, and consequently, by inlet width reduction (Pilkey *et al.*, 1989). Recently, Cacela Inlet (Fig. 2.2) was artificially opened near the eastern part of Ria Formosa and caused the closure of Lacém Inlet, an opening that also placed in the eastern part of the lagoon in a position between Tavira and Cacela inlets.

Cacela inlet typically opens over a wide area during storms, because of the easy inundation of Cabanas Island, and subsequently it narrows while migrating eastwards (Vila-Concejo *et al.*, 2002; Ferreira *et al.*, 2016a). Weinholtz (1964) and Pilkey *et al.* (1989) were the first to analyse Armona Inlet (Fig. 2.2). It is considered to be the only naturally stable inlet of the system. Throughout recent centuries, it occupies the same position although narrowing considerably in the last few decades (Weinholtz, 1964; Andrade, 1990; Salles, 2001; Vila-Concejo *et al.*, 2002) because of the opening and stabilization of Faro-Olhão Inlet that caused changes in the hydrodynamic regime of the western sub-embayment. This modification was particularly impactful since it induced the capture of a large part of the tidal prism from the Armona Inlet (Pacheco *et al.*, 2010), formerly the dominant natural inlet in the system. According to Esaguy (1984) and Dias (1988), during the last century, the width of Armona inlet has narrowed by approximately 2,500 m, from 4,300 m in 1873, to 1,850 m in 1983. The Faro-Olhão Inlet opening and stabilization with long jetties illustrated unpredicted effects of anthropogenic intervention on the system (Pacheco *et al.*, 2008). As mentioned before, the dredging of the channel was carried out in a place where another inlet existed before and its main purpose was to have a more efficient navigability to reach the harbour inside Ria Formosa (Esaguy, 1986b). However, according to Esaguy (1986c) and Silva *et al.* (2002), the distance between the two jetties was too close and, as a consequence, scouring led to local depths of about 40 meters in the inlet throat, due to the intensification of the ebb currents.

Furthermore, the channel was not in equilibrium, due to the jetty configuration. Consequently, a meander in the currents in the channel was set up due to the east jetty, which created an extra difficulty for navigation (Esaguy, 1986c). The scouring process related to the inlet cross-section evolution, greatly reduced the flow through Armona Inlet, resulting in a shift in tidal prism dominance from Armona to Faro-Olhão (Pacheco *et al.*, 2010). For Armona Inlet, the subsequent flow reduction of about 75% resulted in an overabundance of sediment. Ebb-tidal currents decreased over the ebb-tidal delta, allowing waves and flood tidal currents to push the shoals landward. This in turn provided the sediment necessary to extend Culatra Island and to reduce the width of the Armona Inlet to less than 300 m (Pacheco *et al.*, 2011a,b). Due to its (past) width, Armona inlet has a very complex morphology and often shows two or more channels (Vila-Concejo *et al.*, 2002). Nevertheless, it continues to maintain a well-defined navigable channel. Both Armona and Faro-Olhão inlets were capable of flushing sediment out of their cross-section and achieved a new dynamic equilibrium. These two inlets have a strong degree of interconnection (i.e. residual flow), transferring large portions of tidal prism P between them, but draining the embayment more independently for a portion of the neap-spring tidal cycle, and capturing together almost 90% of the total prism of the Ria Formosa (Pacheco *et al.*, 2008, 2010, 2011a,b).

Ancão Inlet is the third migrating inlet of the western embayment. Migrating toward east, the inlet gradually diminishes the connection with Faro-Olhão and Armona Inlets, becoming always more independent: only during certain tide condition (e.g. spring tide), the connection is active (Pacheco *et al.*, 2010). It is only connected with the rest of the system during late flooding or early ebbing stages of the tide. This hydrodynamic semi-independence of Ancão Inlet probably minimized the consequences of the opening and stabilization of Faro-Olhão Inlet over Ancão Inlet. This was also indirectly confirmed by Vila-Concejo *et al.* (2002), who noted that Ancão Inlet width was not affected by the opening of the Faro-Olhão Inlet (Andrade, 1990).

The smaller remaining inlets have lower interconnectivity and a relatively restricted lagoon area where they exert their dominance. For this reason the opening and stabilization of Tavira Inlet did not cause significant changes in the hydrodynamics of the closest Fuzeta, Lacém (before) and Cacela (after) Inlets (Vila-Concejo *et al.*, 2002). The

hydrodynamic efficiency of Tavira Inlet is very low and according to Andrade (1990) it represents a very low percentage (about 4%) of the total tidal prism of the system.

Consistent with the model of van de Kreeke *et al.* (2008), the interconnectivity between the inlets in the same sub-embayment permits their coexistence, changing their characteristics in tidal prism and throat size to reach an equilibrium, while the smaller ones have their own flushing areas, working as single tidal embayments. This configuration and hydrodynamic regime generates a stability situation of the multi tidal inlets system.

2.2 Marano and Grado Lagoon

Marano and Grado Lagoon is located in the North East of Italy (Fig. 2.3) and it is part of the wetlands system distributed along the North Adriatic Sea (Brambati, 1970). The lagoon can be classified as a *restricted* lagoon, according to Kjerfve (1986). It is delimited by the mouth of the Tagliamento River, to the West and the Isonzo River, to the East, and covers a total area of 160 km², about 32 km long and 5 km wide. This size makes it the second largest Italian lagoon after Venice.

Marano and Grado Lagoon is delimited by a system of six barrier islands extending for about 20 km (from West to East: Martignano, S. Andrea, Morgo, Marina dei Manzi and Macia, Grado Island, Fig. 2.3) most of which have been deeply modified by human intervention. A complex system of sandbanks seaward faces the barrier islands of the eastern part of the lagoon, enclosing a para-lagoon environment. Following Brambati *et al.* (1998) and Ulliani (2016), these sandbanks are rapidly evolving, with elevations often close to mean sea level and, only occasionally, crowned by dunes (Gatto and Marocco, 1992). Six tidal inlets interrupt the barrier island and sand bank system. From West to East (Fig. 2.3), these are: Lignano (embanked), S.Andrea (natural), Buso (jettied), Morgo (natural), Grado (jettied) and Primero (embanked) inlets. Among them, the Lignano and Buso inlets have the maximum tidal prism (Dorigo 1965; Fontolan *et al.*, 2007a).

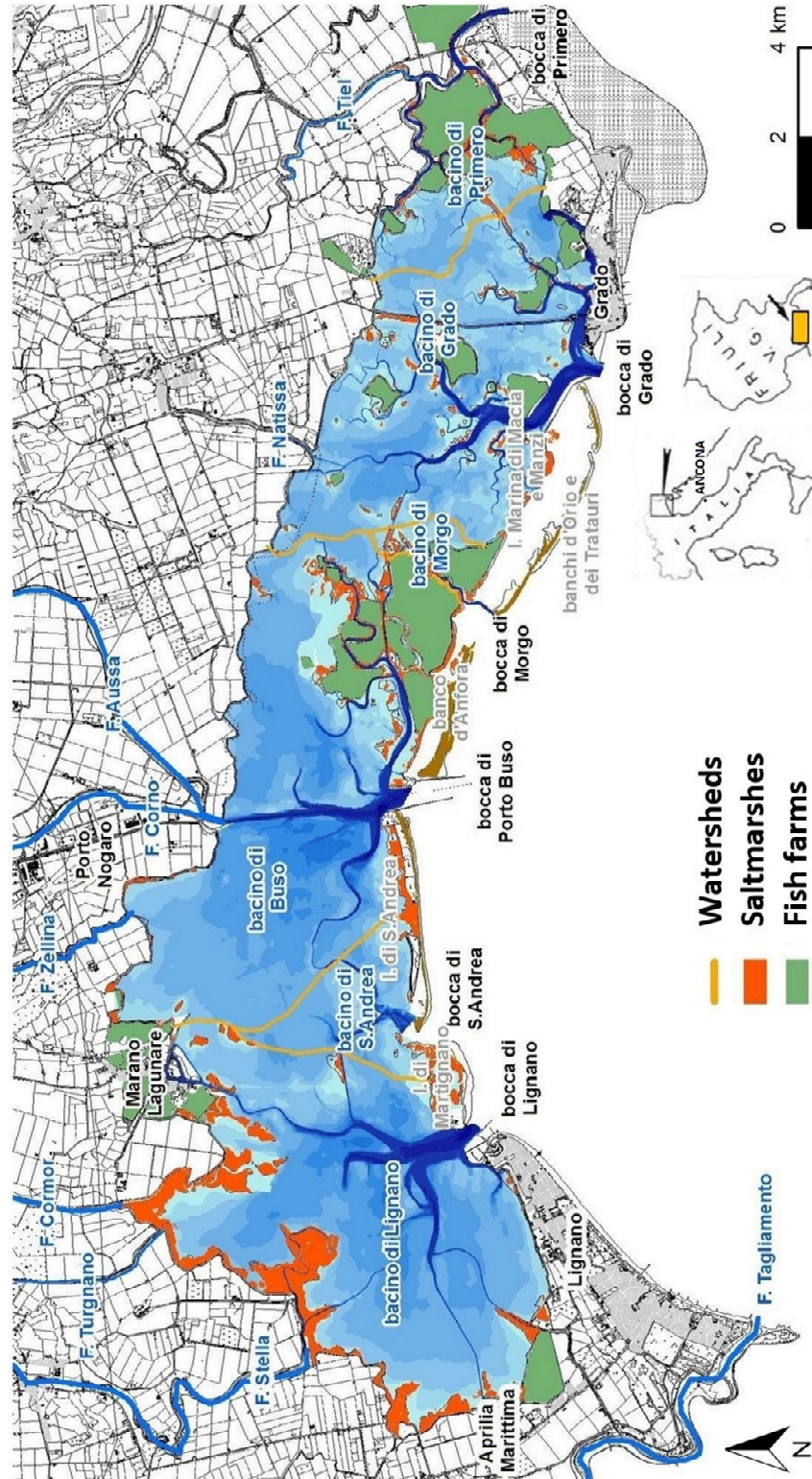


Fig. 2.3 The Marano and Grado Lagoon (from Bezzi, 2013).

The lagoon is divided according by administrative boundaries dating back to the period in which the western part (Marano Lagoon) related to the Kingdom of Italy, while the

eastern one (Grado Lagoon) related to the Austrian-Hungarian Empire (1866-1917, Brambati, 1996). The two sectors have evolved at different time scales. The entire complex formed between 5500 and 2100 years ago. The Marano Lagoon represented the first (embryo) lagoon: it formed progressively through the rapid advancement of the Tagliamento river delta and concomitant formation of barrier islands, following a pulse of sea level, which caused the flooding of the alluvial plain at the eastern side of the river (Brambati, 1983; Marocco, 1991).

Under a morphological point of view, the Marano Lagoon is a simple wide shallow water body dissected by few secondary channels, with intertidal areas limited to the fringing inner margin; the Grado Lagoon is a more complex lagoonal body, due to the presence of a series of positive reliefs (sandy islands) and channel fringing saltmarshes, an irregular hydrographic network, with many secondary channels and creeks (Marocco, 1995).

In the MGL, five main sub-basins are identified, each related to a specific tidal inlet (Dorigo, 1965), as follow: Lignano, S. Andrea, Buso, Morgo, Grado and Primero (Table 2.2). Lignano, S. Andrea and the western part of the Buso sub-basin fall within the administrative limit of the Marano Lagoon, the remnants within the administrative limit of the Grado Lagoon.

Table 2.2 Hydrographic data of the six tidal inlets of Marano and Grado Lagoon (adapted from Fontolan *et al.*, 2007a)

Basin	Lagoon	Tidal prism (x10⁶ m³)	Date of survey and/or reference
Lignano	Marano	40.00	2003
S. Andrea	Marano	3.12	1999 (Segala, 1999)
Buso	Marano	26.30	1960 (Dorigo, 1965)
Morgo	Grado	1.40	1960 (Dorigo, 1965)
Grado	Grado	23.40	2002
Primero	Grado	6.00	1997

During flood tide, the water masses propagate inward and interfere along a line that represents the watershed between each two adjacent basins. In proximity of the tidal watershed, which is generally located at a distance intermediate between two adjacent

inlets, the tidal current velocity reaches a minimum. The watershed lines should not be considered as uniquely determined; each of them could in fact vary in position depending on meteorological conditions and tidal amplitude (Dorigo, 1965).

The sediment input contribution in the lagoon is overall regulated by the Tagliamento and Isonzo Rivers; other minor freshwater tributaries with a very limited solid load flow and influence the hydraulic regime. The main freshwater inputs are: the spring-fed rivers (Stella, Turgnano, Zellina, Aussa-Corno, Natissa, Tiel) and the River Cormor, featuring a mountain watershed and the 30 drainage pumps of the low Friulian plain. In 2009 the Autorità di Bacino Regionale ABR-FVG calculated the mean discharge of the rivers alone as 81.5 m³/s, of which the main contributors are the Stella River (36.1 m³/s) and the Cormor (10.7 m³/s) (Triches *et al.*, 2011). There are no data available regarding sediment load.

The sediment drift by longshore currents is characterized by an overall transport from east to west (Bondesan *et al.*, 1995). A very small amount comes directly from sediment supplies by the Isonzo River; most of the sediment transported alongshore comes from the progressive dismantling of the marine sandbanks in the eastern part of the lagoon, west of the Grado inlet. Due to the presence of the long jetties of Buso Inlet, the material is no longer able to surpass that limit (Brambati, 1970). Only a small amount of sediment comes from the west, from the Tagliamento River to the Lignano Inlet (Brambati, 1970). The S. Andrea barrier represents the only starved island far from the direct sediment contribution due to the longshore sediment supply.

2.2.1 Tide, wind and wave climate

The Northern Adriatic, especially due to its elongated conformation, presents one of the largest tidal ranges in the Mediterranean Sea. The tidal amplitudes range between the minimum values recorded close the amphidromic point, located south of Ancona, and the highest values along the Venetian-Friuli coastlines. Focusing on the study area, tides are semi-diurnal, with a mean range of 0.65 m and spring and neap ranges of 1.05 m and 0.22 m, respectively (Dorigo, 1965). Data on tide propagation inside the entire lagoon are sparse and old. Ferla *et al.* (2008) confirmed the data of Dorigo (1965), who reported that

there is good hydraulic efficiency in the lagoon due to the short propagation delays from the inlets to the lagoon margins, with preserved or sometimes increased amplitudes.

Wind climate in the Northern Adriatic is characterized by a prevalence of winds blowing from the I quadrant, mainly from the ENE (the *Bora*, Carrera *et al.*, 1995). Catani and Marocco (1976), discussing one year of observations, recorded a frequency of about 58% for the winds of this I quadrant (mainly from NE, *Bora* and E, *Levante*) and of 16% for the II quadrant (mainly from SE, *Scirocco* and S, *Ostro*). Current statistics (period 1995-2016) obtained by the elaboration of Osmer-FVG data (www.meteo.fvg.it), confirms the dominance of *Bora* over the *Scirocco* wind, from SE (Fig. 2.4).

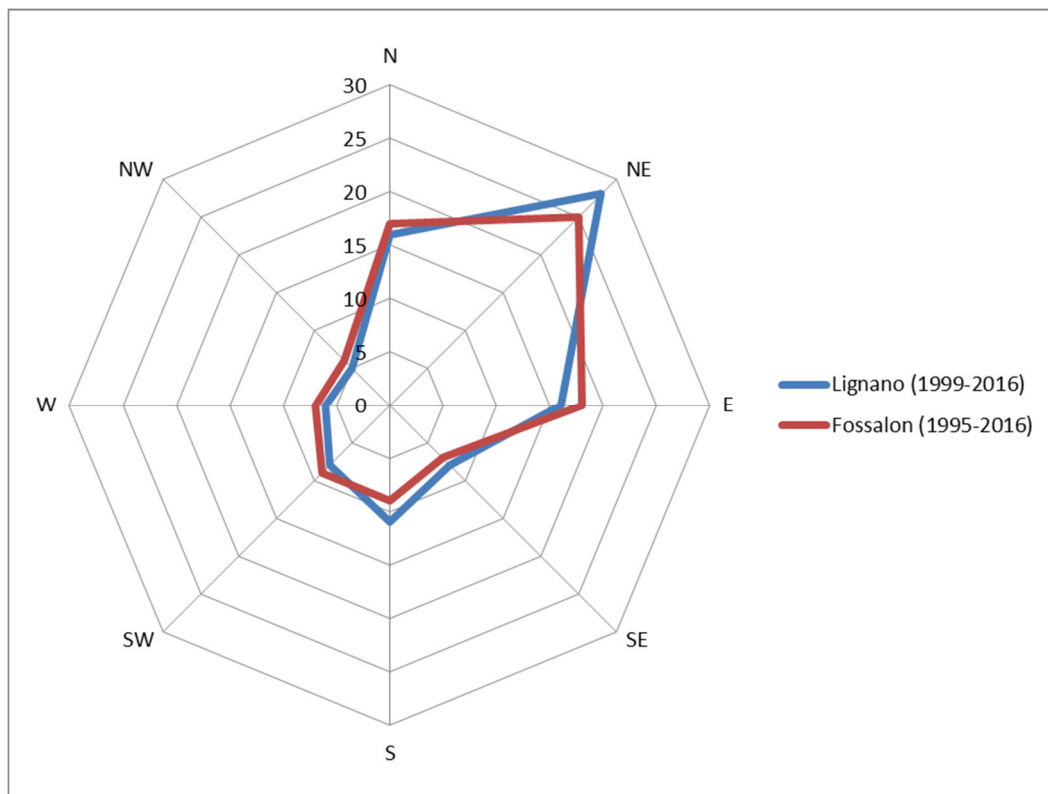


Fig. 2.4 Wind data from the stations of Lignano and Fossalon, along the Marano and Grado Lagoon coastline.

Bora is a cold continental wind and is the strongest wind that affects this part of Italy with gusts reaching 100 km/h and over. *Scirocco*, a southeasterly wet and warm wind, is also important and, after the *Bora*, it is the wind that can reach the maximum speed in this area, due to its long geographical fetch (over 800 km). Periods of persistent *Scirocco*, in concomitance of spring tides, seiches and low atmospheric pressure, can cause a sea surge

up to 160 cm (locally called “acqua alta”). In 1966, water level reached 1.94 m m.s.l. in relation with wind-driven surge, flooding almost the entire coast, towns included. The flooding of 1969 was even worse, with a water level of 2.10 - 2.15 m m.s.l. but the effects were damped by the presence of the reinforced margins (3-m-high) erected along the inner coasts of the lagoon after 1966 (Marocco and Pessina, 1995).

According to Dal Cin and Simeoni, (1994), mean significant annual wave height is lower than 0.5 m, while the maximum offshore wave height, both for *Bora* and *Scirocco* storms, is about 5 m (Cavaleri *et al.*, 1996). Recent analysis from 1958 to 1999 wave data gives a more precise value for the annual-averaged significant wave height, corresponding to 0.27 m (Martucci *et al.*, 2010). Using the complete series of 2000-2003 three-hourly measurements available from a wave gauge located offshore Ancona (Fig. 2.3), an estimate can be obtained of wave energy for the northern Adriatic area in the form of $H_s^2 T^2$ (H_s and T corresponding to the significant wave height and period respectively), and the resulted annual value is 15.61 $m^2 s^2$.

2.2.2 Natural processes and anthropic conflicts

The present configuration of the Marano and Grado Lagoon is the result of a complex interaction between man and the environment, which has led during the time to a progressive transformation of the lagoon, until it becomes a strongly conditioned and controlled system. The analysis of historical maps show how human interventions in the lagoon were numerous and complex, especially during the last century. First of all, the construction of an embankment connecting Grado town to the mainland (1901–1906) isolated the eastern part of the lagoon from the rest of the system (Dorigo, 1965). Successively, the reclamation of territories, since the 1920s, has resulted in the transformation of vast lagoon regions into farmed areas, reducing the lagoonal area by 30% (Gatto and Marocco, 1992). The construction of 70 km of embankments that were raised to an average elevation of 3 m above the m.s.l. along the lagoon perimeter after the disastrous flooding of 1966, further stabilized the lagoonal boundaries. Inside the lagoon basin, the natural hydrography has been changed by the excavation of the Litoranea Veneta (1915-1918), a network of canals that join the Venice Lagoon to the Trieste Gulf,

using the previous existing internal waterways and without exit from the lagoon environment (Dorigo, 1965). In more recent times (1970s), waterways were dredged in order to easily reach the industrial area of Porto Nogaro and the docks of the tourist centres. Finally, the stabilization of Lignano Inlet (works started on 1930s and proceeded through several phases until 1990s), Buso Inlet (1964-1969), Grado Inlet (1927-1934) and Primero (1934) Inlet, slightly altered the water circulation inside the lagoon and the competence of adjacent inlets in term of tidal prism (Brambati, 1987).

The stabilization of Buso Inlet through rigid jetties and the dredging of a straight connection between the inlet and the mainland (straightening the former main channel until the Aussa-Corno mouths, in 1970) to ensure greater draft for navigation (Brambati, 1987; 1996; Ferla *et al.*, 2012) were responsible for a strong reduction of S. Andrea and Morgo tidal prisms and the enlargement of the tidal prism of the adjacent Buso Inlet from 27% to 35% of the total water volume exchanged by the system. This is confirmed, in absolute terms, by an increase of the tidal prism from 25×10^6 to $40 \times 10^6 \text{ m}^3$ (Ferla *et al.*, 2012). In contrast, the Lignano tidal prism reduced from 44% to 35% of the total volume. Despite these significant changes, the overall value of tidal prisms of the system remained substantially the same (Ferla *et al.*, 2012). Nevertheless, Marano and Grado Lagoon multi-inlet system shows a quite good resilience and equilibrium being still able to react and counteract external forcing like natural (floodings) and anthropogenic interventions.

2.1 Final remarks

These two different environments will be further described in the following chapters. Different methodologic-approaches were used to investigate the behaviour and the evolution over time of these two inlets, Ancão and S. Andrea, confronting them also with the hydrodynamic scenario. Brief considerations about the results obtained for each environment are forwarded and a more deep overall discussion is presented in Chapter 5.

3.

The case of Ria Formosa: relocation and life cycle of an artificial opening inlet allowed migrate naturally

3.1 Study area: Ancão Inlet

The Ancão Inlet is the westernmost opening of the Ria Formosa multi tidal inlet system. It presents a cyclic eastward migration, recording three cycles between 1945 and the present, which include western relocations (Vila-Concejo *et al.*, 2002; Popesso *et al.*, 2016). Its behavior reflects the interaction between the regular water circulation and the continuous displacement of the channel as it migrates. Furthermore, its migration represents a challenge for who use this channel as a navigational route because of the recurring changes in the position of the ebb and flood deltas and the main channel.

The Ancão Inlet migration pattern is within the “High-Energy Flank” type (Fig. 3.1; Vila-Concejo *et al.*, 2002): the updrift margin of the inlet is built approximately at the same rate as the downdrift margin is eroded and both ebb and flood-tidal deltas migrate at approximately the same rate as the inlet channel (Pilkey *et al.*, 1989). Furthermore, following the studies of Vila-Concejo *et al.* (2002), about the first two cycles of the inlet, the main channel width is almost constant and therefore independent of inlet migration, except during the last stages of inlet closure. Research on the last Ancão Inlet cycle has shown that the channel width varied many times, especially during the early stages (Popesso *et al.*, 2016).

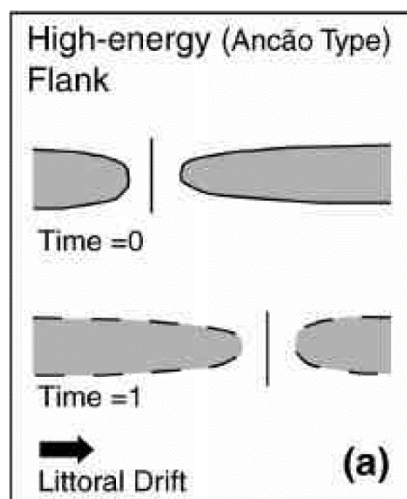


Fig. 3.1 Ancão Inlet migration patterns (adapted from Vila-Concejo *et al.*, 2002).

In 1996, the Ancão Inlet reached its limiting position (Vila-Concejo *et al.*, 2004) and was partially closed by natural infilling and meandering. Following the adopted soft protection program (Dias *et al.*, 2003), on 23 June 1997, the Portuguese Institute of Nature and

Conservation (ICN) then relocated the inlet 3500 m to the west of its closing position, in order to improve water exchange at the western part of the Ria Formosa lagoon system. Vila-Concejo *et al.* (2003) presented a four stage conceptual model for the general natural evolution of such artificially opened inlets (Fig. 3.2): stage 1 describes inlet immediately following artificial opening; stage 2 corresponds to the developed inlet after reaching dynamic equilibrium; stage 3 represents the situation of a “natural” inlet after migration induced by normal longshore drift; and, stage PS “post-storm” represents the inlet morphological features after high energy conditions. According to Vila-Concejo *et al.* (2003; 2004), after an initial instability due to the capture of the tidal prism, the inlet reached dynamic equilibrium one year after opening (July 1998). The eastward migration started in January 1999 after a storm event (Fig. 3.2).

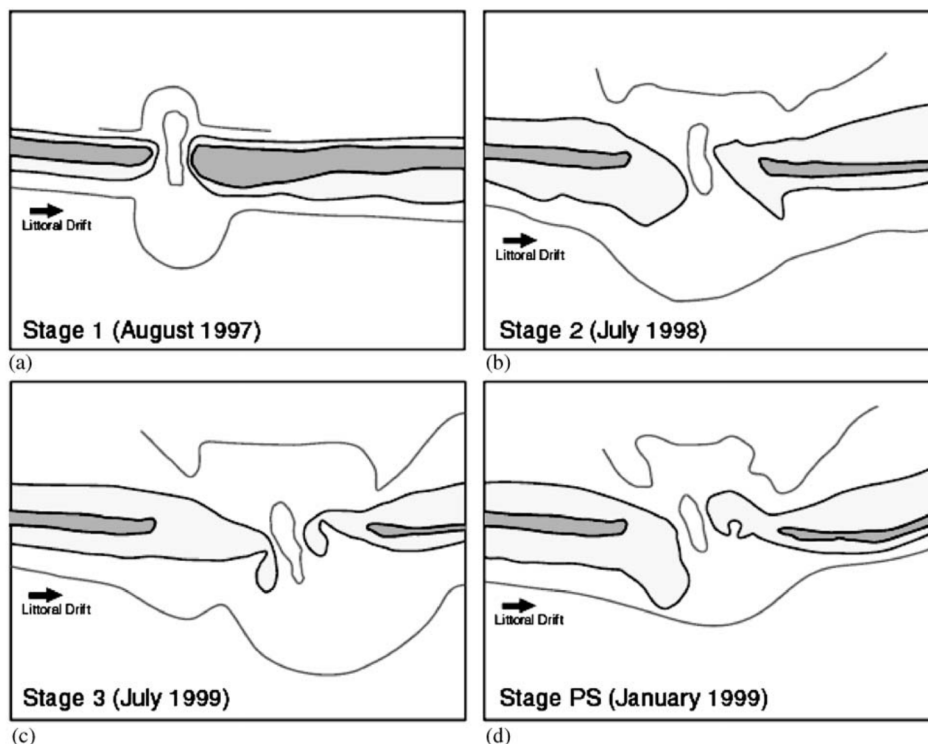


Fig. 3.2 Four stage conceptual model for the natural evolution of Ancão Inlet, after relocation (adapted from Vila-Concejo *et al.*, 2003).

The new Ancão Inlet was monitored since its relocation in 1997 and it has been found to resemble the former inlet in both its hydrodynamic characteristics and morphology (Williams *et al.*, 2003). According to Morris *et al.* (2001; 2004), the Ancão Inlet shows

characteristics of both a tide- and a wave-dominated inlet, as it has a well-defined deep main channel and a relatively small ebb-tidal delta.

During the last migration cycle, storm events breached the barrier updrift (2005) and downdrift (2010 and 2015) of the Ancão Inlet position, forming a new inlet that competed with the older one for dominance of the tidal prism. In 2005, the strong effect of a W-SW Storm (Vince storm) breached the updrift barrier. The new inlet remained open for only three weeks and then closed naturally; in 2010, the new inlet captured a great volume of tidal prism and forced the older inlet to close. “Inlet Jump” is the term used by Popesso *et al.* (2016) to indicate this change in position without migration. Finally, the new downdrift-barrier breach of 2015, caused by an energetic storm event, resembled the event that occurred in 2010 and the breach persisted at the expense of the older inlet. At that time, the inlet reached its final migration position, close to the ending site of the previous migration cycle, and a new western relocation was carried out on 27th November 2015, near to the 1997 opening location.

The adjacent areas of Ancão Inlet, Ancão Peninsula and Barreta Island, are narrow and consist of narrow sand barriers crowned by a single dune ridge that can reach heights of 7 m msl (Vila-Concejo *et al.*, 2002). The updrift margin (Ancão Peninsula) is a prograding spit owing to the net easterly sediment transport (Williams *et al.*, 2003). Inlet migration process is directly related to this fact. As in other tidal inlet systems, the underlying, first order driver of Ancão Inlet evolution is related to storm events (Morris *et al.*, 2001; Popesso *et al.*, 2016). Morris *et al.* (2001) described different morphological responses of Ancão Inlet and adjacent areas to the different hydrodynamic conditions, considering the status of the inlet as a tide-dominated or wave-dominated systems, encompassing relationships between inlet morphology and the present and/or antecedent hydrodynamic conditions. Those authors observed that a combination of large waves during spring high tide resulted in the most dramatic erosion of the vegetated areas along the downdrift margin. Once these areas erode, the inlet migrates rapidly.

Based on the hydrodynamic regimes defined by Morris *et al.* (2001), Williams *et al.* (2003) recognized three morphological states of Ancão Inlet (Table 3.1). A storm forces morphological changes so that the inlet moves from an essentially ebb-tidally dominated condition to a wave-dominated condition (MOR2, Table 3.1). Following passage of the

storm, the inlet must then adjust its morphology back to a configuration determined by fair-weather conditions (MOR1, Table 3.1).

Table 3.1 Three morphological states based on the three hydrodynamic regimes of Ancão Inlet (adapted from Williams *et al.*, 2003). H1 – non-storm conditions (A and L subscripts traduce mean Atlantic, W-SW and “*Levante*”, E-SE, wave approach, respectively), H2 – storm conditions for W-SW waves and H3 – storm conditions for E-SE waves.

Morphological state and frequency	Wave conditions
MOR 1 Ebb-tidally dominated period Frequency \cong 99 % (H1 _A \cong 85%, H1 _L \cong 15%)	H1 _A * 180°< θ <270°, H _s <1 m, 4s <T _p <10 s H1 _L * 90°< θ <180°, H _s <1 m, 4s <T _p <10 s
MOR 2 Post-storm wave-produced period Frequency \cong 0.6 % (Flood-dominated)	H2 245°< θ <275°, H _s > 3 m, 8s <T _p <18 s H3 120°< θ <140°, H _s > 3m, 6s <T _p <14 s
MOR 3 Transitional period Frequency \cong 0.3 %	Establishment of H1 _A conditions

Using video techniques, Morris *et al.* (2004) also proposed a conceptual morphological model for inlet seasonal behavior with three model stages (post-storm, transitional and extended calm morphological stage) that are closely related with the incident waves.

3.2 Material and methods

Since the 1997 inlet relocation, a monitoring program has been in force to study its evolution. Between the relocated inlet’s opening in June 1997 and May 2015, twenty topo-bathymetric surveys were performed (Table 3.2, Vila Concejo *et al.*, 2006; Pacheco *et al.*, 2007; Popesso *et al.*, 2016), including the main channel area and, if the wave conditions permitted, the ebb and flood-tidal delta areas too. The data from the surveys performed at the time of the “inlet jumps” (2010 and 2015) have been divided in two parts: the data relative to the old inlet (a) and the data relative to the new inlet (b). As the exact day of breaching is not known, these dates were arbitrarily assigned, based on the knowledge of previous strong storm events and on the survey date. A *LIDAR* survey was performed at the end of May 2011 and used to improve the database for this work.

Table 3.2 Topo-bathymetric and *LIDAR* surveys performed at Ancão Inlet during the investigated period.

Survey	Date	Days since opening
0	23-06-1997	Not used
1	13-08-1997	0
2	07-04-1998	237
3	24-07-1998	345
4	07-10-1998	420
5	18-12-1998	492
6	06-01-1999	511
7	31-05-1999	656
8	28-07-1999	714
9	10-11-1999	819
10	20-03-2000	950
11	02-06-2000	1024
12	29-09-2000	1143
13	25-01-2001	1261
14	24-04-2001	1350
15	25-07-2001	1442
16	01-12-2002	1936
17	04-06-2004	2487
18	05-05-2006	3187
19a	15-04-2010	4628
19b	26-04-2010	4639
20 (LIDAR)	31-05-2011	5039
21a	04-03-2015	6412
21b	19-05-2015	6488

An accurate topography of the adjacent barriers and of the swash zones was carried out using a total station and a Real Time Kinematic *DGPS*. Navigation and bathymetry transects, more or less perpendicular to the shoreline, were measured using *HYPACK*® 4.3a Gold software, by connecting the *RTK-DGPS* and an echo sounder to a laptop. The *RTK-DGPS* was synchronized with the echo sounder and measurements were taken at a frequency of 1 Hz. Thus, the recorded depth was immediately corrected for water level variations (i.e., tides and waves). During the last survey (May 2015), due to the rough sea conditions, the bathymetry was done following alongshore lines (miming the contour lines), from a depth of 12 m to the shore; the interval between the lines was about 2 m. Each survey was carried out over 2 days during spring tide conditions; the intertidal + supratidal areas were surveyed during low tide, while the subtidal + intertidal areas were

surveyed by boat, during high tide, maximizing the data overlap and permitting a control on accuracy. Due to a scarcity of data (not the entire inlet area was covered), the first survey of June 1997 was not used; as such, the August 1997 survey is herein considered the starting point for the evaluation of the Ancão Inlet evolution.

The topographic and bathymetric datasets were interpolated using the software *Surfer 9*, to produce continuous bathymetric surface maps, following the quality control methods suggested by Hicks and Hume (1997). Various statistics computed for the errors can be used as a quantitative and objective measure of quality for the gridding method. After an interpolator quality check, through the cross-validation function, the Kriging method was selected as the best interpolator (Table 3.3). The spacing was based on data density and spatial distribution. A local metric coordinate system known as the Portuguese Melriça Grid was used for the maps; elevation is always referred to mean sea level.

Table 3.3 Residual statistics using the cross-validation function for the different interpolators. With: Kr=Kriging Method, TWLI=Triangulation with Linear Interpolation Method, IDTAP=Inverse Distance to a Power Method, RBF=Radial Basis Function Method, MC=Minimum Curvature Method.

Statistics of residuals							
Gridding Method	Number of datapoints	Mean (mm)	Minimum (m)	Maximum (m)	Std Dev (mm)	Skewness	Kurtosis
Kr	726	0.0156	-3.5565	3.0098	0.6863	-0.2830	2.4751
TWLI	726	0.0428	-3.9966	3.6057	0.7488	-0.2527	3.8920
IDTAP	726	0.2790	-4.5662	5.3912	1.5631	0.0624	0.7258
RBF	726	0.0846	-18.4394	31.1909	2.7684	3.7498	44.4010
MC	726	-1.0332	-398.2783	71.9114	21.1979	-13.9382	224.4634

Inlet morphological parameters such as minimum cross-sectional area (A_c), inlet width (I_w), maximum depth ($MaxD$), thalweg orientation (O) and migration (M) were determined following the suggestions of the Coastal Engineering Manual (Seabergh, 2002, Table 3.4). On each map, the inlet channel was first defined sketching ten profiles at equal distance from each other through the inlet cross-section, considering the morphology of each situation (e.g., the barrier's width, Fig. 3.3). The direction and the

spacing of the profiles were chosen following the shoreline orientation and the width of the adjacent barriers, respectively. For this reason, in some maps, the profiles are not perpendicular to the thalweg direction and the spacing among them varies from 10 m to 20 m. After the extraction of the data profiles by *Surfer 9*, they were transferred to *Matlab R2009b* in order to extract the parameters Ac , I_w and $MaxD$. The channel orientation O was computed using a wider area than that covered by the profiles. In some more difficult cases, like in Fig. 3.3, it was necessary to measure the mean orientation between segments that covered the channel pathway.

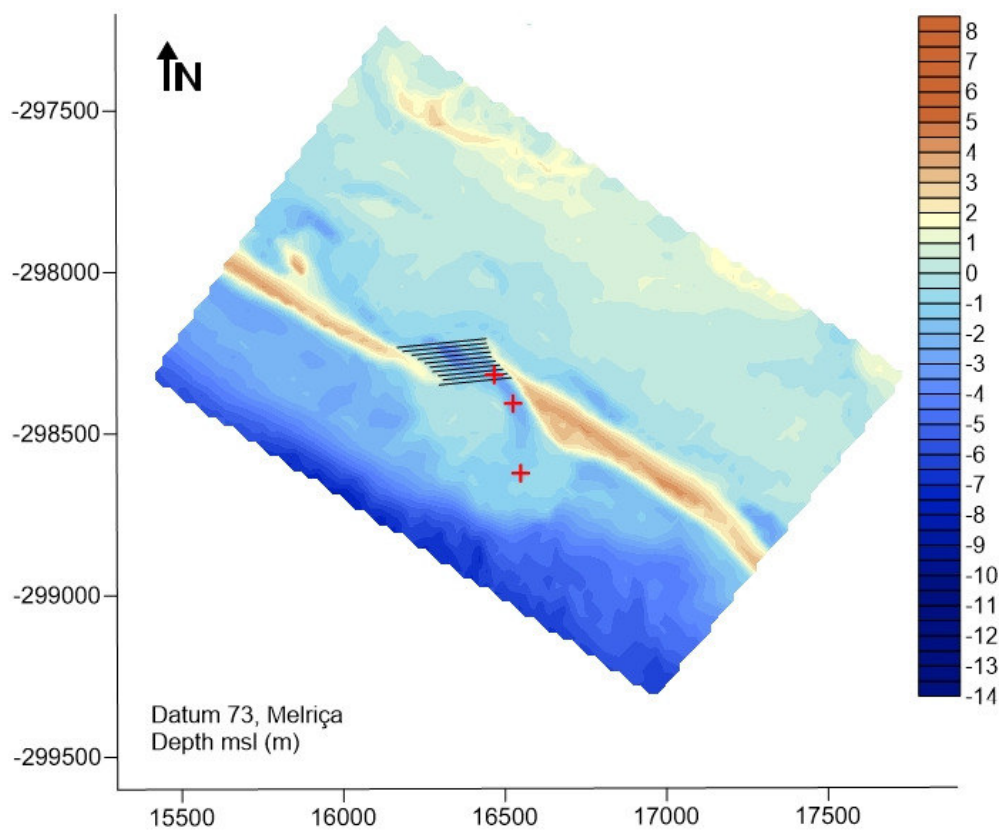


Fig. 3.3 Example of bathymetric surface maps (May 2011), with the sketch of ten profiles (lines in black) to define the minimum cross sectional area and the points (red crosses) to compute the mean orientation between segments that covered the channel pathway.

Inlet migration M was computed by determining the metric difference in the XY coordinates of the maximum depth $MaxD$ at the minimum cross-sectional area Ac between each survey and the reference (August 1997) inlet position. The migration distances between consecutive surveys were then determined and added to obtain the

cumulative (progressive) migration. Different signs were used to refer to eastward (positive) and westward (negative) migration.

The inlet cross-sectional area was used as a tidal prism proxy that could be estimated using the empirical formula developed by Jarrett (1976) for the United States Atlantic Coast (Table 3.4):

$$A_c = 3.039 \cdot 10^{-5} P^{1.05} \quad (\text{Eq. 3.1})$$

where A_c is the minimum cross-sectional area (m^2), measured for each survey, and P is the corresponding tidal prism (m^3).

Wave data from the Instituto Hidrográfico directional wave-rider buoy offshore of Cape Santa Maria (Fig. 2.2, $36^\circ 54.3' \text{ N}$, $7^\circ 53.9' \text{ W}$, in a depth of 93 m) was used in this study (1997–2015). The wave buoy recorded values representing significant wave height (H_s), mean peak period (T_p), and mean wave direction ($^\circ$) for 20 minutes at every three hours, except during storms, when data were recorded at every half hour. Wave data were interpolated to give hourly data and subdivided into intervals between consecutive surveys. The total percentage of missing data was about 3%. To individualize each single high-energy event, the storm threshold used in the present study refers to high-energy events with $H_s \geq 2.5$ m, with a minimum duration of three hours above the storm threshold and 24 hours between consecutive $H_s \geq 2.5$ m. A lower threshold (2.5 m) than proposed by Pessanha and Pires (1981) has been chosen in order to extend the amount of data and to not consider only the extreme cases but also the “normal” storms.

In order to consider the tidal height and the storm surge effects, hourly total water level data were collected from the Spanish gauges of the Puertos del Estado (www.puertos.es): Huelva gauge, now dismissed and substituted in the same place by Huelva5 (37.13° N , 6.83° W), Bonanza, now dismissed and substituted in the same place by Bonanza2 (36.80° N , 34° W). Four gauges at two nearby positions were used in order to cover the entire period investigated. Sometimes the gauges presented missing data for short periods but combining the information by more than one gauge it was possible to reduce the lacking data to less than 1%. The hourly water level data coming from different gauges had different reference level, therefore they were all homogenized, reporting them to the

same reference level (identified in Huelva5 gauge level reference), through a correlation analysis between each couple of data-gauge (Fig. 3.4).

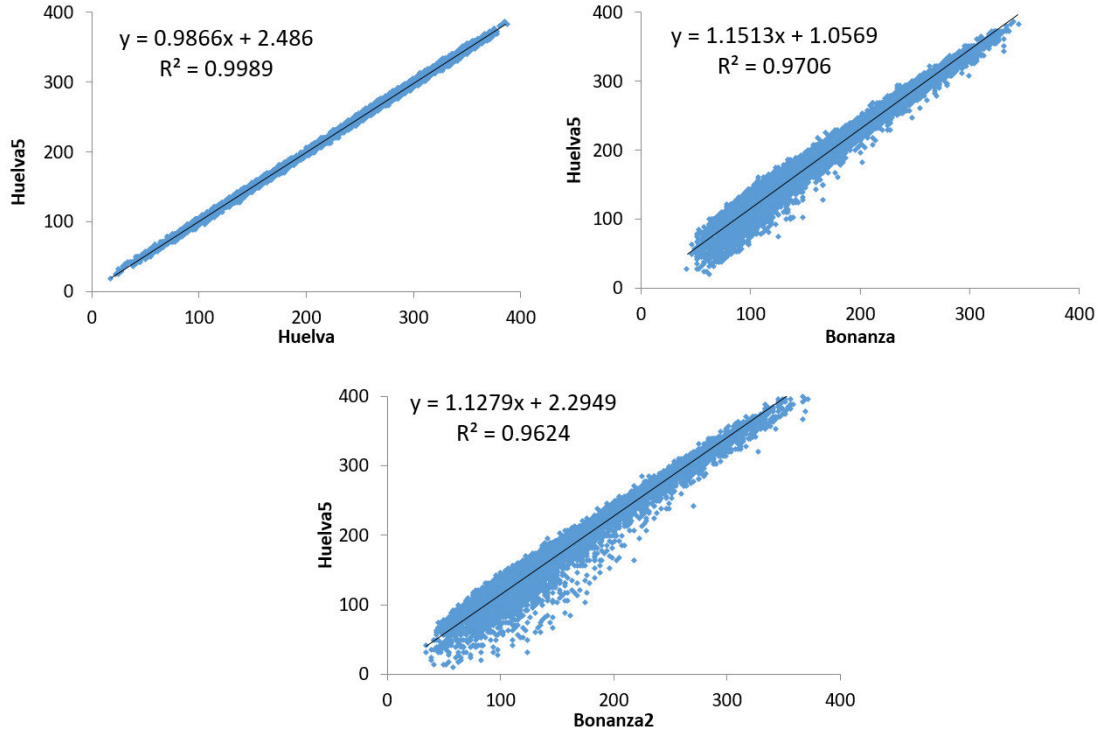


Fig. 3.4 Correlations and tendency lines for data coupling from different gauges.

After that, the hourly water level data were reported to the local datum (Zero Hidrografico Portuguese) that corresponds to about -2 m below the m.s.l.

Mean wave power Wp was evaluated for each storm event (Eq. 3.2):

$$Wp = EC_g \quad (\text{Eq. 3.2})$$

$$\text{with } Ew = \frac{1}{8} \rho g H_s^2 \quad \text{and} \quad C_g = \frac{1}{4\pi} g T_p$$

where Ew is the wave energy (J/m^2), ρ is the water density (assumed as $1,026 \text{ Kg/m}^3$), g is the acceleration due to gravity (9.8 m/s^2), H_s is the significant wave height (m), C_g is the group velocity (m/s) and T_p is the peak period (in seconds) associated to that H_s . Due to the orientation of the barrier system, Wp was divided according to three different wave directions ($\leq 200^\circ$, $200^\circ < \text{dir} < 220^\circ$ and $\geq 220^\circ$), in order to assess their possible different impacts on inlet migration. Each Wp was then multiplied by the relative storm duration (in seconds) to obtain a total wave power value for the single storm ($Wp\#$). Inlet migration

results were then analyzed by comparison with storms $Wp\#$, separated into three directions, to investigate the plausible relation between them. After that, the ratio $P/\sum Wp\#$ was evaluated, where P (tidal prism) is assessed for each survey and $\sum Wp\#$ is the sum of $Wp\#$ of storm events coming from the dominant longshore drift direction ($\geq 220^\circ$, as a proxy of the potential eastward longshore sediment transport), recorded between two surveys.

According to Morris *et al.* (2001), tidal range can exert an important control on the erosion of barrier islands. A combination of large waves and high tides can result in a strong weakening of the area close to the inlet, thus promoting migration. The authors normalized the wave power calculated with hourly wave data, with the tidal level range (Eq. 3.3):

$$Wp_n = Wp \left(\frac{\eta_{dtr}}{\eta_{dtr}^*} \right) \quad (\text{Eq. 3.3})$$

where Wp is the wave power (W/m), η_{dtr} is the daily tidal range (m) and η_{dtr}^* is the maximum tidal range (m). It means that at spring tides $Wp_n \sim Wp$ and at neap tides $Wp_n \sim 0.3P$.

For the purposes of this work, it was decided to use the hourly total water level data instead of the tidal range, to take into account also the contribution of storm surges. Eq. 3.3 was computed with $h\eta_{dtr}$ as the hourly water level and $h\eta_{dtr}^*$ as the maximum water level reached during the period of time examined (since 1997), obtaining, at the end, a normalized wave power (Wp_n) value for each storm event. Similarly to Wp , Wp_n was multiplied for the storm duration (in seconds), thus obtaining $Wp_n\#$.

The existence of a significant dependence between morphological parameters and hydrodynamic ones was investigated. In statistics, the level of significance is, in the simplest case, defined as the probability p to accept or reject the null hypothesis. The most used significance levels are 5%, 1% and 0.1%, corresponding to confidence levels of 95%, 99%, and 99.9%. If the hypothesis test gives a p-value less than the significance level, the null hypothesis is rejected and these results are reported as 'statistically significant'.

The concept tested is that inlet evolution (and associated morphological parameters) during a certain period (interval between two consecutive surveys) is the result of a

combination of the hydrodynamic factors affecting the coast during that period. Following this idea, within the time interval between two consecutive surveys, the differences between morphological data values such as Ac , Iw , $MaxD$ and O (as already expressed) were taken into account and correlated with the sum of $Wp\#$ and $Wpn\#$ for all storm events generated within the same period, previously distinguished in the three main directional classes ($\leq 200^\circ$, $200^\circ < dir < 220^\circ$, $\geq 220^\circ$). The difference between M (migration) within two consecutive surveys was also correlated with the hydrodynamic parameters. *Pearson* and *Spearman* correlations were chosen to identify possible dependences between the couples of parameters, using the three above-mentioned levels of probability to test the significance of the correlations.

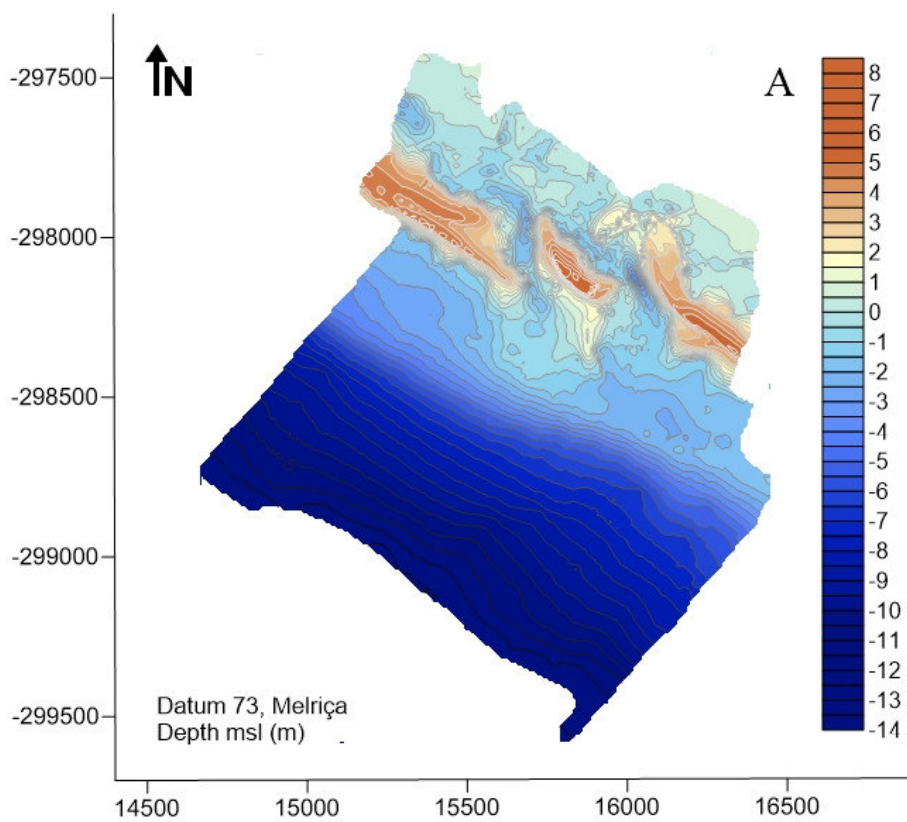
3.3 Results

Two new topo-bathymetric surveys as well as the *LIDAR* survey were added to the surveys already analysed by Vila Concejo *et al.* (2006) and Pacheco *et al.* (2007): April 2010, May 2011 (*LIDAR*) and May 2015 (

Fig. 3.5, A,B,C). The surveys of 2010 and 2015 illustrate the particular situation of downdrift breaching (that resulted in a “jump”), where two inlets compete for the same tidal prism. Being two channels, they were treated as if they were two different surveys (Table 3.4).

In April 2010 (Fig. 3.5 A) both inlets presented a NW-SE-oriented thalweg. The old inlet (on the left) shows a small ebb-tidal delta; the flood delta of the new inlet (on the right) is occupied by the breached/overwashed sediments. A narrow spit on the downdrift side of the old inlet was also present. Furthermore, both the updrift and the downdrift sides were characterized by strong sediment accumulation, for both inlets. The 2011 channel (Fig. 3.5 B) also presented a very oblique orientation; in some points it seemed parallel to the shoreline. It had a large Ac but $MaxD$ was not very deep. Both the updrift and downdrift sides were very narrow and with a reduced elevation. The lengthening of the updrift side, due to the growth of a new spit, induced the channel to shift toward the opposite flank, making the thalweg orientation almost parallel to the shoreline. Four years later, probably as a consequence of a succession of high energy events, it is possible to

observe the downdrift side breached in two points, thus separating two small islands (Fig. 3.5 C). The island at the back of the western side is thus the remnant of the former downdrift barrier. Here the breach evolved rapidly into a channel that rectified and was naturally brought back to a shore perpendicular orientation (see the inlet on the left in Fig. 3.5 C). Later, likely due to an event during the end of February 2015, the downdrift side was further breached, creating a new inlet (inlet on the right in Fig. 3.5 C) showing quite a large channel and hooked sides.



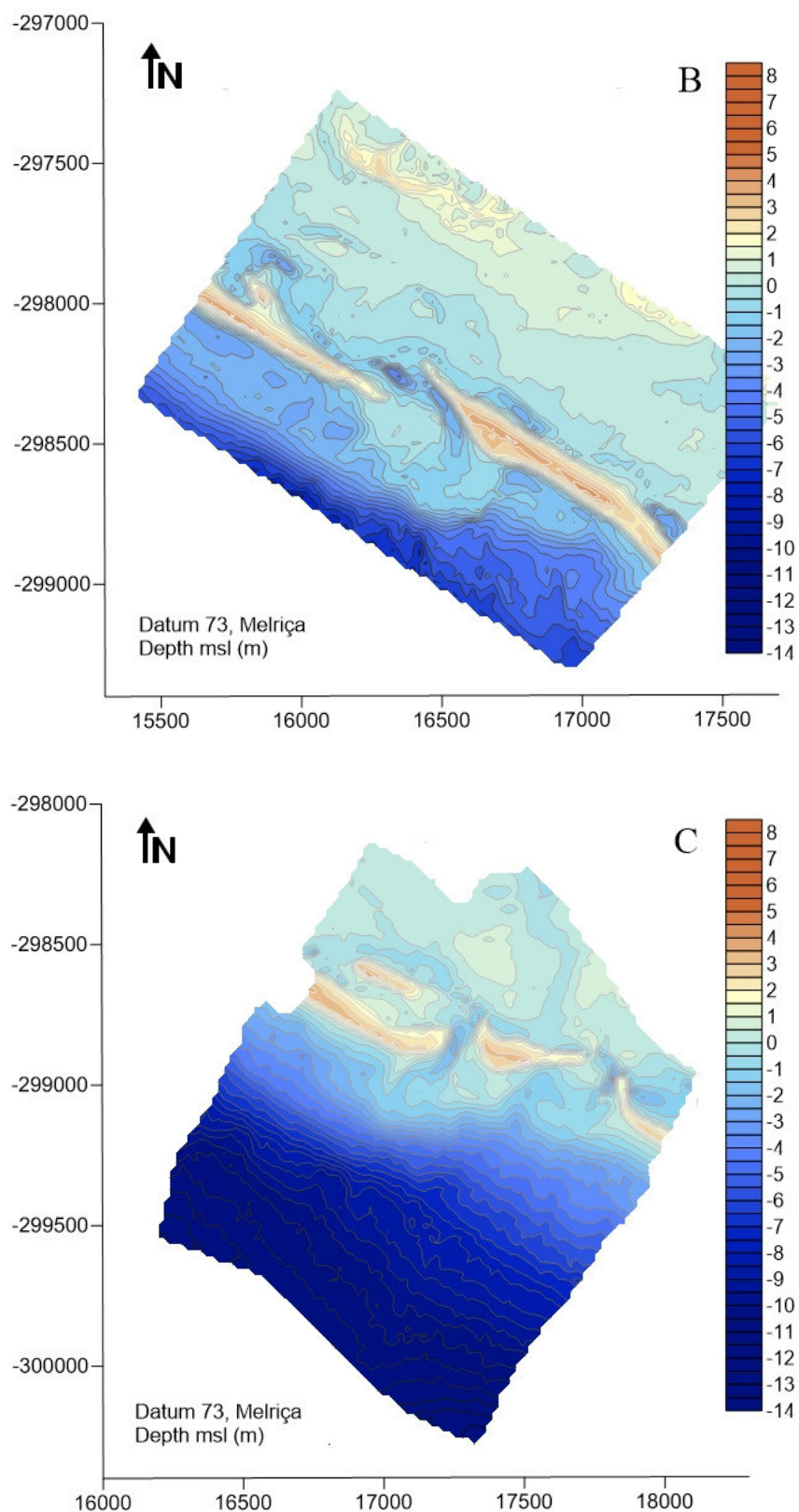
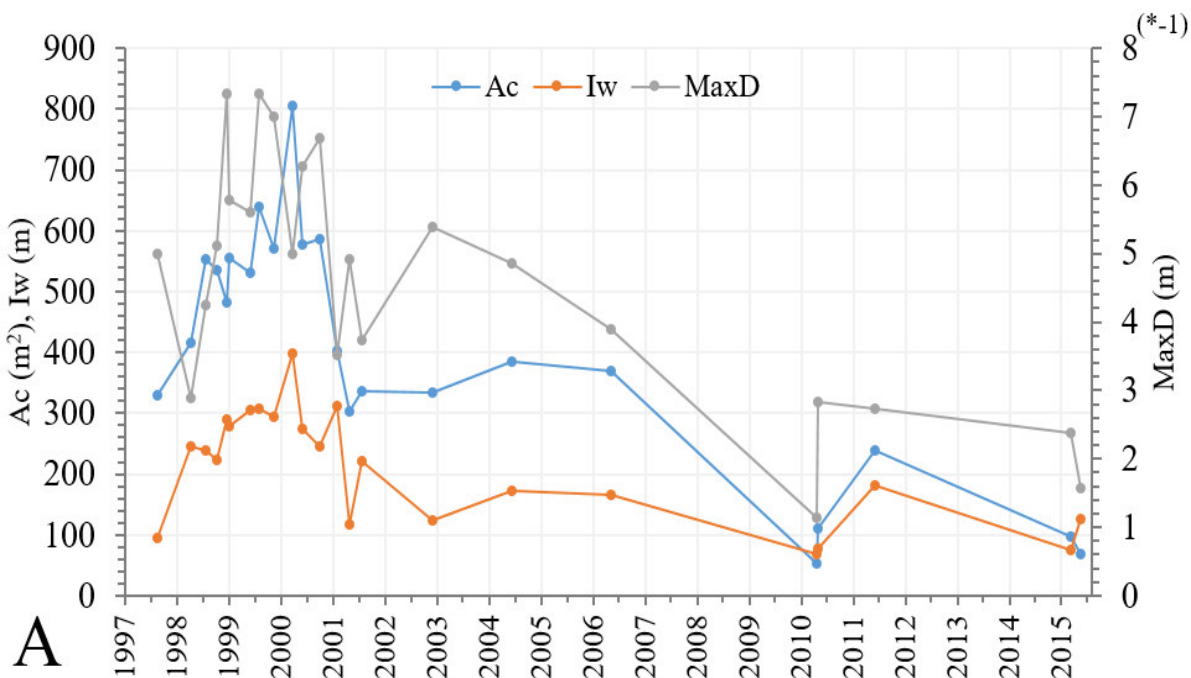


Fig. 3.5 Topo-bathymetric maps corresponding to the three new surveys of April 2010 (A), May 2011 (LIDAR survey, B) and May 2015 (C).

The Ac , Iw and $MaxD$ trends are shown in Fig. 3.6A. Ac and Iw display a similar tendency along time as the increase/decrease of one involves the increase/decrease of the other one (Fig. 3.6A). $MaxD$ becomes deeper when Ac and Iw increase and, viceversa, shallower when a decrease in Ac and Iw is recorded (Fig. 3.6A). The migration trend appears connected with the other parameters (Fig. 3.6B), as the beginning of a regular eastward migration corresponds, more or less, with a decreasing in the Ac , Iw and $MaxD$. All of these extracted parameters highlight an initial period of oscillation (until the year 2000), followed by a continuous and more regular tendency (Fig. 3.6A-B).



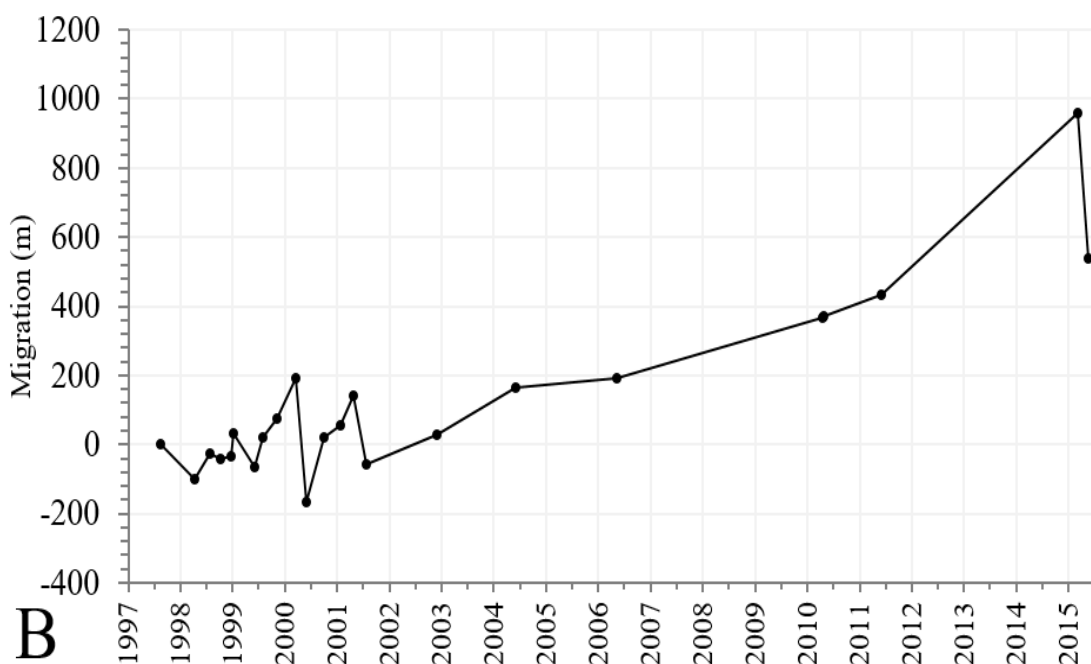


Fig. 3.6 A) Minimum cross sectional area A_c , inlet width I_w and maximum depth $MaxD$ trends and B) migration tendency, for the last Ancão Inlet cycle.

The data described in the previous paragraphs are shown in Table 3.4, for the entire group of 20 surveys. As a consequence of the before mentioned A_c trend, an initial increase in P is highlighted, followed by a progressive decrease after the 2000s (Table 3.4). The orientation of the thalweg O seems not to follow any specific tendency, varying many times during the period investigated (Table 3.4). The M trend and the $cum M$ illustrate the early period of oscillation of the inlet position after the relocation, migrating both eastward and westward. After that, an eastward, very fast migration is recorded (Table 3.4).

Table 3.4 Data of minimum cross sectional area (A_c), tidal prism (P) computed according the empirical relationship by Jarrett (1976), inlet width (I_w), maximum inlet depth, measured on A_c ($MaxD$), thalweg orientation (O), migration (M) and cumulative migration ($cum M$). The – sign in M denotes a westward migration. The new surveys are highlighted in yellow.

	Date	A_c	P	I_w	$MaxD$	O	M	$cum M$
		m ²	m ³	m	m	°	m	m
1	13/08/1997	330	5,018,091	94	-5	55	0	0

2	07/04/1998	415	6,248,628	246	-3	53	-102	-102
3	24/07/1998	553	8,205,152	238	-4	55	-24	-126
4	07/10/1998	535	7,947,192	224	-5	75	-40	-167
5	18/12/1998	483	7,212,857	290	-7	54	-35	-202
6	06/01/1999	555	8,232,149	279	-6	67	33	-169
7	31/05/1999	531	7,897,676	305	-6	15	-63	-233
8	28/07/1999	639	9,414,948	307	-7	75	19	-214
9	10/11/1999	571	8,462,913	295	-7	28	74	-139
10	20/03/2000	804	11,730,453	399	-5	6	193	53
11	02/06/2000	577	8,548,417	275	-6	3	-167	-114
12	29/09/2000	586	8,672,900	245	-7	16	20	-94
13	25/01/2001	402	6,060,157	311	-4	42	57	-37
14	24/04/2001	302	4,614,839	118	-5	33	142	105
15	25/07/2001	337	5,123,188	221	-4	27	-56	49
16	01/12/2002	333	5,066,418	124	-5	6	30	79
17	04/06/2004	384	5,797,142	173	-5	351	165	243
18	05/05/2006	369	5,583,217	166	-4	21	190	434
19a	15/04/2010	52	866,498	68	-1	348	366	800
19b	26/04/2010	110	1,756,518	77	-3	350	370	1170
20	31/05/2011	239	3,693,923	182	-3	340	434	1604
21a	04/03/2015	98	1,581,996	76	-2	39	958	2561
21b	19/05/2015	69	1,130,816	125	-2	35	540	3101

Table 3.5 shows wave-climate data obtained for the study area between August 1997 and May 2015, divided into summer (April-September) and winter (October-March) intervals. Results show that during winter mean significant wave heights (H_s) and peak periods (T_p) are higher than in summer, indicating the higher frequency of swell conditions. Under both summer and winter conditions, incident waves from the west ($\geq 220^\circ$,

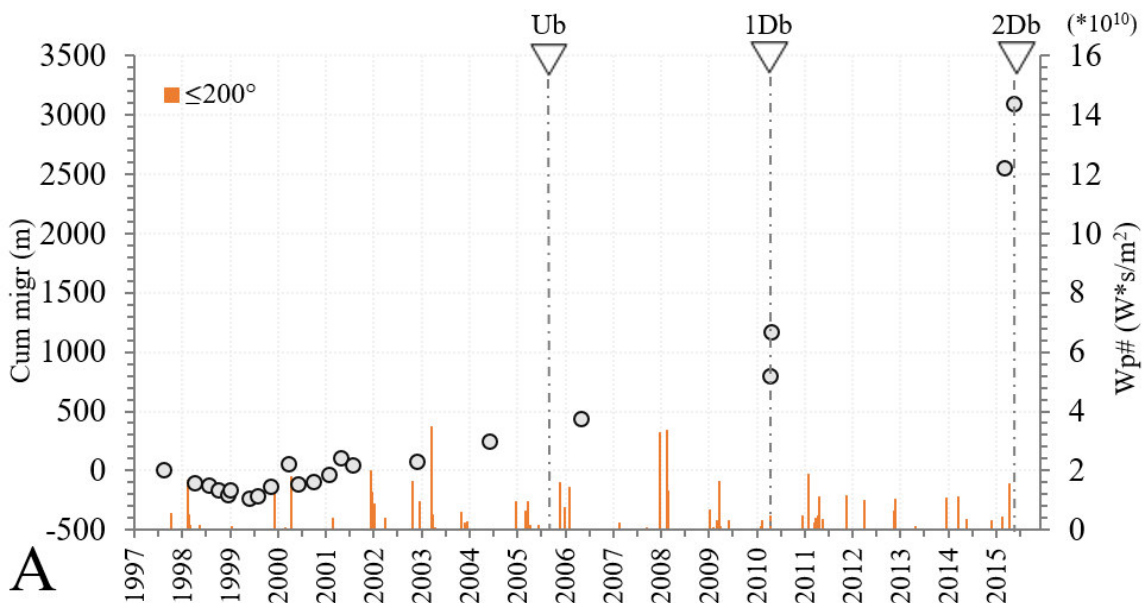
Table 3.5) are dominant while southeast conditions (*Levante*) are infrequent ($\leq 200^\circ$,

Table 3.5). In general, predominant wave directions are from the W-SW ($\geq 220^\circ$), approximately 70%, while waves coming from the SE ($\leq 200^\circ$) only account for 27% of the observations. Percentages of waves from $200^\circ < \text{dir} < 220^\circ$ are limited to only 3.5%. This data are comparable with the data from September 1986 and December 1993 collected by Costa (1994, Table 2.1) and later by Costa *et al.*, (2001).

Table 3.5 Mean and max values of H_s (significant wave height) and T_p (peak period), and percentages of waves occurrence from three directions ($\leq 200^\circ$, $200 < \text{dir} < 220^\circ$ and $\geq 220^\circ$), between August 1997 and May 2015.

	Mean		Directions (%)		
	H_s (m)	T_p (s)	$\leq 200^\circ$	$200^\circ < \text{dir} < 220^\circ$	$\geq 220^\circ$
Summer	0.8	7.1	28.0	3.3	68.7
Winter	1.2	9.5	25.8	3.6	70.5
Entire period	1.0	8.3	26.9	3.5	69.6

Fig. 3.7 A,B,C shows the results of the calculated $Wp\#$ from wave data. Storm events from $\geq 220^\circ$ have higher values than those from other directions and seem to correspond to significant changes in migration rates (as after 2001 or in 2010, when a breaching occurred, with a subsequent inlet jump). $Wp\#$ from the other directions appears not related with visible displacement of the channel. No apparent clustering of storms or energy peaks seems to be responsible for the final breaching in 2015. There is, however, a continuity of the migration irrespective of storm occurrence (Fig. 3.7 A,B,C).



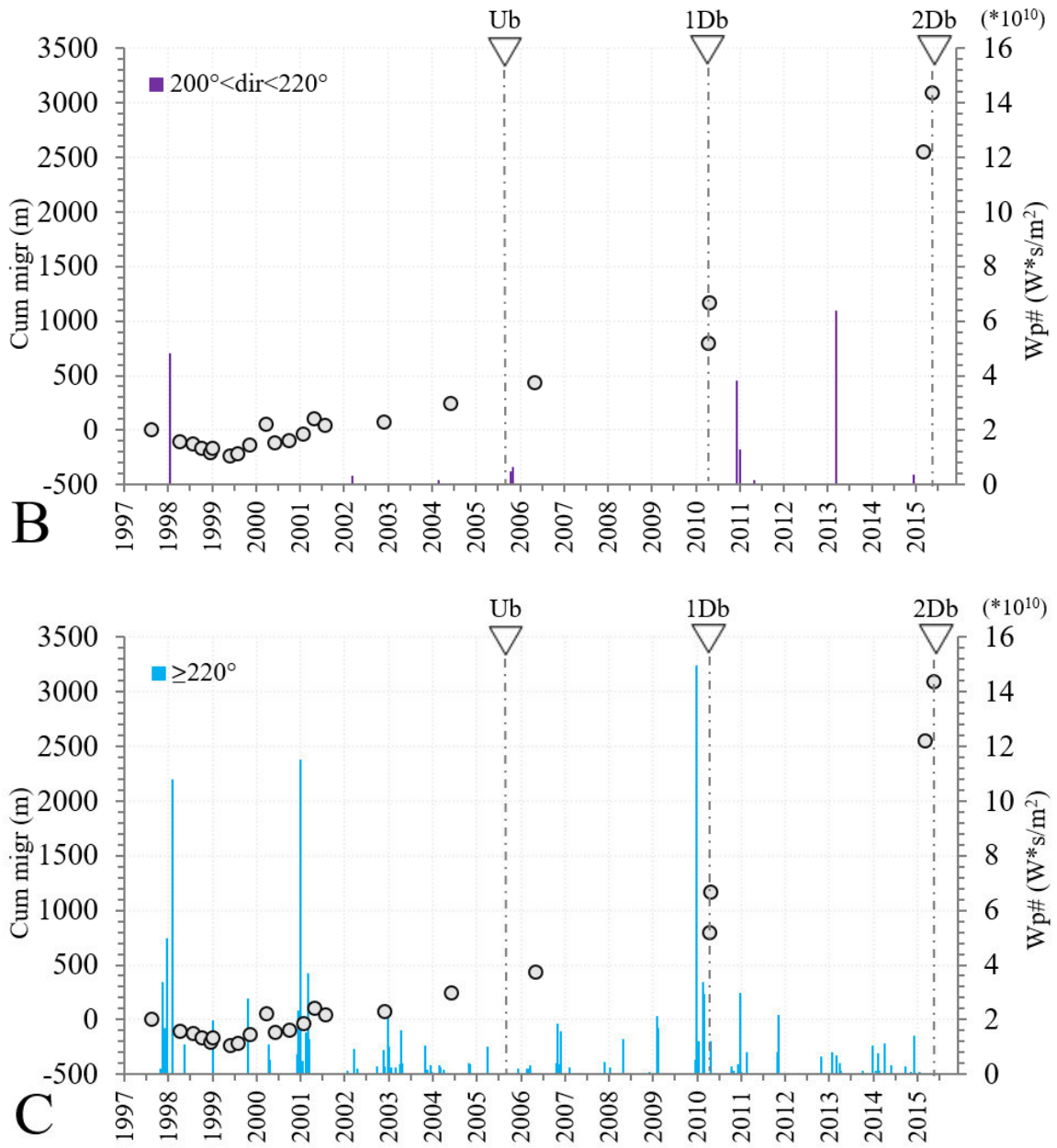


Fig. 3.7 Cumulative migration (gray circles) compared with $Wp\#$ for three directions: $\leq 200^\circ$ (A), $200 < \text{dir} < 220^\circ$ (B), and $\geq 220^\circ$ (C). Updrift breaching (Ub) and downdrift breaching ($1Db$ and $2Db$) events are represented by triangles.

After reaching dynamic equilibrium in July 1998 (Vila-Concejo *et al.*, 2003), the Ancão Inlet had an average cross-sectional area (A_c) of 550 m^2 (Fig. 3.6A, Fig. 3.8). The maximum value of A_c was reached in March 2000 (800 m^2) and was probably related to the dredging of the inner channels close to the inlet that was carried out in February–April 2000 (Dias *et al.*, 2000; Ramos and Dias, 2000). After that, a strong decrease occurred at

the beginning of 2001, reaching a minimum value of 300 m² in April 2001. A stable period followed until 2010, when the inlet almost closed with an A_c of 50 m². The jump recorded during that spring returned the section to a wider value (110 m²) that remained until May 2015 (Fig. 3.8). Mean values of $P/\Sigma Wp\#$ were calculated for longer periods of time (hereafter called macro-intervals; see discussion for their interpretation). The highest values of $P/\Sigma Wp\#$ were recorded from the relocation date until 2001. From 2001 to 2010, the ratio decreased significantly, as well as from 2010 until 2015 (Fig. 3.8). The overall trend is a decreasing cross-sectional area (and corresponding prism) during migration up to a critical position.

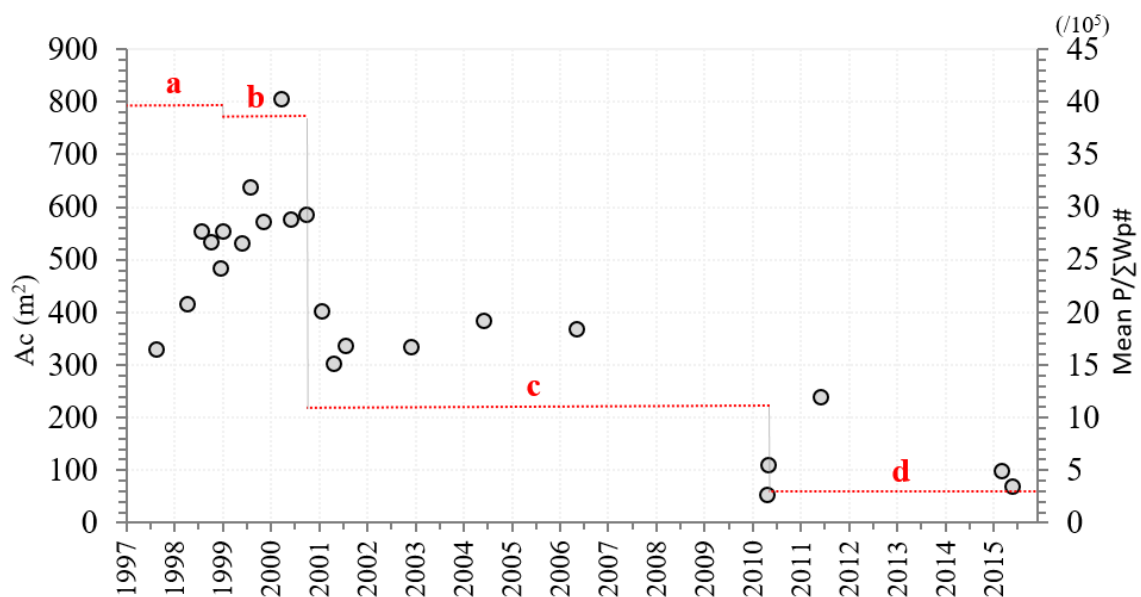


Fig. 3.8 Cross-sectional area (A_c , gray circles) compared with the mean $P/\Sigma Wp\#$ ratio (horizontal lines) for four selected macro-intervals: a) unstable, due to morphological adaptation (which includes the phases described by Vila-Concejo *et al.*, 2003); b) equilibrium 1, while capturing prism and migrating; c) equilibrium 2, without capturing prism but with migration; and d) critical, toward closure/infilling.

The migration trends of the previous Ancão cycles (Vila-Concejo *et al.*, 2002; 2004) integrated with the last Ancão cycle data are shown in Fig. 3.9. After the Ancão Inlet opening in 1997, its migration reproduced the behavior and the path of the oldest inlet, starting with an initial stage of readjustment characterized by low migration rates, followed by a stage of high eastward migration rates (Vila-Concejo *et al.*, 2002). Nonetheless, the migration trend appears to be increasing as the migration cycle lifetime declines (33 years for Ancão1, 22 years for Ancão2, 18 years for Ancão3, for a longer

overall migration), as already noted by Vila-Concejo *et al.* (2002). The migration rates of Ancão2 and Ancão3 are higher than that of the first cycle.

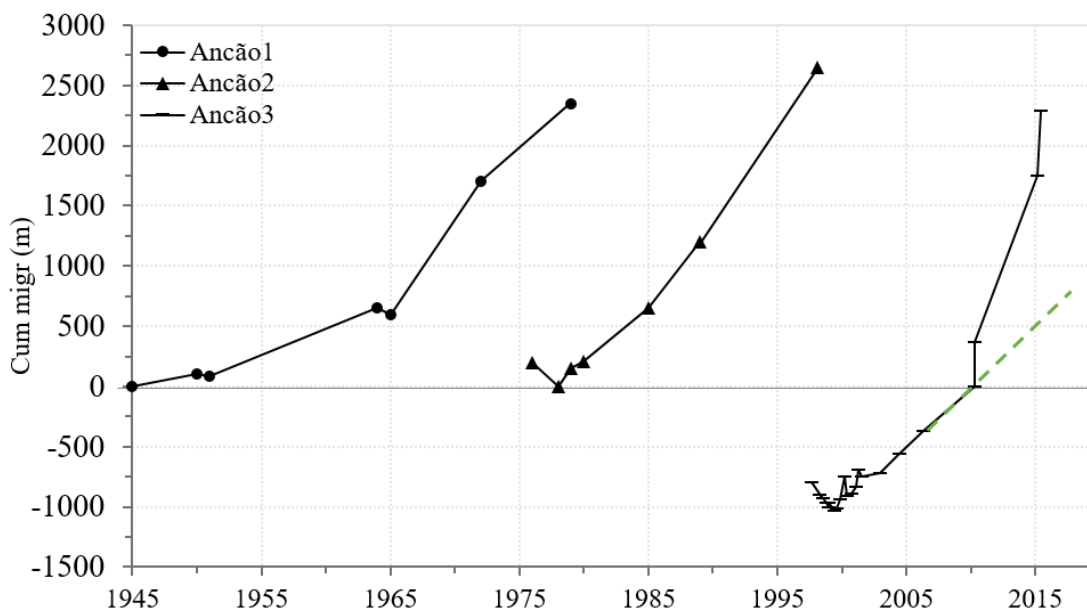


Fig. 3.9 Migration trends of previous Ancão cycles (Vila-Concejo *et al.*, 2002, 2004) integrated with the last Ancão cycle data (1997–2015). Points represent inlet channel positions observed in aerial photographs or surveys. The dashed line represents the supposed continuity of the migration rate before the 2010 and 2015 jumps.

The initial stages of Ancão3, however, displayed lower migration rates. Its relocation site was ~1000 m to the west of the Ancão1 opening (Vila-Concejo *et al.*, 2004) in an area with a high dune system and relatively wide barrier. Once the Ancão1 opening position was reached, the migration trend started to be much faster (see dashed line in Fig. 3.9). From that position to the east (downdrift direction), the barrier was low and narrow and subject to frequent overwashing, and thus, more susceptible to erosion, according to Matias *et al.* (2010).

An important instrument to investigate a possible dependence between morphological and hydrological parameters is to test the significance of the correlations between them. Table 3.6 shows the results of the significance analysis using *Pearson (Pe)* and *Spearman (Sp)* correlations. Hydrological parameters are expressed in the form of wave power and normalized wave power distinguished according to the storm direction for analyzing a possible prevalence of one of them on the changing morphological parameters. Values

lower than the probability thresholds are highlighted in red and can be considered significant.

The correlated data are representative of the interval of time within two consecutive surveys. Each correlation presents three lines: the first line represents the correlation coefficient R , the second one the number of values compared and the third one is the probability p . As already said, if the hypothesis test gives a p-value less than the significance level, the null hypothesis is rejected and these results are 'statistically significant'. As the Table 3.6-Pe reports, ΔAc is significantly, negatively correlated with the total wave and normalized wave power of the storms generated for both $\leq 200^\circ$ (E-SE) and $\geq 220^\circ$ (W-SW) storms. $\Delta MaxD$ is also significantly, negatively correlated with wave power and normalized wave power for both E-SE and W-SW storms but with a considerable stronger and more significant correlation for storms from the W-SW. This trend is clearer than that of Ac and is more responsive mainly for W-SW storms. For higher levels of significance ($p < 0.05$ and $p < 0.01$), it is evident a clear (negative) correlation between maximum depth $\Delta MaxD$ and the sum of wave power and normalized wave power between two consecutive surveys of storm events coming from W-SW, also confirmed by the *Spearman* correlation analysis (Table 3.6-Sp). The other parameters seem to be not significantly influenced by storm events, whatever the direction they come from (Table 3.6).

Table 3.6 *Pearson Pe* and *Spearman Sp* correlation with the evidences of the couples that are statistically significant (red, $p < 0.1$). ΔAc , ΔIw , $\Delta MaxD$, ΔO , ΔM : variations of inlet parameters between two consecutive surveys; $\overline{Wp\#}$ ($\overline{Wpn\#}$) and $\Sigma Wp\#$ ($\Sigma Wpn\#$): mean and sum $Wp\#$ ($Wpn\#$) of the storms coming from three directions ($\leq 200^\circ$, $200^\circ < dir < 220^\circ$, $\geq 220^\circ$), respectively.

Pe	dir < 200°				200° < dir < 220°				dir > 220°			
	$\overline{Wp\#}$	$\overline{Wpn\#}$	$\Sigma Wp\#$	$\Sigma Wpn\#$	$\overline{Wp\#}$	$\overline{Wpn\#}$	$\Sigma Wp\#$	$\Sigma Wpn\#$	$\overline{Wp\#}$	$\overline{Wpn\#}$	$\Sigma Wp\#$	$\Sigma Wpn\#$
ΔAc	-0.3204 N=14 $p=0.264$	-0.3363 N=14 $p=0.081$	-0.4822 N=14 $p=0.086$	-0.4748 N=14 $p=0.086$	-0.0347 N=6 $p=0.948$	-0.0606 N=6 $p=0.909$	-0.1422 N=6 $p=0.788$	-0.1646 N=6 $p=0.755$	-0.0335 N=13 $p=0.913$	-0.0451 N=13 $p=0.884$	-0.4954 N=13 $p=0.085$	-0.4891 N=13 $p=0.090$
ΔIw	-0.1118 N=14 $p=0.704$	-0.0424 N=14 $p=0.886$	-0.2023 N=14 $p=0.488$	-0.1925 N=14 $p=0.510$	0.3566 N=6 $p=0.488$	0.3362 N=6 $p=0.515$	0.1616 N=6 $p=0.760$	0.1359 N=6 $p=0.797$	0.3516 N=13 $p=0.239$	0.3746 N=13 $p=0.207$	0.1183 N=13 $p=0.700$	0.1271 N=13 $p=0.679$
$\Delta MaxD$	0.0561 N=14 $p=0.849$	-0.0304 N=14 $p=0.918$	-0.4633 N=14 $p=0.095$	-0.4589 N=14 $p=0.099$	-0.6148 N=6 $p=0.194$	-0.6096 N=6 $p=0.199$	-0.3574 N=6 $p=0.487$	-0.3404 N=6 $p=0.509$	-0.5531 N=13 $p=0.050$	-0.5736 N=13 $p=0.040$	-0.6990 N=13 $p=0.008$	-0.7000 N=13 $p=0.008$
ΔO	0.1015 N=14 $p=0.730$	0.1373 N=14 $p=0.640$	0.1043 N=14 $p=0.723$	0.0918 N=14 $p=0.755$	0.3541 N=6 $p=0.491$	0.3827 N=6 $p=0.454$	0.5280 N=6 $p=0.282$	0.5474 N=6 $p=0.261$	-0.0964 N=13 $p=0.754$	-0.0833 N=13 $p=0.787$	-0.0962 N=13 $p=0.754$	-0.1031 N=13 $p=0.738$
ΔM	0.0561 N=14 $p=0.849$	0.0858 N=14 $p=0.770$	0.3724 N=14 $p=0.190$	0.3614 N=14 $p=0.204$	0.1573 N=6 $p=0.766$	0.1955 N=6 $p=0.710$	0.6179 N=6 $p=0.191$	0.6481 N=6 $p=0.164$	-0.3216 N=13 $p=0.284$	-0.3010 N=13 $p=0.318$	0.2556 N=13 $p=0.399$	0.2421 N=13 $p=0.426$

Sp	dir<200°				200°<dir<220°				dir>220°			
	$\overline{Wp\#}$	$\overline{Wpn\#}$	$\Sigma Wp\#$	$\Sigma Wpn\#$	$\overline{Wp\#}$	$\overline{Wpn\#}$	$\Sigma Wp\#$	$\Sigma Wpn\#$	$\overline{Wp\#}$	$\overline{Wpn\#}$	$\Sigma Wp\#$	$\Sigma Wpn\#$
ΔAc	-0.2791	-0.2352	-0.3011	-0.3495	0.0857	0.0857	-0.0857	-0.0857	-0.0879	-0.0934	-0.3901	-0.3901
	N=14 p=0.334	N=14 p=0.418	N=14 p=0.296	N=14 p=0.221	N=6 p=0.872	N=6 p=0.872	N=6 p=0.872	N=6 p=0.872	N=13 p=0.775	N=13 p=0.762	N=13 p=0.188	N=13 p=0.188
ΔMw	-0.0902	0.1100	-0.1188	-0.1034	0.2571	0.2571	-0.0857	-0.0857	0.1374	0.1593	0.1978	0.1978
	N=14 p=0.759	N=14 p=0.708	N=14 p=0.686	N=14 p=0.725	N=6 p=0.623	N=6 p=0.623	N=6 p=0.872	N=6 p=0.872	N=13 p=0.655	N=13 p=0.603	N=13 p=0.517	N=13 p=0.517
$\Delta MaxD$	-0.0330	-0.2571	-0.3978	-0.3758	-0.3714	-0.3714	0.0286	0.0286	-0.4176	-0.4615	-0.6044	-0.6044
	N=14 p=0.911	N=14 p=0.375	N=14 p=0.159	N=14 p=0.185	N=6 p=0.468	N=6 p=0.468	N=6 p=0.957	N=6 p=0.957	N=13 p=0.156	N=13 p=0.112	N=13 p=0.029	N=13 p=0.029
ΔO	-0.0374	-0.0462	0.0374	-0.0330	0.6571	0.6571	0.7143	0.7143	-0.0385	0.0110	-0.0330	-0.0330
	N=14 p=0.899	N=14 p=0.876	N=14 p=0.899	N=14 p=0.911	N=6 p=0.156	N=6 p=0.156	N=6 p=0.111	N=6 p=0.111	N=13 p=0.901	N=13 p=0.972	N=13 p=0.915	N=13 p=0.915
ΔM	0.1165	0.1516	0.3319	0.3055	0.0857	0.0857	0.6000	0.6000	-0.2473	-0.2143	0.4505	0.4505
	N=14 p=0.692	N=14 p=0.605	N=14 p=0.246	N=14 p=0.288	N=6 p=0.872	N=6 p=0.872	N=6 p=0.208	N=6 p=0.208	N=13 p=0.415	N=13 p=0.482	N=13 p=0.122	N=13 p=0.122

3.4 Discussions and concluding remarks

Some authors have reported that inlet migration of Ancão Inlet is highly related to western storm events (Morris *et al.*, 2001; Vila-Concejo *et al.*, 2003; Williams *et al.*, 2003), meaning events from a direction $>180^\circ$. This work confirms that westerly storms are the main drivers of inlet migration, although different storm classes have been considered according to their direction ($\leq 200^\circ$, $200^\circ < \text{dir} < 220^\circ$, $\geq 220^\circ$; Fig. 3.7A,B,C) and therefore we include W and SW storms on the same group, in accordance to the dominant wave conditions. It is also clear that the continuity of migration between main storm events is not driven by extreme waves, but seems to be a rather continuous process, most probably dependent on longshore transport induced by waves below the storm threshold. As reported in Fig. 3.6A,B, faster migration M occurs in correspondence with a decrease of Ac , Iw and $MaxD$, denoting an infilling of the channel. Major storms can, however, contribute to migration rate peaks, and especially for inlet “jumps”. Such a consideration relative to the role of the storms and waves in the inlet migration processes is also found in works developed on similar environments, adding also the importance of the tidal currents. For example, Cleary (2002) and Herrling and Winter (2014), analyzing inlets in North Carolina and in the Wadden Sea respectively, reported that morphodynamics at tidal inlets are highly related by the combined action of waves and tides and the relative contribution of these interacting forces largely determines the morphological and sedimentological response. Later De Swart and Zimmerman (2009) and FitzGerald *et al.* (2012) specified that the main drivers determining the morphodynamic development of a tidal inlet system are commonly assumed to be waves that induce mixing, transport and dispersal of the sediment at the ebb-tidal delta and tidal currents in the inlet.

Model experiments with migrating tidal inlets were conducted by Nienhuis and Ashton (2016) to investigate the mechanics and rates of inlet migration. Results suggest that tidal inlet migration occurs due to three mechanisms: (1) littoral sediment deposition along the updrift inlet bank, (2) wave-driven sediment transport preferentially eroding the downdrift bank of the inlet, and (3) flood-tide-driven flow preferentially cutting along the downdrift inlet bank because it is less obstructed by flood-tidal delta deposits. In model experiments to quantify tidal inlet migration, both updrift littoral sediment and the eroded downdrift inlet bank are sediment sources to the growing updrift barrier and the flood-

tidal delta, such that tidal inlets can be net sink of up to 150% of the littoral sediment flux. According to the same authors, with flood-tidal deltas acting as a littoral sediment sink, migrating tidal inlets can drive erosion of the downdrift barrier beach.

Considering these data and following the M and A_c trends, the migration cycle of the Ancão Inlet was divided into four macro-intervals (Fig. 3.8 a,b,c,d): the first from the opening of the inlet in 1997 to the beginning of the eastward migration (January 1999); the second from January 1999 to September 2000; the third from September 2000 until the breaching of 2010; and the final period from 2010 until the end of the monitoring, with the inlet almost in its closing position (i.e., very shallow and meandering channel). The first interval corresponds to the unstable situation caused by the morphological behavior subsequent to the relocation (“a” in Fig. 3.8). The prevailing migration was opposite to what was expected, as already shown by Vila-Concejo *et al.* (2003). Although some storms from the east occurred during this period, it is difficult to establish a clear relationship between storms and westward migration. A possible reason for the observed migration is the adaptation of the inlet to its position in the context of a new hydrodynamic setting. The existence of main channels (and relevant currents) to the west (Ancão and Ramallete channels) probably helped this migration pattern. The subsequent ~2-year interval highlights the increasing cross-sectional area A_c while the inlet migrated eastward. Maximum efficiency is indicated by the high $P/\sum Wp\#$ that likely occurred after the capture of the backbarrier channel network close to the inlet (“b” in Fig. 3.8). The results show that the inlet cross-sectional area during the third interval was almost constant, and therefore, not affected by the inlet’s migration. Migration occurred undisturbed until 2010 (“c” in Fig. 3.8). That date marks an abrupt change in the history of the inlet, as the breaching caused by a severe storm occurred in the 1975 position of the Ancão inlet. From this position, until the last survey, migration trends increased significantly (Fig. 3.9), while the inlet featured an unstable/critical condition toward a possible closure (“d” in Fig. 3.8). This rapid migration is most likely associated with the morphology of the affected area, which corresponded to a narrow overwash terrace (Matias *et al.*, 2010) with no dunes, thus causing less resistance. The dashed line in Fig. 3.9 shows how the migration would likely have continued with a fully developed dune system (as before the jump). Observing the last migration cycle, Ancão seems to be unable to capture the local drainage pattern at the end of its migration. This is exacerbated

by the residual washover fans and old flood tidal delta bodies that are now intercepted and drained by the last terminations of creeks connected to the neighboring Faro–Olhão system. The inlet is too far to the east to have an efficient connection to the main drainage system, even during spring tides and is clogged by the deposited sand banks. The inlet acts more independently, draining the surrounding area as a single (with a reduced tidal prism) inlet system (Pacheco *et al.*, 2010). Hence, this behavior seems to resemble the behavior of the previous migration-cycle.

Other migrating and relocated inlets in the world follow more or less the same cycle, passing from an initial adaptation period to a new begin of the migration process. This is the case of Mason Inlet (NC), when the new inlet position (the relocated inlet) resulted stable for the first year after relocation, but then it started to infilling and re-started to migrate (Erickson *et al.*, 2003). It is also the case of Captain Sam’s Inlet that, after three relocations, it still continues to migrate (Kana, 1989; Kana and McKee, 2003). For all of these cases, the same authors affirmed that the process of the infilling, directly and also indirectly connected to the wave climate, is considered one of the responsible of the migration, to allow the inlet to preserve its efficiency.

Table 3.6 shows that ΔAc is negatively and significantly correlated with the total wave power and normalized wave power of a storm (for both E-SE and W-SW storms) and therefore an increase in wave power (storms with stronger power) will cause a reduction of Ac . The results of the present work show that larger storms contribute to bring sediment to the inlet and to a reduction on Ac and even on the flushing capacity of the inlet. The maximum depth $\Delta MaxD$, is also negatively and significantly correlated with wave power and normalized wave power (for both E-SE and W-SW storms but with a considerably stronger correlation for W-SW storms). This implies that stronger storms can contribute to a stronger reduction of the $MaxD$, mainly the events from the west-southwest. This also states that during storms the sediment is infilling the inlet and that sediment most probably come from the littoral drift and/or from the previous ebb-tidal deltas. Cleary (2002) confirmed that an infilling of the tidal inlet system (with its backbarrier zone) can carry to a dramatically reduction of tidal prism and then to an increase of the migration rate.

Other consideration of management aspects, with the comparison of other cases examples in the world, will be presented in Chapter 5.

3.5 Chapter summary

The evolution of the unconstrained Ancão tidal inlet, located in South of Portugal, in a human-affected multi-tidal inlet system, is the topic of this chapter. Through an analysis of morphological and hydrodynamic data, some results-points can be expressed to draw more attention to how natural features of tidal inlets can be indirectly conditioned by the presence of man and by the natural events happened in the system.

- The migration trend appears connected with the modification of morphologic parameters (Fig. 3.6B), as the beginning of a regular eastward migration corresponds, more or less, with a decreasing in the Ac , Iw and $MaxD$, because this bring to a change in tidal prism (Table 3.4) and to a modification of the inlet efficiency;
- Results show that during winter mean significant wave heights (H_s) and peak periods (T_p) are higher than in summer, indicating the higher frequency of swell conditions (Table 3.5);
- Storm events from $\geq 220^\circ$ have higher values than those from other directions (Fig. 3.7C) and seem to correspond to significant changes in migration rates (as after 2001 or in 2010, when a breaching occurred, with a subsequent inlet jump). Followed the worldwide cases, this is probably linked to the infilling of the tidal inlet system due to strong storm event but also due to the fair-weather longshore sediment transport. In fact, a continuity in the migration is shown even though in absence of storms (Fig. 3.7);
- The maximum value of Ac was reached in March 2000 (800 m², Fig. 3.8) and was probably related to the dredging of the inner channels close to the inlet that was carried out in February–April 2000 (Dias *et al.*, 2000; Ramos and Dias, 2000).

- As Table 3.6 reports, ΔA_c is significantly, negatively correlated with the total wave and normalized wave power of the storms generated for both $\leq 200^\circ$ (E-SE) and $\geq 220^\circ$ (W-SW) storms. $\Delta MaxD$ is also significantly, negatively correlated with wave power and normalized wave power for both E-SE and W-SW storms but with a considerable stronger and more significant correlation for storms from the W-SW (Table 3.6). This means that more energetic storm events carry sediment to the inlet zone and contribute to infill it, enhancing the migration processes.

The documented history of the Ancão inlet subsequent to its relocation in 1997 allows the acquisition of knowledge of both its morphodynamic and hydraulic behaviors in order to provide for a good management and avoid or at least reduce the conflicts between the natural modification and the human needs (and viceversa). This consideration will be treated in the Chapter 5.

4.

***The case of Marano Lagunare: past, present
and future trends of a natural inlet in a
lagoon system highly changed by anthropic
actions***

4.1 Study area: S. Andrea Inlet

S. Andrea Inlet is one of two natural openings located in the Marano and Grado lagoon. Following Cirilli (2004), it is a tide-dominated tidal inlet (Fig. 2.1). There is little morphological information about the area. Sartori (1995) and Segala (1999) performed part of the evolutionary analysis reworking the cartographic archive data as well as interpreting aerial photographs related to the study site. Later Cirilli (2004) added further information. On maps, S. Andrea Inlet already appeared in the 1600s (Fig. 4.1). By that time, all the current openings were already present, along side six other inlets that are all now closed.

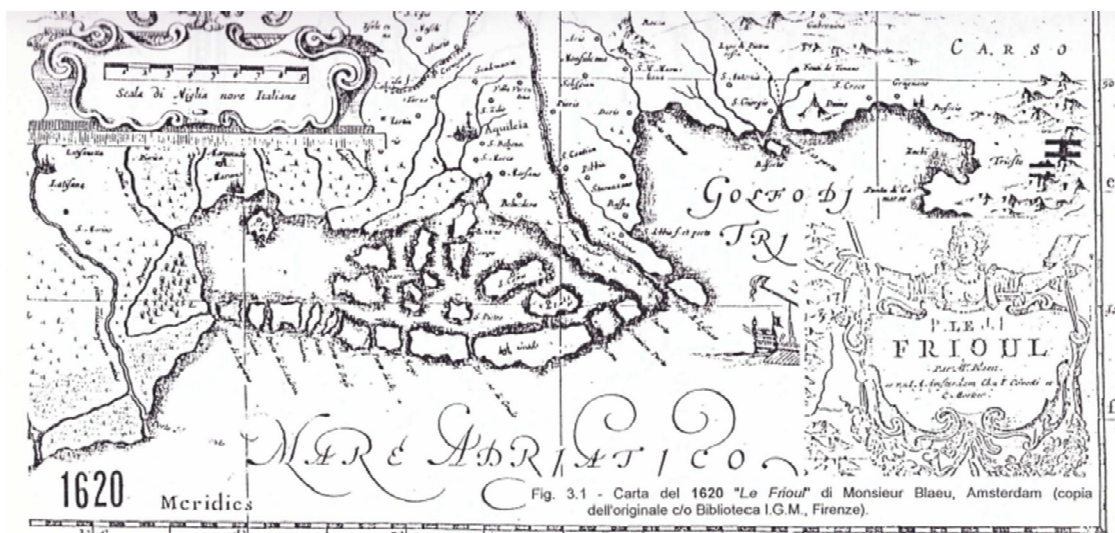


Fig. 4.1 Detail of “Le Frioul” by Monsieur Blaeu, 1620, Amsterdam (copy from the original, Library I.G.M., Firenze).

Sartori (1995) gave a detailed description of the evolution of S. Andrea Inlet. In 1891, S. Andrea Inlet is approximately 225 m wide. In 1927, the mouth has more than halved its width not exceeding 100 m. This net occlusion trend is associated with the development, on the western side, of the Martignano Island. In the cartography of 1938, the inlet was about 225 m wide and migrated to the east. In front of Martignano Island a small sandy bar is reported for the first time on the map, probably representing the visible part of a largest submerged bank. In 1951, S. Andrea had a width of about 250 m and a significant growth of the spit along the western tip of S. Andrea Island, occupying a portion of the

channel, caused the translation of the channel westward. As a consequence, the channel also eroded the eastern side of Martignano Island, in order to maintain its cross-section area. Most changes occurred in the period between 1951 and 1974. In 1974 the inlet entrance had its largest documented width of about 400 m. This width is due to the retreat toward the east of the island of S. Andrea, caused by erosion, which destroyed a long part of its beach. Probably the configuration of 1974 is the result of the intense period of storms and surge (“acqua alta”) that occurred in the late 1960's (i.e. the catastrophic floodings of 1966 and 1969) as well as of a decreasing in sediment budget from the east, caused by the construction of the jetties of Buso Inlet between 1964 and 1969 (Sartori, 1995).

A cartographic survey in 1990 highlights the growth of the western end of the island of S. Andrea and the emergence of the aforementioned sand body, at that time represented as a well-developed bank either in width, either in length and elevation. The inlet resulted further narrowed: the presence of a new coastal revetment constructed along the eastern side of Martignano Island since 1985 prevented the migration of the inlet westward, caused by the push of the updrift barrier. The response of the inlet was the deepening of the main channel, while narrowing the thalweg, in order to maintain the cross section. Segala (1999) continued the description of the area observing that in 1995 the western tip of S. Andrea barrier island moved northward, accompanying a further decrease in inlet width. At that time, the ebb tidal delta was diverged westward and the emerged sandbank, by now welded to the Martignano Island, was thinner, likely due to a rectifying action by tidal currents moved through a small marginal channel, connected to the S. Andrea inlet. Later, Cirilli (2004) described the inlet-area conformation as a result of a topobathymetric survey carried out in 2002. He recognized two marginal channels, along the opposite sides of the inlet, with the western channel more developed than the other. The analysis of data highlighted a westward migration of the main ebb channel of about 25 m between 1994 and 1999, caused by the progradation of the S. Andrea Island spit. The westward longshore sediment transport in the same interval then caused a partial reduction of the channel section, with an accumulation of about 20,000 m³ of sediment and a consequent erosion of the western margin of the channel. Cirilli (2004) highlighted that the tidal currents removed only the 65% of the sediment transported by the longshore currents, causing a progressive occlusion.

The spring tidal prism of S. Andrea was first calculated in 1965 by Dorigo (1965) as 9,700,000 m³ during ebb and 11,150,000 m³ during flood. With the expansion of the neighboring Buso basin, Brambati (1996) reported that the S. Andrea Inlet basin had undergone the greatest change with an area reduction by 2,150 ha in 1965 to about 700 ha in 1995.

Martignano Island and the S. Andrea Inlet are placed in a particular convergence point, where two longshore currents meet, one from east to west (the strongest current) and the other from the opposite direction.

4.2 Material and methods

The purpose of a topo-bathymetric survey is principally to define the morphology of the tidal channel and the surrounding area, in order to obtain important morphodynamic elements that allow the study of past and current hydraulic behavior of the system.

In this thesis, data from such a survey carried out in July 2016 were compared to previous data collected by Sartori (1995), Segala (1999), Burla (2003) and Cirilli (2004) (Table 4.1). A brief illustration of their methods is reported here.

Table 4.1 List of surveys used in this thesis for the investigated area.

Survey	N. of profiles	Area surveyed	Topo-bathymetric tools
July 1994 (Sartori, 1995)	15	Main channel	analogue echo-sounder Lowrance leveling rod
2-6 August 1999 (Segala, 1999)	18	Main channel Ebb tidal delta Area fronting Martignano Island	analogue echo-sounder Lowrance leveling rod
Between 2002-2003 Burla (2003) Cirilli (2004)	Relative to the ebb delta area	Ebb tidal delta Area fronting Martignano Island	analogue echo-sounder Lowrance echo-sounder SIMRAD DGPS Trimble Ag 132
19 July 2016 (new survey)	18	Main channel Ebb tidal delta Area fronting Martignano Island	echo-sounder Ohmex SonarMite v3.0 GNSS Stonex S9III receiver

In July 1994, a series of bathymetric surveys in the S. Andrea Inlet area were performed to develop the thesis studies of Sartori (1995, Table 4.1). Combining a study regarding the sea bottom and channel configuration with sediment sampling data, Sartori (1995) gave an exhaustive view of the area configuration at that time, extracting data by 15 profiles (Fig. 4.2A).

The bathymetric profiles were carried out from the backshore of Martignano Island to the inlet and were performed by using an analogue echo-sounder Lowrance, placed on board of a small boat with the transducer positioned at 15 cm from the water line. The alignment and positioning of the sections were verified by a series of cross targets performed by theodolites located on the ground, in points previously measured. Due to the shallow water, some parts were surveyed by a leveling rod, pre-calibrated with the last point measured by Lowrance.

Later, Segala (1999) followed and continued the previous studies with another survey (Table 4.1). She improved the studies increasing the number of profiles and sediment samplings, in order to survey a larger inlet area, from the shallow area facing Martignano Island to the westernmost side of the S. Andrea Island, including also the entire part of the ebb-tidal delta (Fig. 4.2B). During this survey, 18 profiles were performed, distributed in a slightly different configuration than that followed by Sartori (1995, Fig. 4.2A). The methodology followed by Segala (1999) was similar to that one used by Sartori (1995). Between 2002 and 2003, the Coastal Group of the University of Trieste carried out an extended survey, from the Lignano to the Grado inlets (see Burla, 2003). A series of profiles, orthogonal to the shoreline, and a small bathymetric campaign were performed (Fig. 4.3). They were useful for this thesis only for the part concerning the S. Andrea ebb tidal delta. The main channel has not been surveyed. The instrumentation used during this last survey was more modern than that one used for the previous surveys, with the employ of *DGPS* and a digital echo-sounder. Cirilli (2004) studied the ebb tidal delta conformation and volume, producing a *DEM* for the delta region, using the same data of Fig. 4.3.

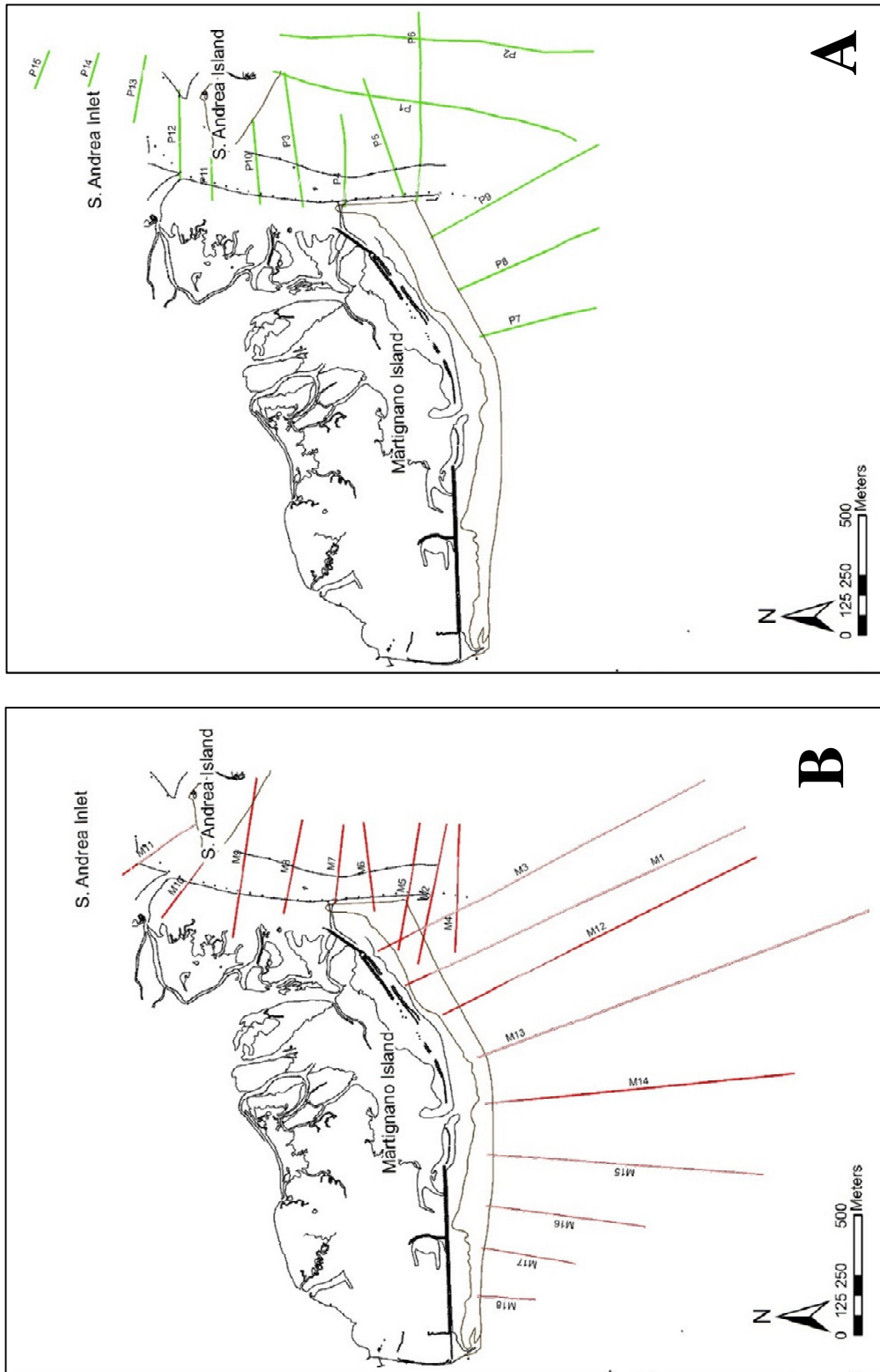


Fig. 4.2 Profiles tracks from Sartori (1995, A) and from Segala (1999, B). Base: restitution from a 1990 orthophoto.

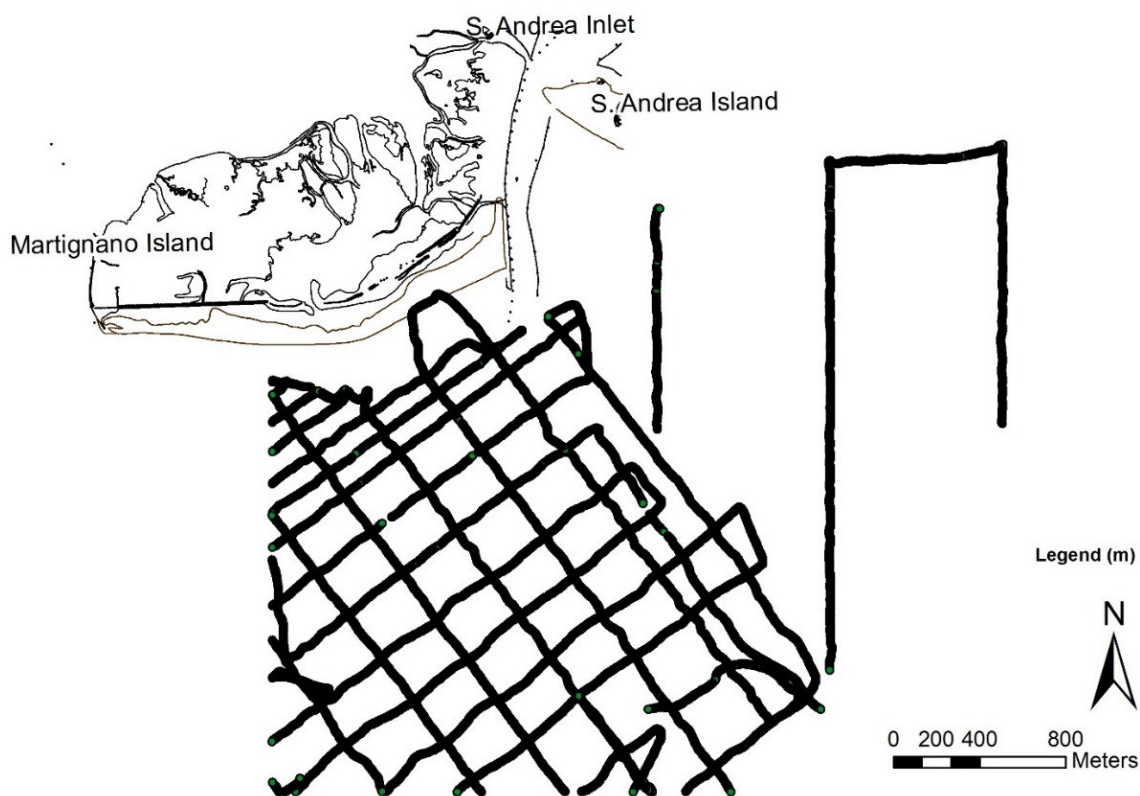


Fig. 4.3 Tracks followed during the 2002 survey (Cirilli, 2004).

No more surveys were performed in the area until July 2016. Following the tracks of the Segala (1999) profiles, a new topo-bathymetric survey was carried out with the aim to obtain indications about the current morphology of the area, adding further information to the evolution of this inlet during the last 20 years.

The 2016 survey, being the most recent, took advantage of a more innovative instrumentation compared to that one used for the 1994 and 1999 topo-bathymetric surveys (Fig. 4.4). The data are digital and more numerous and accurate. The topographic survey was conducted with a GNSS Stonex S9III receiver, from the backshore until a depth of about 1 m, while the bathymetric campaign was performed on a flat-bottomed boat, interfacing between them the GNSS receiver and the digital echo-sounder Ohmex SonarMite v3.0 using a special software, *NAVPRO* of Communication Technology. This software allows the complete planning of the bathymetric campaign, by tracking the route to follow with the boat, and recording the data into a file. It also performs simultaneous correction of the measures for tidal and wave height during the bathymetric survey operations. The data from bathymetric and topographic profiles were then combined in

order to obtain a single complete profile of the beach (backshore+shoreface). The profiles were then compared with previous profiles of 1994 and 1999, in order to identify morphological changes undergone by the inlet during these time frames.

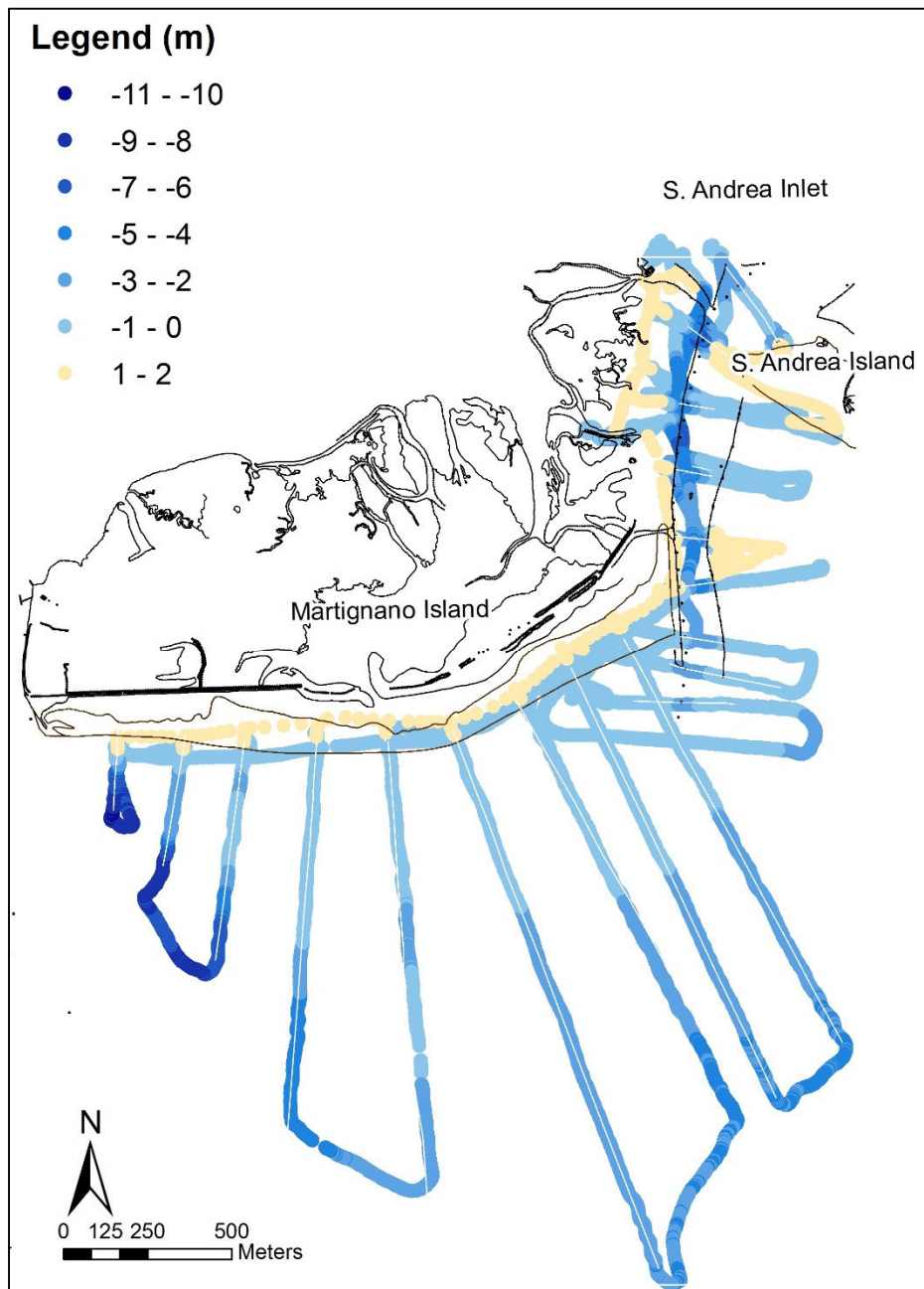


Fig. 4.4 Topo-bathymetric tracks of the 2016 survey. Base: restitution from a 1990 orthophoto.

ESRI ArcGIS™ 10.3 software was used to store and analyze all topo-bathymetric data. Digital Elevation Models (*DEMs*) of the area were produced for the 1994, 1999 and 2016 (Fig. 4.7, Fig. 4.8 and Fig. 4.9, respectively). As the available data is not regularly spaced, the Triangulated Irregular Networks techniques (*TIN*) were employed as interpolator method. In order to avoid artefacts, the models were improved by introducing vector elements, inferred from collected data. The resulting topo-bathymetries were converted to raster format, a grid of regularly spaced cells. Cell spacing was chosen according to survey data resolution. A local metric coordinate system known as the Gauss-Boaga Grid was used for the maps; elevation was based on mean sea level (m.s.l.).

The next step was to observe the volumetric changes in the ebb-tidal delta area, as it is one of the inlet features whose evolution can give some information about the stability condition of the inlet. Fontolan *et al.* (2007a,b) and Delli Quadri (2007) developed the Semi-Automatic Detrending Procedure (*ADP*), a GIS geostatistical procedure based on the original depth data (surveyed during the topo-bathymetric campaigns), in order to calculate the ebb delta volume. One of their major challenges was finding a method that could minimize the operator intervention in the construction of a reliable virtual “no-delta” bathymetric configuration, used as initial sea-bottom state on which the ebb tidal delta structure was set. Instead of using 2 or 4 lateral profiles located in the area not affected by the ebb-tidal delta structure, the entire dataset was used to create different polynomial trend surfaces of no-delta bathymetry (Fontolan *et al.*, 2007a,b; Delli Quadri, 2007). The use of the entire dataset resulted in a less subjective and more precise procedure, because it avoided operator errors when selecting lateral profiles. First and second-order polynomial trend surfaces were created. To make this operation, some data from the survey of 2002 were used (Burla, 2003). Finally, the Different Residual Maps were created by subtraction of the no-delta surfaces from the real bathymetry (*DEMs*). The *DEM* for the 2002 survey (regarding only the ebb tidal delta region, Cirilli, 2004) was also used, in order to estimate the ebb-tidal delta size in that period. Volumes were evaluated for the different configurations within a specific area that includes only the ebb tidal delta region. Cells with positive values are used to compute the volume in the different residual surface. The Residual Method (Walton and Adams, 1976; Hicks and Hume, 1996) consists of the calculation of the positive anomalies while negative anomalies identify mainly channel morphologies.

An evaluation of the changing volume of the main channel bottom was also computed in order to analyze its possible infilling and/or shifting. The evaluations were computed within a limited region.

Inlet morphological parameters such as minimum cross-sectional area (A_c), inlet width (I_w) and maximum depth ($MaxD$) were determined for each year following the same methodology used for Ancão Inlet:

- the inlet throat was first defined sketching ten profiles with equal intervals through the inlet cross-section (Fig. 4.5); the direction and the spacing of the profiles were chosen following the shoreline orientation and the width of the adjacent barriers, respectively. The spacing among them varies from 5 to 10 m;
- extraction of the data from the profiles using *ESRI ArcGIS™ 10.3* software;
- elaboration of the data by *Matlab R2009b* in order to define A_c and extract the parameters of I_w and $MaxD$.

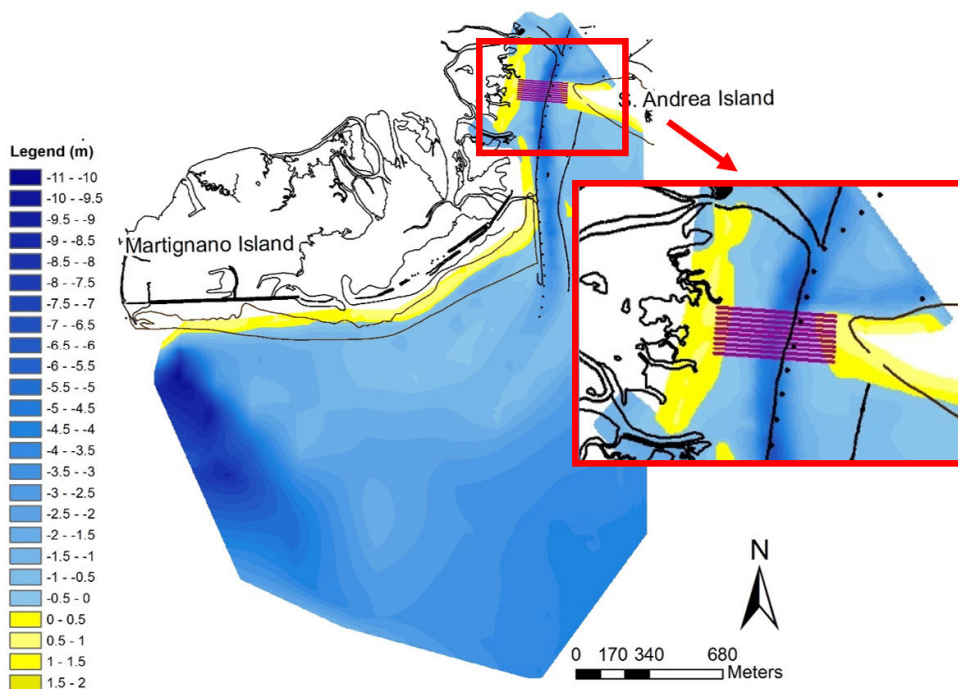


Fig. 4.5 Ten profiles with equal intervals through the inlet cross-section in order to identify the A_c (example for the 2016 survey).

The $MaxD$ variation and displacement was computed by determining the metric difference between the position of $MaxD$ and its depth value, respectively, of the same topo-bathymetric profile, taken in different surveys.

The inlet cross-sectional area A_c was used as a tidal prism proxy that could be estimated using the empirical formula developed by Fontolan *et al.* (2007a,b) for the North Adriatic Coasts (Table 4.4):

$$A_c = 0.0068 p^{0.7439} \quad (\text{Eq. 4.1})$$

where A_c is the minimum cross-sectional area (m^2), measured for each survey, and P is the corresponding tidal prism (m^3).

Regarding the analysis of the wave height and the individuation of storm events, in the center-north Adriatic different thresholds are proposed. According to Corsini *et al.* (2004), a storm event is isolated if the significant wave height (H_s) at Ancona buoy exceeds the threshold of 1.0 m for at least 12 consecutive hours and two subsequent events are considered independent if they are separated by at least 6 consecutive hours of H_s below that threshold. Another definition for the northern Adriatic is provided by Bertotti *et al.*, (1996), which sets the H_s threshold to 2.0 m. Perini *et al.* (2011) identified events where the H_s exceeds the reference value of 1.5 m for at least 6 consecutive hours. Two events are considered separate if H_s drops below 1.5 m for at least 3 hours. Analyzing data between 2004 and 2016 from the directional wave-rider buoy DWGR1, offshore of MGL (Fig. 4.6), managed by the Protezione Civile della Regione FVG, in collaboration with the Istituto nazionale di Oceanografia e Geofisica Sperimentale di Trieste (OGS), a mixing between the proposals it is chosen: an H_s should exceed the reference value of 1 m for at least 6 consecutive hours; two events are considered separate if H_s drops below 1 m for at least 12 hours. This choice was made to have more statistical data to analyze.

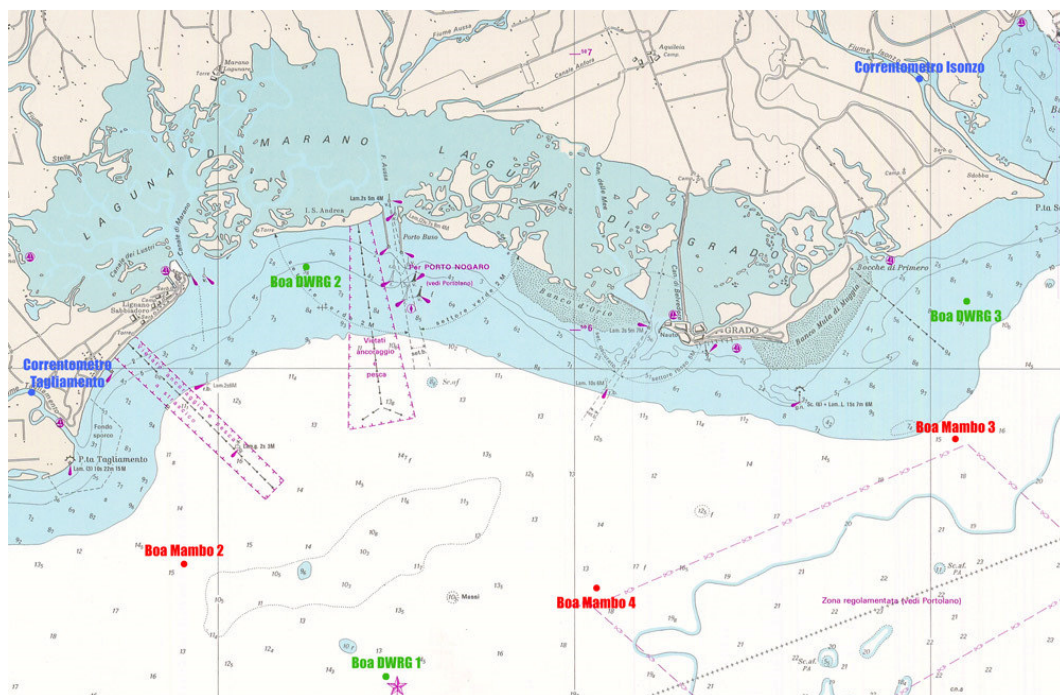


Fig. 4.6 Localization of DWRG1 wave-directional buoy offshore the MGL (www.protezionecivile.fvg.it).

4.3 Results

The *DEMs* for the surveys of 1994, 1999 and 2016 were created and later converted in *raster* format using *ESRI ArcGIS™ 10.3* software, following the methods described in the previous paragraph. The map for the survey of 1994 is shown in the Fig. 4.7. Due to the scarcity of data collected during that survey, the area covered by the *DEM* is very small but denotes a well developed main channel and a sand-bank in front of the south-eastern side of Martignano Island. The subsequent survey (1999) covered a bigger part of the S. Andrea Inlet region, also including the ebb-tidal delta area (Fig. 4.8). The channel seems to be better defined and developed, while the south-eastern part of Martignano Island starts to suffer erosion. Finally, Fig. 4.9 illustrates the most recent configuration of the tidal inlet area. The channel is clearly shallower than in the previous surveys and a small island starts to emerge in the central-eastern part of it (see Fig. 4.9); the sand bank of the Martignano Island appears further eroded.

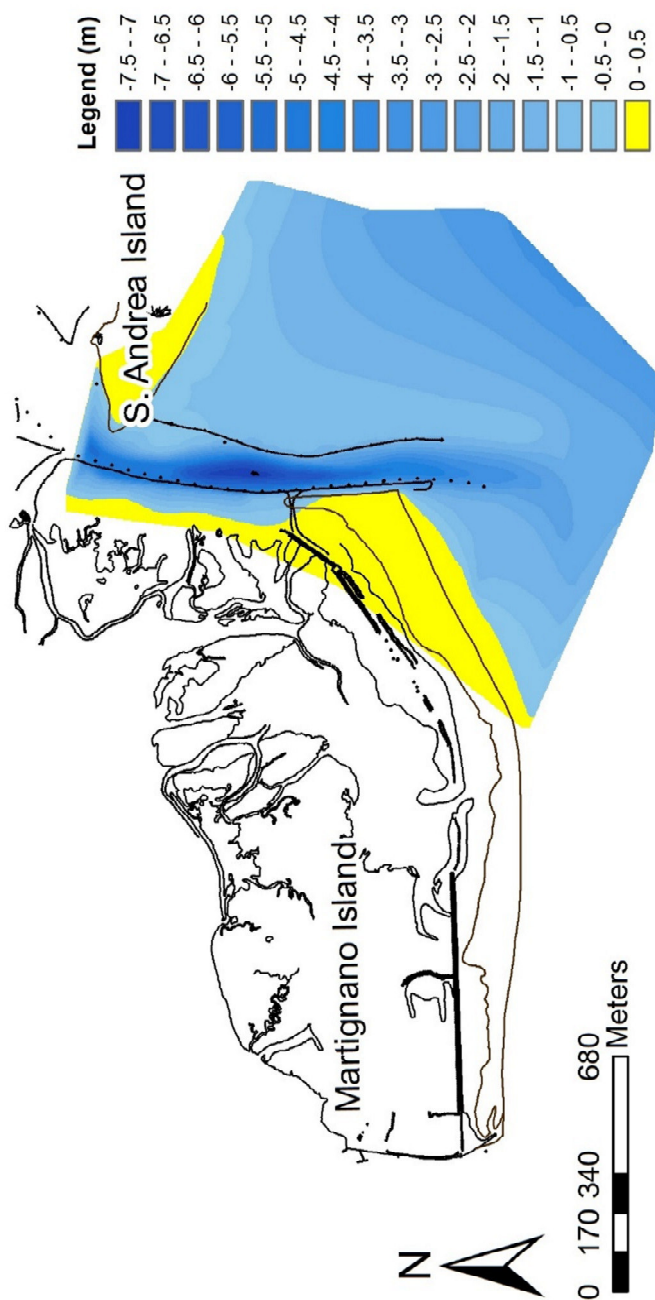


Fig. 4.7 DEM for the 1994 survey (using the data collected by Sartori, 1995). Base: restitution from a 1990 orthophoto.

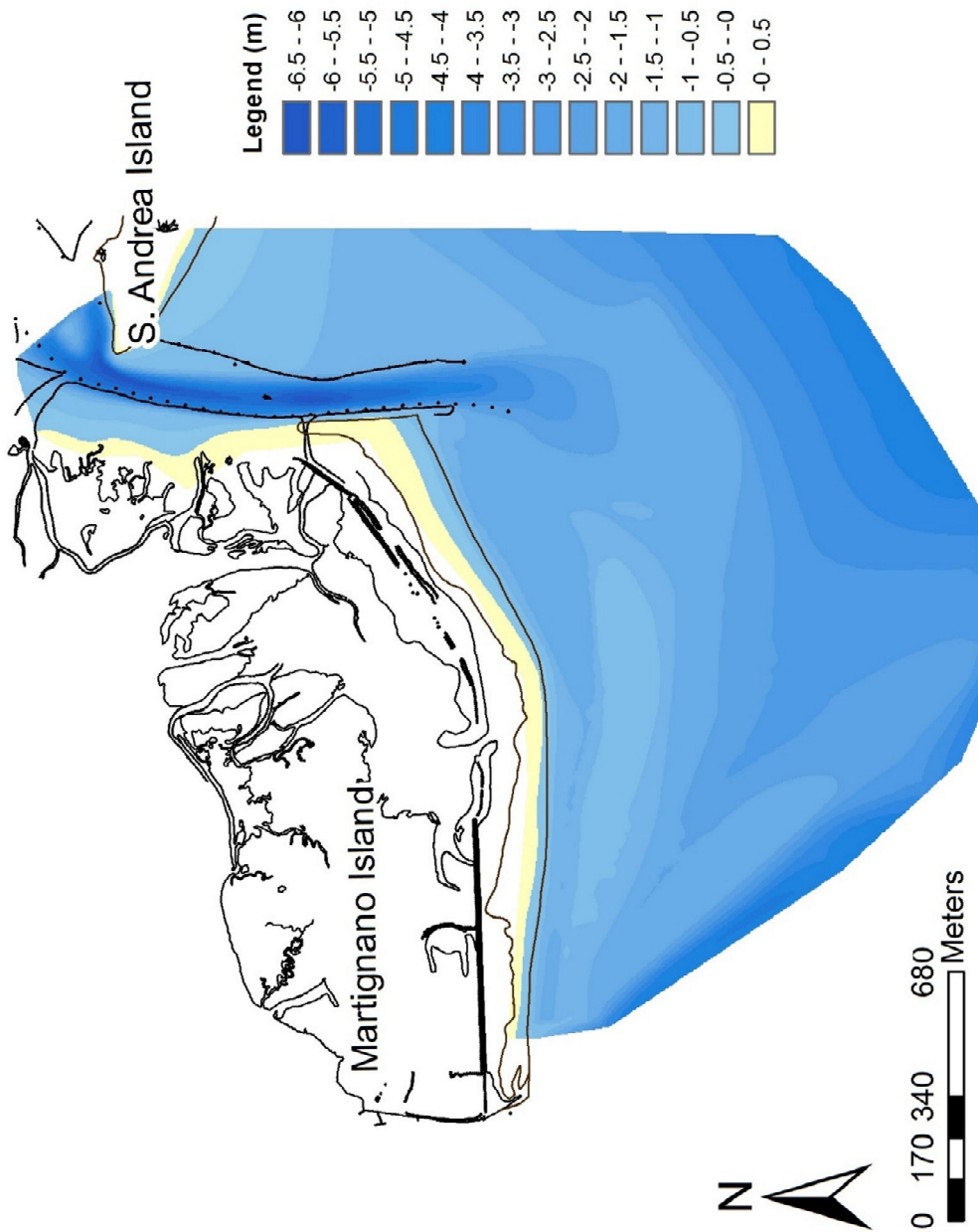


Fig. 4.8 DEM for the 1999 survey (using the data collected by Segala, 1999). Base: restitution from a 1990 orthophoto.

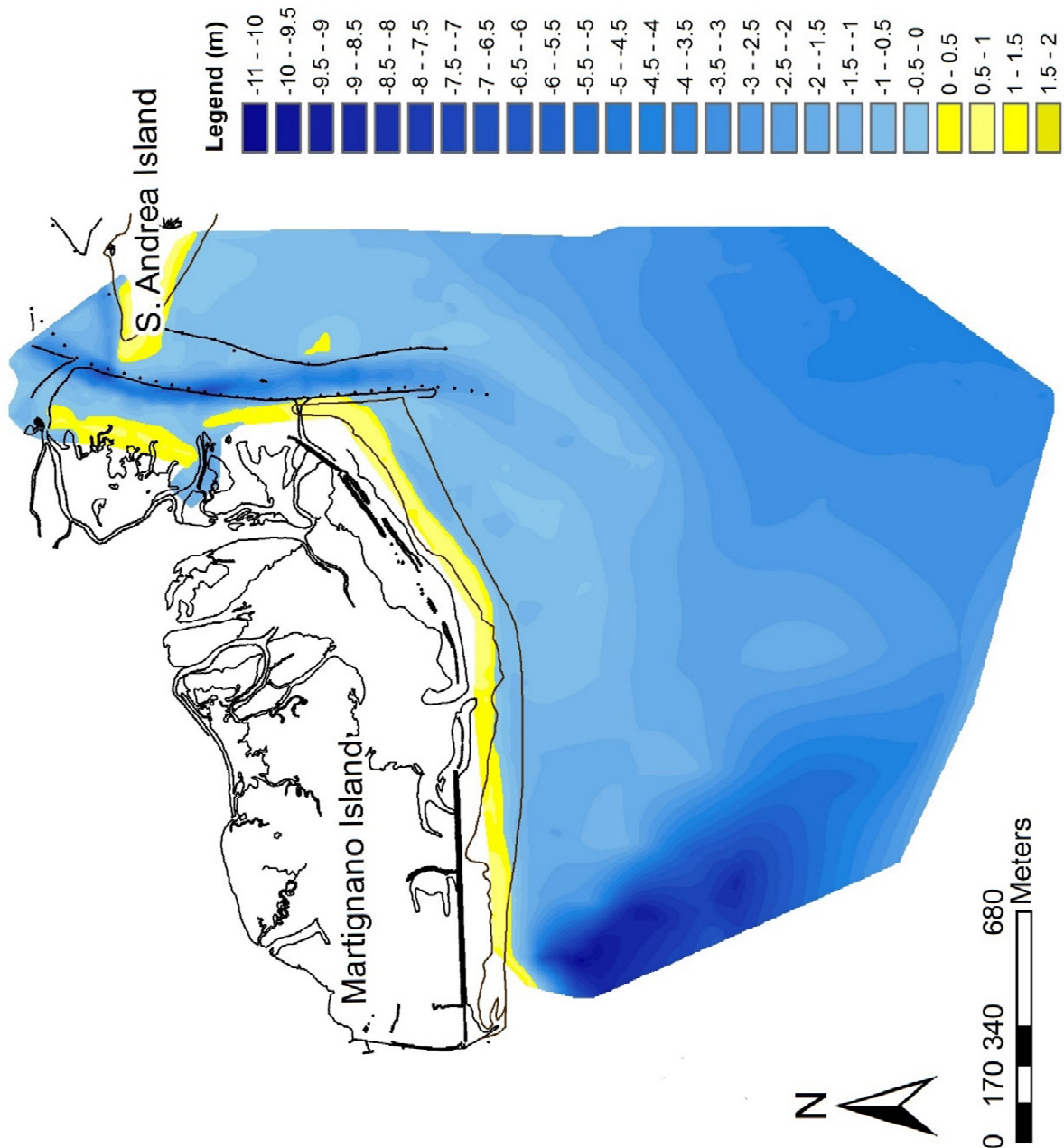
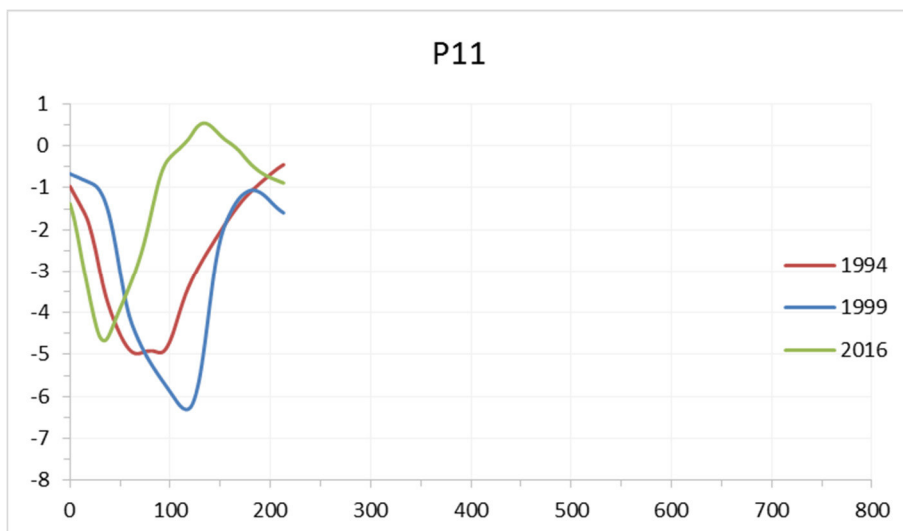
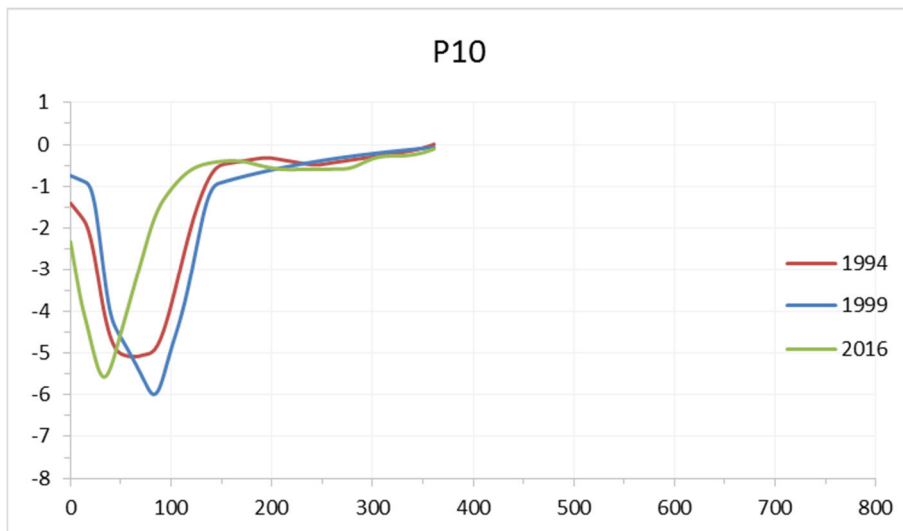
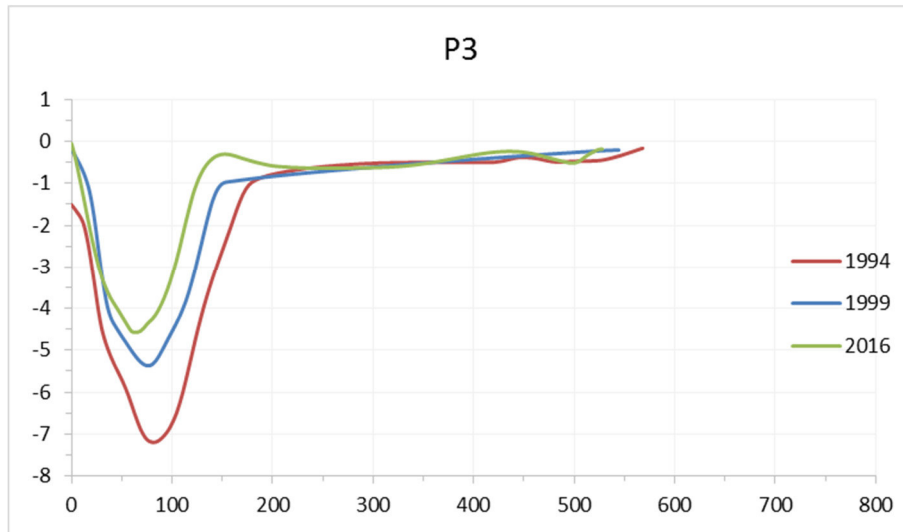


Fig. 4.9 DEM for the 2016 survey (using the data collected during July 2016). Base: restitution from a 1990 orthophoto.

Fig. 4.10 and Fig. 4.11 show the main channel sections along the tracks followed by Sartori (1995) and Segala (1999), extracted by the 1994, 1999 and 2016 maps. In the figures, sections are grouped in northern sector and southern sector, according to their position along the channel. Table 4.2 summarizes the information about the maximum depth of each section in order to investigate its evolution over time.



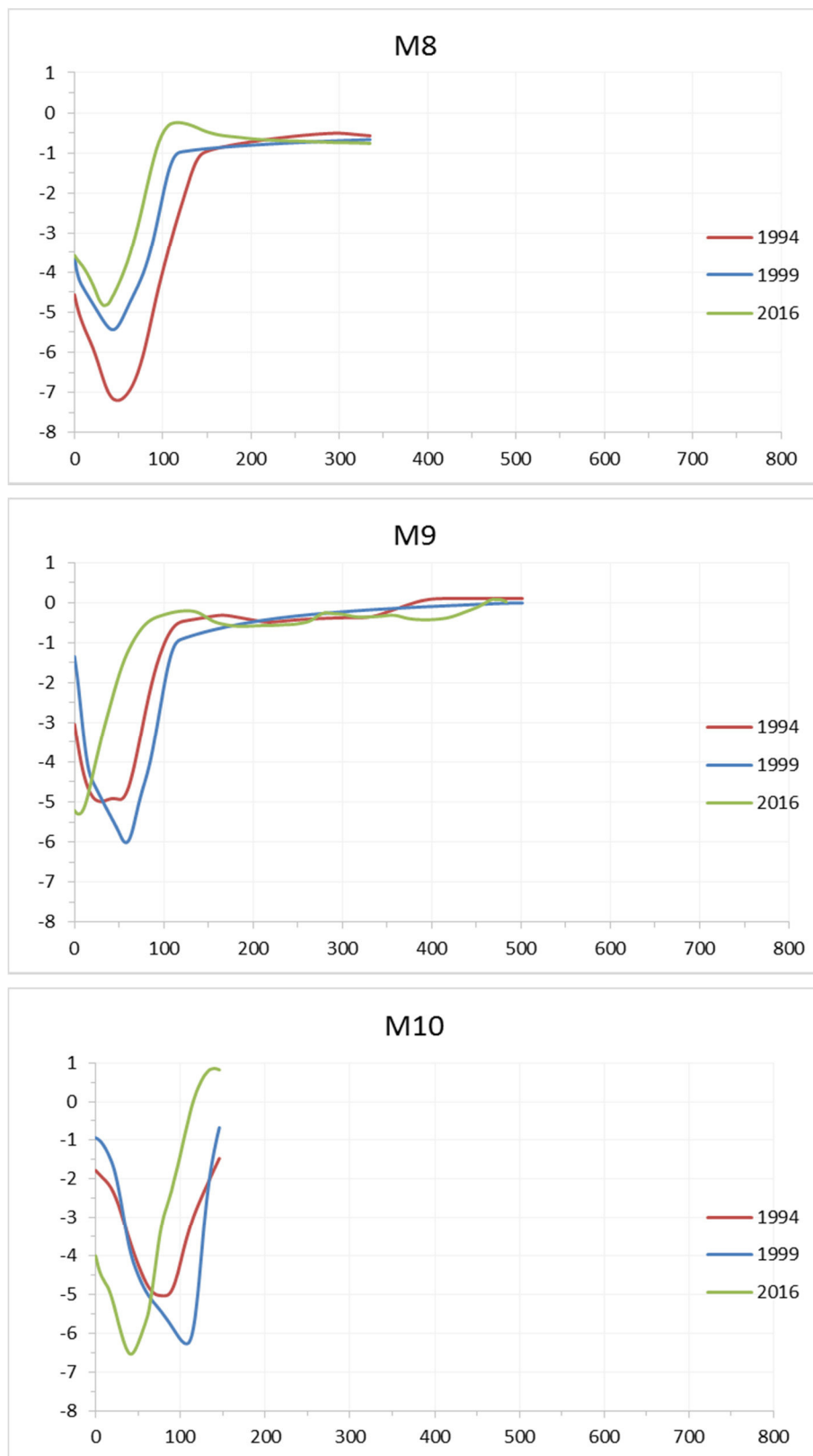
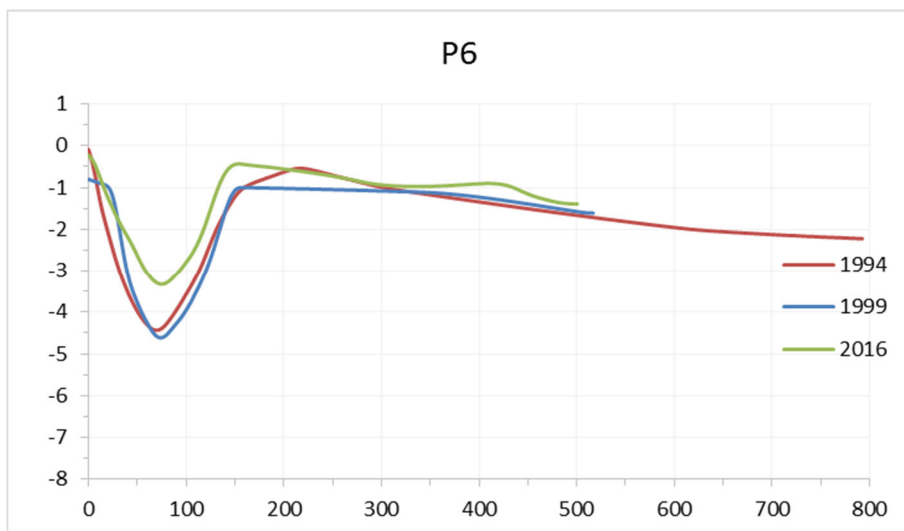
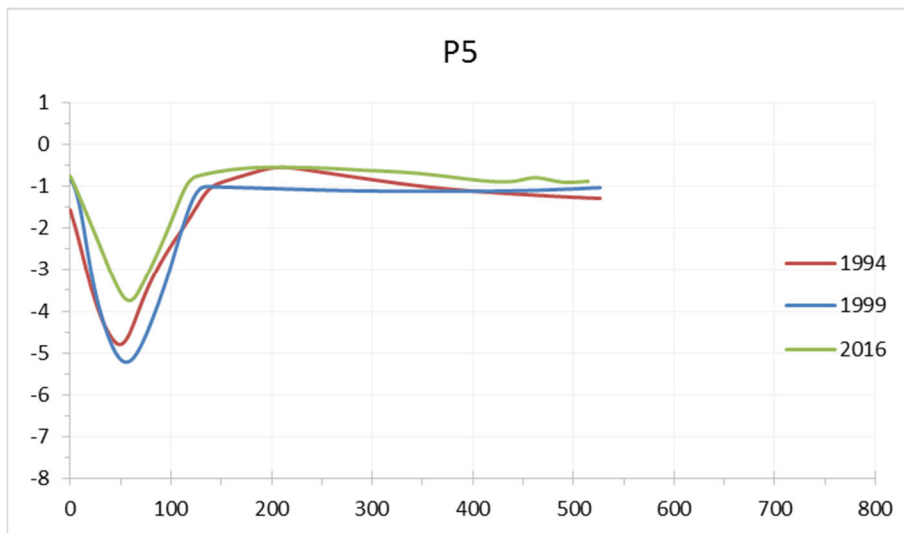
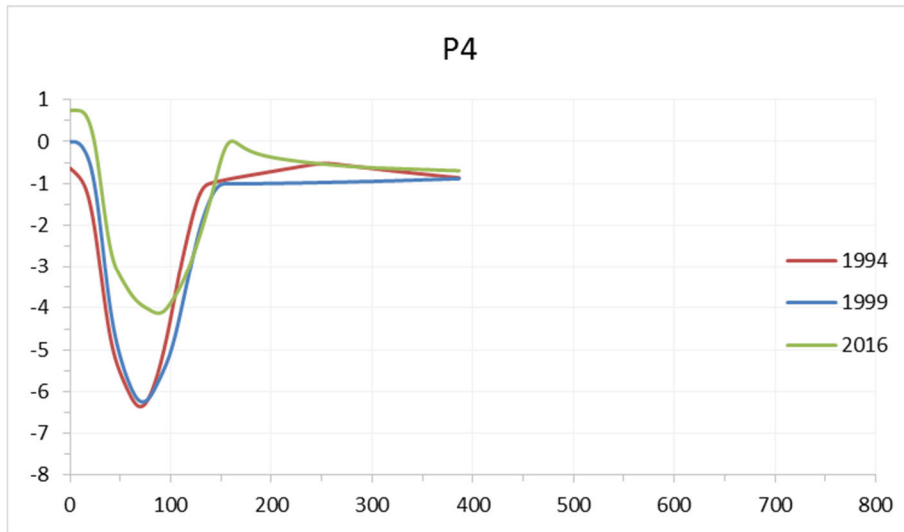


Fig. 4.10 Northern sector. P3 – P10 – P11: sections on Sartori (1995) tracks; M8 –M9 – M10: sections on Segala (1999) tracks.



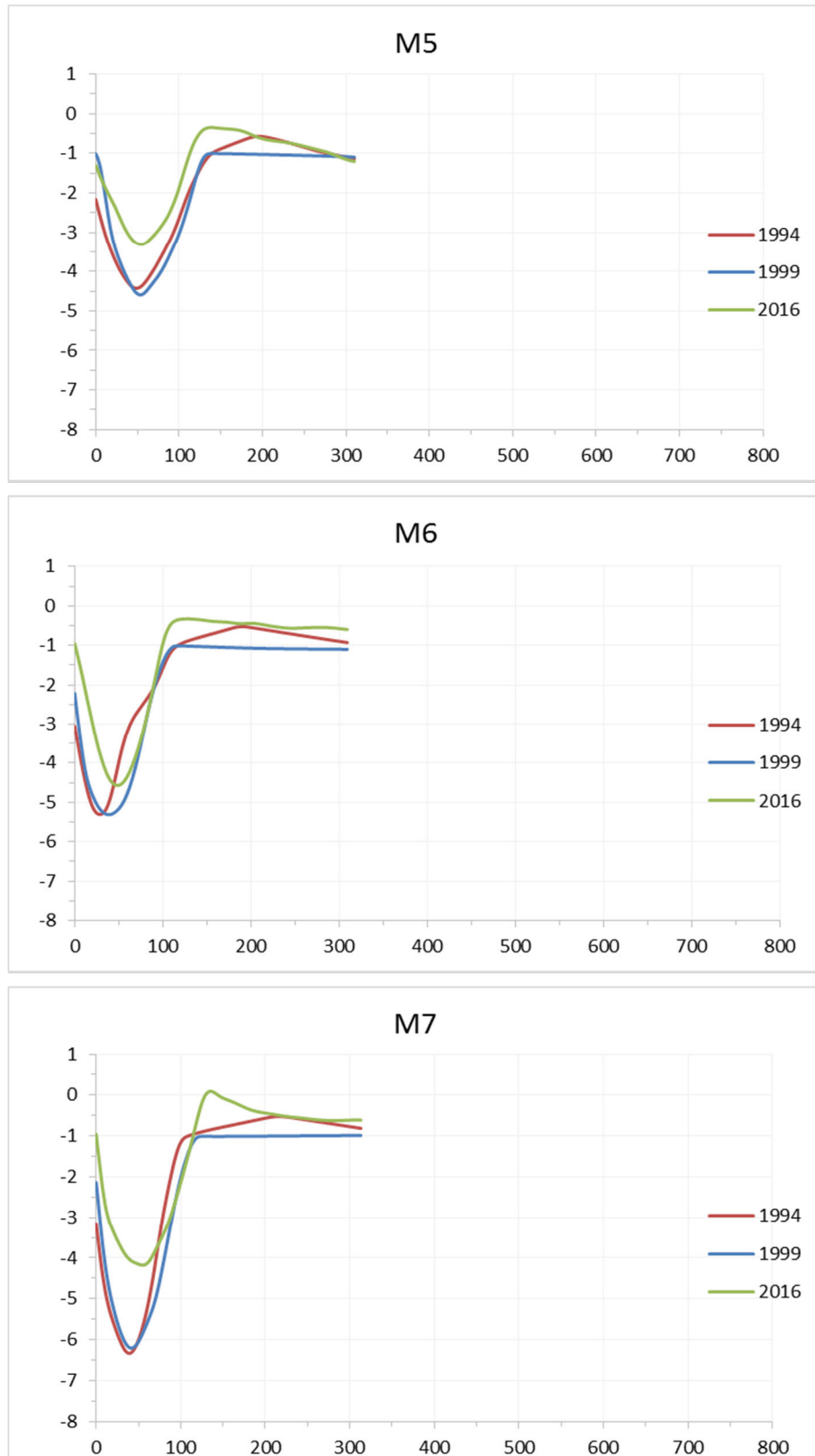


Fig. 4.11 Southern sector. P4 – P5 – P6: sections on Sartori (1995) tracks; M5 –M6 – M7: sections on Segala (1999) tracks.

The sections of Fig. 4.10 regarding the northern sector of the main channel, underline a displacement toward the west that leads to the erosion of the north-eastern side of Martignano Island. Fig. 4.11 reports the sections of the southern sector of the main channel, pointing out the eastward displacement of the maximum depth between 1994 and 2016. Furthermore, a general decrease in depth from the 1994' to the 2016' survey is evident. Table 4.2 reports, in meters, the horizontal and vertical displacement of *MaxD*, along the profile tracks, measured in the interval of time between surveys. Negative and positive values mean, respectively, a westward or eastward movement (for *horizontal displ.*) or a deepening or infilling situation (for *vertical displ.*). Results obtained between 1994 and 2016, clearly indicate a westward movement of the northern sector (negative values) and an eastward movement of the southern one (positive values). A progressive infilling of the channel is indicated by the positive values of vertical displacement.

Table 4.2 Evolution of *MaxD* in depth (*vertical displ.*) and position (*horizontal displ.*), along the main-channel sections, during the investigated period. Negative and positive values mean, respectively, a westward or eastward movement (for horizontal displ.) or a deepening or infilling situation (for vertical displ.).

NORTHERN SECTOR		1994-1999 (m)	1999-2016 (m)	1994-2016 (m)
P3	horizontal displ.	-5.9	-12.1	-18.1
	vertical displ.	1.8	0.8	2.6
P10	horizontal displ.	20.9	-50.7	-29.8
	vertical displ.	-0.9	0.4	-0.5
P11	horizontal displ.	47.3	-82.9	-35.5
	vertical displ.	-1.3	1.7	0.3
M8	horizontal displ.	-3.0	-12.0	-14.9
	vertical displ.	1.8	0.6	2.4
M9	horizontal displ.	26.9	-50.4	-23.5
	vertical displ.	-1.0	0.7	-0.3
M10	horizontal displ.	26.8	-65.5	-38.7
	vertical displ.	-1.2	-0.3	-1.5
SOUTHERN SECTOR		1994-1999 (m)	1999-2016 (m)	1994-2016 (m)
P4	horizontal displ.	3.0	15.0	18.0
	vertical displ.	0.1	2.1	2.2
P5	horizontal displ.	9.0	3.0	12.0
	vertical displ.	-0.4	1.5	1.0

P6	horizontal displ.	6.0	0.0	6.0
	vertical displ.	-0.2	1.3	1.1
M5	horizontal displ.	3.0	0.0	3.0
	vertical displ.	-0.2	1.3	1.1
M6	horizontal displ.	8.9	8.9	17.8
	vertical displ.	0.0	0.7	0.7
M7	horizontal displ.	3.0	11.9	14.9
	vertical displ.	0.1	2.0	2.2

Residual maps created using *ESRI ArcGIS™ 10.3* software, illustrated below, also highlight the general channel infilling. In general, between 1994 and 1999 the channel suffered erosion along its length and a shift of the Northern sector toward the East, evidenced by sediment accumulation on the opposite side, clearly visible in the residual map (Fig. 4.12). After this early stage, almost the entire channel has undergone sedimentation along the updrift side, as reported in Fig. 4.13, for 1999 and 2016. The overall evolution for the entire period investigated is illustrated in the Fig. 4.14. The channel was infilled with quite thick sediment (more than 1.5 m in some parts).

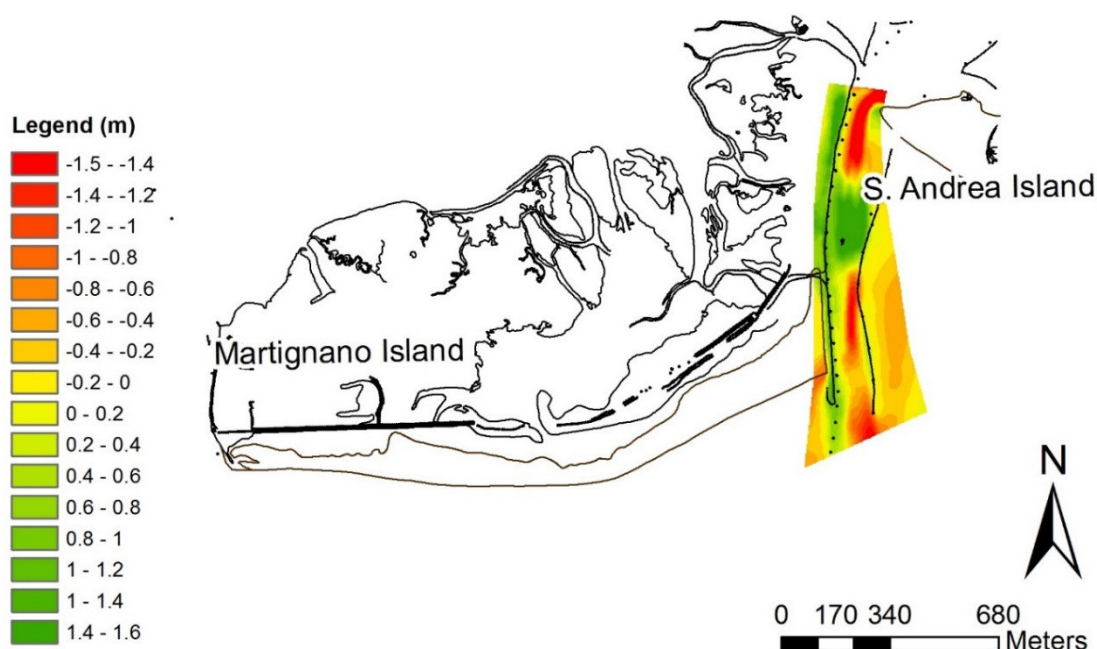


Fig. 4.12 Residual map of the differences in volume of the main channel area for the period 1994 – 1999. Base: restitution from a 1990 orthophoto.

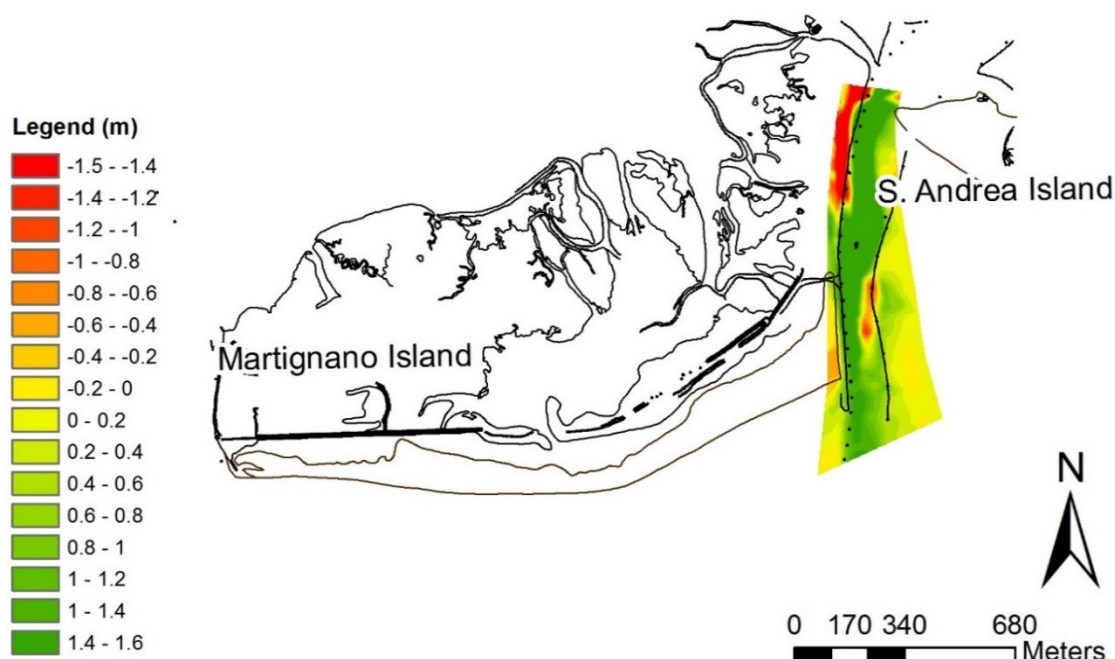


Fig. 4.13 Residual map of the differences in volume of the main channel area for the period 1999 – 2016. Base: restitution from a 1990 orthophoto.

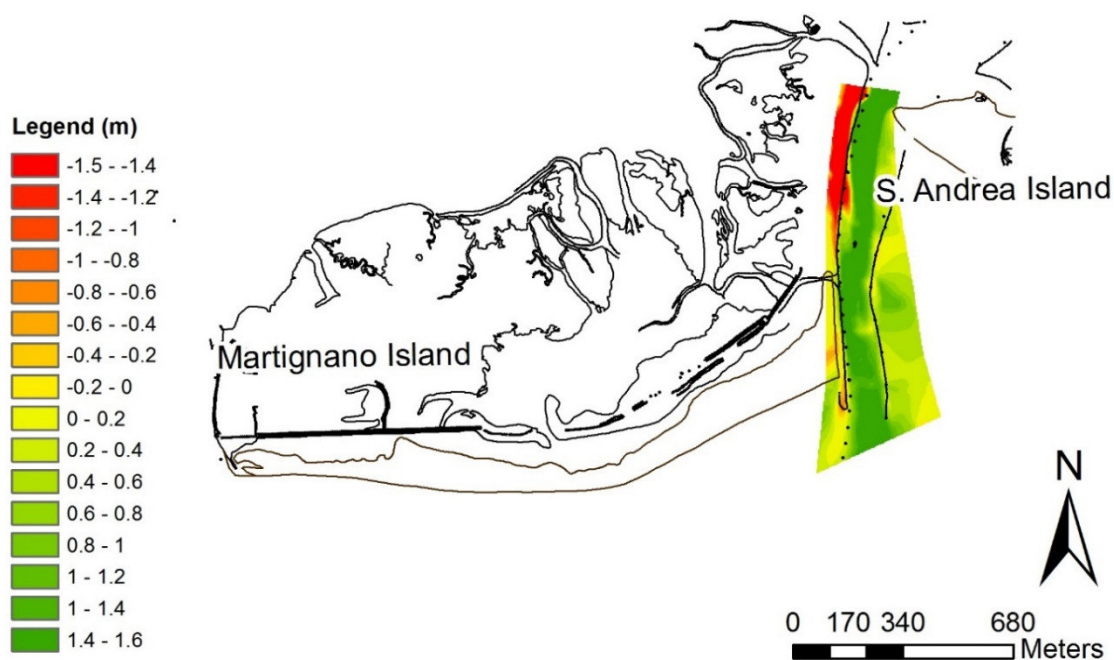


Fig. 4.14 Residual map of the differences in volume of the main channel area for the entire period investigated: 1994 – 2016. Base: restitution from a 1990 orthophoto.

The values of positive and negative anomalies resulting by residual maps of the main channel area are summarized in Table 4.3. The volume analysis confirms that already noted in the profiles analysis, that is an increase of sediment (Table 4.3).

Table 4.3 Differences of volume (m³) calculated by comparison of DEMs in the main channel area.

Year	Positive anomaly (m ³ , above 0 m.s.l.)	Negative anomaly (m ³ , below 0 m.s.l.)	Volume difference (m ³)	Figures
1994-1999	91,600	81,900	+9,700	Fig. 4.12
1999-2016	267,400	59,300	+208,100	Fig. 4.13
1994-2016	257,500	39,300	+218,200	Fig. 4.14

The tidal prism was computed for each year using the North Adriatic empirical relationship (Fontolan *et al.*, 2007a,b) with A_c evaluated through a *Matlab R2009b* computation. Using the A_c measured by Dorigo (1965), a value of tidal prism was calculated also for the 1960s. Results are reported in Table 4.4. Between 1960 and 1994, P (and A_c) seems drastically reduced of about 2.5 times. During last twenty years, these values halved, reaching an A_c of about 300 m² and a P volume of circa 1,700,000 m³ (Table 4.4).

Table 4.4 Tidal prism computation for each year using the North Adriatic empirical relationship.

Map	A_c (m ²)	Tidal Prism (m ³ , from N.A.)	A_c from:
1960	1,232	11,703,000	Dorigo (1965)
1994	522	3,686,000	<i>Matlab R2009b</i> computation
1999	527	3,736,000	<i>Matlab R2009b</i> computation
2016	295	1,713,000	<i>Matlab R2009b</i> computation

The Semi-Automatic Detrending Procedure (*ADP*, Fontolan *et al.*, 2007a,b) was used to compute the volume of the ebb tidal delta according to the 2002 and 2016 bathymetric configuration. A mask covering only the delta region was created and used to extract the

positive anomalies, subtracting the different ‘no delta’ (regional trend) maps from the DEMs representing the 2002 (Fig. 4.15) or 2016 (Fig. 4.16) tidal inlet configuration. Two different polynomial surfaces of the first and second order were extrapolated by the entire topographic database for the survey of 2002 or 2016 (Fig. 4.15 and Fig. 4.16). Using a first-order polynomial surface, the ebb tidal delta increased its volume from 2002 to 2016, gaining $\sim 200,000 \text{ m}^3$ of sand. Using the second-order polynomial, the ebb tidal delta had a stable volume during the same period (Table 4.5).

Table 4.5 Positive anomalies from the ADP deployment.

Year	Ebb delta volume (m ³ , positive anomaly)	Polynomial surface order	References/data	Figures
2002	233,300	1	DEM: Cirilli (2004) Polynomial surface: data from 2002	Fig. 4.15
2002	320,450	2	DEM: Cirilli (2004) Polynomial surface: data from 2002	Fig. 4.15
2016	434,100	1	DEM and polynomial surface: data from 2016	Fig. 4.16
2016	319,150	2	DEM and polynomial surface: data from 2016	Fig. 4.16

Fig. 4.15 and Fig. 4.16 easily describe the ADP procedure, step by step. In both cases, the second-order polynomial surface seems to best fit the ‘no delta’ configuration, as it follows the trend of the contour lines in a marked asymmetric context, due to the offset between the two adjacent barriers. The same was observed by Fontolan *et al.* (2007a, b) for the case of a jettied inlet, where a strong bathymetric offset between the opposite sides of the inlet is better represented by an interpolation that uses a higher polynomial order. The 2016 ebb-delta configuration, compared with the one for 2002, shows the ebb delta body considerably compressed toward the Martignano island (Fig. 4.15 and Fig. 4.16), although remaining stable in volume (Table 4.5).

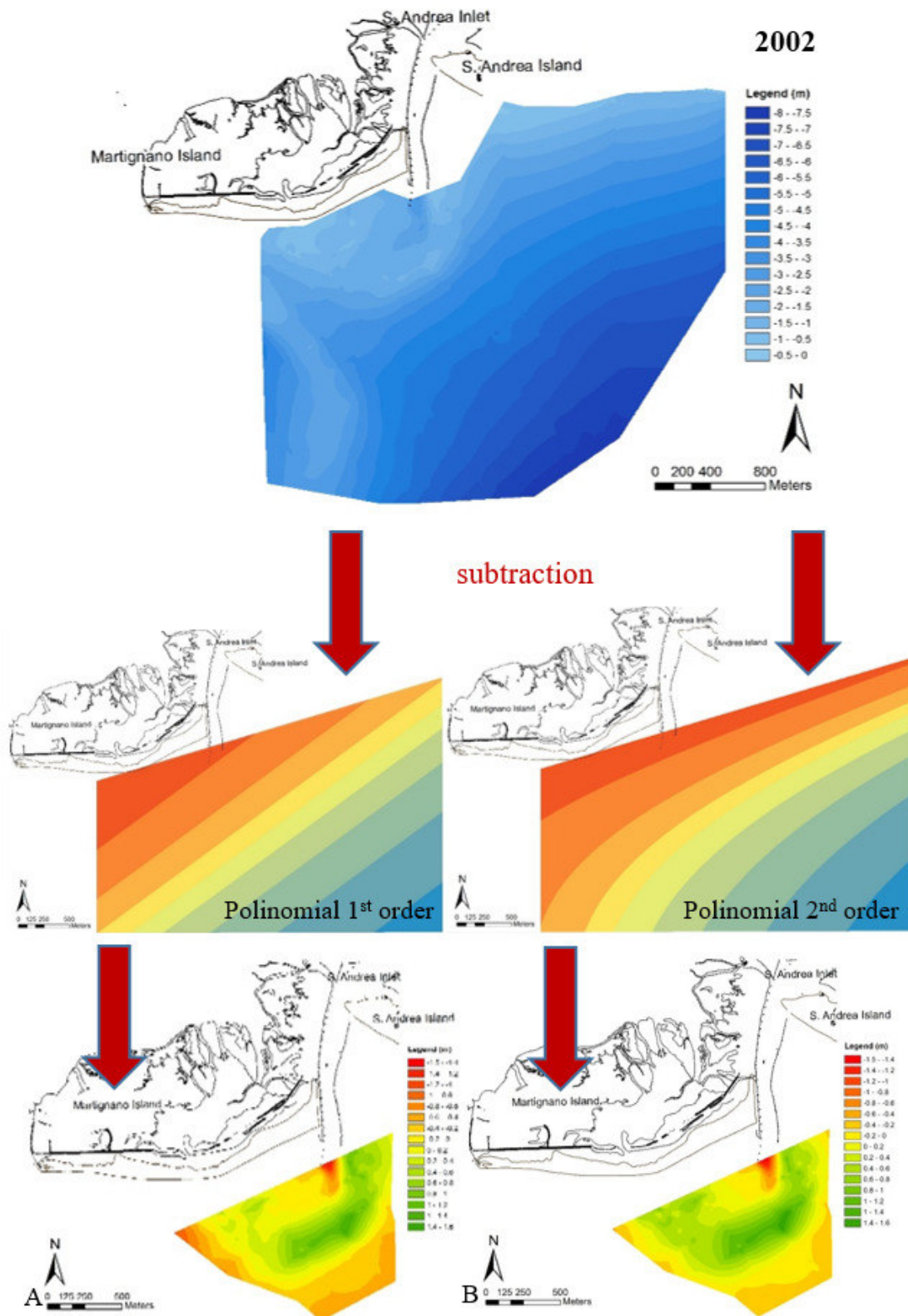


Fig. 4.15 Ebb tidal delta volume computation following the *ADP* procedure: polynomial surfaces of first (on the left) or second on the right) order were subtracting to the *DEM* of 2002 configuration, obtaining two different Residual Map (A and B).

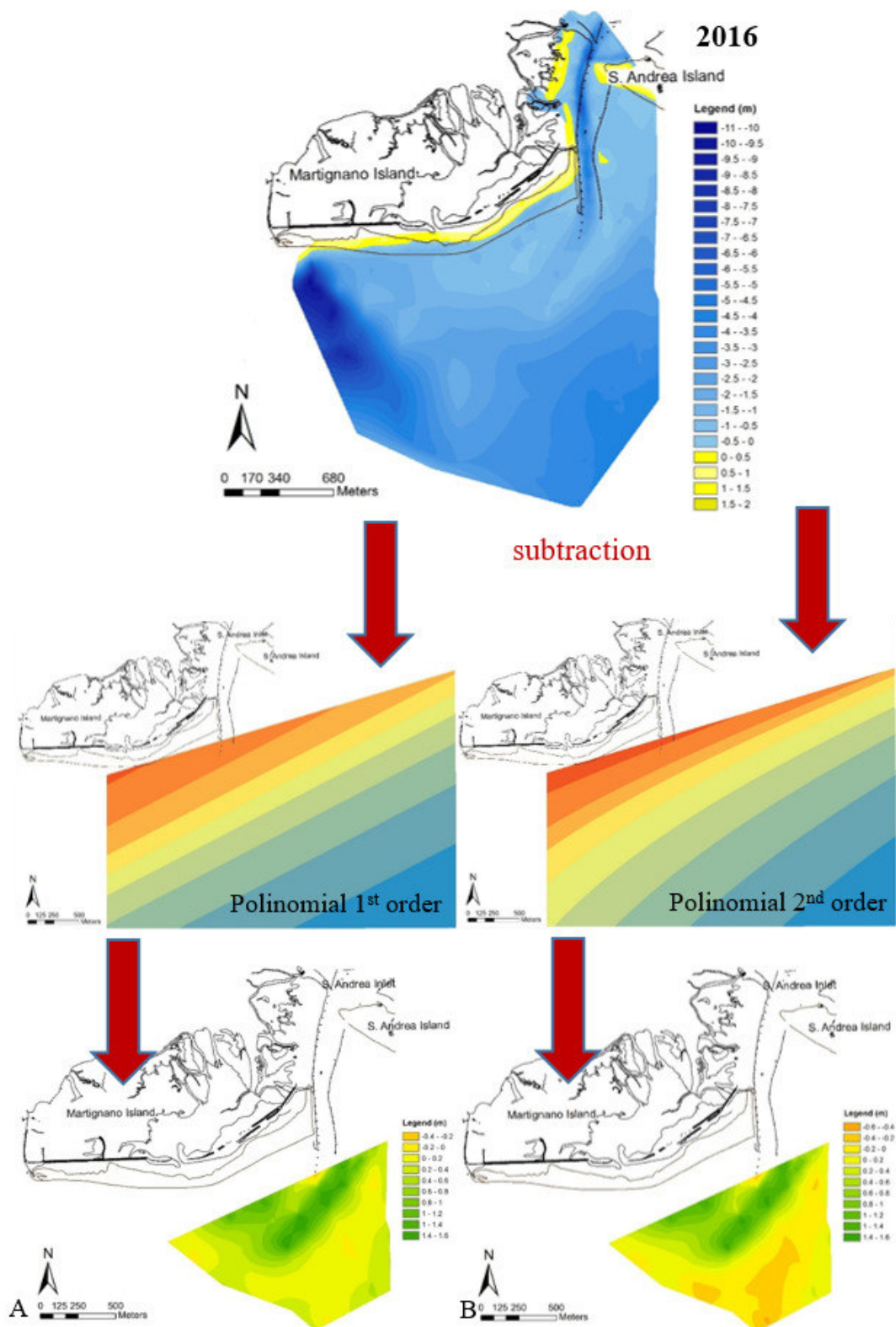


Fig. 4.16 Ebb tidal delta volume computation following the *ADP* procedure: polynomial surfaces of first (on the left) or second order on the right) were subtracting to the *DEM* of 2016 configuration, obtaining two different Residual Map (A and B).

The analysis of the wave data between 2004 and 2016 from the wave directional buoy DWRG1 of Protezione Civile della Regione FVG, according the above mentioned methodology and thresholds, reveals a net prevalence of waves and storms comes from the first quadrant (ENE, mainly *Bora*, 55%), followed by waves coming from SE (mainly *Scirocco*, 32%), while the remaining 13% is the result of waves coming from the III and VI quadrant (Fig. 4.17). These findings are in agreement with Catani and Marocco (1976), Carrera *et al.* (1995) and Osmer-FVG (www.meteo.fvg.it) regarding the wind directional statistics (Fig. 2.4).

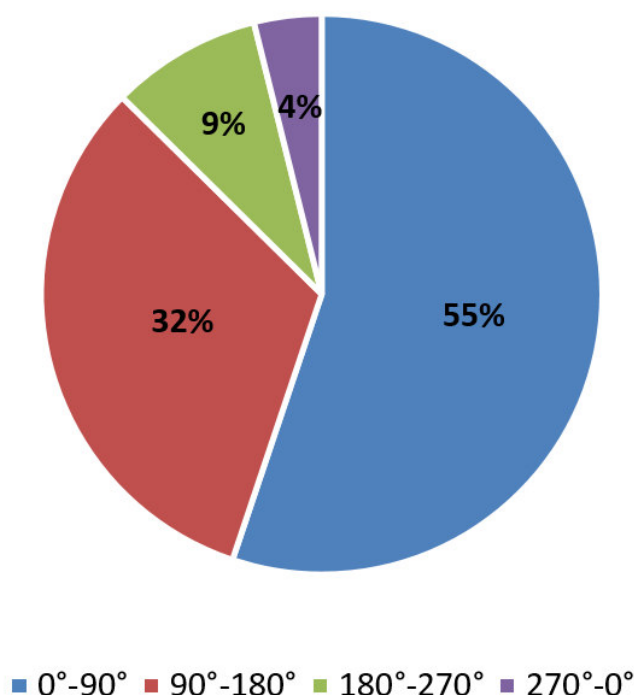


Fig. 4.17 Storm event directions distribution between 2004 and 2016.

4.4 Discussions and concluding remarks

S. Andrea Inlet has always been an important navigation route. Especially during recent decades, it is a crucial point for natural-tourism, allowing the connection between Martignano and S. Andrea Islands. It is also important in water exchange for this part of the lagoon. On the nearby backbarrier are some aquaculture plants that need good circulation of water. This inlet has always remained open in historical times (see old

maps, Fig. 4.1), highlighting a strong resilience and capacity to adapt to new conditions, in contrast to the important man-made changes to the nearby inlets aimed to increase their efficiency. Nevertheless, from the analysis conducted, nowadays S. Andrea inlet seems to be at risk of closing. The analysis of the cross sections during the time of investigation, denote a different pattern of migration of the northern sector of the main channel compared to the southern one (Fig. 4.18).

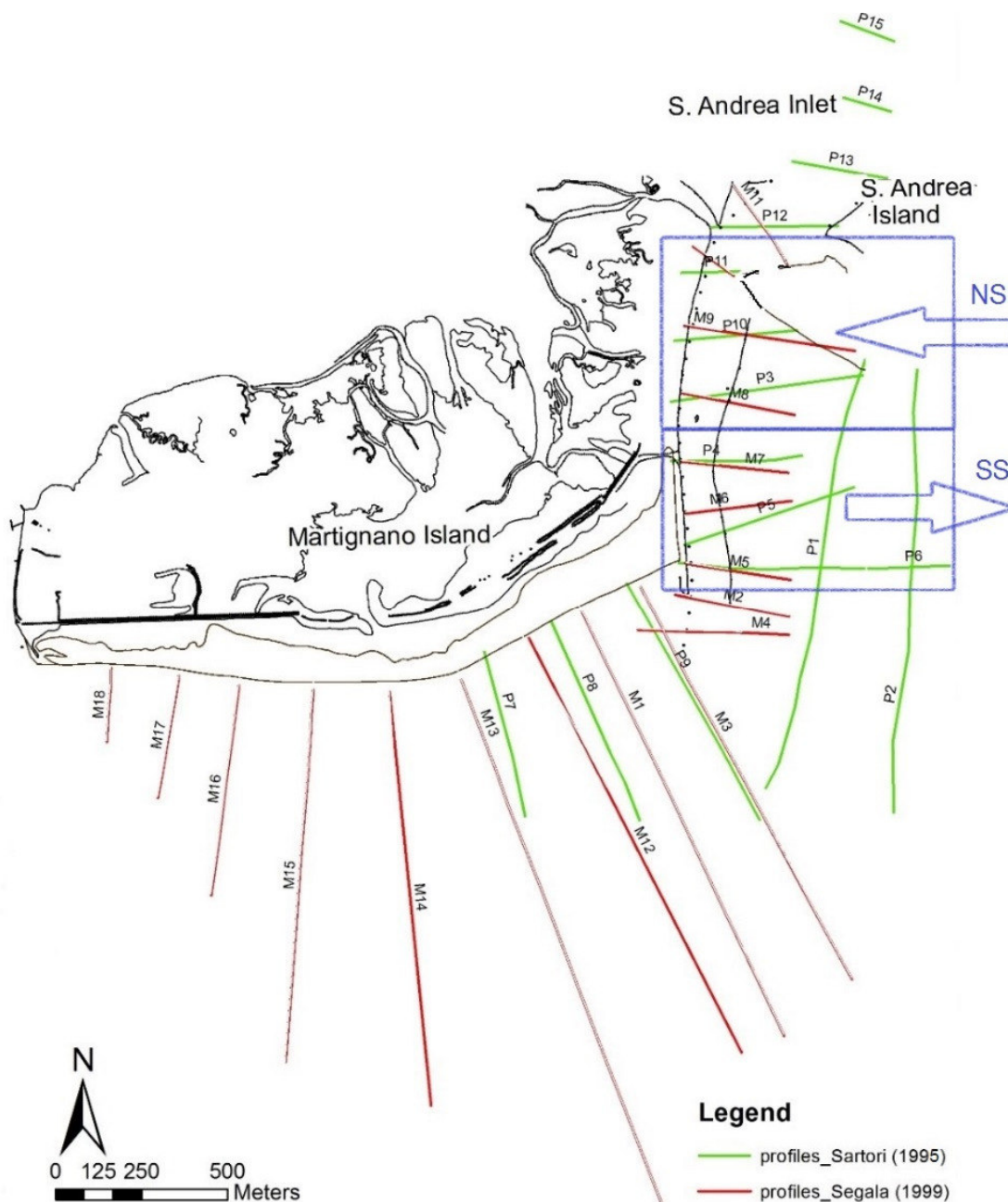


Fig. 4.18 Main channel displacement trend during the last 20 years, differentiated in northern NS and southern SS sector. Base: restitution from a 1990 orthophoto.

The advancement of S. Andrea Island spit could have prompted the northern sector of the channel to migrate westward; instead, the southern sector results tend to oscillate according to wave climate –but has overall since 1994 shifted eastward, due to the lesser effect of the longshore drift that influences the inner sector, Fig. 4.18). Sha and Van den Berg (1993) developed a descriptive model to explain the orientation of the seaward inlet channel as a response to the relative direction of waves to the interplay of tidal currents alongshore and within the inlet.

General infilling of the channel from 1994 to 2016 is recorded along the entire channel length through various methods: profiles analysis, comparison of residual maps, calculation of positive/negative sediment volume anomalies. The positive anomalies of Table 4.3 represent the amount of sediment transported by the westward longshore currents in the area. A rough estimation is 11,700 m³/y during the monitored 22 years. However, we cannot exclude the possibility that part of this amount comes from other source (e.g. from the lagoon itself).

As a result, the tidal prism almost halved from the 1960s to today (2016, Table 4.4). According to different authors (e.g. Ferla *et al.*, 2012) this drastic decrease is probably a result of the expansion of the prism (capture) of the nearby inlets of Lignano and Buso, whose artificial stabilization began in those years. Therefore, there is a general decline in efficiency of the channel. This is possibly related to the increasing efficiency of the adjacent mouths (Lignano, reinforced, and Buso, jettied) that gradually carried S. Andrea Inlet toward atrophy. The capture of tidal prism by the neighboring inlets is a well known phenomena in multi tidal inlet systems. In the previous chapter (especially Chapter 1) many example of this happening are reported that can reinforce this consideration (see the example of Matagorda Bay, Kraus and Batten, 2008).

Special attention should be given to the ebb tidal delta: according to the literature (Walton and Adams, 1976), the size of the ebb tidal delta is proportional to the tidal discharge. The delta should be the expression of the mouth efficiency as its volume can change with the modification of the inlet hydraulics. For this reason, with a decreasing in tidal prism, it would be expected to find a decrease in volume of the ebb tidal delta. Cleary and FitzGerald (2003), studying the case of Mason Inlet, a migrating opening in North Carolina, report that the long-term decline in tidal prism at the inlet resulted in a

concomitant reduction in the size of the ebb-tidal delta. As the ebb discharge decreased in the inlet channel, the amount of sand transported seaward to the ebb delta also decreased. A comparison between aerial photographs from 1986 and 2001 indicate the extent of the delta decreased markedly during this period of time (Cleary, 2002). Data on the ebb tidal delta of S. Andrea, instead, show that the delta is still conserving its volume, despite the significant reduction in tidal prism, as inferred by the significant reduction in cross section area. This could be explained by inertia of the sedimentary body to adapt to changes, being in a low wave energy regime that struggles to rework sediment and dismantle the delta. The only evidence of adaptation to the new hydrodynamic situation is the delta compression (shift) toward north-west. This might be an effect of increasing relative wave dominance on the terminal lobe. According to Cleary and FitzGerald (2003), the reduction of ebb flow, due to a decrease in tidal prism, allowed wave action and flood currents to move ebb delta sand onshore. No other example has been found in the literature that describes conservation of the ebb tidal volume during a decreasing tidal prism.

The only example that can help the discussion of this phenomena, comes from Hicks and Hume (1996). Studying several natural inlets on the open-sea (North Island, New Zeland), the authors report that the major controls on ebb delta sand volume are primarily the volume of tidal prism and secondarily the angle of inlet outflow with respect to the shoreline. Furthermore, delta volume also appears to increase with decreasing wave energy. Thus, S. Andrea ebb tidal delta volume could be in decrease due to the decline of tidal prism but the limited wave action “replenishes” the sand body, allowing the sedimentation. At the same time, similarly to what observed by Cleary and FitzGerald (2003), the wave action and the flood currents seem to shift the delta onshore. Data on wave climate indicates that almost 90% of the more energetic events comes from the first and second quadrant (Fig. 4.17) that have a marked western longshore component. Easterly waves can have pushed the ebb delta toward the eastern side of Martignano Island due to the pronounced offset of the island, which is located downdrift of the S. Andrea Inlet. As conclusive consideration, at the same time, the continuous sediment supply by the longshore currents over the delta and the strong downdrift offset that limits the accommodation could further maintain the local sedimentation, thus slowing down the possible future destruction of the ebb-tidal delta.

4.5 Chapter summary

The unconstrained S. Andrea tidal inlet, located in Italy (North Adriatic Sea), in a human-affected multi-tidal inlet system and its evolution was the subject of this chapter. Through different analysis of morphological data and using dedicated software, some results-points can be outlined:

- The *DEMs* for the surveys of 1994, 1999 and 2016 were created using *ESRI ArcGIS™ 10.3* software. The map for the survey of 1994 (Fig. 4.7) denoted a well developed main channel and a sand-bank in front of the south-eastern side of Martignano Island. In the successive survey (1999, Fig. 4.8) the channel seems to be better defined and developed, while the south-eastern part of Martignano Island starts to suffer erosion. Finally, Fig. 4.9 illustrates the 2016 configuration. The channel is shallower and a small island (swash bar) starts to emerge in the central-eastern part of it; the sand bank of the Martignano Island appears further eroded;
- Topo-bathymetric profiles from the northern sector of the main channel (Fig. 4.10), underline a displacement toward west that leads to the erosion of the north-eastern side of Martignano Island. The profiles from the southern sector (Fig. 4.11) point out the eastward displacement of the maximum depth between 1994 and 2016. Furthermore, a general decrease in depth from the 1994 to the 2016 survey is evident, causing a difficult access to the boats and a reduced exchange of water;
- Residual maps created using *ESRI ArcGIS™ 10.3* software (Fig. 4.12, Fig. 4.13 and Fig. 4.14) as well as the positive/negative anomalies calculation (Table 4.3) also highlight the general channel infilling. Between 1994 and 2016 the channel was infilled with quite thick sediment (more than 1.5 m in some parts, Fig. 4.14);
- Tidal prism calculations computed using the North Adriatic empirical relationship (Fontolan *et al.*, 2007a,b) with *Ac* evaluated through a *Matlab R2009b* computation (and *Ac* measured by Dorigo (1965) for the 1960 value) reveal a drastic reduction of about 2.5 times between 1960 and 1994; during the last twenty years, the *P* value halved, reaching a volume of circa 1,700,000 m³ (Table 4.4);
- Positive anomalies, subtracting the different ‘no delta’ (regional trend) maps from the *DEMs* representing the 2002 (Fig. 4.15) or 2016 (Fig. 4.16) tidal inlet

configuration have been extracted using the Semi-Automatic Detrending Procedure (ADP, Fontolan *et al.*, 2007a,b). Two different polynomial surfaces of the first and second order were extrapolated by the entire topographic database for the survey of 2002 or 2016 (Fig. 4.15 and Fig. 4.16) and used to compute the ebb tidal delta volume. According to the elaboration with the second-order polynomial, the ebb tidal delta resulted to have a stable volume during the 14-years period (Table 4.5). In both 2002 and 2016 cases, the second-order polynomial surface seems to best fit the ‘no delta’ configuration, as it follows the trend of the contour lines in a marked asymmetric context, due to the offset between the two adjacent barriers. The same has been observed by Fontolan *et al.* (2007a, b) for a case of jettied inlet, where a strong bathymetric offset between the opposite sides of the inlet is better represented by an interpolation that uses a higher polynomial order;

- Despite having the same volume (Table 4.5), the 2016 ebb-delta body, compared to the 2002 delta, is considerably compressed toward the Martignano island (Fig. 4.15 and Fig. 4.16). This is possibly correlated with poor wave energy and the marked downdrift offset of the inlet that limits the accommodation;
- The analysis of the wave data between 2004 and 2016 from the wave directional buoy DWRG1 of Protezione Civile della Regione FVG, reveals a net prevalence of waves and storms comes from the first quadrant (ENE, mainly *Bora*, 55%), followed by waves coming from SE (mainly *Scirocco*, 32%), while the resting 13% is the results of waves coming from the III and VI quadrant (Fig. 4.17). These findings are in agreement with that already reported by Catani and Marocco (1976), Carrera *et al.* (1995) and Osmer-FVG (www.meteo.fvg.it) regarding the wind directional data (Fig. 2.4). Thus, almost 90% of the events hit against the downdrift side of S. Andrea inlet, compressed the delta onshore, toward Martignano Island.

According to these results, local Authorities should now schedule a monitoring plan, in order to control the evolution of the inlet in the following years, in order to plan possible

actions aimed to conserve this important lagoon waterway. Consideration of management perspectives will be treated in Chapter 5.

5.
Management practices and perspectives

Since a great number of inlets have direct and indirect impacts on human economy (navigation, aquaculture, etc.), knowledge on the behaviour of this morphological element is fundamental to effective management, in order to protect the littoral zone and exploit wisely the coastal environment, respecting its functionality.

5.1 Inlet stabilization practices

Inlet stabilization has become the traditional engineering approach to the maintenance of navigation routes. Jetties are intensively used, as they are intended to make navigation safer and channel maintenance cheaper. The effects of inlet stabilization, however, may modify different features of the environment. For example they can change the shape and seaward extent of the ebb-tidal delta (Pope, 1991), by interrupting the longshore sediment transport and thus changing the hydrodynamics of the entire system and its surroundings. According to Dean (1988), at natural entrances, sand transport processes and the associated effects on adjacent shorelines depend substantially on the magnitude of longshore sediment transport. Modified inlet entrances may consequently cause additional impact on the adjacent shorelines and sediment losses to adjacent beaches. Furthermore, a small change in the conditions of one inlets in a multi-tidal inlet system, can cause unexpected consequences (see Chapter 1). The construction of jetties can block the net longshore sediment transport on the updrift side and remove sand from the channel and jet it farther seaward to the ebb tidal delta (Dean, 1988). As a consequence, the delta would shift to a greater depth (Marino and Mehta, 1988, Fig. 5.1) and the hydrodynamics of the inlet would change.

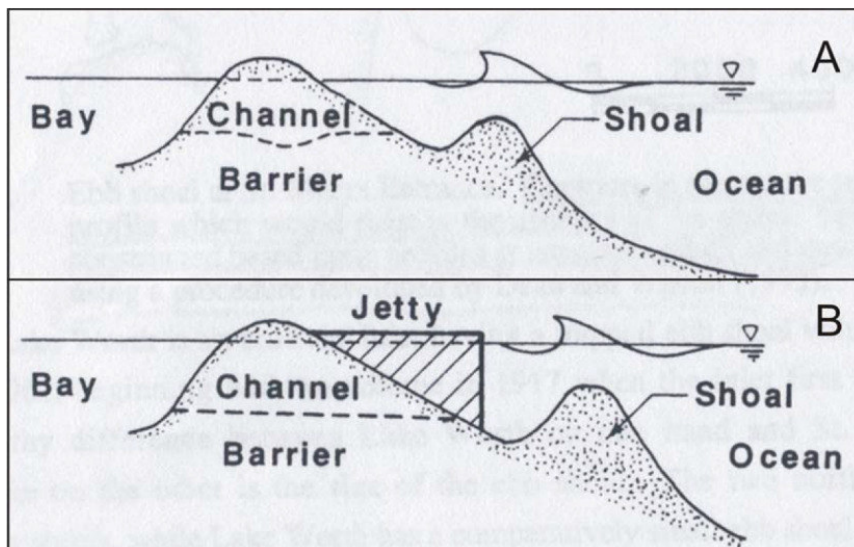


Fig. 5.1 Ebb-tidal delta development at untrained (A) and trained (B) inlets (adapted from Marino and Mehta, 1988).

As an example, Tomlinson (1991) analysed the development of the ebb-tidal delta at a tidal river inlet located in Northern New South Wales, Australia (Tweed River Entrance), after first stabilization by jetties during the beginning of XX century and, subsequently, after a jetty extension in the 1960s. He found that, since the extension of the jetties (1962-1964), the ebb-tidal delta morphology and natural sand bypassing mechanism changed extensively. A new delta formed further offshore due the constriction of the ebb discharge by the jetties (Fig. 5.2).

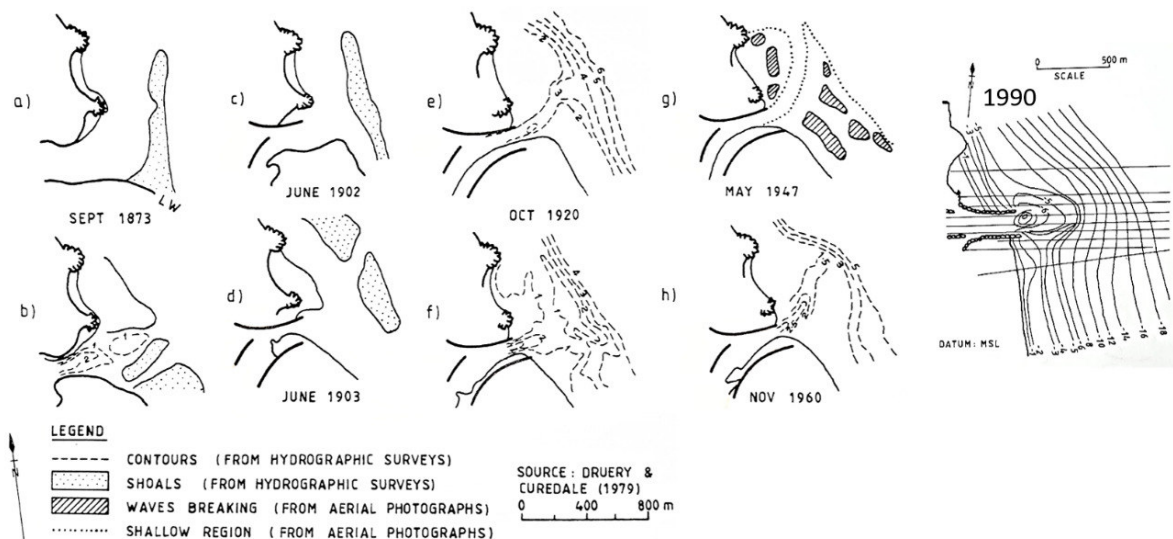


Fig. 5.2 Ebb tidal delta morphology prior and after jetties extension (adapted from Tomlinson, 1991).

Pope (1991) analyzed the behavior of four ebb-dominated inlets, between North Carolina and northern Florida, after stabilization by jetties. He showed that the inlet evolution after the stabilization included initial thalweg channelization and a fairly rapid collapse of the natural ebb-delta lobe as waves scoured the delta and transported the sediment toward the beach (Fig. 5.3A). Finally, the associated ebb-delta platform steepened as waves release materials to the downdrift side (Fig. 5.3B). However, this phenomenon may take many years to fully evolve (Pope, 1991).

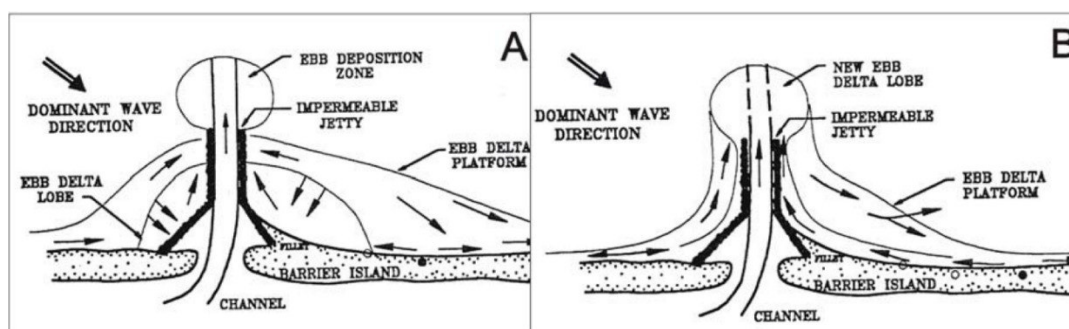


Fig. 5.3 Conceptual model of a stabilized ebb-dominated tidal inlet (adapted from Pope, 1991). A: collapse of ebb-tidal delta lobe. B: erosion of ebb-tidal delta platform.

At S. Mary's Entrance, one of the four inlets analyzed by Pope (1991), after the construction of the massive rock jetties, a large quantity of sediment from the natural ebb-tidal delta was reworked and transported offshore in response to jetty construction and channel dredging, creating a new ebb-tidal delta (Byrnes and Hiland, 1995). Following the same authors, the ebb-tidal delta shifted approximately 3 km seaward and its deposition occurred at the downdrift side of the inlet, due to a reversal in sand transport caused by localized wave refraction across the historical ebb-tidal delta, confirming the observation of FitzGerald and Hayes (1980).

Long jetties extending thousands of meters into the sea may trap and retain millions of cubic meters of sand on the updrift side (e.g. Penland, 1979; Pilkey and Neal, 1980). This is the case of Lido Inlet in the Venice Lagoon (North Italy) According to Helsby (2008), the construction of the two long jetties has changed the morphodynamic features of the inlet; prior to their construction a large spit, formed through longshore transport, extended from Punta Sabbioni (the updrift side, Fontolan *et al.*, 2007) and an extensive flood tidal delta was present (Fig. 5.4). Delli Quadri (2007) reported that, after the creation of the jetties, sediment were stored on the updrift side, causing the accretion of

that beach and resulting in sediment starvation of the ebb-tidal delta. Punta Sabbioni beach, located updrift, grew at a rate of more than 10 m/y since 1886, and more precisely the rate of growth has been 15.8 m/y between 1908 and 1933 and 10.7 m/y between 1933 and 1968. Since 1968, the rate of beach accretion has decreased, to 8.7 m/y in the period 1968-1980, to 8.5 m/y in the period 1980-1987 (Fig. 5.4, Consorzio Venezia Nuova, 1989).

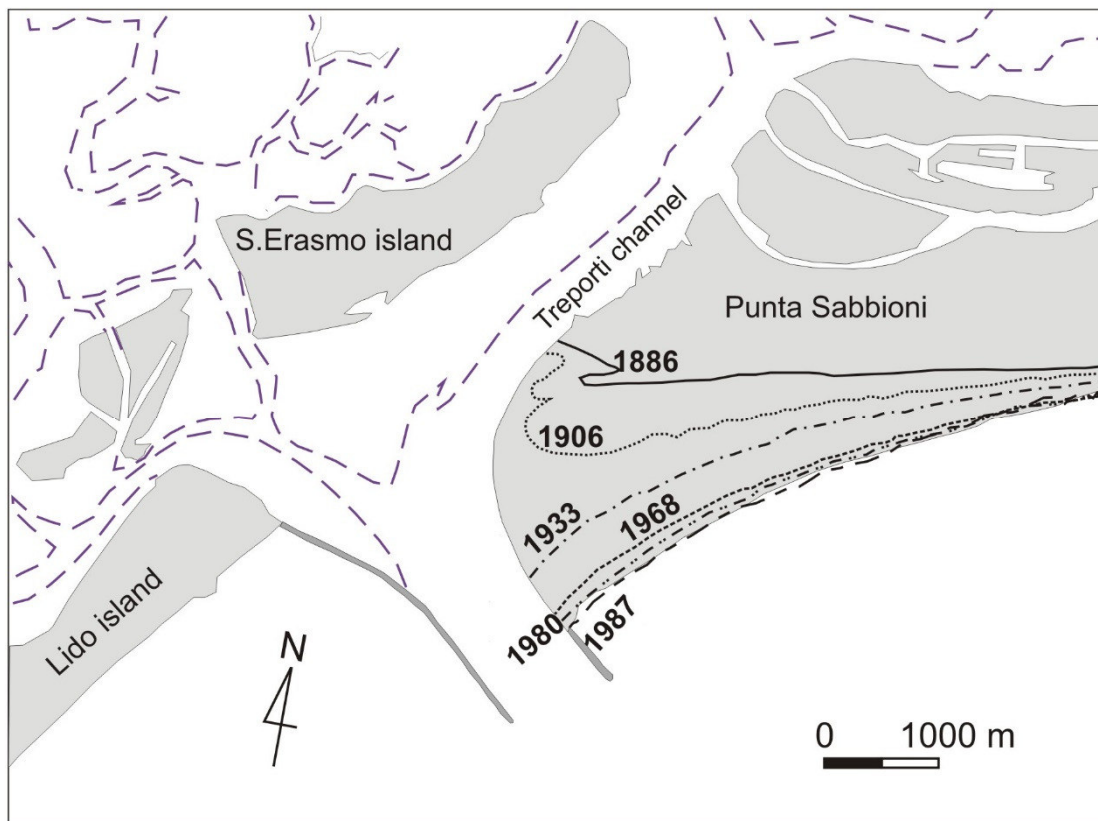


Fig. 5.4 Beach accretion at Punta Sabbioni beach after jettiy construction (adapted from Consorzio Venezia Nuova, 1989).

Hence, changing the sediment budget and longshore transport conditions at a tidal inlet means a modification of its sedimentary/accumulation bodies, first of all the ebb-tidal delta. Relationships between P and V (e.g. Walton and Adams, 1976) affirmed that a variation of tidal prism (P) of the inlet leads to a variation in ebb tidal delta volume (V). If an opening is created in a multi-tidal inlet system, any hydraulic change can bring to a modification in tidal prism/morphology of the adjacent tidal inlets relating to the same system.

Furthermore, jetties can improve the efficiency of an inlet that often assimilates the tidal prism of nearby tidal inlets relating to the same multi-inlet system. Different examples are before described in Chapter 1 and 2 (e.g. Faro-Olhão Inlet, Esaguy, 1984).

The sediment budget and wave conditions over a broad section of the coast nearby the inlet are then influenced by the stabilization by jetties (Pope, 1991). For the assumption and studies above-mentioned (Chapter 1), the loss in sediment as well as the displacement of the ebb-delta or the channelization of the thalweg, can change the stability status of the opening and lead to modifications, first of all, to the inlet morphology and then to the entire multi-tidal inlet system.

5.2 Relocation management practices

Many coastal regions are affected by quite large longshore sediment transport. This can cause an accumulation of sand on the updrift side of a tidal inlet and on its ebb-tidal delta, resulting in a modification of the thalweg (Bruun and Gerritsen, 1959), which adversely affects the normal tidal flow and could cause hydraulic efficiency issues. Since the sediment carried by currents can accumulate on the updrift side of an inlet, in some cases, the opposite side can be eroded, thus causing migration (Johnson, 1919). The rate of migration depends on various factors. First of all the contribution of sediments; secondly, the wave energy, tidal currents and the size of the main channel (Vila-Concejo *et al.*, 2002; Popesso *et al.*, 2016). Where inlet migration represents a risk to the population or can affect the navigability or the regular passage of water and nutrients, coastal managers have acted using different methods. Inlet stabilization with jetties is widespread but, as before mentioned, can cause some unexpected problems. Only recently, coastal managers began to use relocation as a particular soft engineering technique that, when applied to migrating inlets, involves the artificial opening of a new tidal inlet along the historic migration path of the inlet. Inlet relocation is a management practice that permits the use of the coastal zone, preserves natural dynamics and does not imply a large environmental impact. The concept of this approach is to work with natural processes, rather than confronting nature. It simply reproduces, when done correctly, the natural evolution of a migrating inlet and consists of relocating the opening along its historical path, leaving the

old inlet open, waiting for the capture of its prism by the new inlet, or closing it artificially. Kana (2003) reports that another benefit of inlet relocation is the release of sediment from the abandoned inlet, especially of the sediment accumulated in the ebb tidal delta that can move onshore and naturally nourish the downdrift beach.

Vila-Concejo (2003) found that the most important factor for a relocation action to succeed is the correct choice of the location of the opening. A theoretical procedure to enhance the possibilities of relocation success was suggested: (1) Hydrodynamic studies are needed in order to determine if the present conditions are similar to the historical ones. (2) The position for the inlet opening is chosen according to the hydrodynamic conditions but there are other factors to be taken into account, i.e., the historical migration paths and typical inlet width of the natural inlet; the hydrodynamics of the backbarrier; the morphology of the backbarrier and, for multi-inlet barrier island systems, the proximity to adjacent inlets. (3) Once the position is chosen, environmental impact studies should be made in order to assess the risk of the relocation for the ecosystems of the area. According to the same author, only if the environmental impact studies are favorable, should a relocation action be performed. Once the inlet is relocated, the degree of success depends on: (1) the hydrodynamic efficiency of the new inlet to remain open and (2) that the new inlet is not causing the same problems as the old one (Vila-Concejo *et al.*, 2003).

As already mentioned, only few examples of inlet relocation are reported in literature, and it is quite difficult to give a reasonable judgment about its effectiveness. Nevertheless, from the few studies, important considerations can be expressed. Briefly, it is important to describe here the few cases already mentioned in the introduction. The oldest record of relocation regards Tubbs Inlet (North Carolina, USA). The history of Tubbs Inlet before the relocation (1969-1970) was characterized by a westward migration. During the XX century, the inlet migrated westward along a 2.0 km (Marden and Cleary, 1999). The most active migration was between 1956 and 1966 when the gorge moved 810 m (Masterson *et al.*, 1973). Fig. 5.5 illustrates the adjacent shoreline from 1859 to 1970.

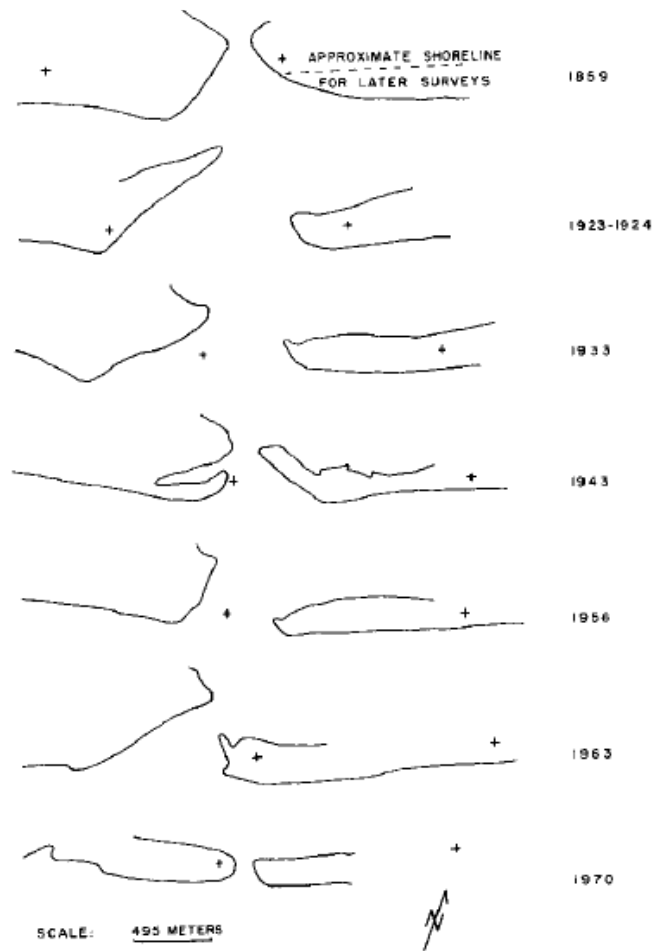


Fig. 5.5 Tubbs inlet evolution between 1959 and 1970. The + marks are in the same positions on all drawings (adapted from Masterson *et al.*, 1973).

In order to mitigate the rapid erosion of the downdrift littoral and to contrast the damages to roads and houses, the inlet was artificially relocated in December 1969 to a position 1.0 km eastward that approximated the former location of the inlet in 1938. This was accomplished by the dredging of the new channel and fill operations on the downdrift side (Masterson *et al.*, 1973). According to the same authors, since the relocation, the position of the inlet remained relatively stable but there is no information on possible channel deepening because the original depth was not known. The inlet width, instead, increased to about 333 m during 22 months from Spring 1970. After this first period of adjustment to the new hydrodynamic conditions, Tubbs Inlet reversed its migration direction going eastward, although the longshore sediment drift comes from the opposite direction (Marden and Cleary, 1999). According to Budde & Cleary (2006), this reversal

was due to the alteration of the backbarrier channel network, effectuated in those years. Not subsequent relocations are known.

The relocation of Captain Sam’s Inlet (South Carolina, USA) is one of the best-known cases. According to many authors (i.e., Mason, 1986; Kana and Mason, 1988; Kana and McKee, 2003), Captain Sam’s is a small mesotidal inlet that was relocated a first time in February 1983 because its southwestern migration and realignment of the channel was threatening the coastal population (Fig. 5.6).

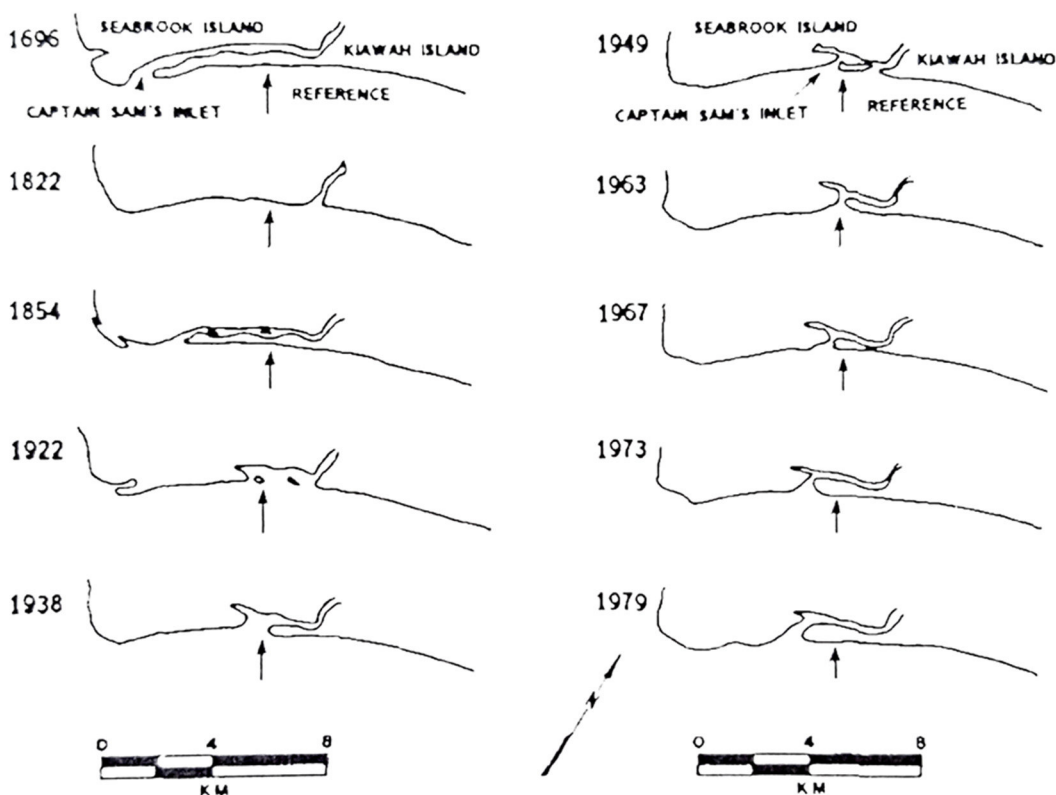


Fig. 5.6 Historical changes in the position of Captain Sams Inlet between 1696 and 1979 (adapted from Hayes *et al.*, 1979).

During the 1970s, in fact, the erosion processes threatened developments on the downdrift side. For this reason, a series of shore-protection measures were implemented (Kana, 1989). According to the same author, sandbag revetments, groins, sheetpile walls, riprap stones and eventually larger rocks were used with the hope of mitigate the erosion processes. But the erosion went on. Then, Hurricane David seriously damaged the shore-protections and the relocation-practice was taken into account (1983). Captain Sams Inlet

was relocated at its historical northernmost location 4 km from the 1979 position. The old opening was artificially closed. The excavated sand was used to reinforce the adjacent littorals (Kana, 1989). Soon the new inlet reached channel equilibrium (after six months) and the shoals from the abandoned tidal delta began to move toward the new inlet. But, because the project did not include any attempt to stabilize the new channel, the process of inlet migration continues. Five years after this first relocation, the inlet position shifted by about 500 m (Kana, 1989) and in 1996 the inlet had returned about 65% of the way to its former position: a second relocation was accomplished in April 1996 (Kana and McKee, 2003). Also in this case, the inlet continued to migrate in the same direction, and a third relocation was undertaken in July 2015. Nevertheless, the relocation of Captain Sams Inlet demonstrated that cost-effective management of migrating tidal inlets can be accomplished (Kana, 1989). Furthermore, the continuous relocations, allowed a gain of more than 1 million of cubic meters of sand for the downdrift side, since 1990 (CSE, 2017).

Although it has several advantages linked to the environmental sustainability as well as the possibility to re-use the dredged sediment from the new opening to nourish erosional adjacent beaches, this practice is not yet widely used. Relocation, as a soft intervention, is not a definitive solution. From the above-listed cases from the world, it is clear that after some time (typically decades), the inlet will likely reach the same starting position, causing the same problems as before the relocation and it is necessary to program a new intervention. It is also evident that the relocation intervention cannot be effective unless it is accompanied by other management solutions.

5.3 Dredging operations practices

One practice to improve inlet efficiency is channel dredging. The sediments taken from the dredged channels can then be used to provide sediment to sediment-starved locations, such as the downdrift side. Dredging operations (to maintain the navigable channel) must be planned properly and based on accurate sediment budget estimations to avoid potential problems and changes in the conformation of the adjacent coastlines. Pacheco *et al.* (2007) developed a conceptual coastal management program considering different

aspects and several interests socio-economical involved in a coastal management practice. The case of Gordon Pass, in the city of Naples (Florida) illustrates the issues well. Following Dabees and Moore (2011), historical survey data on the inlet show that from 1930s to 1957, prior to the dredging, the Gordon Pass shoal system had been growing. Growth was in response to increases in tidal prism principally from the closure of an inlet that existed approximately 1 mile south of Gordon Pass. From 1960 to 2003, the inlet was dredged 7 times at an average interval of approximately 7 years (Dabees and Moore, 2011). The same authors concluded that the dredged material was disposed on the downdrift beach but the studies showed that the cumulative effects of management of the inlet system through maintenance dredging and downdrift beach disposal have been insufficient to address the erosion of beaches adjacent to the inlet.

Another approach to improve inlet efficiency is to dredge the backbarrier channels connecting the inlet to the internal lagoon. A good example of this practice is from the migrating Mason Inlet, North Carolina, already mentioned. The inlet was relocated due to the shoaling of navigable waterways and due to the southerly migration that threatened some infrastructures on the nearby shoreline (Cleary and FitzGerald, 2003). The southerly longshore sediment transport, high energy wave events, and the landward movement of sand through the inlet and into the backbarrier reduced the tidal prism. The accumulation of sand, drastically diminished the water exchange between the opening and the Atlantic Intracoastal Waterway (an important artificial channel connecting the south-eastern states of USA), reducing the inlet tidal prism. FitzGerald (1988; 1996) observed that the infilling processes were most active during storms when large quantities of sand are delivered to the inlet via high-energy waves and flood tidal currents. At the same time, the storm surge caused strong landward-directed flow into the backbarrier. According to Cleary and FitzGerald (2003), several measures were undertaken to increase the tidal prism of the new inlet, as the relocation of the inlet channel 920 m to the north and the revitalization of the backbarrier channel (Mason Creek), through dredge-practice. Furthermore, a settling basin was dredged inside the inlet to help prevent rapid shoaling that is normally a product of flood-tidal delta formation. The same authors confirmed that these efforts increased the tidal prism by $3.5 \times 10^6 \text{ m}^3$ resulting in a larger equilibrium sized tidal inlet compared to the old inlet. The sediment dredged from Mason Creek was finally destined

to nourish the neighboring beaches and to close off the old Mason inlet (Cleary and FitzGerald, 2003).

5.4 Ancão inlet perspective

Ancão Inlet is in a wave-dominated environment in which there is a strong action by the western wind and, waves. This results in a very strong eastward migration process of the mouth, mainly triggered, by the wave climate. The migration leads to prism atrophy and the inability to maintain a stable mouth, hampers the navigation and makes difficult to use the western territory of Ria Formosa, poorly served by the mouth (bad circulation of water serving the backbarrier etc.). These consequences are nowadays creating conflict with the human needs.

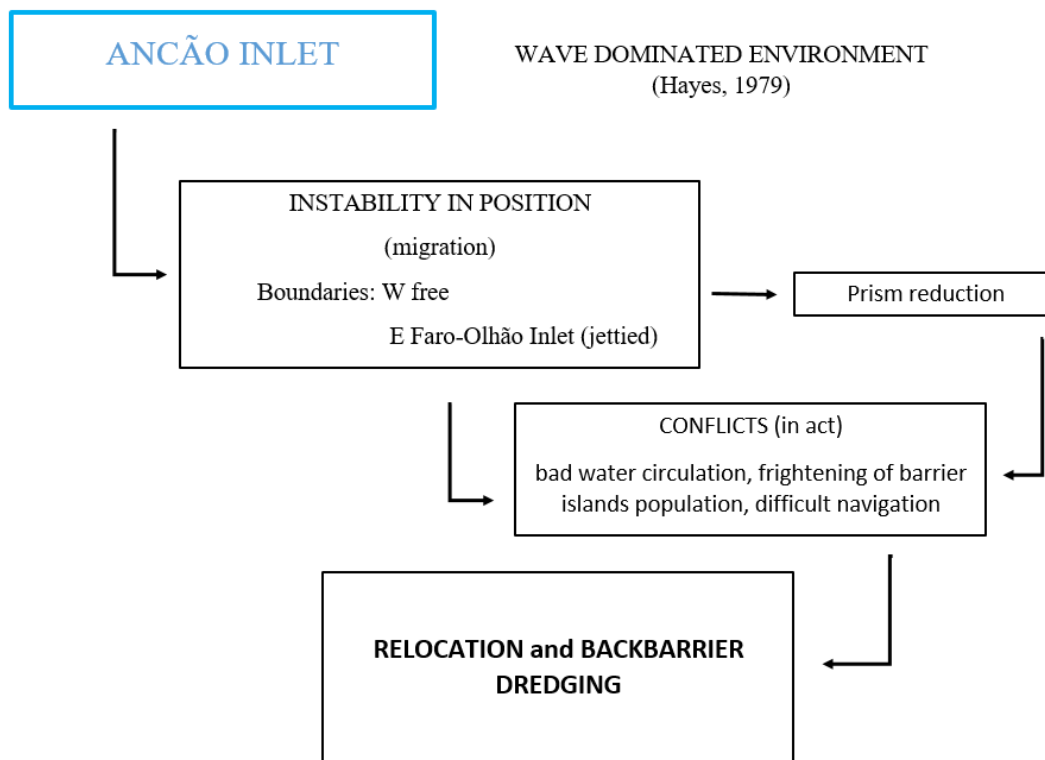


Fig. 5.7 Conceptual scheme for Ancão Inlet situation.

Managers cannot allow a tidal flow interruption through inlet closure, nor wait for an abrupt or extreme event to cause a natural break to restore the circulation process. For this reason, over the decades, the inlet has been relocated several times, repositioning it

along the old path followed by it (Fig. 5.7). After a short period of settling, the inlet starts again its migration path, denoting the ineffectiveness of this management procedure. As the migration rate of the inlet along the common path seems to increase over time for the progressive fragility of the barrier involved by migration, the main question is what is the possible management solution for this inlet? The procedure of fixing the mouth through jetties would seem to be inappropriate because, although it would improve the inlet efficiency, it would generate large offsets and weaken the already precarious conditions of the downdrift side (see Lido Inlet case, Fig. 5.4). A possible solution could be coupling management of inlet relocation and dredging of the backbarrier channels connecting the opening to the internal lagoon. Following the example of Mason Inlet, this practice could enhance circulation on the backbarrier area, largely occupied by washover bodies and flood delta remnants, thus improving water exchanges, increasing the tidal prism and making the tidal inlet size more stable. If it is feasible, the dredged sediments should be used to reinforce the adjacent downdrift beach and or nourish nearby beaches that need a refill of sand.

5.5 S. Andrea Inlet perspective

The case of S. Andrea Inlet is an indirect consequence of the stabilization of the two neighbouring openings, Lignano (to the West) and Buso Inlet (to the East). The geomorphological analysis confirmed a tidal prism reduction (Chapter 3) and a contraction toward Martignano Island of the ebb tidal delta body, although its volume seems to be unaltered (2002-2016).

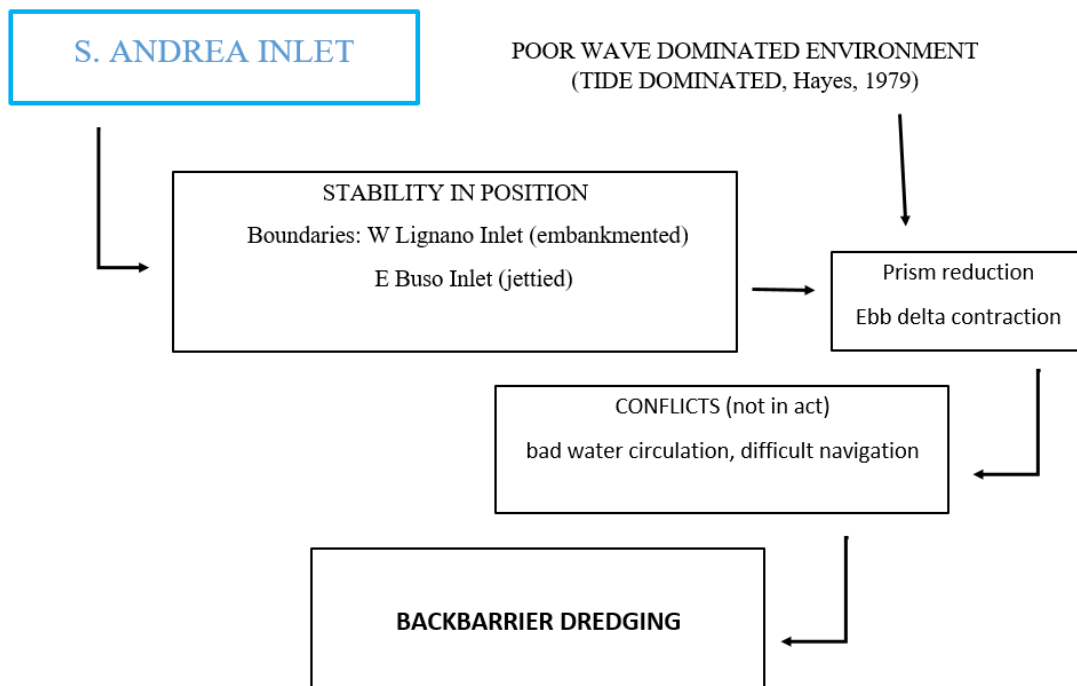


Fig. 5.8 Conceptual scheme for S. Andrea Inlet situation.

The Italian lagoons of the Northern Adriatic (Venice and Marano and Grado) are heavily used environments for the exploitation of resources within the lagoon. In these environments, the wave forcing is much smaller. They occur in a semi-closed fetch-limited basin (northern Adriatic) and therefore waves have a minor effect on inlet dynamics. These lagoons are more regulated by tidal flow, resulting in tide-dominated environments.

S. Andrea Inlet experiences stability in its position, in the middle of the two largest and most efficient mouths of the system, Lignano and Buso inlets. Over the last few decades, S. Andrea inlet underwent a substantial decrease of the tidal prism that was mostly captured by the two nearby mouths, whose hydraulic efficiency was enhanced by inlet stabilization and dredging. The mouth is unconstrained and has never been affected by any management intervention. Due to these characteristics, the tidal prism reduction, the channel infilling and the contraction of the ebb tidal delta are significant signals of changes that could soon generate, as in Ancão Inlet case, a poor water circulation in the backbarrier and an unsafe navigation (Fig. 5.8). No real conflict currently exists, but if the trend proceeds, possible issues could arise. The flood delta zone is an important site for shellfish activities that need good oxygenation and a sandy bottom. Possible atrophy

of the mouth could lead to the inlet closure, with cessation of all the economic exploitation.

S. Andrea and Ancão Inlet have very different behaviour, but the conflicts that could be generated are the same. For this reason, also for the case of S. Andrea Inlet the suggested management is the dredging of the backbarrier channels. This could allow an improvement in efficiency of water exchange and guarantee longer survival of the opening and of the activities that rely on it. A stabilization could possibly increase the competence of the inlet but it is likely to generate too strong currents as well as possible large offset along the updrift side, thus inducing critical erosion issues to Martignano Island, located downdrift. Furthermore, a stabilized S. Andrea Inlet, as placed in such delicate multi-tidal inlet system, can disrupt the equilibrium of the other nearby inlets, as predicted by different authors (see Chapter 1). Dredging the internal channels would lead to an increase in efficiency, but less drastic than that one caused by a permanent inlet stabilization.

6.
Concluding remarks

The world's coastline extends for about 440,000 km. Because nearly half of the global population lives within less than 100 km of the coastline, the coastal zone has become perhaps the most critical part of the Earth's surface in term of global economy, strategies and management needs (Davis and FitzGerald, 2009).

The development of lagoons is closely related to several interacting factors, such as the tidal range, wave energy, solid and liquid flow rates from sea and rivers, transport of the sediment due to the longshore currents, the wind effects and in general the climate, that controls the whole system and, at long term, the eustatic and isostatic processes (Brambati, 1988).

The life of a lagoon is related to its degree of freedom, thus meaning the possibility of evolution of the environment as a whole, from the surfaces periodically subjected to the action of the tides, to the inlet positions, to the morphology of the barrier islands. Tides, waves, sediment sources, eustasy and climate determine the dynamic equilibrium of the system. The changing of one of these basic parameters through direct or indirect human intervention can alter this balance, causing modifications very different from those due to the natural behavior.

The lagoons, in a certain sense, can be understood as natural harbors, already inherently protected from energy from the sea or ocean. For this reason, they are often places of important trading ports and conservation zones. Hence the need to understand their evolutionary processes thoroughly, monitoring them in order to preserve these environments and, at the same time, to gain the benefits they offer (trade, tourism etc.). Proper management of this environment is essential in order to limit natural upheavals that can also be countered by man.

The aim of this thesis was to focus on the sensitivity of certain environments to natural and man-made changes and how they can respond to this kind of stress. The intention is to verify the behavior of unconstrained tidal inlets that can undergo modifications related to forcing that are natural or man-made. The goal is to understand what effects and conflicts can arise from this natural behavior with respect to man's manners. Finally, to investigate solutions for reducing these conflicts thus possibly conserving both the natural equilibrium and the human uses.

In both multi-inlet lagoon systems examined, the most important morphological changes are attributable to the ongoing works and management by man that still characterize the entire lagoon area. Over the years, land reclamations, consolidation of the lagoon embankments and, especially, the dredging of channels for navigation, sea defenses construction and the stabilization of tidal inlets were more and more invasive. Several conflicts between natural processes and human needs have arisen, altering the natural evolution of the lagoons. The example of the opening and stabilization of Faro-Olhão Inlet is striking, leading to a significant change of the hydrodynamic regime of the nearby Armona Inlet. In the case of Ancão inlet, its tendency to migrate and the human needs for good oxygenation of the backbarrier area and an easy and sure navigation through the inlet generated a conflict. The stabilization of the nearby Faro-Olhão inlet did not cause substantial changes on it. Moving to the Italian case, the need to guarantee an adequate waterway to the commercial vessels stabilizing Buso and Lignano Inlets and dredging the main channels, greatly influenced the evolution of S. Andrea Inlet, threatening its stability and efficiency.

The cases reported, although different, are both linked to the natural response of a human modification carried out in a multi-inlet system, as examples of a reaction of this type of environment. In contrast to this behavior, sometimes there are no other solutions than the maintenance of the openings through dredging or fixing. In extreme cases, as Ancão, the inlet relocation is the obvious choice. The proposal of dredging the channels connecting the openings with the backbarrier could be an efficient management action, because it is not so invasive and, furthermore, the sediments dredged could be re-use to reinforce weak part of the shoreline.

Thus this thesis wants also to stress the need for a correct and sustainable approach in order to avoid high impact of the human action. The alteration of environmental equilibrium derived, overall, from the frequent inability of natural forms to react (quickly) to the changes induced by man. The use of a fragile and ephemeral environment like a lagoon tends unavoidably to create disequilibrium. This occurs in a chain of effects that lead all to the changing in hydrodynamics, starting from or leading to the inlets.

References

ALMEIDA, L.P., FERREIRA, Ó., AND PACHECO, A. 2011a - Thresholds for morphological changes on an exposed sandy beach as a function of wave height. *Earth Surface Processes and Landforms*, 36(4), 523-532pp.

ALMEIDA, L.P., FERREIRA, Ó., VOUSDOKAS, M.I., AND DODET, G. 2011b - Historical variation and trends in storminess along the Portuguese South Coast. *Natural Hazards and Earth System Sciences*, 11(9), 2407-2417pp.

ANDRADE, C.F. 1990 - O Ambiente de Barreira da Ria Formosa. Lisbon, Portugal: University of Lisbon, unpublished Ph.D. dissertation, 626p. (in Portuguese)

AUBREY, D.G. 1986 - Hydrodynamic Controls on Sediment Transport in well-mixed Bays and Estuaries. In: J. Vand de Kreeke, Ed.: *Physics of Shallow estuaries and Bays*. Coastal and Estuarine Studies, 16. Springer-Verlag, New York, NY, 245-258pp.

AUBREY, D.G. AND SPEER, P.E. 1983 - Sediment transport in a tidal inlet. Technical Report WHOI-83-20, Woods Hole Oceanographic Institution, Woods Hole, MA, 110p.

AUBREY, D.G. AND SPEER, P.E., 1985. A Study of Non-Linear Tidal Propagation in Shallow Inlet/Estuarine Systems. Part I: Observations. *Estuar. Coast. Shelf Sci.* 21, 185-205 pp.

BALL, M.M., SHINN E.A., AND STOCKMAN K.W. 1967 - The geologic effects of Hurricane Donna in South Florida. *Journal Geology*, 75(5), 583-597pp.

BARNES, R.S.K. 1980 - *Coastal Lagoons*. Cambridge University Press, Cambridge: 106pp.

BATTEN, B. K., KRAUS, N. C., AND LIN, L. 2007. Long-term inlet stability of a multiple inlet system, Pass Cavallo, Texas. In *Coastal Sediments' 07*, 1515-1528 pp.

BERTOTTI, L., CAVALERI, L., AND TESCARO, N. 1996 - Long term wave hindcast in the Adriatic Sea. *Il Nuovo Cimento*, 19C (1), 91-108pp.

- BETTENCOURT, P. 1994 - Les environnements sédimentaires de la côte sotavento (Algarve, Sud Portugal) et leur évolution holocène et actuelle. Bordeaux, France: University Bordeaux I, unpublished Ph.D. dissertation, (in French)
- BEZZI, A. 2013 - Le barene della laguna di Marano e Grado: analisi degli aspetti morfo-evolutivi nella prospettiva gestionale. Trieste, Italy: University of Trieste, unpublished Ph.D. dissertation, 154p. (in Italian)
- BIRD, E.C.F. 1994 - Physical setting and geomorphology of coastal lagoons. In: (Kierfve B. J. Ed.) Coastal Lagoon Processes. Elsevier Oceanography Series, 60, Elsevier Science Publishers B. V., New York, 9-39pp.
- BOON, J.D. AND BYRNE, R.J. 1981 - On basin hypsometry and the morphodynamic response of coastal inlet systems. *Marine Geology* 40, 27-48pp.
- BOOTHROYD, J.C. AND HUBBARD, D.K. 1975 - Genesis of bedforms in mesotidal estuaries. *Estuarine Research*, 2, Academic Press, New York, 129-149pp.
- BONDESAN, M., CASTIGLIONI, G.B., ELMI, C., GABBIANELLI, G., MAROCCO, R., PIRAZZOLI, P.A., AND TOMASIN, A. 1995 - Coastal areas at risk from storm surges and sea-level rise in north eastern Italy. *Journal of Coastal Research*, 11 (4), 1354-1379pp.
- BOUMA, A. H. AND W. R. BRYANT. 1969. Rapid delta growth in Matagorda Bay, Texas. In *Coastal Lagoons, A Symposium*. Universidad Nacional Autónoma de México, San Antonio, TX, 171-189 pp.
- BRAMBATI, A. 1970 - Provenienza, trasporto e accumulo dei sedimenti recenti nelle lagune di Marano e di Grado e nei litorali tra i fiumi Isonzo e Tagliamento. *Memorie della Società Geologica Italiana, Arti Grafiche Pacini Mariotti, Pisa, IX*, 281-329pp.
- BRAMBATI, A. 1983 - Modificazioni costiere nell'arco lagunare dell'Adriatico settentrionale. *Antichità Altoadriatiche*, 27, 13-47pp. (in Italian)
- BRAMBATI, A. 1987 - Studio sedimentologico e marittimo-costiero dei litorali del Friuli-Venezia Giulia. Ipotesi di intervento per il recupero ambientale e la valorizzazione della fascia costiera. Regione Autonoma Friuli-Venezia Giulia, Direzione Regionale dei Lavori Pubblici, Servizio all'Idraulica, Trieste, 67p.

BRAMBATI, A. 1988 - Lagune e stagni costieri: due ambienti a confronto. In: (a cura di Carrada G. C., Cicogna F. e Fresi E.) *Le lagune costiere: ricerca e gestione*. Ed CLEM, Massa Lubranense (Na), 9-33pp. (in Italian)

BRAMBATI, A. 1996 - *Metalli pesanti nelle lagune di Marano e Grado - Piano di studi finalizzato all'accertamento della presenza di eventuali sostanze tossiche presenti nel bacino lagunare di Marano e Grado e al suo risanamento*. Regione Autonoma Friuli-Venezia Giulia, Direzione dell'Ambiente- Servizio dell'idraulica, Trieste, 174p. (in Italian)

BRAMBATI, A., DE MURO, S., MAROCCO, R., AND SELIVANOV, A. 1998 - Barrier island evolution in relation to sea-level changes: the example of Grado Lagoon (northern Adriatic Sea, Italy). *Bollettino di Geofisica Teorica ed Applicata*, 39(2), 145-161pp.

BRODERS, S. 2002. *Masons Inlet relocation project completed*. The Seahawk. UNCW Student Newspaper. Available at www.surfrider.org/capefear/beachrenourishmentMasonsInlet.htm.

BROUWER, R.L. 2013 – *Cross sectional stability of double inlets systems*. Delft, Netherlands: Delft University of Technology, Ph.D. dissertation, 135p.

BROUWER, R.L., ZITMAN, T.J., SHUTTELAARS, H.M., AND VAN DE KREEKE, J. 2008 - Effects of amplitude differences on equilibrium and stability of a two-inlet bay system. In Dohmen-Janssen and Hulscher, editors, *River, Coastal and Estuarine Morphodynamics 2008*, London, 2007. RCEM 2007, Taylor & Francis, 33-40pp.

BROUWER, R.L., VAN DE KREEKE, J. AND SCHUTTELAARS, H.M., 2012 - Entrance/exit losses and cross-sectional stability of double inlet systems. *Estuarine Coastal and Shelf Science* 107, 69-80pp.

BROUWER, R.L., SCHUTTELAARS, H.M., AND ROOS, P.C. 2013 - Modelling the influence of spatially varying hydrodynamics on the cross-sectional stability of double inlet systems. *Ocean Dynamics*, 63(11), 1263-1278pp.

BROWN, E.I. 1928 - *Inlets on sandy coasts*. Proceedings, American Society of Civil Engineers, 54, 505-553pp.

BRUUN, P. 1966 - *Tidal inlets and littoral drift*. Oslo, Univ. Book Co., 193pp.

BRUUN, P. 1978 - Stability of tidal inlets, theory and engineering. Elsevier, Amsterdam, The Netherlands.

BRUUN, P. AND GERRITSEN, F. 1959 - Natural by-passing of sand at coastal inlets. Journal of the Waterways and Harbors Division, 85(4), 75-108pp.

BRUUN, P. AND GERRITSEN, F. 1960 - Stability of coastal inlets. Coastal Engineering Proceedings, 1(7), 23p.

BRUUN, P., BHAKTA, N.P. AND GERRITSEN, F. 1974 - Evaluation of overall entrance stability at tidal entrances. Proceedings 14th Conference Coastal Eng., A. S. C. E., Copenhagen, 1655-1684pp.

BUDDE, L.E. AND CLEARY, W.J. 2006 - Barrier progradation related to inlet spacing and migration patterns. Journal of Coastal Research, 117-121pp.

BURLA, I. 2003 - Metodologie di valutazione del rischio costiero associate a diverse valenze territoriali. Trieste, Italy: University of Trieste, unpublished Ph.D dissertation, 201p. (in italian)

BYRNES M. R. AND HILAND M. W. 1995 - Large-scale sediment transport patterns on the continental shelf and influence on shoreline response: St. Andrew Sound, Georgia to Nassau Sound, Florida, USA. Marine Geology, 126: 19-43pp.

C.E.R.C. 1984. Shore Protection Manual. 4th edition. Coastal engineering research unit. Department of the Army Washington D.C., 354 pp.

CARRASCO, A.R., FERREIRA, Ó., MATIAS, A., PACHECO, A., AND FREIRE, P., 2011. Short-term sediment transport at a backbarrier beach. J Coast Res 27(6):1076–1084 pp.

CARRERA, F., CERASUOLO, M., TOMASIN, A., AND CANESTRELLI, P., 1995 - La nebbia a Venezia nel quarantennio 1951e1990. Analisi comparata degli andamenti di visibilità, pressione, temperatura e vento. In: Rapporti e Studi, XII. Istituto Veneto di Scienze, Lettere ed Arti, Commissione di Studio dei provvedimenti per la conservazione e difesa della laguna e della città di Venezia, 235-271pp. (in Italian).

CATANI, G. AND MAROCCO, R. 1976 - Considerazioni sulle caratteristiche mareografiche e anemografiche a S. Nicolò di Lido, Punta Tagliamento e Grado. In: (a

cura di Versino L.) Ricerche sul regime e la conservazione dei litorali. CNR, Quaderni de la Ricerca Scientifica, 92, 21-25pp. (in Italian)

CAVALERI, L., BERGAMASCO, L., BERTOTTI, L., BIANCO, L., DRAGO, M., IOVENITTI, L., LAVAGNINI, A., LIBERATORE, G., MARTORELLI, S., MATTIOLI, F., OSBORNE, A.R., PEDULI, L., RIDOLFO, R., SCLAVO, M., SERIO, M., TESCARO, N., RIBALDI, S., TOSI, E., AND VIEZZOLI, D. 1996 - Wind and waves in the northern Adriatic Sea. *Il Nuovo Cimento* 19(1), 136pp.

CAVAZZONI S. & GOTTARDO D., 1983. Processi evolutivi e morfologici nella laguna di Venezia - Proceedings of the Conference 'Laguna, fiumi, lidi: cinque secoli di gestione delle acque nelle Venezia', 10-12, June, 1983, Venezia.

CIALONE, M.A., SEABERGH, W.C. AND WATSON, K.D., 1999. Flood shoal response to inlet modifications at Barnegat Inlet, New Jersey. Proceedings Coastal Sediments '99 Conference (New York, U.S.A., ASCE), 1434-1449 pp.

CIAVOLA, P., TABORDA, R., FERREIRA, Ó., AND DIAS, J.A. 1997 - Field measurements of longshore sand transport and control processes on a steep meso-tidal beach in Portugal. *Journal of Coastal Research*, 13(4), 1119-1129pp.

CIRILLI, S. 2004 - Morfodinamica delle bocche lagunari e potenzialità di utilizzo delle sabbie di delta di riflusso come cave di prestito per interventi di rifluimento. Trieste, Italy: University of Trieste, unpublished Ph.D. dissertation, 172p. (in Italian)

CLEARY, W.J. 2002 - Variations in Inlet Behavior and Shoreface Sand Resources: Factors Controlling Management Decisions, Figure Eight Island, NC, USA. *Journal of Coastal Research*, 148-163pp.

CLEARY, W.J. AND FITZGERALD, D.M. 2003 - Tidal inlet response to natural sedimentation processes and dredging-induced tidal prism changes: Mason Inlet, North Carolina. *Journal of Coastal Research*, 1018-1025pp.

CLEARY, W.J. AND PILKEY, O.H. 1996 - Environmental coastal geology: Cape Lookout to Cape Fear, North Carolina; Regional overview. In: (W. J. Cleary Ed) *Environmental Coastal Geology: Cape Lookout to Cape Fear, NC*. Carolina Geological Society Fieldtrip Guidebook, 87-128pp.

CONSORZIO VENEZIA NUOVA, 1989 - Progetto preliminare di massima delle opere alle bocche. Descrizione dell'ecosistema, parte II, Venezia, 2: 254 pp.

CORSINI, S., INGHILESI, R., FRANCO, L., AND PISCOPIA, R. 2004 - Atlante delle onde nei mari italiani - Italian wave atlas. Agenzia per la Protezione dell' Ambiente e per i Servizi Tecnici (APAT) e Università di Roma "3".

COSTA, M. 1994 - Agitação marítima na costa portuguesa. Anais do Instituto Hidrográfico 13, 35-40pp. (in Portuguese).

COSTA, M., SILVA, R., AND VITORINO, J. 2001 - Contribuição para o estudo do clima de agitação marítima na costa Portuguesa. Actas das 2as Jornadas Portuguesas de Engenharia Costeira e Portuária (Sines, Portugal), Associação Internacional de Navegação, CD-ROM, 20p. (in Portuguese)

CSE, 1995. Relocation of Captain Sams Inlet and Beach Restoration Plan. Seabrook Island, South Carolina. Coastal Science & Engineering Inc. Technical Report CSE-738R. 153 pp.

CSE, 2001. Seabrook Island, South Carolina. Captain Sams Inlet Relocation Project. Survey Report no.5. Coastal Science & Engineering, Inc. Technical Report CSE-2056R. 40 pp.

CSE, 2017. Captain Sams Inlet Relocation - 2015 Seabrook Island South Carolina. Monitoring Report - Year 2 to Seabrook Island POA. CSE, Columbia, SC, 61 pp + appendices.

DABEES, M.A. AND MOORE, B.D. 2011 - Evaluation of inlet management practices at navigation inlets in southwest Florida, USA. Coastal Engineering Proceedings, 1(32), 89pp.

DAL CIN, R. AND SIMEONI, U. 1994 - A model for determining the classification, vulnerability and risk in the Southern coastal zone of the Marche (Italy). Journal of Coastal Research, 10(1), 18-29pp.

DAVIES, J.L. 1964 - A Morphogenic approach to World Shoreline. Zeitschrift für Geomorphologie, 8, 27-42pp.

DAVIS, R. A. Jr, 1989. Morphodynamics of the west-central Florida barrier system: the delicate balance between wave and tide-domination. Coastal Lowlands, Geology and Geotechnology, Dordrecht, 225-235 pp.

DAVIS, R.A. AND BARNARD, P.L. 2000 - How anthropogenic factors in the back-barrier area influence tidal inlet stability: examples from the Gulf Coast of Florida, USA. Geological Society, London, Special Publications, 175(1), 293-303pp.

DAVIS, R. A. JR AND BARNARD, P. 2003. Morphodynamics of the barrier-inlet system, west-central Florida. Marine Geology, 200: 77-101 pp.

DAVIS JR, R.A. AND FITZGERALD, D.M. 2009 - Beaches and coasts. John Wiley & Sons. 432pp.

DAVIS JR, R.A. AND GIBEAUT, J.C. 1990 - Historical morphodynamics of inlets in Florida, models for coastal zone planning. Technical Paper 55, Florida Sea Grant College Program, Gainesville, Florida.

DAVIS R.A. AND HAYES M.O. 1984 - What is a wave-dominated coast?. In: (Elsevier Science Publishers) Marine Geology, n. 60: 313- 329pp.

DAVIS, R.A., HINE, A.C., AND BLAND, M.J., 1987. Midnight Pas, Florida: inlet instability due to non-related activities in Little Sarasota Bay. In: Kraus, N.C. (Ed.), Coastal Sediments, ASCE, 2062-2077 pp.

DAY J. W., SCARTON F., RISMONDO A. e ARE D., 1998. Rapid Deterioration of a Salt Marsh in Venice Lagoon. Italy. Journal of Coastal Research, 14 (2): 583-590 pp.

DEAN R. G., 1988 - Sediment interaction at modified coastal inlets: processes and policies. In: Hydrodynamics and Sediment Dynamics of Tidal Inlets (Eds. Aubrey D. G. and Weishar L.), Springer-Verlag: 412-439 p.

DELLI QUADRI, F. 2007 - Coastal sedimentary traps as potential borrow sources for nourishment of neighbouring erosional beaches. Trieste, Italy: University of Trieste, unpublished Ph.D. dissertation, 122p. (in Italian)

DE SWART, H.E. AND VOLP, N.D. 2012. Effects of hypsometry on the morphodynamic stability of single and multiple tidal inlet systems. Journal of sea research, 74, 35-44 pp.

- DIAS, J.A. 1988 - Aspectos geológicos do litoral algarvio. *Geonovas* (Lisboa) 10, 113-128pp. (in Portuguese)
- DIAS, J.M.A., FERREIRA, Ó, SÁ-PIRES, C., DUARTE, C. 2000 - Relatório de Monitorização da Repulsão de Dragados para a Zona de Barreira do Sistema da Ria Formosa. CIACOMAR Technical Report n. 06/00, 55p. (in Portuguese)
- DIAS, J.A., FERREIRA, Ó., MATIAS, A., VILA-CONCEJO, A., AND SÁ-PIRES, C. 2003 - Evaluation of soft protection techniques in barrier islands by monitoring programs: case studies of the Ria Formosa (Algarve-Portugal). In: Klein A.H.F. (ed.), *Proceedings of the Brazilian Symposium on Sandy Beaches: Morphodynamics, Ecology, Uses, Hazards and Management* (Spring, 2003), *Journal of Coastal Research*, Special Issue 35, 117-131pp.
- DORIGO, L. 1965 - La laguna di Grado e le sue foci. *Ricerche e rilievi idrografici*. Magistrato alle Acque, Ufficio Idrografico 155, Grafiche Gasparoni, Venezia, 231p. (in Italian)
- DRONKERS, J.J. 1964 - *Tidal computations in rivers and coastal waters*, John Wiley & Sons, Inc., New York. (in Russian)
- EELKEMA, M., WANG, Z.B., AND STIVE, M.J. 2013 - Ebb-tidal delta morphology in response to a storm surge barrier. In *Coastal Dynamics 2013: 7th International Conference on Coastal Dynamics*, Arcachon, France, 24-28 June 2013. Bordeaux University.
- ELIAS, E.P.L. 2006. *Morphodynamics of Texel Inlet*, Ph.D. Thesis, Delft University of Technology, Faculty of Civil Engineering and Geosciences, Delft, The Netherlands, 261 pp.
- ELIAS E. P. L. AND VAN DER SPEK A. J. F., 2006 - Long-term morphodynamic evolution of Texel Inlet and its ebb-tidal delta (The Netherlands). *Marine Geology*, 225: 5-21 pp.
- EYSINK, W.D. 1990 - Morphologic response of tidal basins to changes. In: B.L. edge (ed), *Coastal Engineering 1990 Proc.*, ASCE, New York, 1948-1961pp.

ERICKSON, K.M., KRAUS, N.C., AND CARR, E.E. 2003 - Circulation change and ebb shoal development following relocation of Mason Inlet, North Carolina. Engineer Research and Development Center Vicksburg Ms Coastal and Hydraulics Lab.

ESAGUY, A.S. 1984 - Ria de Faro, Barra da Armona. Evolução 1873–1983. Direcção Geral de Portos Internal Report, 5p. (in Portuguese)

ESAGUY, A.S. 1986a - Ria de Faro, Ilha do Ancão. Evolução 1950–1985. Direcção Geral de Portos Internal Report, 7p. (in Portuguese)

ESAGUY, A.S., 1986b - Ria de Faro, Barra de Faro-Olhao. Evolucao 1955-1985. Direcção geral de Portos Internal Report, 10p. (in Portuguese)

ESAGUY, A.S. 1986c - Ria de Faro, Ilha do Tavira. Evolução 1950–1985. Direcção Geral de Portos Internal Report, 8p. (in Portuguese)

ESAGUY, A.S. 1987 - Ria de Faro, Barra de Tavira. Evolução. Direcção Geral de Portos Internal Report, 13p. (in Portuguese)

ESCOFFIER, F.F. 1940 - The Stability of Tidal Inlets. *Shore and Beach*, 8(4), 114-115pp.

ESCOFFIER, F.F. 1977 - Hydraulics and stability of tidal inlets. general investigation of tidal inlets (GITI) Report 13, U.S. Army Engineer Waterway Experience Station, Vicksburg , MS, 72p.

FERLA, M., CORDELLA, M., MICHIELLI, L., AND RUSCONI, A. 2008. Analisi delle variazioni di lungo periodo del livello del mare dell'area nord adriatica e del regime di marea delle lagune di Venezia e di Marano-Grado. *L'Acqua*, 5, 65-76pp. (in italian)

FERLA, M., CROSATO, F., AND RAGAZZO, M. 2012 - Litorali e lagune del Nord est. ISPRA, 47p.

FERREIRA, Ó., MARTINS, J. C., & DIAS, J. A. 1997. Morfodinâmica e vulnerabilidade da Praia de Faro. Seminário sobre a zona costeira do Algarve, 67-76 pp. (in portuguese)

FERREIRA, Ó., GARCIA, T., MATIAS, A., TABORDA, AND R., DIAS, J.A. 2006. "An integrated method for the determination of set-back lines for coastal erosion hazards on sandy shores," *Continental Shelf Research*, 26, 1030-1044 pp.

FERREIRA, Ó., MATIAS A., AND PACHECO A. 2016a - The East Coast of Algarve: a Barrier Island Dominated. *Coast. Thalassas: An International Journal of Marine Sciences*, 32.2, 75-85pp.

FERREIRA, O., VIAVATTENE, C., JIMÉNEZ, J., BOLE, A., PLOMAITIS, T., COSTAS, S., AND SMETS, S. – 2016b CRAF Phase 1, a framework to identify coastal hotspots to storm impacts. *E3S Web of Conferences, FLOODrisk 2016 - 3rd European Conference on Flood Risk Management*.

FITZGERALD, D.M. 1984 - Interaction between the ebb-tidal delta and landward shoreline: Price Inlet, South Carolina. *Journal of Sedimentary Petrology*, 54, 1303-1308pp.

FITZGERALD, D.M. 1988 - Shoreline erosion-depositional processes associated with tidal inlets. In: *Hydrodynamics and sediment dynamics of tidal inlets* (Ed. Aubrey D. G.e Weishar L.), Springer-Verlag, New York, 29, 189-225pp.

FITZGERALD, D.M. 1996 - Geomorphic variability and morphologic and sedimentologic controls on tidal inlets. In: Mehta, A.J. (ed.), *Proceedings, An International Forum for the Littoral Sciences*. *Journal of Coastal Research, Special Issue 23*, 47-71pp.

FITZGERALD, D.M. AND HAYES, M.O. 1980 - Tidal inlet effects on barrier island management. In: *Proceedings of Coastal Zone '80, ASCE/Hollywood, FL, November 17–20, 1980*, 2355–2380pp.

FITZGERALD, D.M., HUBBARD, D.K., AND NUMMEDAL, D. 1978 - Shoreline changes associated with tidal inlets along the South Carolina coast. *Proceedings Coastal Zone 1978, American Society of Civil Engineers*, 1973-1994pp.

FITZGERALD, D.M., KRAUS, N.C., AND HANDS, E.B. 2001 - Natural Mechanisms of Sediment Bypassing at Tidal Inlets. ERDC/CHL CHETN-IV-30, U.S. Army Engineer Research and Development Center, Vicksburg, MS, 10p.

FITZGERALD, D.M., BUYNEVICH, I.V., AND HEIN, C.J., 2012, Morphodynamics and facies architecture of tidal inlets and tidal deltas, In: Davis, R.A., and Dalrymple,

R.W. (eds.), Principles of tidal sedimentology, Springer, New York. Chapter 12, p. 301-333 pp.

FONTOLAN, G., PILLON, S., QUADRI, F.D., AND BEZZI, A. 2007a - Sediment storage at tidal inlets in northern Adriatic lagoons: Ebb-tidal delta morphodynamics, conservation and sand use strategies. *Estuarine, Coastal and Shelf Science*, 75(1), 261-277pp.

FONTOLAN, G., PILLON, S., DELLI QUADRI, F., AND BEZZI, A. 2007b - Sediment storage in the northern Adriatic ebb-tidal deltas, Italy: sand use potential and GIS database. *Proceedings of the 9th International Coastal Symposium, Journal of Coastal Research, Special Issue 50*, 917-921pp.

FORBES, D.L. AND SOLOMON, S.M. 1999. Inlet division and coastal instability following tidal prism diversion. *Proceedings Coastal Sediments '99 Conference* (New York, U.S.A., ASCE), 1418-1433 pp.

FRIEDRICH, C.T. AND AUBREY, D.G., 1988. Non-linear tidal distortion in shallow wee-mixed estuaries: a synthesis. *Estuar. Coast. Shelf. Sci.* 27, 521-545 pp.

FRIEDRICH, C.T. AND MADSEN, O.S., 1992. Nonlinear Diffusion of the Tidal Signal in Frictionally Dominated Embayments. *J. Geophys. Res.* 97, 5637-5650 pp.

FRIEDRICH, C.T., AUBREY, D.G., GIESE, G.S., AND SPEER, P.E. 1993 - Hydrodynamic modelling of a multiple-inlet/barrier system. Insight into tidal inlet formation and stability. In *Formation and evolution of multiple tidal inlets*. Aubrey, D.G., Giese, G.S. (eds.), American Geophysical Union, Coastal and estuarine studies, 44, 95-112pp.

FRY, V.A. AND D.G. AUBREY. 1990. Tidal Velocity Asymmetries and Bedload Transport in Shallow Embayments. *Estuarine, Coastal and Shelf Science*, v. 30, p. 453-473 pp.

GALGANO, F.A. AND LEATHERMAN, S.P. 1999. Beach erosion, tidal inlets and politics: The Fire Island story. *Shore and Beach*, 67(2/3), 26-32 pp.

- GAO, S. AND COLLINS, M. 1994a - Tidal inlet equilibrium, in relation to cross-sectional area and sediment transport patterns. *Estuarine Coastal and Shelf Science*, 38, 157-172pp.
- GAO, S. AND COLLINS, M. 1994b - Tidal inlet stability in response to hydrodynamic and sediment dynamic conditions. *Coastal Engineering*, 23(1), 61-80pp.
- GATTO, F. AND MAROCCO, R. 1992 - Caratteri morfologici ed antropici della laguna di Grado (alto Adriatico). *Atti del Museo Friulano di Storia Naturale*, 14, Gortania, Udine, 19-42pp. (in Italian)
- GERRITSEN, F. 1990 - Morphological stability of inlets and channels in the Western Wadden Sea. Rijkswaterstaat, Report GWAO-90.019.
- GOMES, N., ANDRADE, C., NEVIN, C., MCCLUSKEY, J., AND JACKSON, D., 1994. Aeolian sand transport in Culatra barrier, Ria Formosa (Portugal). *Proceedings of 2nd International Symposium Littoral '94*, 509–516 pp.
- HARWOOD, P.J.W. 1973. "Stability and geomorphology of Pass Cavallo and its flood delta since 1856, central Texas coast," M.A. thesis, The U. of Texas at Austin, Austin, TX, 185 p.
- HAYES, M.O. 1969 - Coastal Environments: NE Massachussets and New Hampshire. Guidebook fieldtrip for eastern section of S. E. P. M., May 9-11, 1969, 462p.
- HAYES, M.O. 1975 - Morphology of sand accumulation in estuaries: an introduction to the symposium. In: (Cronin L. E. Ed.) *Estuarine Research*, 2: Geology and Engineering, New York: Accademic, 3-22pp.
- HAYES, M.O. 1979 - Barrier Island Morphology as a Function of Tidal and Wave Regime. In: (S. P. Leatherman Ed.) *Barrier Islands from the Gulf of St. Lawrence to the Gulf of Mexico*. Academic Press, New York, 1-27pp.
- HAYES, M.O. 1980 - General morphology and sediment patterns in tidal inlets. *Sedimentary Geology*, 26, 139-156pp.
- HAYES, M.O. 1994 - The Georgia Bight Barrier System. Chap. 7, 233- 304pp. In: (Davis R. A. Jr Ed.) *Geology of Holocene Barrier Island Systems*. Berlin, Germany: Springer-Verlag: 464 pp.

HAYES, M.O. AND KANA, T.W. 1976 - Terrigenous clastic depositional environments: some modern examples. AAPG Field Course Guidebook and Lecture Notes. Coastal Research Div. Geol. Dep., Univ. S.C., Technical Report, 11 - C.R.D., 131p.

HAYES, M.O., HUBBARD, D.K., AND ABELE, R.W. 1973 - The investigation of forms and processes in the coastal zone. In: (Coates D. R. Ed.) Coastal Geomorphology. Publ. in Geomorphology: Binghampton, New York, 2, 41p.

HAYES, M.O., SEXTON, W.J., DOMERACKI, D.D., KANA, T.W., MICHEL, J., BARWIS, J.H., AND MOSLOW, T.M. 1979 - Assessment of shoreline changes, Seabrook Island. South Carolina. Tech. Report to Seabrook Island Company (SIC); Research Planning Inst. (RPI), Columbia, S.C., 82pp.

HELSEBY, R. 2008 - Sand transport in northern Venice lagoon through the tidal inlet of Lido. Doctoral dissertation, University of Southampton. 262 pp.

HERRLING, G. AND WINTER, C., 2014. Morphological and sedimentological response of a mixed-energy barrier island tidal inlet to storm and fair-weather conditions. *Earth Surf. Dyn.* 2 (1), 363–382 pp.

HERRLING, G., AND C. WINTER 2015. Tidally-and wind-driven residual circulation at the multiple-inlet system East Frisian Wadden Sea. *Continental Shelf Research* 106: 45-59 pp.

HICKS, D.M. AND HUME, T.M. 1996 - Morphology and size of ebb-tidal deltas at natural inlets on open sea and pocket bay coasts, North Island, New Zealand. *Journal of Coastal Research*, 12(1), 47-63pp.

HICKS, D.M. AND HUME, T.M. 1997 - Determining sand volumes and bathymetric change on an ebb-tidal delta. *Journal of Coastal Research*, 13(2), 407-416pp.

HINE, A.C. 1975 - Bedform Distribution and Migration Patterns on Tidal Deltas in the Chatham Harbor Estuary, Cape Cod, Massachusetts. In: (L. E. Cronin Ed.) *Estuarine Research*, Academic Press, New York, 235-252p.

HUBBARD, D.K. 1977 - Variation in tidal inlet processes and morphology in the Georgia Embayment. Coastal Research Div. Geol. Dep., Univ. S. C., Teach. Rep., 14- C. R. D., 79p.

HUBBARD, D. K., OERTEL, G., AND NUMMEDAL, D. 1979. The role of waves and tidal currents in the development of tidal-inlet sedimentary structures and sand body geometry: examples from North Carolina, South Carolina, and Georgia. *Journal of Sedimentary Research*, 49(4).

HUME, T.M. AND HERDENDORF, C. 1993 - On the use of empirical stability relationships for characterising estuaries. *Journal of Coastal Research*, 9(2), 413-422pp.

HUNTLEY, D.A., NUMMEDAL, D., 1978. Velocity and stress measurements in a tidal inlet. *Proceedings 16th Coastal Engineering Conference (New York U.S.A.)*, 1320-1335 pp.

ISLA, F.I. 1995 - Coastal Lagoons. In: (Perillo G. M. E. Ed.) *Geomorphology and Sedimentology of Estuaries. Developments in Sedimentology*, 53, Elsevier Science B. V., Amsterdam, 241-267pp.

JARRETT, J.T. 1976 - Tidal prism-inlet area relationships. Vicksburg, U.S.A.: U.S. Army Corps of Engineers, Waterways Experiment Station, GITI Report 3, 32p.

JOHNSEN, C.D., CLEARY, W.J., FREEMAN, C.W., SAULT, M., 1999. Inlet induced shoreline changes, high energy flank of the Cape Fear foreland, SE; NC. *Proceedings Coastal Sediments '99 Conference (New York, U.S.A., ASCE)*, 1402-1417pp.

JOHNSON, D.W. 1919 - *Shore processes and shoreline development*. New York, Wiley, 504p.

JOHNSON, J.W. 1972 - Tidal inlets on the California, Oregon and Washington Coasts. Report HEL 24-12, Hydraulic Engineering Laboratory, University of California, Berkeley, CA.

KANA, T.W. 1989 - Erosion and beach restoration at Seabrook Island, South Carolina. *Shore and Beach*, 57(3), 3-18pp.

KANA, T.W., 2003. *Coastal Erosion and Solutions - A Primer*. Coastal Science and Engineering, Columbia, SC, 23pp.

KANA, T.W., MASON, J.E., 1988. Evolution of an ebb tidal-delta after an inlet relocation. *Lecture Notes on Coastal and Estuarine Studies*, 29, 382-409 pp.

KANA, T.W. AND MCKEE, P.A. 2003 - Relocation of Captain Sams Inlet - 20 years later. In Proceedings of Coastal Sediments, 3. American Society of Civil Engineers, New York, NY.

KEULEGAN, G.H. 1967 - Tidal flow in entrances. Water-level fluctuations of basins in communication with seas. Committee of Water Hydraulics, US Army Corp of Engineers, Technical Bulletin, 14, 89p.

KING, C.A.M. 1972 - Beaches and coasts. London, Edward Arnold, 570p.

KING, D.B. 1974 - The dynamics of inlets and bays. Coastal and Oceanographic Engineering Laboratory, College of engineering, University of Florida, technical report, 22, 82p.

KJERFVE, B. 1986 - Comparative oceanography of coastal lagoons. In Estuarine Variability, Ed. By DA Wolfe. Academic Press, New York, 63-81pp.

KRAUS, N. C. 2007. Coastal Inlets, Texas, USA, Proceedings Coastal Sediments '07, ASCE.

KRAUS, N.C. AND BATTEN, B.K. 2008 - Morphologic examination of the stability of Pass Cavallo, Texas. Engineer Research and Development Center Vicksburg MS Coastal and Hydraulics Lab.

KRAUS, N. C., AND MILITELLO, A. 1999. Hydraulic study of multiple inlet system: East Matagorda Bay, Texas. Journal of Hydraulic Engineering, 125(3), 224-232 pp.

KRAUS, N.C., LIN, L., BATTEN, B.K., AND BROWN, G.L. 2006. Matagorda Ship Channel, Texas: Jetty stability study, Technical Report ERDC.CHL-06-7, U.S. Army Engineer Research and Development Center, Coastal and Hydraulics Laboratory, Vicksburg, MS, 153 p.

LE CONTE, L. 1905 - Discussion of "Notes on the improvement of river and harbour outlets in the United States" by D.A. Watts. Trans. Amer. Soc. Civil Eng. LV, 2, 306-308pp.

LYNCH-BLOSSE, M.A. AND KUMAR N. 1976 - Evolution of downdrift-offset tidal inlets: a model based on the Brigantine Inlet system of New Jersey. Journal of Geology, 84, 165-178pp.

LYNCH-BLOSSE, M. A. AND DAVIS, R. A. 1977. Stability of Dunedin and Hurricane Passes, Pinellas County, Florida. In: Coastal Sediments '77, American Society of Civil Engineers, New York, 774-789 pp.

MARDEN, T.P. AND CLEARY, W.J. 1999 - Barrier morphology and inlet types; low-energy flank of the Cape Fear foreland, NC. Proceedings Coastal Sediments '99 Conference (New York, U.S.A., ASCE), 1295-1310pp.

MARINO, J.N. AND METHA, A.J. 1987 - Inlet ebb tide shoals related to coastal parameters. Coastal Sediments 1987, New York, ASCE, 1608-1622pp.

MARINO J.N. AND METHA A.J. 1988 - Sediment trapping at Florida's East Cost inlets. In: Hydrodynamics and sediment dynamics of tidal inlets (Eds. Aubrey D. G. and Weishar L.), Springer- Verlag, New York: 284-296pp.

MAROCCO, R. 1991 - Evoluzione tardo pleistocenica-olocenica del delta del F. Tagliamento e delle lagune di Marano e Grado (Golfo di Trieste). Il Quaternario, IV, 1b, 223-232pp. (in Italian)

MAROCCO, R. 1995 - Sediment distribution and dispersal in northern Adriatic lagoons (Marano and Grado paralic system). Giornale di Geologia, ser.3, 57/1-2, Bologna, 77-89pp.

MAROCCO, R. AND PESSINA, M. 1995 - Il rischio litorale nell'area circumlagunare del Friuli Venezia Giulia. Gortania – Atti del Museo Friulano di Storia Naturale, 17, 5-35pp. (in Italian)

MARTIN, L. AND DOMINGUEZ, J. 1994 - Geological history of coastal lagoons. In: (Kierfve B. J. Ed.) Coastal Lagoon Processes. Elsevier Oceanography Series, 60, Elsevier Science B. V., Amsterdam, 41-68pp.

MARTUCCI, G., CARNIEL, S., CHIGGIATO, J., SCLAVO, M., LIONELLO, P., AND GALATI, M.B. 2010 - Statistical trend analysis and extreme distribution of significant wave height from 1958 to 1999 – an application to the Italian Seas. Ocean Sci 6: 525-538pp.

MASON, J.E. 1986 - Morphologic evolution of a relocated mesotidal inlet: Captain Sam's Inlet, South Carolina. Technical Report, Dept. Geol., University South Carolina, 149p.

MASTERTON, R.P., MACHEMEHL, J.L., AND CAVAROC, V.V. 1973 - Sediment Movement in Tubbs Inlet, North Carolina. The Center for Marine Coastal Studies – North Carolina State University. Report N. 73-2, 117pp.

MATIAS, A., FERREIRA, Ó., AND ALVEIRINHO-DIAS, J. M. (1999). Preliminary results of the Cacela Peninsula (southern Portugal) replenishment. BOLETIN- INSTITUTO ESPANOL DE OCEANOGRAFIA, 15(1/4), 283-288 pp.

MATIAS, A., FERREIRA, Ó., VILA-CONCEJO, A., GARCIA, T., AND DIAS, J.A. 2008 - Classification of washover dynamics in barrier islands. *Geomorphology* 97, 655–674pp.

MATIAS, A., FERREIRA, Ó., VILA-CONCEJO, A., MORRIS, B., AND DIAS, J.A. 2010 - Short-term morphodynamics of non-storm overwash. *Marine Geology*, 274(1), 69-84pp.

MEHTA, A.H., JONES, C.P. AND ADAMS, W.D. 1976. Johns Pass and Blind Pass. Glossary of Inlets Report, Florida Sea Grant Program, Rept. No. 18.

MILITELLO, A. AND HUGHES, S.A. 2000 - Circulation Patterns at Tidal Inlets with Jetties. US Army Corp of Engineers, Technical Note ERDC/CHL CETN-IV-29, 10p.

MORANG, A., 1999. Shinnecock Inlet, New York, Site Investigation; Report 1, Morphology and Historical Behavior. Technical Report CHL-98-32, U.S. Army Engineer Waterways Experiment Station, Vicksburg, MS. 94 pp.

MORRIS, B.D., DAVIDSON, M.A., AND HUNTLEY, D.A. 2001 - Measurements of the response of a coastal inlet using video monitoring techniques. *Marine Geology*, 175(1-4), 251-272pp.

MORRIS, B.D., DAVIDSON, M.A., AND HUNTLEY, D.A. 2004 - Estimates of the seasonal morphological evolution of the Barra Nova Inlet using video techniques. *Continental Shelf Research*, 24, 263-278pp.

MURACA, A. 1982. Shore protection at Venice: a case study. In *Coastal Engineering 1982* 1078-1093 pp.

NIENHUIS J.H. AND ASHTON A.D. 2016 - Mechanics and rates of tidal inlet migration: Modeling and application to natural examples. *Journal of Geophysical Research: Earth Surface*, 121 (11): 2118-2139pp.

NIXON, S.W. 1982 - Nutrient dynamics, primary production and fisheries yields of lagoons. *Oceanologica Acta. Proceedings International Symposium on Coastal Lagoons. SCOR/ IABO/ UNESCO, Bordeaux, 8-14 September, 1981*, 357-371pp.

NUMMEDAL, D. AND HUMPHRIES, S.M., 1978. *Hydraulics and Dynamics of North Inlet, SC, 1975-1976. GITI Report 16, U.S. Army Engineer Research and Development Center, Vicksburg, MS. 214pp.*

NUMMEDAL, D.N., OERTEL G.F., HUBBARD D.K., AND HINE, A.C. 1977 - Tidal Inlet Variability- Cape Hatteras to Cape Canaveral. *Proceedings Coastal Sediments 77, American Society of Civil Engineers*, 543-562pp.

O'BRIEN, M.P. 1931 - Estuary tidal prism related to entrance areas. *Civil Engineering*, 1(8), 738-739pp.

O'BRIEN, M.P. 1969 - Equilibrium flow areas of inlets on sandy coasts. *Journal Waterways and Harbors Division. American Society of Civil Engineers*, 95, 43-52pp.

OERTEL, G.F. 1988 - Processes of sediment exchange between tidal inlets, ebb deltas and barrier islands. In: (D.G. Aubrey and L. Weishar, Eds) *Hydrodynamics and sediment dynamics of tidal inlets. Lecture Notes on Coastal and Estuarine Studies*, 29. Springer-Verlag, New York, 297-318pp.

OOST, A. P. 1995. *Dynamics and sedimentary developments of the Dutch Wadden Sea with a special emphasis on the Frisian Inlet: a study of the barrier islands, ebb-tidal deltas, inlets and drainage basins. Faculteit Aardwetenschappen.*

PACHECO, A., VILA-CONCEJO, A., FERREIRA, Ó., AND DIAS, A. 2007 - Present hydrodynamics of Ancão Inlet, 10 years after its relocation. In: *Coastal Sediments' 07*, 1557-1570pp.

PACHECO, A., VILA-CONCEJO, A., FERREIRA Ó., AND DIAS, J.A. 2008 - Assessment of tidal inlet evolution and stability using sediment budget computations and hydraulic parameter analysis. *Marine Geology*, 247(1-2), 104-127pp.

PACHECO, A., FERREIRA, Ó., WILLIAMS, J.J., GAREL, E., VILA-CONCEJO, A., AND DIAS, J.A. 2010 - Hydrodynamics and evolution of a multiple-inlet system. *Marine Geology*, 274(1-4), 32-42pp.

PACHECO, A., WILLIAMS, J.J., FERREIRA, Ó., GAREL, E. AND REYNOLDS, S. 2011a - Application of sediment transport models to a multiple-inlet system. *Estuarine, Coastal and Shelf Science* 95, 119-134pp.

PACHECO, A., FERREIRA, Ó., AND WILLIAMS, J.J. 2011b - Long-term morphological impacts of the opening of a new inlet on a multiple inlet system. *Earth Surface Processes and Landforms* 36, 1726–1735pp.

PENLAND, S. 1979 - Influence of a jetty system on tidal inlet stability and morphology: Fort George Inlet, Florida. *Proceedings of the Specialty Conference on Coastal Structures* 79, ASCE, Virginia, USA, March 14-16, 665-689.

PERINI, L., CALABRESE, L., AND LUCIANI, P. 2011 - Il monitoraggio dei danni da mareggiata. Comunicazione nell'ambito del convegno "Monitoraggio del Sistema Costiero in Emilia-Romagna", Palazzo della Provincia di Ravenna, 15 Marzo 2011.

PESSANHA, L.E.V. AND PIRES, H.O. 1981 - Elementos sobre o Clima de Agitação Marítima na Costa Sul do Algarve. Lisbon, Portugal: Instituto Nacional de Meteorologia e Geofísica. Internal Report, 66p. (in Portuguese)

PILKEY, O.H. And NEAL, W.J. 1980 - Barrier island hazard mapping. *Oceanus*, 23(4), 38-46.

PILKEY, O.H., NEAL, W.J., MONTEIRO, J.H., AND DIAS, J.M.A. 1989 - Algarve barrier islands: a noncoastal-plain system in Portugal. *Journal of Coastal Research*, 5(2), 239–261pp.

POPE, J. 1991 - Ebb delta and shoreline response to inlet stabilization, examples from the southeast Atlantic Coast. In *Coastal Zone '91*, pp. 643-654pp.

POPESSO, C., PACHECO, A., FERREIRA, Ó., AND FONTOLAN, G. 2016 - Evolution of a relocated inlet migrating naturally along an open coast. In: Vila-Concejo, A., Bruce, E., Kennedy, D.M., and McCarroll, R.J. (eds.), *Proceedings of the 14th International*

Coastal Symposium (Sydney, Australia). *Journal of Coastal Research*, Special Issue, 75, 233-237pp.

POSTMA, H., 1961. Transport and accumulation of suspended matter in the Dutch Wadden Sea. *Netherlands Journal of Sea Research* 1: 148-190 pp.

POSTMA, H., 1967. Sediment transport and sedimentation in the estuarine environment. In: Lauff, G.H. (ed) *Estuaries*. American association for the Advancement of Science 16: 651-668 pp.

PRICE, W.A. 1952. Reduction of maintenance by proper orientation of ship channels through tidal inlets, *Proceedings 2nd Coastal Engineering Conference*, Council on Wave Research, 243-255 pp.

RAMOS, L. AND DIAS, J.A. 2000 - Atenuação da vulnerabilidade a galgamentos oceânicos no sistema da Ria Formosa mediante intervenções suaves *overwash vulnerability attenuation in Ria Formosa system through soft interventions*. 3º Simpósio sobre a Margem Ibérica Atlântica, 361-362pp. (in Portuguese)

RANASINGHE, R. AND PATTIARATCHI, C., AND MASSELINK, G., 1998. Seasonal inlet closure: Governing processes. *Journal of Coastal Research*, SI(26), 32-41pp.

RANASINGHE, R. AND PATTIARATCHI, C., 1999. The seasonal closure of tidal inlets: Wilson Inlet - a case study. *Coastal Engineering*, 37, 37-56 pp.

RAVERA, O. 2000. The lagoon of Venice: the result of both natural factors and human influence. *Journal of Limnology*, 59 (1), 9-30 pp.

RIEDEL, H.P. AND GOURLAY, M.R. 1980 - Inlets/estuaries discharging into sheltered waters. *Proceedings International Conference of Coastal Engineering*, ASCE Press, NY, 2250-2562pp.

ROOS, P.C., SCHUTTELAARS, H.M., AND BROUWER, R.L., 2013 - Observations on barrier island length explained using an exploratory morphodynamic model. *Geophysical Research Letters*, 40(16), 4338-4343pp.

SALLES, P. 2001 - Hydrodynamic Controls on Multiple Tidal Inlet Persistence. Woods Hole, Massachusetts: Massachusetts Institute of Technology and Woods Hole Oceanographic Institution, unpublished Ph.D. dissertation, 272p.

SALLES, P., VOULGARIS, G., AND AUBREY, D. 2005 - Contribution of nonlinear mechanisms in the persistence of multiple tidal inlet systems. *Estuarine Coastal and Shelf Science*, 65, 475-491pp.

SARTORI, M. 1995 - Caratteri morfodinamici e sedimentologici della bocca di S. Andrea (Laguna di Marano). Trieste, Italy: University of Trieste, unpublished thesis, 99p. (in Italian)

SARRETTA A., PILLON S., MOLINAROLI E., GUERZONI S., FONTOLAN G., 2010. Sediment budget in the Lagoon of Venice. *Continental Shelf Research*, 30 (8): 934-949 pp.

SEABERGH, W.C. 2002 - Hydrodynamics of tidal inlets. In: Vincent, L. and Demirebilek, Z. (Eds), *Coastal Engineering Manual, Part II, Coastal Hydrodynamics, Chapter II-6, Engineer Manual*. Washington, DC: U.S. Army Corps of Engineers, 1110-2-1100, 73p.

SEGALA, C. 1999 - Morfodinamica sedimentaria ed aspetti evolutivi del sistema di bocca di S. Andrea- Isola di Martignano. Trieste, Italy: University of Trieste, unpublished thesis, 98p. (in Italian)

SHA, L.P. 1989 - Cyclic morphologic changes of the ebb-tidal delta, Texel Inlet, The Netherlands. *Geologie en Mijnbouw*, 68, 35-48pp.

SHA, L.P., 1990. Sedimentological studies of the ebb-tidal deltas along the West Frisian Islands, the Netherlands. Phd Thesis, University of Utrecht, Geol. Ultraiectina, 64, Utrecht. 160 pp.

SHA, L.P. AND VAN DEN BERG, J.H. 1993 - Variation in Ebb-Tidal Delta Geometry along the Coast of the Netherlands and the German Bight, *J. Coast. Res.*, 9, 730–746pp.

SHIGEMURA, T. 1981 - Tidal prism-throat width relationships of the bays of Japan. *Shore and Beach*, 49(3), 34-39pp.

SILVA, J.R.A., LEITAO, P.C., BRAUNSCHWEIG, F., AND NEVES, R., 2002. Ria Formosa 3D hydrodynamic model. A contribution for the understanding of the Faro-Olhao Inlet processes. *Proceedings of Littoral 2002*, 197-207 pp. (in Portuguese).

SPEER, P.E. AND AUBREY, D.G., 1985. A Study of the Non-Linear Propagation in Shallow Inlet/Estuarine Systems Part II: Theory. *Estuar. Coast. Shelf. Sci.* 21: 207-224 pp.

STAUBLE, D., 1998. Techniques for Measuring and Analysing Inlet Ebb Shoal Evolution. Coastal Engineering Technical Note IV-13, U.S. Army Engineer Waterways Experiment Station, Vicksburg, MS. 12 pp.

STEIJN, R.C. 1991 - Some Considerations on Tidal inlets. A literature survey on hydrodynamic and morfodynamic characteristics of tidal inlets with special attention to "Het Friesche Zeegat". Delft Hydraulics, Coastal Genesis, Rep. H 840.45.: 109 pp.

SWART, H.E., ZIMMERMAN, J.T.F. 2009 - Morphodynamics of tidal inlet systems. *Annual Review of Fluid Mechanics*, 41, 203-229pp.

TEIXEIRA, S. 2013 - Evolução da gestão da erosão costeira nos últimos 50 anos. Caso de estudo do litoral Quarteira-Garrão (Algarve-Portugal).

TOMLINSON, R.B. 1991 - Processes of sediment transport and ebb tidal delta development at a jettied inlet. *Coastal Sediments 1991*: 1404-1418 pp.

TRICHES A., PILLON, S., BEZZI A., LIPIZER M., GORDINI E., VILLALTA R., FONTOLAN G., AND MENCHINI G. 2011 - Carta batimetrica della Laguna di Marano e Grado. *Arti Grafiche Friulane, Imoco spa (UD)*, 39p. + 5 Maps.

TUNG, T.T, WALSTRA, D.R., VAN DE GRAAFF, J., AND STIVE, M.J.F. 2009 - Morphological modelling of tidal inlet migration and closure. *Journal of Coastal Research, Special Issue 56*, 1080-1084pp.

ULLIANI, A. 2016 - Struttura morfologica, dinamica evolutiva e indicatori gestionali delle isole-barriera della laguna di Marano e Grado. Trieste, Italy: University of Italy, Master thesis, 160p.

USACE, U.S. ARMY CORPS OF ENGINEERS 2002 - Coastal Engineering Manual. Volume IV- Ch. 3, Washington D.C.

VAN DE KREEKE, J. 1985 - Stability of tidal inlets – Pass Cavallo, Texas. *Estuarine Coastal and Shelf Science*, 21(1), 33-43pp.

VAN DE KREEKE, J. 1990. Can multiple tidal inlets be stable? *Estuarine Coastal and Shelf Science*, 30, 261-273 pp.

VAN DE KREEKE, J., 1998. Adaptation of the Frisian Inlet to a Reduction in Basin Area with Special Reference to the Cross-sectional Area of the Inlet Channel. In: Dronkers, J., Scheffers, M.B.A.M. (Eds.), *Physics of Estuaries and Coastal Seas. Proceedings 8th International Biennial Conference Physics of Estuaries and Coastal Seas (PECS)*, 355–362 pp.

VAN DE KREEKE, J. 2004. Equilibrium and cross-sectional stability of tidal inlets: application to the Frisian Inlet before and after basin reduction. *Coastal Engineering*, 51(5), 337-350 pp.

VAN DE KREEKE, J., BROUWER, R.L., ZITMAN, T.J., AND SCHUTTELAARS, H.M. 2008 - The effect of a topography high on the morphological stability of a two-inlet bay system. *Coastal Engineering*, 55, 319-332pp.

VILA-CONCEJO, A., 2003 - Sediment Dynamics and Tidal Inlet Relocation in Mixed-Energy Settings: The case of Ancão Inlet (Algarve - Portugal) Ph.D Dissertation.

VILA-CONCEJO, A., MATIAS, A., FERREIRA, Ó., DUARTE, C., AND DIAS, J.M.A. 2002 - Recent evolution of the natural inlets of a barrier island system in Southern Portugal. In: Cooper, J.A.G. and Jackson, D.W.T. (eds.), *Proceedings of the International Coastal Symposium (Northern Ireland) Journal of Coastal Research, Special Issue 36*, 741-752pp.

VILA-CONCEJO, A., FERREIRA, Ó., MATIAS, A., AND DIAS, J.M.A. 2003 - The first two years of an inlet: sedimentary dynamics. *Continental Shelf Research*, 23, 1425-1445pp.

VILA-CONCEJO, A., FERREIRA, Ó., MORIS, B.D., MATIAS, A., AND DIAS, J.M.A. 2004 - Lessons from inlet relocation: examples from southern Portugal. *Coastal Engineering*, 51(10), 967-990pp.

VILA-CONCEJO, A., MATIAS, A., FERREIRA, Ó., AND DIAS, J.M.A. 2006 - Inlet sediment bypassing to a downdrift washover plain. *Journal of Coastal Research, Special Issue 39*, 401- 405pp.

WADSWORTH, A. H. 1966. Historical delatation of the Colorado River, Texas. In *Deltas in their geological framework*, ed. M. L. Shirley, 99–105. Houston, TX: Houston Geological Society.

WALTON, T.L. AND ADAMS, W.D. 1976 - Capacity of inlet outer bars to store sand. In: *Proceedings of the Fifteenth Coastal Engineering Conference, 1919- 1937pp.*

WARD, G. H. 1982. Pass Cavallo, Texas: Case study of tidal-prism capture, *Journal of Waterway, Port, Coastal and Ocean Division* 108(WW4), ASCE, 513-525 pp.

WEINHOLTZ, M.B. 1964 - Contribuição para o estudo da evolução das flechas de areia na costa sotavento do Algarve. Separata do Boletim Trimestral de Informação do D G.S.H., 14, 14p. (in Portuguese)

WILLIAMS, G.L., MORANG, A., AND LILLYCROP, L., 1998. Shinnecock Inlet, New York, Site Investigation; Report 2, Evaluation of Sand Bypass Options. Technical Report CHL-98-32, U.S. Army Engineer Waterways Experiment Station, Vic.

WILLIAMS, J.J., O'CONNOR, B.A.O., ARENS, S.M., ABADIE, S., BELL, P., BALOUIN, Y., VAN BOXEL, J.H., DO CARMO, A.J., DAVIDSON, M., FERREIRA, ´O, HERON, M., HOWA, H., HUGHES, Z., KACZMAREC, L.M., KIM, H., MORRIS, B., NICHOLSON, J., PAN, S., SALLES, P., SILVA, A., SMITH, J., SOARES, C., AND VILA-CONCEJO, A., 2003. Tidal inlet function: field evidence and numerical simulation in the INDIA project. *Journal of Coastal Research*, 19(1), 189-211 pp.

ZIMMERMAN, J.T.F., 1976. Mixing and flushing of tidal embayments in the Western Dutch Wadden Sea I. Distribution of salinity and calculation of mixing time scales. *Neth. J. Sea Res.*, 10, 149-191pp.

WEBSITES:

OSMER: www.osmer.fvg.it

PROTEZIONE CIVILE DELLA REGIONE FVG: www.protezionecivile.fvg.it

PUERTOS DEL ESTADO: www.puertos.es

Appendix

Evolution of a relocated inlet migrating naturally along an open coast

Chiara Popesso^{**}, André Pacheco[‡], Óscar Ferreira[‡] and Giorgio Fontolan[†]

[†]Coastal Group, Dipartimento di Matematica e Geoscienze
Università degli studi di Trieste
Trieste, Italia

[‡]CIMA, Centro de Investigação Marinha e Ambiental,
Universidade do Algarve, Campus de Gambelas
Faro, Portugal



www.cerf-jcr.org



www.JCRonline.org

ABSTRACT

Popesso, C.; Pacheco, A.; Ferreira, Ó., and Fontolan, G., 2016. Evolution of a relocated inlet migrating naturally along an open coast. *In: Vila-Concejo, A.; Bruce, E.; Kennedy, D.M., and McCarroll, R.J. (eds.), Proceedings of the 14th International Coastal Symposium (Sydney, Australia). Journal of Coastal Research, Special Issue, No. 75, pp. 233-237. Coconut Creek (Florida), ISSN 0749-0208.*

Ancão Inlet is a small migrating inlet that was relocated in 1997 and has been monitored since then. In October 2015, it was about to conclude its third eastward migrating cycle since the 1940s. Morphological parameters and migration rates were correlated with oceanographic settings to evaluate the importance of different mechanisms in the evolutionary phases of the inlet. The migration trend is related to the dominant southwest sea conditions, inducing the alongshore sediment transport from west to east. The inherited features of the downdrift side area were also considered as rate of migration constraints. In this paper, we show how storm events, a constant longshore sediment supply from the west, and a lower downdrift barrier island volume control migration rates, noting that inlet efficiency is also strongly influenced by the reshaping of the barrier area.

ADDITIONAL INDEX WORDS: *Ancão Inlet, migrating inlet, relocation, accommodation space.*

INTRODUCTION

Tidal inlets are one of the most important and dynamic coastal features that play a significant role in coastal systems as navigation routes, sediment suppliers to adjacent beaches, and conduits that allow an exchange of nutrients between backbarrier systems and the coastal zone (FitzGerald, 1996). Once inlet and backbarrier basins have formed, their medium-term evolution (on a timescale of decades) depends on the competing effects of waves and tides that attempt to close and widen the inlet, respectively. These two factors determine, to a large extent, the direction and magnitude of sediment transport, which can lead to erosion or deposition, and thus, to shifts in the inlet's morphology and position (Pacheco *et al.*, 2008). Tidal inlet migration is linked to barrier growth/erosion; migration and barrier spit growth/erosion are common features of many coasts in the world where wave-induced alongshore sediment transport is dominant in one direction. As an inlet migrates, the channel connecting the inlet to the bay elongates and sometimes meanders, thus increasing frictional factors, attenuating tidal flow, and decreasing tidal prism (FitzGerald, 1996). Breaching can lead to the formation of a new inlet that may compete for dominance of the tidal prism and threaten the stability of existing inlets in the same bay system, possibly promoting their closure. Understanding and predicting the morphological behavior and determining optimal flow management schemes of tidal inlet systems is crucial for coastal

zone management, in order to allow tidal inlets to function as naturally as possible and to minimize the risk of inlet closure.

In this paper, the natural evolution of the Ancão Inlet, a relocated inlet in southern Portugal, is evaluated. Using 18 years of data from a monitoring program, morphological and oceanographic parameters were compared to evaluate the importance of different factors in inlet migration and associated rates. During this period of time, all of the above-mentioned processes occurred (migration, inlet breaching, tidal prism shifts, and inlet closure).

Study Area

The Ancão Inlet is a small migrating inlet situated in southern Portugal. It is part of Ria Formosa, a coastal lagoon protected by a multi-inlet barrier island system consisting of five islands and two peninsulas separated by six tidal inlets (Figure 1). Tides in the area are semi-diurnal; average ranges are 2.8 m for spring tides and 1.3 m for neap tides, although maximum ranges of 3.5 m can be reached. Wave climate in the area is moderate to high (Ciavola *et al.*, 1997). Predominant wave directions, approximately 71%, are from the W-SW, while waves coming from the E-SE only account for 23% of the observations (Costa *et al.*, 2001). The storm threshold for this region has been defined as significant wave height (H_s) >3 m (Pessanha and Pires, 1981) or 2.5 m (*e.g.*, Costa *et al.*, 2001). This region is affected by a high sediment longshore transport (Q) that recent studies evaluated as 1.1×10^5 m³/year (Teixeira and Does, 2013), which is in accordance with the values determined in the early 1990s by Andrade (1990), $\sim 0.9 \times 10^5$ m³/year.

DOI: 10.2112/SI75-47.1 received 15 October 2015; accepted in revision 15 January 2016.

*Corresponding author: chiara.popesso@phd.units.it

©Coastal Education and Research Foundation, Inc. 2016

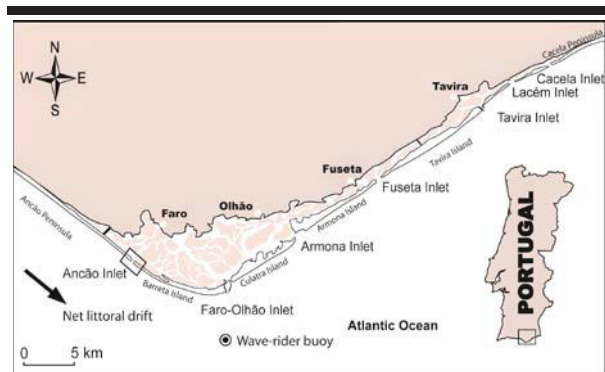


Figure 1. Ria Formosa Barrier Island System and location of study area (Ancão Inlet).

The Ancão Inlet presents a cyclic eastward migration. Three cycles were recorded between 1945 and the present (see Vila-Concejo *et al.*, 2002 and references therein). The Ancão Inlet pattern migration type is “High-Energy Flank” (Vila-Concejo *et al.*, 2002). In 1996, the Ancão Inlet was in its limiting position (Vila-Concejo *et al.*, 2004) and was partially closed by natural infilling and meandering. Following the adopted soft protection program (Dias *et al.*, 2003), on 23 June 1997, the inlet was relocated 3500 m to the west of its closing position, in order to improve water exchange at the western part of the Ria Formosa lagoon system. According to Vila-Concejo *et al.* (2003; 2004), the inlet reached dynamic equilibrium one year later (July 1998). The eastward migration started in January 1999 after an energy storm event. Since its relocation, the new Ancão Inlet has been monitored and has been found to resemble the old inlet in both its hydrodynamic characteristics and its morphology (Williams *et al.*, 2003). According to Morris *et al.* (2001), the Ancão Inlet shows characteristics of both a tide- (well-defined deep main channel and migrating flood channels) and a wave-dominated inlet (relatively small ebb delta).

During the current cycle, storm events breached the barrier updrift (2005) and downdrift (2010 and 2015) of the Ancão Inlet position, forming a new inlet that competed with the older one for dominance of the tidal prism. In 2005, the new inlet remained open for only three weeks and then closed naturally; in 2010, the new inlet captured a greater volume of tidal prism and forced the older inlet to close. Here we use the term “jump” to indicate this changed position without migration. Finally, the new opening of 2015 was still active in October 2015, with both inlets becoming too narrow and very shallow. A new relocation to a position close to the 1997 location is programmed for the end of 2015.

METHODS

Since the 1997 inlet relocation, a monitoring program has been in place to study its evolution. Twenty topobathymetric surveys were performed between the relocated inlet’s opening in June 1997 and May 2015. Topography was carried out using a total station and a RTK-DGPS positioning. Navigation and bathymetry transects were measured using HYPACK® 4.3a Gold software, by connecting the RTK-DGPS and an echo

sounder to a laptop. The RTK-DGPS and echo sounder were synchronized and measurements were taken at a frequency of 1 Hz. Thus, the recorded depth was immediately corrected for water level variations (*i.e.*, tides and waves). Due to a scarcity of data (not the entire inlet area was covered), the first survey of June 1997 was not used; as such, the August 1997 survey is herein considered the starting point for the evaluation of the Ancão inlet.

Using Surfer® 9, the topographic and bathymetric datasets were interpolated to produce continuous bathymetric surface maps, following the quality control methods suggested by Hick and Hume (1997). After an interpolator quality check, through the cross-validation function, the Kriging method was selected as the best interpolator. The spacing was based on data density and spatial distribution. A local metric coordinate system known as the Portuguese Melriça Grid was used for the maps; elevation is based on mean sea level.

Inlet morphological parameters such as minimum cross-sectional area (A_c) and migration (M) were determined following the suggestions of the Coastal Engineering Manual (Seabergh, 2002). The inlet throat was first defined on each map in order to sketch ten profiles with equal intervals through the inlet cross-section, considering the morphology of each situation (*e.g.*, the barrier’s width). Inlet migration was computed by determining the metric difference in the XY coordinates of the maximum depth at the minimum cross-sectional area between each survey and the August 1997 inlet position. The migration distances between consecutive surveys were then determined and added to obtain the cumulative migration. The different migration sign (plus or minus) is due to the fact that values are positive if migration is eastward and negative if westward.

The inlet cross-section area was used as a tidal prism proxy that could be estimated using the empirical formula developed by Jarrett (1976) for the Atlantic Coast (Equation 1):

$$A_c = 3.039 \cdot 10^{-5} P^{1.05} \quad (1)$$

where A_c is the minimum cross-sectional area (m^2), measured for each survey, and P is the corresponding tidal prism (m^3).

Wave data from the Instituto Hidrografico directional wave-rider buoy offshore of Cape Santa Maria (Figure 1) was used in this study (1997–present). The wave buoy recorded values representing significant wave height (H_s), mean peak period (T_p), and mean wave direction ($^\circ$) for 20 minutes every three hours, except during storms, when data were recorded every half hour. Wave data were interpolated to give hourly data and subdivided into intervals between consecutive surveys. The total percentage of missing data was about 3%. To individualize each single high-energy event, the storm threshold used in the present study refers to high-energy events with $H_s \geq 2.5$ m, with a minimum duration of three hours above the storm threshold and 24 hours between consecutive $H_s \geq 2.5$ m.

Due to the orientation of the barrier system, mean wave power (Wp) for the storm events was evaluated coming from three different directions ($<200^\circ$, $200 \div 220^\circ$, and $>220^\circ$), following Vila-Concejo *et al.* (2004), in order to assess their possible different impacts on inlet migration M . Wp was then multiplied by storm duration in seconds ($Wp\#$) to obtain total storm wave power.

The ratio $P/\sum Wp\#$ was evaluated, where P is assessed for each survey and $\sum Wp\#$ is the sum of $Wp\#$ of storm events coming from the dominant longshore drift direction ($>220^\circ$, as a proxy of the potential eastward longshore sediment transport), recorded between two surveys.

RESULTS

Storm events from $>220^\circ$ have higher $Wp\#$ values than those from other directions and seem to correspond to significant changes in migration rates (as after 2001 or in 2010, when a breaching occurred, with a subsequent inlet jump). No apparent clustering of storms or energy peaks seems to be responsible for the final breaching in 2015. There is, however, a continuity of the migration despite the existence (or absence) of storms (Figure 2A,B,C).

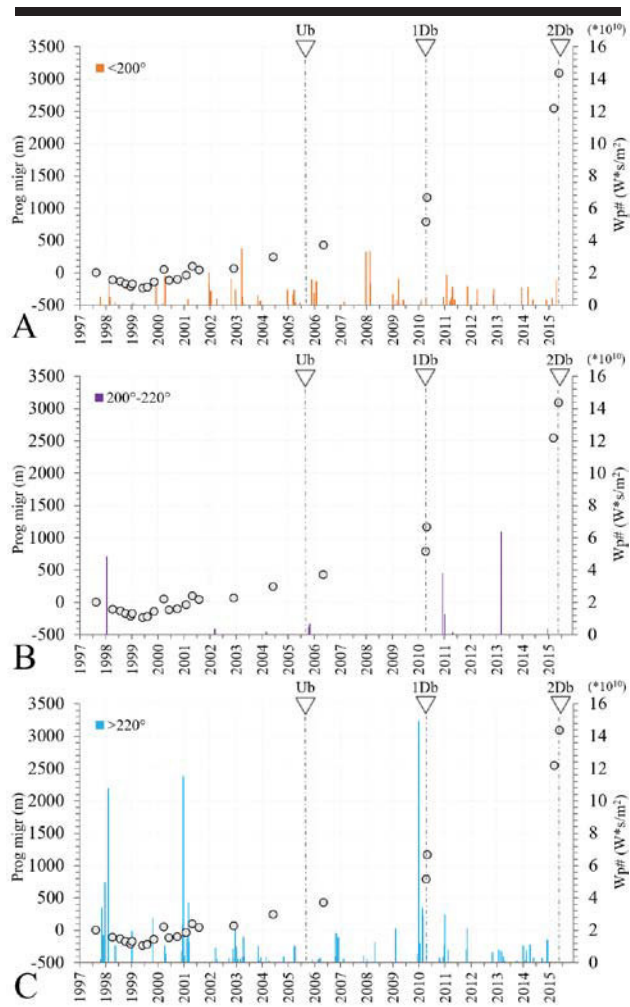


Figure 2. Progressive migration (gray circles) compared with $Wp\#$ for three directions: $<200^\circ$ (A), $200^\circ-220^\circ$ (B), and $>220^\circ$ (C). Updrift breaching (Ub) and downdrift breaching (1Db and 2Db) events are represented by triangles.

After reaching dynamic equilibrium in July 1998 (Vila-Concejo *et al.*, 2003), the Ancão Inlet had an average cross-section area (A_c) of 550 m^2 (Figure 3). The maximum value of A_c was reached in March 2000 (800 m^2) and was probably related to the dredging of the inner channels close to the inlet that was carried out February–April 2000 (Dias *et al.*, 2000). After that, a strong decrease occurred at the beginning of 2001, reaching a minimum value of 300 m^2 in April 2001. A stable period followed until 2010, when the inlet almost closed with an A_c of 50 m^2 . The jump recorded that spring took back the section to a wider value (110 m^2) that remained until May 2015 (Figure 3). Mean values of $P/\sum Wp\#$ were calculated for longer periods of time (hereafter called macro-intervals; see discussion for their interpretation). The highest values of $P/\sum Wp\#$ were recorded from the relocation date until 2001. From 2001 to 2010, the ratio decreased significantly, as well as from 2010 until 2015 (Figure 3). The overall trend is a decreasing cross-sectional area (and corresponding prism) during migration up to a critical position.

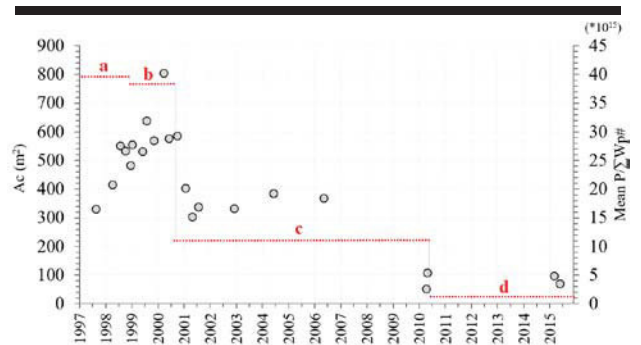


Figure 3. Cross-section area (A_c , gray circles) compared with the mean $P/\sum Wp\#$ ratio (horizontal lines) for four selected macro-intervals: a) unstable, due to morphological adaptation (which includes the phases described by Vila-Concejo *et al.*, 2003); b) equilibrium 1, while capturing prism and migrating; c) equilibrium 2, without capturing prism but with migration; and d) critical, toward closure/infilling.

The migration trends of the previous Ancão cycles (Vila-Concejo *et al.*, 2002; 2004) integrated with the last Ancão cycle data are shown in Figure 4. After the Ancão Inlet opened in 1997, its migration reproduced the behavior of the oldest inlet, starting with an initial stage of readjustment characterized by low migration rates, followed by a stage of high eastward migration rates (Vila-Concejo *et al.*, 2002). Nonetheless, the migration trend appears to be increasing as the migration cycle lifetime declines (33 years for Ancão1, 22 years for Ancão2, 18 years for Ancão3, for a longer overall migration), as already noted by Vila-Concejo *et al.* (2002). The migration trends of Ancão2 and Ancão3 are steeper than that of the first cycle. The Ancão2 opening position was located along the previous migration cycle path, and the overall migration was faster than that of the first cycle.

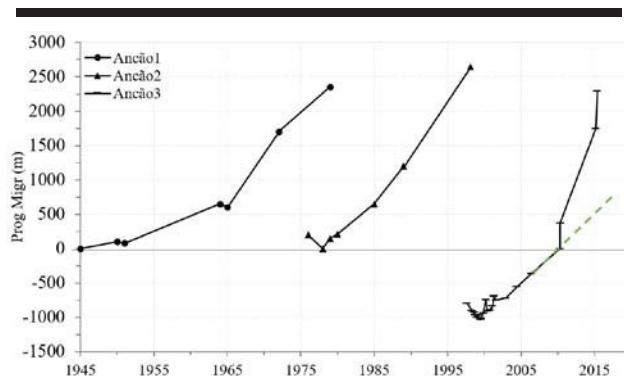


Figure 4. Migration trends of previous Ancão cycles (Vila-Concejo *et al.*, 2002, 2004) integrated with the last Ancão cycle data (1997–2015). Points represent inlet channel positions observed in aerial photographs or surveys. The dashed line represents the supposed continuity of the migration rate before the 2010 jump.

The initial stages of Ancão3, however, displayed lower migration rates. Its relocation site was ~1000 m to the west of the Ancão1 opening (Vila-Concejo *et al.*, 2004) in an area with a high dune system and relatively wide barrier. Once the Ancão1 opening position was reached, the migration trend started to be much faster (see dashed line in Figure 4). From that position to the east (downdrift direction), the barrier was low and narrow and subject to frequent overwashing, and thus, more susceptible to erosion, according to Matias *et al.* (2010).

DISCUSSION

Some authors have reported that migration is highly related to western storm events (Morris *et al.*, 2001; Vila-Concejo *et al.*, 2003; Williams *et al.*, 2003), referring to them as events from a direction $>180^\circ$. We also found that western storms are the main drivers of relevant changes at the inlet migration, although herein we have considered different storm classes according to their direction ($<200^\circ$, $200^\circ\text{--}220^\circ$, $>220^\circ$; Figure 2A,B,C). It is also visible that the continuity of migration between main storm events is not driven by storms, but seems to be a rather continuous process, most probably dependent mainly on longshore transport.

Considering these data and following the M and A_c trends, the migration cycle of the Ancão Inlet was divided into four macro-intervals (Figure 3, a,b,c,d): the first from the opening of the inlet in 1997 to the start of the eastward migration (January 1999); the second from January 1999 to September 2000; the third from September 2000 until the breaching of 2010; and the final period from 2010 until the end of the monitoring, with the inlet almost in its closing position (*i.e.*, very shallow and meandering channel).

The first interval corresponds to the unstable situation caused by the adapting morphological behavior subsequent to the relocation (“a” in Figure 3). The prevailing migration is opposite to what was expected, as already shown by Vila-Concejo *et al.* (2003). Although some storms from the east occurred during this period, it is difficult to establish a sole relationship between

storms and westward migration. A possible reason for the observed migration is the adaptation of the inlet to its position in the context of a new hydrodynamic setting. The existence of main channels (and relevant currents) to the west (Ancão and Ramallete channels) probably helped this migration pattern. The subsequent ~2-year interval highlights the increasing cross-section area A_c while the inlet migrated eastward. Maximum efficiency is indicated by the high $P/\sum Wp\#$ that likely occurred after the capture of the backbarrier channel network close to the inlet (“b” in Figure 3).

The results show that the inlet cross-section area during the third interval was almost constant, and therefore, not affected by the inlet’s migration. Migration occurred undisturbed until 2010 (“c” in Figure 3). That date marks an abrupt change in the history of the inlet, as the breaching caused by a severe storm occurred in the original (1975) position of the Ancão inlet. From this position, until the last survey, migration trends increased significantly (Figure 4), while the inlet featured an unstable/critical condition toward a possible closure (“d” in Figure 3). This rapid migration is most likely associated with the morphology of the affected area, which corresponded to a narrow overwash terrace (Matias *et al.*, 2010) with no dunes, thus causing less resistance. The dashed line in Figure 4 shows how the migration would have continued with a fully developed dune system (as before the jump).

Observing the present cycle, Ancão seems to be unable to capture the local drainage pattern at the end of its migration. This can be seen in the residual washover fans and old flood tidal delta bodies that are now intercepted and drained by the last terminations of creeks connected to the neighboring Faro–Olhão system. Indeed, the inlet is too far to the east to have an efficient connection to the main drainage system, even during spring tides. The inlet acts more independently, draining the surrounding area as a single (reduced tidal prism) inlet system (Pacheco *et al.*, 2010).

Therefore, the stability/instability conditions of the inlet can be categorized according to the macro-intervals reported in Figure 3: a) unstable, due to morphological adaptation (which includes the phases described by Vila-Concejo *et al.*, 2003); b) equilibrium 1, while capturing prism and migrating; c) equilibrium 2, without capturing prism but with migration; d) critical, toward closure/infilling.

CONCLUSIONS

The documented history of the Ancão inlet subsequent to its relocation in 1997 allows the acquisition of knowledge of both its morphodynamic and hydraulic behaviors. Southwestern storm events can increase the sediment longshore supply and help migration, while events coming from the east and from directions more perpendicular to the shoreline can fill the flood deltas and disrupt the eastward migration. The constant longshore transport, however, is the major driver of migration continuity, as the main storms are the drivers of rapid migration events or migration by jumps.

Knowing that a new inlet will be open at the 1997 position but that dunes are not yet established, the entire migration area will behave as a low and narrow barrier. After a two-year period of adjustment, the migration rate will most likely be similar to that observed in the last five years of the third cycle.

Better comprehension of the mechanisms linked with inlet migration, mainly associated with the current barrier situation, can be achieved through the collection of other physical data, such as determining the adjacent barrier dune elevation and barrier sediment volumes. The ongoing work will analyze nonlinear effects related to migration and morphological inlet features with controlling parameters (waves, levels, and morphologies).

Only a precise knowledge of the complex relationships among inlet, the barrier sediment volumes involved in the erosion processes, and the backbarrier inundation/drainage potential can furnish the basic elements needed for more effective management plans that consider complementary actions rather than the simple relocation of the Ancão Inlet.

LITERATURE CITED

- Andrade, C.F., 1990. O Ambiente de Barreira da Ria Formosa. Lisbon, Portugal: University of Lisbon, Ph.D. dissertation, 626p. (in Portuguese)
- Ciavola, P.; Taborda, R.; Ferreira, Ó., and Dias, J.A., 1997. Field measurements of longshore sand transport and control processes on a steep meso-tidal beach in Portugal. *Journal of Coastal Research*, 13(4), 1119-1129.
- Costa, M.; Silva, R., and Vitorino, J., 2001. Contribuição para o estudo do clima de agitação marítima na costa Portuguesa. *Actas das 2as Jornadas Portuguesas de Engenharia Costeira e Portuária* (Sines, Portugal), Associação Internacional de Navegação, CD-ROM, 20 p. (in Portuguese)
- Dias, J.M.A.; Ferreira, Ó.; Sá-Pires, C., and Duarte, C., 2000. *Relatório de Monitorização da Repulsão de Dragados para a Zona de Barreira do Sistema da Ria Formosa*. Algarve, Portugal: Centro de Investigação dos Ambientes Costeiros e Marinhos da Universidade do Algarve, *Technical Report No. 06/00*, 55p. (in Portuguese)
- Dias, J.A.; Ferreira, Ó.; Matias, A.; Vila-Concejo, A., and Sá-Pires, C., 2003. Evaluation of soft protection techniques in barrier islands by monitoring programs: case studies of the Ria Formosa (Algarve-Portugal). In: Klein A.H.F. (ed.), *Proceedings of the Brazilian Symposium on Sandy Beaches: Morphodynamics, Ecology, Uses, Hazards and Management (Spring, 2003)*. *Journal of Coastal Research*, Special Issue No. 35, pp. 117-131.
- FitzGerald, D.M., 1996. Geomorphic variability and morphologic and sedimentologic controls on tidal inlets. In: Mehta, A.J. (ed.), *Proceedings, An International Forum for the Littoral Sciences*. *Journal of Coastal Research*, Special Issue No. 23, pp. 47-71.
- Hicks, D.M. and Hume, T.M., 1997. Determining sand volumes and bathymetric change on an ebb-tidal delta. *Journal of Coastal Research*, 13(2), 407-416.
- Jarrett, J.T., 1976. *Tidal prism-inlet area relationships*. Vicksburg, U.S.A.: U.S. Army Corps of Engineers, Waterways Experiment Station, *GITI Report No. 3*, 32p.
- Matias, A.; Ferreira, Ó.; Vila-Concejo, A.; Morris, B., and Dias, J.A., 2010. Short-term morphodynamics of non-storm overwash. *Marine Geology*, 274(1), 69-84.
- Morris, B.D.; Davidson, M.A., and Huntley, D.A., 2001. Measurements of the response of a coastal inlet using video monitoring techniques. *Marine Geology*, 175(1-4), 251-272.
- Pacheco, A.; Vila-Concejo, A.; Ferreira Ó., and Dias, J.A., 2008. Assessment of tidal inlet evolution and stability using sediment budget computations and hydraulic parameter analysis. *Marine Geology*, 247(1-2), 104-127.
- Pacheco, A.; Ferreira, Ó.; Williams, J.J.; Garel, E.; Vila-Concejo, A., and Dias, J.A., 2010. Hydrodynamics and evolution of a multiple-inlet system. *Marine Geology*, 274(1-4), 32-42.
- Pessanha, L.E.V. and Pires, H.O., 1981. *Elementos sobre o Clima de Agitação Marítima na Costa Sul do Algarve*. Lisbon, Portugal: Instituto Nacional de Meteorologia e Geofísica. *Internal Report*, 66 p. (in Portuguese)
- Seabergh, W.C. 2002. Hydrodynamics of tidal inlets. In: Vincent, L. and Demirbilek, Z. (Eds), *Coastal Engineering Manual, Part II, Coastal Hydrodynamics, Chapter II-6, Engineer Manual*. Washington, DC: U.S. Army Corps of Engineers, pp. 1110-2-1100.
- Teixeira, S.B. and Does, A., 2013. Characterization of accidents in sea cliffs dissociated of natural geodynamics in the Algarve (Portugal) coast during the last decade (2003-2012). *Comunicações VII Congresso sobre Planeamento e Gestão das zonas Costeiras dos Países de Expressão Portuguesa* (Maputo, Moçambique), pp.3. (in Portuguese)
- Vila-Concejo, A.; Matias, A.; Ferreira, Ó.; Duarte, C., and Dias, J.M.A., 2002. Recent evolution of the natural inlets of a barrier island system in Southern Portugal. In: Cooper, J.A.G. and Jackson, D.W.T. (eds.), *Proceedings of the International Coastal Symposium (Northern Ireland)* *Journal of Coastal Research*, Special Issue No. 36, pp. 741-752.
- Vila-Concejo, A.; Ferreira, Ó.; Matias, A., and Dias, J.M.A., 2003. The first two years of an inlet: Sedimentary dynamics. *Continental Shelf Research*, 23, 1425-1445.
- Vila-Concejo, A.; Ferreira, Ó.; Morris, B.D.; Matias, A., and Dias, J.M.A., 2004. Lessons from inlet relocation: Examples from Southern Portugal. *Coastal Engineering*, 51(10), 967-990.
- Williams, J.J.; O'Connor, B.A.O.; Arens, S.M.; Abadie, S.; Bell, P.; Balouin, Y.; Van Boxel, J.H.; do Carmo, A.J.; Davidson, M.; Ferreira, Ó.; Heron, M.; Howa, H.; Hughes, Z.; Kaczmarek, L.M.; Kim, H.; Morris, B.; Nicholson, J.; Pan, S.; Salles, P.; Silva, A.; Smith, J.; Soares, C., and Vila-Concejo, A., 2003. Tidal inlet function: Field evidence and numerical simulation in the INDIA project. *Journal of Coastal Research*, 19(1), 189-211.